Vol. 5 No. 4 2020
ISSN:1390-9347

Bionatura

Latin American journal of Biotechnology and Life Sciences

The race for a coronavirus vaccine

Scientifically unproven therapeutic treatments for COVID-19

Therapeutic approach for COVID-19 – clinical challenges and implementation

Development of research on COVID-19 by the World Scientific Community in the first half of 2020

Comparative Pilot Study Between a Tomographic Score and RT-PCR to Determine Diagnostic Prediction in Patients with COVID 19

Es el momento de los que se atreven a soñar y luchan por alcanzar sus metas.

En la UCO te acompañamos

UCO Universidad Católica de Oriente
Acreditación Institucional en ALTA CALIDAD

Vigilada Mineducación

Pregrados

Tecnología en Operaciones Financieras
SNIES 104841 Registro Calificado - Res. 12903 del 21-09-2015 M.E.N.
95 créditos - A distancia tradicional - Rionegro Ant.

Contaduría Pública
SNIES 13018 Registro Calificado - Res. 9256 del 07- 06- 2018
Acreditación de Alta Calidad 4610 del 21- 03 - 2018 M.E.N.
165 créditos Presencial - Rionegro

Comercio Exterior
SNIES 1854 Registro Calificado - Res.14314 del 11-12-2019 M.E.N.
159 créditos - Presencial - Rionegro Ant.

Administración de Empresas
SNIES 55096 Registro Calificado - Res. 7658 del 18-04-2017 M.E.N.
152 créditos - Presencial - Rionegro Ant.

Tecnología Agropecuaria
SNIES 1850 Registro Calificado - Res. 8684 del 10-07-2013 M.E.N.
113 créditos - Presencial - Rionegro Ant.

Agronomía
SNIES 4443 Registro Calificado - Res. 8087 del 17-05-2018
Acreditación de Alta Calidad N° 29149 del 26-12-2017
157 créditos - Presencial - Rionegro Ant.

Zootecnia
SNIES 53037 Registro Calificado - Res. 14466 del 04-09-2014 M.E.N.
156 créditos - Presencial - Rionegro Ant.

Psicología
SNIES 8562 Registro Calificado - Res. 9902 del 31-07-2013 M.E.N.
Acreditación de Alta Calidad N° 17227 del 24 - 10 - 2018
175 créditos - Presencial - Rionegro Ant.

Comunicación Social
SNIES 53045 Registro Calificado - Res. 14892 del 11-09-2014 M.E.N.
146 créditos - Presencial - Rionegro Ant.

Trabajo Social
SNIES 106586 Registro Calificado - Res. 26741 del 29-11-2017 M.E.N.
141 créditos - Presencial - Rionegro Ant.

Derecho
SNIES 53539 Registro Calificado - Res. 10542 del 14-07-2015 M.E.N.
166 créditos - Presencial - Rionegro Ant.

Nutrición y Dietética
SNIES 104601 Registro Calificado - Res. 7823 del 01-06-2015 M.E.N
166 créditos - Presencial - Rionegro Ant.

Gerontología
SNIES 1853 Registro Calificado - Res. 14839 del 22-10-2013 M.E.N.
138 créditos - A distancia con apoyo virtual - Rionegro Ant.

Enfermería
SNIES 91027 Registro Calificado- Res. 12600 del 03-08-2018 M.E.N.
166 créditos - Presencial - Rionegro Ant.

Licenciatura en Filosofía
SNIES 106542 Registro Calificado - Res. 22108 del 24 - 10 - 2017 M.E.N.
164 créditos - Presencial - Rionegro Ant.

Licenciatura en Lenguas Extranjeras con énfasis en Inglés
SNIES 106647 Registro Calificado - Res. 29529 del 29-12-2017 M.E.N.
164 créditos - Presencial - Rionegro Ant.

Licenciatura en Educación Física, Recreación y Deportes
SNIES 106436 Registro Calificado - Res. 17481 del 31-08-2017 M.E.N.
164 créditos - Presencial - Rionegro Ant.

Licenciatura en Educación para la Primera Infancia
SNIES 105359 Registro Calificado - Res. 02848 del 16-02-2016 M.E.N.
164 créditos - Presencial - Rionegro Ant.

Licenciatura en Ciencias Naturales
SNIES 105898 Registro Calificado - Res.19869 del 18-10-2016 M.E.N.
164 créditos - Presencial - Rionegro Ant.

Licenciatura en Educación Religiosa
SNIES 106705 Registro Calificado - Res. 2084 del 13 - 02 - 2018 M.E.N.
164 créditos - Presencial - Rionegro Ant.

Técnico Profesional en Programación Web
SNIES 103704 Registro Calificado - Res.14454 del 04-09-2014 M.E.N.
67 créditos - Presencial - Rionegro Ant.

Ingeniería Ambiental
SNIES 4361 Registro Calificado - Res. 3654 del 02-03-2018 M.E.N.
Acreditación de Alta Calidad No. 6543 del 18 - 04 - 2018
173 créditos - Presencial - Rionegro Ant.

Ingeniería de Sistemas
SNIES 1855 Registro Calificado - Res. 0178 del 05-01-2019 M.E.N.
164 créditos - Presencial- Rionegro Ant.

Ingeniería Industrial
SNIES 1856 Registro Calificado - Res. 1293 del 04-02-2019 M.E.N.
160 créditos - Presencial- Rionegro Ant.

Ingeniería Electrónica
SNIES 20271 Registro Calificado - Res. 24646 del 14-11-2017 M.E.N.
178 créditos - Presencial- Rionegro Ant.

Teología
SNIES 103450 Registro Calificado - Res. 10638 del 09-07-2014 M.E.N.
130 créditos - A distancia - Rionegro Ant.

¡HAGAMOS QUE PASE!

www.uco.edu.co @uconiano universidad catolica de oriente 322 569 90 90

Docencia, investigación, extensión y proyección social al servicio del territorio

UCO
Universidad Católica de Oriente
Vigilada Mineducación

Fortalezas **institucionales**

- Biotecnología
- Limnología
- Derechos Humanos – Posconflicto
- Internacionalización
- Inclusión Social
  - SER Servicio Educativo Rural
  - Educación de Alfabetización
- MIS – Instituto de formación para el trabajo y el desarrollo humano
- Formación humanística "Ruta Humanística en el currículo - Cátedra abierta Madre de la Sabiduría"
- Investigación y desarrollo tecnológico
- Comprometida con la calidad
- Centro de Estudios Territoriales
- Biodiversidad
  - Herbario
  - Ictiología
  - Litoteca

Áreas del **conocimiento**

- Ciencias Agropecuarias
- Ciencias de la Educación
- Ciencias de la Salud
- Ciencias Económicas y Administrativas
- Ciencias Sociales
- Derecho
- Ingenierías
- Teología y Humanidades

- 26 programas de pregrado
- 16 programas de posgrado
  - 1 doctorado
  - 8 maestrías
  - 7 especializaciones

www.uco.edu.co Universidad catolicadeoriente @uconia

Contacto institucional Universidad Católica de Oriente
Sector 3, Cra. 46 No. 40B 50 - **PBX:** (57)(4) 569 90 90. Ext. 694
Fax: (57)(4) 531 09 72 - **Email:** uco@uco.edu.co

Vol. 5 No. 4 2020

Bionatura

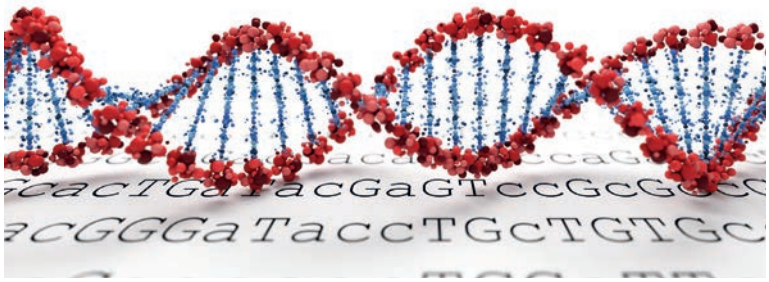

La Revista Bionatura publica trimestral en español o inglés trabajos inéditos de investigaciones básicas y aplicadas en el campo de la Biotecnología, la Inmunología, la Bioquímica, Ensayos Clínicos y otras disciplinas afines a las ciencias biologícas, dirigidas a la obtención de nuevos conocimientos, evaluación y desarrollo de nuevas tecnologías, productos y procedimientos de trabajo con un impacto a nivel mundial.

Equipo editorial

latindex

Index in directory of open access journals

Instrucciones para los Autores

Los Trabajos serán Inéditos: Una vez aprobados, no podrán someterse a la consideración de otra revista, con vistas a una publicación múltiple, sin la debida autorización del Comité Editorial de la Revista. La extensión máxima será 8 cuartillas para los trabajos originales, 12 las revisiones y 4 las comunicaciones breves e informes de casos, incluidas las tablas y figuras. Los artículos se presentarán impresos (dos ejemplares). Todas las páginas se numerarán con arábigos y consecutivamente a partir de la primera. Estos deben acompañarse de una versión digital (correo electrónico o CD) en lenguaje Microsoft Word, sin sangrías, tabuladores o cualquier otro atributo de diseño (títulos centrados, justificaciones, espacios entre párrafos, etc.). Siempre se ha de adjuntar la carta del consejo científico que avala la publicación y una declaración jurada de los autores.

Referencias Bibliográficas. Se numerarán según el orden de mención en el texto y deberán identificarse mediante arábigos en forma exponencial. Los trabajos originales no sobrepasarán las 20 citas; las revisiones, de 25 a 50 y las comunicaciones breves e informes de casos.

En las Referencias en caso de que las publicaciones revisadas esten online se debe proveer un enlace consistente para su localización en Internet. Actualmente, no todos los documentos tienen DOI, pero si lo tienen se debe incluir como parte de la referencias. Si no tuviese DOI, incluir la URL.

Tablas, modelos y anexos: Se presentarán en hojas aparte (no se intercalarán en el artículo) y en forma vertical numeradas consecutivamente y mencionadas en el texto. Las tablas se ajustarán al formato de la publicación se podrán modificar si presentan dificultades técnicas.

Figuras: Las fotografías, gráficos, dibujos, esquemas, mapas, salidas de computadora, otras representaciones gráficas y fórmulas no lineales, se denominarán figuras y tendrán numeración arábiga consecutiva. Se presentarán impresas en el artículo en páginas independientes y en formato digital con una resolución de 300 dpi. Todas se mencionarán en el texto. Los pies de figuras se colocarán en página aparte. El total de las figuras y tablas ascenderá a 5 para los trabajos originales y de revisión y 3 para las comunicaciones breves e informes de casos.

Abreviaturas y siglas: Las precederá su nombre completo la primera vez que aparezcan en el texto. No figurarán en títulos ni resúmenes. Se emplearán las de uso internacional.

Sistema Internacional de Unidades (SI): Todos los resultados de laboratorio clínico se informarán en unidades del SI o permitidas por este. Si se desea añadir las unidades tradicionales, se escribirán entre paréntesis. Ejemplo: glicemia: 5,55 mmol/L (100 mg/100 mL).

Para facilitar la elaboración de los originales, se orienta a los autores consultar los requisitos uniformes antes señalados disponibles en: http://www. fisterra.com/recursos_web/ mbelvancouver. htm#ilustraciones%20 (figura)

Los trabajos que no se ajusten a estas instrucciones, se devolverán a los autores. Los aceptados se procesarán según las normas establecidas por el Comité Editorial. El arbitraje se realizará por pares y a doble ciego en un período no mayor de 60 días. Los autores podrán disponer de no más de 45 días para enviar el artículo con correcciones, se aceptan hasta tres reenvíos. El Consejo de Redacción se reserva el derecho de introducir modificaciones de estilo y /o acotar los textos que lo precisen, comprometiéndose a respetar el contenido original.

El Comité Editorial de la Revista se reserva todos los derechos sobre los trabajos originales publicados en esta.

Bionatura

La **Revista Bionatura** es un medio especializado, interinstitucional e interdisciplinario, para la divulgación de desarrollos científicos y técnicos, innovaciones tecnológicas, y en general, los diversos tópicos relativos a los sectores involucrados en la biotecnología, tanto en Ecuador como en el exterior; así mismo, la revista se constituye en un mecanismo eficaz de comunicación entre los diferentes profesionales de la biotecnología.

Es una publicación sin ánimo de lucro. Los ingresos obtenidos por publicidad o servicios prestados serán destinados para su funcionamiento y desarrollo de su calidad de edición. (http://revistabionatura.com/media-kit.html)

Es una revista trimestral, especializada en temas concernientes al desarrollo teórico, aplicado y de mercado en la biotecnología.

Publica artículos originales de investigación y otros tipos de artículos científicos a consideración de su consejo editorial, previo proceso de evaluación por pares (peer review) sin tener en cuenta el país de origen.

Los idiomas de publicación son el Español e Inglés.

Esta revista utiliza Open Journal Systems, que es un gestor de revistas de acceso abierto y un software desarrollado, financiado y distribuido de forma gratuita por el proyecto Public Knowledge Project sujeto a la Licencia General Pública de GNU.

Nuestros contactos deben ser dirigidos a:
Revista Bionatura: editor@revistabionatura.com

ISSN: 1390-9347 (Versión impresa)
Formato: 21 x 29,7 cm
ISSN: 1390-9355 (Versión electrónica)
Sitio web: **http://www.revistabionatura.com**

Publicación periódica trimestral
Esta revista utiliza el sistema peer review para la evaluación de los manuscritos enviados.

Instrucciones a los autores en:
http://revistabionatura.com/instrucciones.html

Asistente de publicación / Publication assistant
Evelyn Padilla Rodriguez (sales@revistabionatura.com)

ÍNDICE / INDEX

EDITORIAL

LETTER TO EDITOR / CARTA AL EDITOR

RESEARCH / INVESTIGACIÓN

CASE REPORTS / REPORTE DE CASO

REVIEW / ARTÍCULO DE REVISIÓN

NEWS AND VIEWS / NOTICIAS Y OPINIONES

BIOETHICS /BIOÉTICA

ESCUELA DE CIENCIAS BIOLÓGICAS E INGENIERÍA

YACHAY TECH

www.yachaytech.edu.ec

YACHAY TECH
UNIVERSIDAD DE INVESTIGACIÓN DE TECNOLOGÍA EXPERIMENTAL

/YachayTech @YachayTech /YachayTech /YachayTech

EDITORIAL

The race for a coronavirus vaccine

Gerardo Ferbeyre[1], Nelson Santiago Vispo[2]

DOI. 10.21931/RB/2020.05.04.1

The international race to find a preventive vaccine and effective treatments against COVID 19 has been influenced by two fundamental factors. Firstly, by the molecular characterization of the causative virus and the pathology it produces, and secondly, by access to this information, mostly free of charge by the international scientific community causing a synergy to obtain results in such a short time.

Several vaccines preparations against Covid19 have entered Phase 3 clinical trials. Although it is uncertain the degree of protection that they will achieve, preliminary data from Phase 1 and 2 trials and studies in animals indicate that they trigger an antiviral immune response without serious side effects. The current formulations include viral vectors, RNA vaccines, inactivated viruses, and recombinant proteins particles. They all have advantages and disadvantages, but only the results of Phase 3 clinical trials will ultimately decide the best candidates for vaccination campaigns.

The tremendous impact of the SARS-CoV-2 in our society has triggered an unprecedented effort to find a vaccine to control the pandemic. Billions of dollars have already been invested in multiple vaccination schemes. According to the WHO, more than 170 vaccines were in different phases of development in August 2020. Here is a summary of the advantages and disadvantages of the front runner strategies categorized according to their delivery method (Figure 1).

Viral Vectors

Several vaccines against SARS-CoV-2 take advantage of viral vectors to express the viral proteins in the host. These vectors mimic a natural viral infection leading to the presentation of viral antigens to the immune system. Vectors based on human adenovirus were used before to make a vaccine against Ebola with excellent results and were the first to be used to make a vaccine against Coronavirus. The main disadvantage of these vectors is the presence of antibodies against adenovirus in the human population[1]. Also, after the first shot, patients will make antibodies against the viral vector making it very difficult to make a booster, second shot. The most widely used adenovirus vector comes from the strain Ad5. The CanSino/China vaccine is based on Ad5 expressing the full-length spike gene[2]. One potential problem with Ad5 is that it is a widespread strain and most people have antibodies against it[1].To circumvent this problem, the Gamaleya Research Institute in Russia designed a vaccine based on two adenoviruses. The first is Ad26, which is relatively rare, and the second is Ad5. The use of two vectors facilitates the administration of the booster shot, but still, the use of Ad5 may reduce its efficacy. This vaccine, called Sputnik V, also showed immunogenicity and short term safety in phase I/II trials published recently in the Lancet online. The University of Oxford partnered with AstraZeneca to make a vaccine using an adenovirus from chimpanzees, which is not recognized by

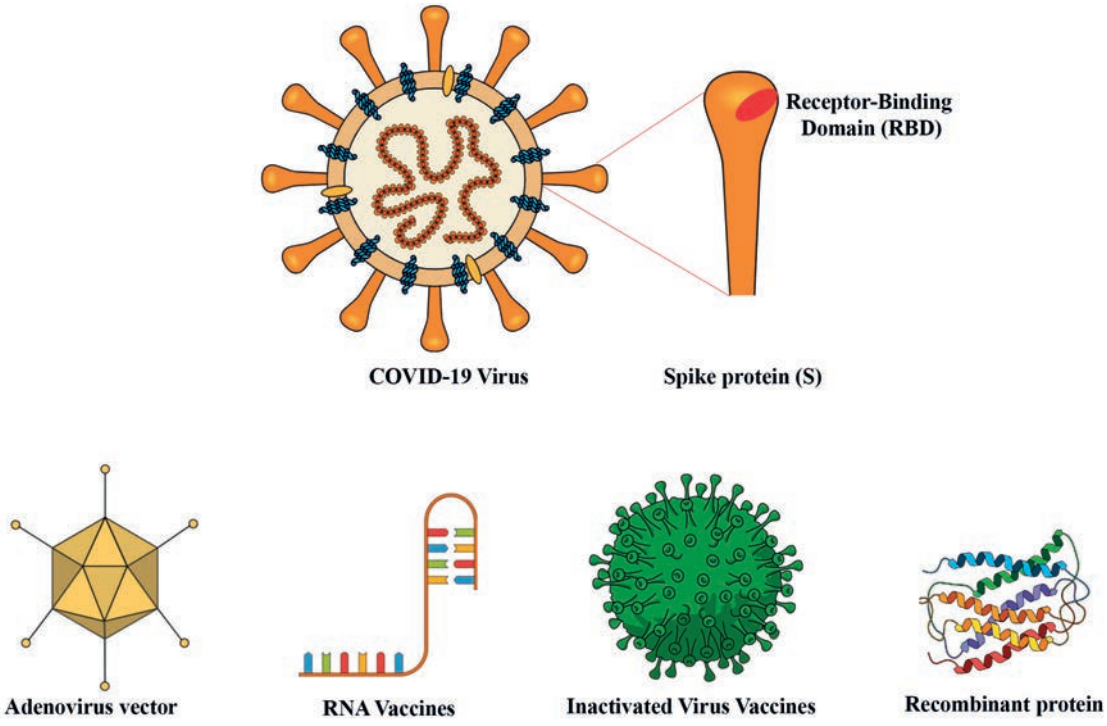

Figure 1. Different design strategies for new vaccine candidates based on nucleic acids, Adenovirus viral vectors, inactivated COVID virus or peptide sequences.

[1] Université de Montréal, Faculté de médicine, Département de biochimie et médecine moléculaire, Montréal, Canada.
[2] Universidad Yachay Tech, Imbabura, Ecuador.

Corresponding author: g.ferbeyre@umontreal.ca

human anti-adenovirus antibodies. This was the first vaccine that reported successful safety and immunogenicity data back in July 2020[3]. The main disadvantage of this vaccine is that it is based on only one adenovirus. Antibodies developed against this vector will reduce the efficacy of a second shot.

RNA Vaccines

RNA vaccines have been experimentally tested in animals with success for many years but never approved for use in humans. These vaccines express antigens in host cells transiently mimicking a natural viral infection[4,5]. The Covid19 pandemic provided an opportunity for several companies to develop this innovative vaccination technology. Moderna tested their RNA vaccine mRNA-1273 encoding for the SARS-CoV-2 spike protein in a phase 1 trial documenting a good immunogenicity and safety profiles[6]. The German company BioNtech has partnered with Pfizer to perform Phase 3 clinical trials with their mRNA vaccine BNT162b2, which also encodes for the spike protein. They reported good immunogenicity both in young and older patients, and it is the first vaccine to demonstrate that they could protect the population at higher risk[7]. CureVac is also developing mRNA vaccines[5], and they have one against Covid-19 in Phase I trials. One potential difficulty with RNA vaccines is that they require freezing at shallow temperatures to keep the RNA-lipid emulsion homogenous.

Inactivated Virus Vaccines

The anti-polio vaccine, widely used all over the world, is an inactivated virus[8]. This strategy was followed by SinoPharm in China, reporting a low rate of adverse effects and good immunogenicity with their SinoVac inactivated virus[9]. However, in a recent interview published in Science, Moncef Saloui, head of Operation Warp Speed, considered that this strategy is not a good idea[10]. Inactivated viruses may enhance the disease as reported for the inactivated respiratory syncytial virus vaccine. Also, there are safety concerns associated with producing high amounts of inactivated viruses. A single nucleotide change that arose during the preparation of the inactivated polio vaccine increased the neurovirulence of this vaccine[8].

Recombinant protein and Virus-Like Particles

Recombinant proteins are poorly immunogenic, and when given alone, they require the use of adjuvants to elicit a long-lasting immune response[11]. The formation of virus-like particles (VLP) can increase the immunogenicity of recombinant proteins. VLP has been used before to create vaccines against HPV and Hepatitis B. The HPV vaccine is prepared from purified HPV L1 protein that self assembles to form the VLP capable of triggering a protective immune response[12]. The Hepatitis B vaccine is prepared from recombinant HBsAg (Hepatitis B surface Antigen) produced in yeast[13,14]. The Quebec company Medicago has optimized the production of VLP from influenza haemagglutinin trimers in plants[15], and they are now making Coronavirus Like particles using this technology to initiate Phase 2/3 trials in October. These particles need adjuvants that Medicago will add to their formulation using technologies from GSK and Dynavax. The company Novavax, reported a very successful phase 1-2 trial with the recombinant SARS-CoV-2 vaccine. Their vaccine is based on recombinant spike glycoproteins expressed in insect cells from a baculovirus vector with matrix M1, a saponin based adjuvant[16]. One advantage of this formulation is that it can be stored at 2-8oC.

On August 18, the Cuban Ministry of Public Health announced that the Finlay Vaccine Institute in Havana began a clinical trial of a vaccine for Covid-19. The vaccine, called Soberana 1, contains a part of the spike protein, called RBD, along with the meningococcal outer membrane vesicle system and alumina; the basis of VA-MENGOC, BC meningococcal vaccine[17].This institution has widely studied the vesicle of the outer membrane of the meningococcal bacteria for many years as an enhancer of the innate immune response, and in fact, it has been studied as one of the pre-existing Cuban drugs in the fight against COVID-19 since the beginning of the pandemic[18].

Concluding remarks

Many more vaccine candidates are at the initial stages of the investigation, but we should know the real potential and challenges of making a coronavirus vaccine from the results we will get with these initial candidates. All phase II trials demonstrated the presence of neutralizing antibodies in the blood of vaccinated patients, but it is not known whether these antibodies correlate with protection. There have been several anecdotal reports that people can be reinfected with SARS-CoV-2, but the frequency of these events is still unknown. If reinfections are common, we may need to re-vaccinate the population as long as the virus remains circulating. Therefore the use of viral vectors may be compromised for frequent administration. Only one vaccine (BNT162b2) has shown good immunogenicity in old patients that are at high risk of both acquiring and dying from Covid-19. However, this only means that BioNtech/Pfizer tested this population in their Phase 2 trials, and data from other vaccine candidates are not yet available. Although adenovirus-based vaccines are now among the front runners, we cannot discard mRNA vaccines that can be used without the risk of inactivation. For similar reasons, other vaccines now in Phase 1-2 trials should be considered in the future.

All vaccines tested in Phase 1-2 trials have shown so far to have a good safety profile. If the results of Phase 3 trials that have enrolled thousands of patients confirm this trend, there is no reason to refuse vaccination for fear or political reasons. Even the low-risk population should be vaccinated to avoid passing the virus to high-risk populations. Nevertheless, the final word on both efficacy and toxicity is up to Phase 3 clinical trials that should be completed at the end of the year. It is remarkable that the Covid19 pandemic has shortened the time to develop a vaccine, which traditionally has taken as long as ten years. This is due in part to previous knowledge of another coronavirus (SARS) that identified the spike protein as a target for vaccine development[19,20]. We are lucky that we have many candidate vaccines in the pipeline. It is hard to believe that they will all fail and will not confer any degree of protection. In fact, although many vaccine trials fail, once they make it to phase 3 trials, they have an 85% chance of success. The CDC reports that the flu vaccines are regularly under 50% effective, but the influenza virus is known to mutate every season. Although there is evidence of mutations in SARS-CoV-2, we still do not know the magnitude of this phenomenon and whether these mutants are actually resistant to the previous immunity. Covid-19 has put science and health care systems to the test. It is clear that a rapid response was only possible due to advances in molecular biology and medical sciences. Further investment in basic research is the only way to be ready for future challenges.

Bibliographic references

1. Barouch, D. H. et al. International seroepidemiology of adenovirus serotypes 5, 26, 35, and 48 in pediatric and adult populations. Vaccine 29, 5203–5209 (2011).
2. Zhu, F. C. et al. Immunogenicity and safety of a recombinant adenovirus type-5-vectored COVID-19 vaccine in healthy adults aged 18 years or older: a randomised, double-blind, placebo-controlled, phase 2 trial. Lancet 396, 479–488 (2020).
3. Folegatti, P. M. et al. Safety and immunogenicity of the ChAdOx1 nCoV-19 vaccine against SARS-CoV-2: a preliminary report of a phase 1/2, single-blind, randomised controlled trial. Lancet 396, 467–478 (2020).
4. Alameh, M.-G., Weissman, D. & Pardi, N. Messenger RNA-Based Vaccines Against Infectious Diseases. in Current topics in microbiology and immunology (Curr Top Microbiol Immunol, 2020). doi:10.1007/82_2020_202.
5. Thran, M. et al. mRNA mediates passive vaccination against infectious agents, toxins, and tumors. EMBO Mol. Med. 9, 1434–1447 (2017).
6. Jackson, L. A. et al. An mRNA Vaccine against SARS-CoV-2 — Preliminary Report. N. Engl. J. Med. (2020) doi:10.1056/nejmoa2022483.
7. Walsh, E. E. et al. RNA-Based COVID-19 Vaccine BNT162b2 Selected for a Pivotal Efficacy Study. medRxiv 2020.08.17.20176651 (2020) doi:10.1101/2020.08.17.20176651.
8. Evans, D. M. A. et al. Increased neurovirulence associated with a single nucleotide change in a noncoding region of the Sabin type 3 poliovaccine genome. Nature 314, 548–550 (1985).
9. Xia, S. et al. Effect of an Inactivated Vaccine Against SARS-CoV-2 on Safety and Immunogenicity Outcomes. Jama 1–10 (2020) doi:10.1001/jama.2020.15543.
10. Cohen, J. Leader of U.S. vaccine push says he'll quit if politics trumps science. Science (80-.). (2020) doi:10.1126/science.abe6380.
11. Pérez, O. et al. Human prophylactic vaccine adjuvants and their determinant role in new vaccine formulations. Brazilian Journal of Medical and Biological Research vol. 45 681–692 (2012).
12. Garbuglia, A. R., Lapa, D., Sias, C., Capobianchi, M. R. & Del Porto, P. The Use of Both Therapeutic and Prophylactic Vaccines in the Therapy of Papillomavirus Disease. Front. Immunol. 11, 1–14 (2020).
13. Ho, J. K. T., Jeevan-Raj, B. & Netter, H. J. Hepatitis B Virus (HBV) Subviral Particles as Protective Vaccines and Vaccine Platforms. Viruses 12, 1–26 (2020).
14. Hardy, E. et al. Large-scale production of recombinant hepatitis B surface antigen from Pichia pastoris. J. Biotechnol. 77, 157–167 (2000).
15. Phane Pillet, S. et al. Immunogenicity and safety of a quadrivalent plant-derived virus like particle influenza vaccine candidate-Two randomized Phase II clinical trials in 18 to 49 and 50 years old adults. (2019) doi:10.1371/journal.pone.0216533.
16. Keech, C. et al. First-in-Human Trial of a SARS CoV 2 Recombinant Spike Protein Nanoparticle Vaccine. medRxiv 2020.08.05.20168435 (2020) doi:10.1101/2020.08.05.20168435.
17. Corum, J. & Zimmer, C. Coronavirus vaccine tracker - The New York Times. The New York Times 1–17 (2020).
18. Tahimi Arboleya. Cuban Soberana 01 vaccine | OnCubaNews English. https://oncubanews.com/ https://oncubanews.com/en/cuba/cuban-soberana-01-vaccine/ (2020).
19. Walls, A. C. et al. Structure, Function, and Antigenicity of the SARS-CoV-2 Spike Glycoprotein. Cell 181, 281-292.e6 (2020).
20. Zamora-Ledezma, C.; C., D.F.C.; Medina, E.; Sinche, F.; Santiago Vispo, N.; Dahoumane, S.A.; Alexis, F. Biomedical Science to Tackle the COVID-19 Pandemic: Current Status and Future Perspectives. Molecules 2020, 25 , 4620.

LETTER TO EDITOR / CARTA AL EDITOR

Estudios “Solidaridad” a la medida de Latinoamérica

"Solidarity" studies tailored to Latin America

Samuel Pecho-Silva[1], Ana Claudia Navarro-Solsol[2], Vicky Panduro-Correa[3], Alfonso J. Rodriguez-Morales[4], Kovy Arteaga-Livias[5]

DOI. 10.21931/RB/2020.05.04.2

Desde que los primeros casos de la infección con el coronavirus del síndrome Respiratorio agudo severo por coronavirus 2 (SARS-CoV-2) fueron descritos en Wuhan, provincia de Hubei en China, comenzó una carrera contra reloj por la búsqueda de un tratamiento efectivo, que pueda disminuir la carga de morbimortalidad ocasionada por la enfermedad por coronavirus 2019 (COVID-19). Muchos estudios fueron planteados para probar la conveniencia de múltiples drogas, tanto conocidas, como otras de reciente fabricación[1,2].

Uno de los hitos más importantes en este contexto fue el anuncio del estudio “*Solidarity*” por parte de la Organización Mundial de la Salud (OMS), el cual se llevaría a cabo en algunos países de Europa. Debido a la importancia de este estudio muchos países que no fueron inicialmente considerados, fueron sumándose en el resto del mundo. El objetivo de este estudio era valorar distintos tratamientos propuestos y utilizados contra el COVID-19. Del mismo modo la Universidad de Oxford y los sistemas de salud del Reino Unido dieron inicio al estudio RECOVERY (Randomized Evaluation of COVid-19 Therapy) también con varios tratamientos a ser probados.

Sin embargo, la OMS el 17 de junio del 2020 para su estudio “*Solidarity*” y los investigadores del estudio “*Recovery*” el 4 de junio decidieron suspender definitivamente de ambos estudios el grupo compuesto por Hidroxicloroquina[3,4]. Esto basado en los hallazgos de que el medicamento en mención no ofrecía ningún beneficio clínico y más bien presentaba un aumento de los riesgos cardiovasculares, reportados por múltiples estudios observacionales y algunos ensayos clínicos aleatorizados (ECA)[5].

A la luz de la evidencia actual (Julio 20, 2020) la decisión que han tomado los investigadores de ambos estudios al suspender el grupo de tratamiento con Hidroxicloroquina ha sido la mejor opción. Sin embargo, existen aún esquemas en evaluación por el estudio “*Solidarity*”, que deberían también valorarse bajo la evidencia disponible.

Se debe considerar que adicionalmente a la hidroxicloroquina tendría que suspenderse otra terapia también en evaluación como es el caso del lopinavir/ritonavir, que en un ensayo aleatorizado no logró demostrar beneficios clínicos cuando se le comparó con los cuidados habituales que recibieron pacientes con COVID-19[6] y que adicionalmente fue inferior a la terapia triple lopinavir/ritonavir más Interferón beta-1b más ribavirina en cuanto a la reducción del tiempo de eliminación viral, rapidez de alivio de síntomas y estancia hospitalaria[7].

Figura 1. El conocimiento del covid-19 requiere de estudios acorde a latinoamerica.

[1] Hospital Nacional Edgardo Rebagliati Martins. Maestría en Epidemiología Clínica y Bioestadística, Universidad Científica del Sur, Lima, Perú.
[2]Universidad Nacional de Ucayali. Pucallpa, Perú.
[3]Facultad de Medicina. Universidad Nacional Hermilio Valdizán. Huánuco, Perú.
[4] Maestría en Epidemiología Clínica y Bioestadística, Universidad Científica del Sur, Lima, Perú. Grupo de Investigación Salud Pública e Infección, Facultad de Ciencias de la Salud, Universidad Tecnológica de Pereira. Grupo de Investigación Biomedicina, Facultad de Medicina, Fundación Universitaria Autónoma de las Américas, Sede Pereira, Pereira, Risaralda, Colombia.
[5] Maestría en Epidemiología Clínica y Bioestadística, Universidad Científica del Sur. Facultad de Medicina. Universidad Nacional Hermilio Valdizán. Huánuco, Perú.

Corresponding author: jcastillo@yachaytech.edu.ec

Actualmente la información científica crece a una velocidad acelerada, resultado de los ECA realizados en pacientes con COVID-19, como el caso del beneficio clínico observado por el uso de dosis bajas de dexametasona gracias al estudio "*Recovery*". Es importante realizar seguimientos de los ensayos clínicos, evitar la duplicación innecesaria de esfuerzos, pero sobre todo valorar cuales son los tratamientos que deben continuarse estudiando y cuales ir desechando[8]. Al evaluar el uso de lopinavir/ritonavir se observa que existen más de 25 ensayos clínicos en curso, por lo cual invertir más esfuerzos en este fármaco que, según los primeros resultados no sería de utilidad, no parece ser correcto[9].

Además de los fármacos mencionados, existen otros medicamentos bastante interesantes y tal vez prometedores, que se vienen utilizando ampliamente en algunos de nuestros países para el manejo de pacientes con COVID-19. Uno de estos fármacos es la ivermectina, un antiparasitario de fácil disponibilidad en nuestra región sudamericana, bastante seguro y con infrecuentes efectos adversos y que ha demostrado tener cierta actividad antiviral *in vitro* frente a una gran variedad de virus, incluso frente al SARS-CoV-2. Este efecto *in vitro* ha llevado a que sea ampliamente utilizado en Perú, Bolivia y Ecuador de manera empírica para el COVID-19, basado en la plausibilidad biológica, llegando a indicarse incluso en casos leves[10].

Múltiples autores han hecho las precisiones de que las dosis de ivermectina estudiadas *in vitro*, son varias veces más altas a las que se alcanzaría con las dosis aprobadas para uso humano y no se alcanzarían incluso utilizando las máximas dosis tolerables. Lamentablemente, el Ministerio de Salud del Perú lo incluye dentro de sus esquemas terapéuticos como una alternativa de tratamiento incluso para pacientes clasificados como leves para COVID-19, a pesar de la escasa evidencia clínica actual, lo que ha llevado que muchos médicos prescriban la ivermectina en sus esquemas de tratamiento sin tener en cuenta la gran cantidad de estudios clínicos que se requieren para evaluar nuevas indicaciones de fármacos conocidos[11]. Además, este uso indiscriminado del medicamento, ha llevado a escasez del producto, ocasionando que médicos, personal de salud e incluso médicos veterinarios recomienden a la población el uso de ivermectina veterinaria, lo cual ha llevado a la aparición de complicaciones debido al uso de presentaciones parenterales[12].

A pesar de la emergencia que significa en todo el mundo la presencia de esta nueva enfermedad que ya ha causado más de medio millón de muertes, no podemos como médicos e investigadores, dejar de buscar una solución para mitigar la gravedad de esta enfermedad[13], por lo cual es urgente evaluar cuál es la efectividad de los medicamentos que vienen siendo utilizados por la población a través de los pasos correctos de la investigación científica. En Colombia, por ejemplo, se recomienda su uso únicamente dentro de estudios clínicos, debidamente aprobados y regulados[14].

Conclusiones

Por todo lo expuesto, nosotros planteamos adaptar el ensayo clínico "*Solidarity*" a Latinoamérica, proponiendo las siguientes modificaciones: 1) suspender adicionalmente a la hidroxicloroquina el grupo de tratamiento lopinavir/ritonavir. 2) agregar al grupo compuesto por lopinavir/ritonavir más interferón beta 1-b el antiviral rivabirina y 3) agregar un nuevo grupo de tratamiento conformado por la ivermectina. De esta manera, estaríamos coincidiendo plenamente con los médicos y personal de salud a nivel mundial, que requieren respuestas rápidas, urgentes y el uso de medicamentos con efectividad probada frente a la pandemia del coronavirus que es un grave problema de salud global.

Fuentes de financiamiento

El estudio fue de carácter autofinanciado.

Conflictos de interés

Ninguno declarado por los autores.

Referencias bibliográficas

1. Song Y, Zhang M, Yin L, et al. COVID-19 Treatment: Close to a Cure? - A Rapid Review of Pharmacotherapies for the Novel Coronavirus. Int J Antimicrob Agents. Published online July 4, 2020:106080. doi:10.1016/j.ijantimicag.2020.106080
2. Dhama K, Khan S, Tiwari R, et al. Coronavirus Disease 2019–COVID-19. Clin Microbiol Rev. 2020;33(4). doi:10.1128/CMR.00028-20
3. "Solidarity" clinical trial for COVID-19 treatments. Accessed June 19, 2020. https://www.who.int/emergencies/diseases/novel-coronavirus-2019/global-research-on-novel-coronavirus-2019-ncov/solidarity-clinical-trial-for-covid-19-treatments
4. No clinical benefit from use of hydroxychloroquine in hospitalised patients with COVID-19 — RECOVERY Trial. Accessed June 19, 2020. https://www.recoverytrial.net/news/statement-from-the-chief-investigators-of-the-randomised-evaluation-of-covid-19-therapy-recovery-trial-on-hydroxychloroquine-5-june-2020-no-clinical-benefit-from-use-of-hydroxychloroquine-in-hospitalised-patients-with-covid-19
5. Pecho-Silva S, Navarro-Solsol AC, Arteaga-Livias K, et al. Esperar a la evidencia antes de tratar a casos leves de COVID-19. An Fac Med. 2020;81(1):123-124. doi:10.15381/anales.v81i1.17693
6. Cao B, Wang Y, Wen D, et al. A Trial of Lopinavir–Ritonavir in Adults Hospitalized with Severe Covid-19. N Engl J Med. 2020;382(19):1787-1799. doi:10.1056/NEJMoa2001282
7. Hung IF-N, Lung K-C, Tso EY-K, et al. Triple combination of interferon beta-1b, lopinavir–ritonavir, and ribavirin in the treatment of patients admitted to hospital with COVID-19: an open-label, randomised, phase 2 trial. The Lancet. Published online May 2020:S0140673620310424. doi:10.1016/S0140-6736(20)31042-4
8. Thorlund K, Dron L, Park J, Hsu G, Forrest JI, Mills EJ. A real-time dashboard of clinical trials for COVID-19. Lancet Digit Health. 2020;2(6):e286-e287. doi:10.1016/S2589-7500(20)30086-8
9. Meini S, Pagotto A, Longo B, Vendramin I, Pecori D, Tascini C. Role of Lopinavir/Ritonavir in the Treatment of Covid-19: A Review of Current Evidence, Guideline Recommendations, and Perspectives. J Clin Med. 2020;9(7):2050. doi:10.3390/jcm9072050
10. Sharun K, Dhama K, Patel SK, et al. Ivermectin, a new candidate therapeutic against SARS-CoV-2/COVID-19. Ann Clin Microbiol Antimicrob. 2020;19(1):23. doi:10.1186/s12941-020-00368-w
11. Pecho-Silva S. COVID-19 y la "locura" por la ivermectina. Rev Peru Investig En Salud. 2020;4(3):95-96. doi:10.35839/repis.4.3.747
12. Echeverria RR, Sueyoshi JH, Caceres OJ. Ivermectina: ¿La respuesta de Latinoamerica frente al SARS-CoV-2? Kasmera. 2020;48(2):48232453. doi:10.5281/zenodo.392976
13. Soto A, Quiñones-Laveriano DM, García PJ, Gotuzzo E, Henao-Restrepo AM. Respuestas rápidas a la pandemia de COVID-19 a través de la ciencia y la colaboración global: el ensayo clínico Solidaridad. Rev Peru Med Exp Salud Pública. 2020;37(2):356-360. doi:10.17843/rpmesp.2020.372.5546
14. Trujillo CHS. Consenso colombiano de atención, diagnóstico y manejo de la infección por SARS-COV-2/COVID 19 en establecimientos de atención de la salud. Recomendaciones basadas en consenso de expertos e informadas en la evidencia. Infectio. 2020;24(3):1-153. doi:10.22354/in.v24i3.851

Recibido: 20 julio 2020
Aprobado: 21 agosto 2020

LETTER TO EDITOR / CARTA AL EDITOR

Scientifically unproven treatments for COVID-19

Martín S. Marcial-Coba

DOI. 10.21931/RB/2020.05.04.3

Detected for the first time in late December 2019, a novel severe acute respiratory syndrome coronavirus 2 (SARS-CoV-2), is the causative agent of an international outbreak of coronavirus disease 2019 (COVID-19). In late August 2020, approx. 24 000 000 cases, including 815 038 deaths, have been confirmed worldwide[1]. The WHO declared the outbreak of COVID-19 as a Public Health Emergency of International Concern, and it has been proposed that its spread may be interrupted by early detection, isolation, the implementation of a robust system to trace contacts, and a prompt treatment[2]. Nevertheless, there has not yet been any vaccine or effective treatment that has received approval[3]. Despite this, the FDA has recently issued an emergency use authorization for the investigational antiviral drug Remdesivir to treat COVID-19 in patients with severe disease[4]. Although there is still limited information regarding the safety and efficacy of this novel prodrug, it has shown potent *in vitro* antiviral activity against SARS-CoV-2 isolates, and therapeutic efficacy in animal models[5].

Furthermore, patients treated with this investigational drug, in clinical trials, have shown a significant shortening in recovery time in comparison with control subjects[6]. Besides Remdesivir, other antiviral agents, including nucleoside analogs (e.g., ribavirin and favipiravir), protease inhibitors (e.g., Lopinavir/Ritonavir), endosomal acidification inhibitors (e.g., chloroquine/hydroxychloroquine), among others, have also been investigated as drug candidates for the treatment of COVID-19. However, detrimental side effects and variable efficiency have been associated with its application on several patients[6]. Likewise, it has been reported that ivermectin, an anti-parasitic agent, inhibits the replication of SARS-CoV-2 *in vitro*, but clinical trials are still underway to test possible therapies[7]. Additionally, the potential interferon 1 (IFN1) treatment has been tested against SARS-CoV-2 both *in vitro* and *in vivo*, and combination or not with some of the above-mentioned antiviral agents, and it has been suggested that it may account for a safe and efficient treatment against COVID-19 in the early stages of infection[8].

The lack of standardized treatments has led to the emergence of unproven health advice, which doesn't rely on a scientific basis, for fictitiously treating or preventing COVID-19. In this context, the utilization of these fake therapies might be considered useless, but the consequences on human health can be innocuous to relatively harmless, or even absolutely dangerous. For instance, rumors indicating that garlic can be used as a home remedy for preventing COVID-19 have been widely spread. Even though garlic is considered a healthy food ingredient, there is no evidence suggesting that it can cure or prevent SARS-CoV-2 infection[9]. Additionally, the intake of copious amounts of garlic can result in throat inflammation and burns[10]. Other home recipes include drinking or gargling herbal tea and warm purified water, eucalyptus inhalant, essential oils, alcoholic beverages, and tinctures[11–13].

Remarkably, non-evidence-based information also proposes drinking disinfectant substances, such as colloidal silver and chlorine dioxide, not only as a home remedy but also as commercial products specifically "targeted" against SARS-CoV-2 infection[14]. It has been demonstrated that surface disinfection, and even wastewater treatment, using chlorine dioxide (ClO_2) is effective against coronaviruses, when appropriate (over 2.2 mg/L) concentrations are applied[15,16]. However, to the best of the current knowledge, there is no research describing the safety and efficiency of these products for treating any pathology. Furthermore, regulatory institutions, like the FDA,

Figure 1. The consumption of non-tested or fraudulent medicines may lead to adverse events, including serious and life-threatening harm.

Pontifical Catholic University of Ecuador.

Corresponding author: msmarcial85@gmail.com

have warned about the risks related to the intake these formulations, since they have received several reports of people suffering severe adverse effects (i.e., nausea, severe vomiting and diarrhea, acute liver failure, life-threatening low blood pressure caused by dehydration) after drinking chlorine dioxide products[17].

Conclusions

The promotion of fraudulent products, claiming to prevent or cure COVID-19, is not ethical, and its consumption may mislead a correct diagnostic, interfere with the appropriate medical treatment, and harm the patient's health. Therefore, the efforts of governmental regulatory agencies and legislation, all over the world, should be focused on preventing and sanctioning the occurrence of fraudulent products claiming to prevent or cure COVID-19. At the same time, scientists keep investigating multiple candidate therapies or vaccines against the novel coronavirus, authorities, health care professionals, and society, in general, reinforce biosecurity and social isolation strategies as preventive actions to avoid exposure to the virus. Additionally, scientific publications, mainly reviews, regarding the current state of research involving potential therapies against SARS-CoV-2, should be promoted and widely diffused, through appropriate mechanisms, to inform the majority of society.

Bibliographic references

1. World Health Organization. WHO Coronavirus Disease (COVID-19) Dashboard. WHO. [Internet]. 2020. Available from: https://covid19.who.int
2. Sohrabi C, Alsafi Z, O'Neill N, Khan M, Kerwan A, Al-Jabir A, et al. World Health Organization declares global emergency: A review of the 2019 novel coronavirus (COVID-19). Int J Surg 2020; 76: 71–76.
3. Lotfi M, Hamblin MR, Rezaei N. COVID-19: Transmission, prevention, and potential therapeutic opportunities. Clin Chim Acta 2020; 508: 254–266.
4. Food and Drug Administration. Coronavirus (COVID-19) Update: FDA Issues Emergency Use Authorization for Potential COVID-19 Treatment. FDA News Release. [Internet]. 2020. Available from: https://www.fda.gov/news-events/press-announcements/coronavirus-covid-19-update-fda-issues-emergency-use-authorization-potential-covid-19-treatment.
5. Williamson BN, Feldmann F, Schwarz B, Meade-White K, Porter DP, Schulz J et al. Clinical benefit of Remdesivir in rhesus macaques infected with SARS-CoV-2. Nature 2020. doi:10.1038/s41586-020-2423-5.
6. Wang D, Li Z, Liu Y. An overview of the safety, clinical application and antiviral research of the COVID-19 therapeutics. J Infect Public Health 2020. doi:10.1016/j.jiph.2020.07.004.
7. Caly L, Druce JD, Catton MG, Jans DA, Wagstaff KM. The FDA-approved drug ivermectin inhibits the replication of SARS-CoV-2 in vitro. Antiviral Res 2020; 178: 3–6.
8. Sallard E, Lescure FX, Yazdanpanah Y, Mentre F, Peiffer-Smadja N. Type 1 interferons as a potential treatment against COVID-19. Antiviral Res 2020; 178. doi:10.1016/j.antiviral.2020.104791.
9. Alschuler L, Weil A, Horwitz R, Stamets P, Marie A. Integrative considerations during the COVID-19 pandemic. Explore 2020.
10. Vargo RJ, Warner BM, Potluri A, Prasad JL. Garlic burn of the oral mucosa: A case report and review of self-treatment chemical burns. J Am Dent Assoc 2017; 148: 767–771.
11. Tasnim S, Hossain M, Mazumder H. Impact of rumors and misinformation on COVID-19 in Social Media. J Prev Med Public Heal 2020; 53: 171–174.
12. Love JS, Blumenberg A, Horowitz Z. The Parallel Pandemic: Medical Misinformation and COVID-19: Primum non nocere. J Gen Intern Med 2020; 35: 2435–2436.
13. Adams KK, Baker WL, Sobieraj DM. Myth Busters: Dietary Supplements and COVID-19. Ann Pharmacother 2020; 54: 820–826.
14. Larson HJ. A call to arms: helping family, friends and communities navigate the COVID-19 infodemic. Nat Rev Immunol 2020; 20: 449–450.
15. Wang XW, Li JS, Jin M, Zhen B, Kong QX, Song N et al. Study on the resistance of severe acute respiratory syndrome-associated coronavirus. J Virol Methods 2005; 126: 171–177.
16. Foladori P, Cutrupi F, Segata N, Manara S, Pinto F, Malpei F et al. SARS-CoV-2 from faeces to wastewater treatment: What do we know? A review. Sci Total Environ 2020; 743: 140444.
17. Food and Drug Administration. (COVID-19) Update: FDA Warns Seller Marketing Dangerous Chlorine Dioxide Products that Claim to Treat or Prevent COVID-19. FDA News Release. [Internet]. 2020.Available: https://www.fda.gov/news-events/press-announcements/coronavirus-covid-19-update-fda-warns-seller-marketing-dangerous-chlorine-dioxide-products-claim.

Received: 5 August 2020
Accepted: 27 August 2020

RESEARCH / INVESTIGACIÓN

Comparative Pilot Study Between a Tomographic Score and RT-PCR to Determine Diagnostic Prediction in Patients with COVID 19

Jorge Luis Vélez-Paez[1,2], Rafael Salazar-Montesdeoca[3], Juan Pablo Echeverría[3], Steffy Reinthaller-Subía[3], Sebastián Vásquez-Barzallo[3], Andrea Villegas-Polanco[3], Santiago Xavier Aguayo-Moscoso[2]

DOI. 10.21931/RB/2020.05.04.4

Abstract: In today's COVID-19 pandemic, application of RT-PCR is the diagnostic standard; however, such factors as the delayed availability of its results and the false negatives that are stemming from technical-dependent factors, the anatomical site of sampling, the time of the evolution of the symptoms and the viral load, make it possible to fail. Therefore, finding a diagnostic alternative becomes crucial, and pulmonary computed tomography (CT), using characteristic COVID-19 patterns, can fulfill this function by building tomographic scores. A prospective and observational cohort study was conducted in March-July 2020 in 30 patients with suspicion of SARS COV-2, admitted to the emergency department (ED) at Pablo Arturo Suárez Hospital. The purpose of the study was to compare the diagnostic correlation of a tomographic score and biomarkers, such as ferritin and D-dimer, with the standard RT-PCR diagnostic test. The score has a maximum value of 11 points, made up of bilateral involvement (2 points), peripheral distribution (2 points), posterior distribution (2 points), multilobar involvement (2 points), ground-glass opacification (2 points), and consolidation (1 point). The ROC curve was used to determine positive PCR predictors for COVID-19 by determining cut-off points and calculating the parameters corresponding to the diagnostic tests. At the multivariate level, the logistic regression approach was applied. The average age of the participants was 52 years, being higher in the positive ones (57 vs. 46, p: 0.045); there was no difference in gender, comorbidities, and prognostic scales. With the ROC curve, the cut-off points were established for positive or negative diagnoses: for the CT score it was 7 (AUC: 0.77 S: 93.33% and NPV: 88.89%), and it presented an adjusted OR of 53.51 (95% CI: 3-1036, p: 0.008), while for ferritin it was 883 ng/ml (AUC: 0.74 S: 93.33% and NPV: 90.91%) and had an adjusted OR of 80.18 (95% CI: 4-1475, p: 0.003), the AUC for D-dimer was not significant. The tomographic score, created for this pilot study, yielded promising results, giving an excellent diagnostic correlation with RT-PCR, being augmented with the ferritin biomarker, and reaching a predictive diagnostic level.

Key words: COVID-19, RT-PCR, ferritin, D-dimer.

Introduction

In Wuhan, a city in China's Hubei province, an outbreak of pneumonia began in late 2019, quickly associated with the coronavirus family, and later spread worldwide. The SARS-CoV-2 virus, declared a pandemic, causes severe acute respiratory syndrome and the pathology, known as COVID-19 (Coronavirus Disease 2019), called so by the World Health Organization[1].

Viral genome sequencing was available to WHO on January 12, 2020, allowing laboratories in different countries to produce specific diagnoses via RT-PCR tests, which is currently the standard diagnostic test, but which, however, has false negatives dependent on the sampling site, operator experience, and viral load, so finding a complementary or supplementary test is desirable[2].

Chest computed tomography (CT) has a high sensitivity to show patterns suggestive of COVID 19; however, this study is generally intended for hospitalized patients[3]. Different studies have been conducted worldwide to determine the diagnostic value of CT in SARS-CoV-2, finding sensitivity and specificity of 97% and 68%, respectively. Tao Ai *et al.* conducted a study involving 1014 patients, which attempted to determine the diagnostic value of chest CT scan in SARS-CoV-2 compared to RT-PCR. It was determined that the tomography has a high sensitivity for the diagnosis of COVID-19, especially in epidemic areas, and that it should be taken into account for patient screening, evaluation, and follow-up[4,5].

In this study, we aim to compare a CT score created based on the most common radiological patterns in chest CT scan with the results of the RT-PCR in patients entering the ED with a presumptive diagnosis of COVID-19, and to determine whether analytical biomarkers, such as ferritin and the D-dimer, can interact with the score and improve the diagnostic efficiency of the score.

Materials and methods

A prospective observational cohort study was conducted in 30 patients with suspicion of SARS COV-2 admitted to the Pablo Arturo Suárez Hospital ED in March-July 2020, comparing the diagnostic correlation of a tomographic score and biomarkers, such as ferritin and D-dimer, with the standard RT-PCR diagnostic test.

Tomographic score

It was built by assigning a score based on CT findings reported in the Japanese Coronavirus Disease 2019 (COVID-19) study: A Systematic Review of Imaging Findings in 919 Patients[6], The following scores were determined: bilateral involvement in 12 meta-analysis studies was for a whole of 497 patients, where 435 presented this finding, corresponding to 87.5% (2 points); peripheral distribution - 12 meta-analysis studies were evaluated for a total of 121 patients, out of which 92

[1] Critical Care Service-Pablo Arturo Suárez Hospital, Ecuador.
[2] Medical Science School-Central University of Ecuador.
[3] Emergency Department-Pablo Arturo Suárez Hospital., Ecuador.

Corresponding author: jlvelez@uce.edu.ec

presented this type of lesion, corresponding to 76% (2 points); posterior involvement - 1 meta-analysis study is for 51 patients, 41 of whom had these findings, corresponding to 80.4% (2 points); a multilobar involvement - with 5 meta-analysis studies of 137 patients, of whom 108 had these findings, corresponding to 78.8% (2 points); ground glass opacities were evaluated in 22 meta-analysis studies with 393 patients, out of whom 346 had this, corresponding to 88%; the consolidation - in 10 meta-analysis studies, where 204 patients were assessed, 65 had this complication, corresponding to 31.8% (1 point).

PATTERN	SCORE
Bilateral involvement	2
Peripheral distribution	2
Posterior distribution	2
Multilobar involvement	2
Ground glass opacification	2
Consolidation	1

Inclusion and exclusion criteria

Within the inclusion criteria are patients over 18 suspected of having SARS COV-2.

Patients under the age of 18 and over 85, and those who are carriers of primary immune pathologies, HIV-like infectious and neoplastic pathologies, were excluded from the study.

Statistical processing

The analyses were performed using the RStudio and IBM SPSS version 25 statistical packages, using descriptive statistics, using tables and charts, representing absolute and relative values of qualitative variables, and measures of central tendency and scatter for quantitative variables.

The assumption of normality of quantitative variables was verified using the Shapiro-Wilk test, where the t-test was used for quantitative variables with a normal distribution (age), and the Mann Whitney test for non-normal quantitative variables, such as SOFA (it is a daily measurement system of multiple organ failure: respiratory, cardiovascular, coagulation, hepatic, renal, neurological; it is a prognostic indicator), APACHE II (it estimates the probability of death of a patient according to the values of a series of physiological variables, plus age and previous health status), CT score, ferritin, and D-dimer.

The Chi-square test or Fisher's exact test was used for qualitative variables.

To compare the CT score, ferritin, and D-dimer per PCR result for COVID 19, the graphic function of the RStudio program and the gstatsplot, and ggbetweenstats packages were used.

The Receiver Operating Characteristic (ROC) curve was applied to determine positive PCR prognosticators for COVID-19 by determining cut-off points and calculating the parameters for diagnostic tests: sensitivity, specificity, positive predictive value, negative predictive value, accuracy, and odds ratio. At a multivariant level, the logistic regression approach was used, determining predictors and defining the predictive equation. Statistical significance was set for p-value <0.05.

Ethical Considerations

Researchers have respected the bioethical principles of human research. The data obtained is secondary, obtained from the blogs and medical records; the identification of the patients will not be disclosed and has been recorded to avoid recognition. We also have permission to publish this work from the authorities and the Department of Teaching and Research.

Results

30 patients were tested with PCR for COVID-19, of which 15 PCR test results were positive and 15 negatives. The average age of patients stood at 52 years; significant differences were observed between the PCR results with p-value 0.045,

Clinical Characteristics	General	PCR		p-value
		Positive	Negative	
Age (Average (SD))[1/]	52 (14)	57 (14)	46 (12)	0,045*
Sex (n (%))[2/]				
Masculine	24 (80,00)	14 (58,33)	10 (41,67)	0,068
Feminine	6 (20,00)	1 (16,67)	5 (83,33)	
Comorbidities (n (%))[2/]				
DM	7 (23,33)	4 (57,14)	3 (42,86)	1,000
AH	5 (16,67)	2 (40,00)	3 (60,00)	1,000
Obesity	4 (13,33)	2 (50,00)	2 (50,00)	1,000
COPD	3 (10,00)	2 (66,67)	1 (33,33)	1,000
Apache II (Mean (SD))[3/]	12,77 (6,26)	14,93 (6,02)	10,60 (5,90)	0,053
Sofa (Mean (SD))[3/]	3,87 (2,98)	4,47 (3,04)	3,27 (2,89)	0,186
Mortality (n (%))	5 (16,67)	2 (13,33)	3 (20,00)	1,000
Nota: SD=Standard Deviation; * differences in means; 1/ based on t-test, 2/ based on Chi-square or Fisher's exact test, 3/ based on Mann Whitney test				
Source: own work				

Table 1. Clinical Characteristics of Patients who were Tested with PCR for COVID-19.

with the average age of 57 years for positive PCR vs. 46 years for negative PCR results. The sample was made up of 80% male majority. Among the most frequent comorbidities was diabetes mellitus - 23.33%, Arterial Hypertension (AH) - 16.67%, obesity - 13.33%, COPD - 10%, among others. Parameters associated with mortality risk showed an average of 12.77 for APACHE II and 3.87 for SOFA, the mortality rate was 16.67% with no differences observed in these parameters relative to the PCR outcome (see table 1).

When comparing CT score between patients with positive or negative results, significant differences with p-value 0.009 were observed, where the mean was 5.13 (95% CI 3.83-7.07) for negative PCR vs. 8.33 (95% CI 7.3-9.17) for positive PCR; for this test, the effect size r was observed (0,48), which indicates that the relationship between CT score and PCR result for COVID-19 is medium. (see Figure 1)

For ferritin, when comparing patients with positive and negative PCR, significant differences were observed with a p-value of 0.022, where the means were 839.31 ng/ml (95% CI 542.64-1201.48) for negative PCR vs. 1327.25 ng/ml (CI 95% 1198.52-1491.76) for positive PCR, for this test the effect size r (0.42) was observed, indicating that the relationship between ferritin and the PCR result for COVID-19 is medium. (see Figure 2)

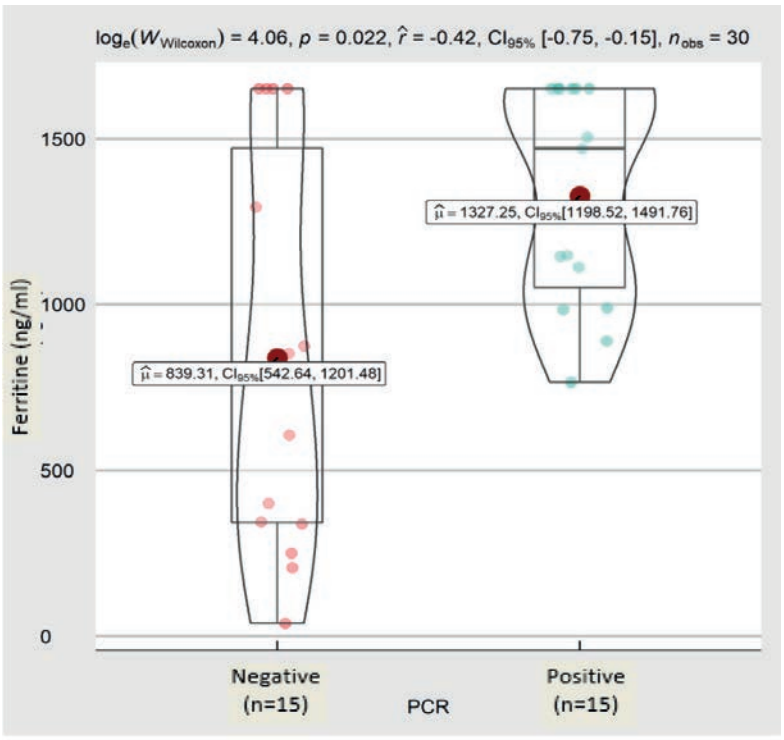

Figure 1. CT score comparison with PCR results for COVID-19.

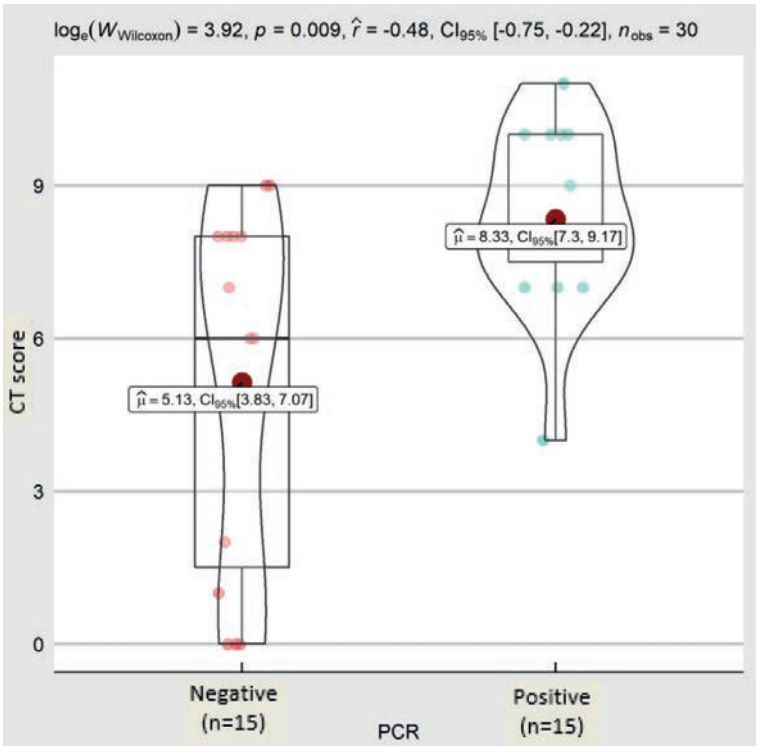

Figure 2. Comparison of ferritin by PCR results for COVID-19.

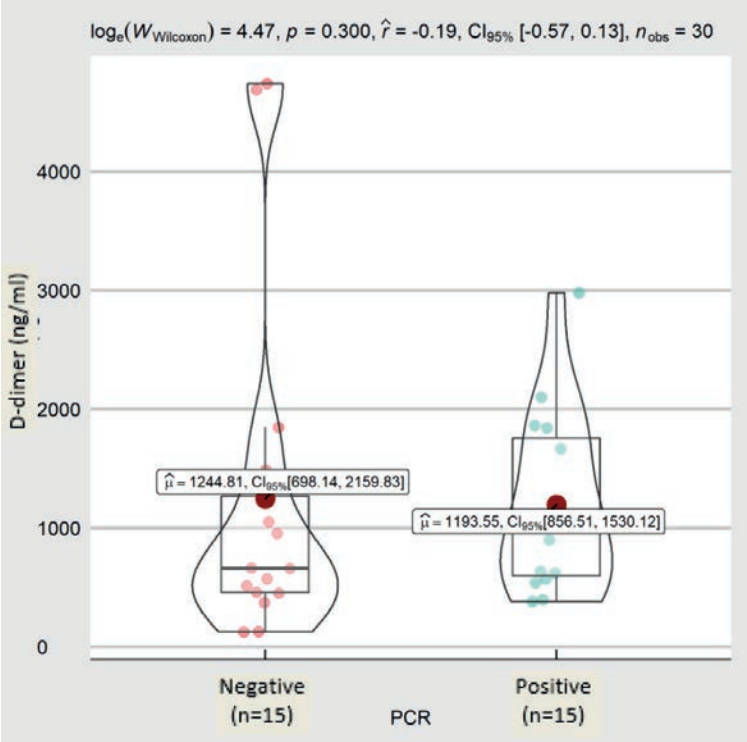

Figure 3. D-dimer comparison by PCR results for COVID-19.

Comparing the D-dimer between patients with positive and negative PCR did not find any significant differences; however, their averages were 1244.81ng/ml (CI 95% 698.14-2159.83) for negative PCR and 1193.55 ng/ml (CI 95% 856.51-1530.12) for positive PCR. (See Figure 3)

The CT score, ferritin, and D-dimer variables were considered to determine if they could be positive PCR predictors for COVID-19.

Targeted evaluation of the area below the ROC curve to estimate positive PCR results for COVID-19 was for a CT score of 0.776 (0.613-0.938) and ferritin 0.742 (0.551-0.933). These areas showed confidence intervals that do not include the value 0.5, which proved to be significant to predict positive PCR for COVID-19, whereas the D-dimer, whose area under the curve was 0,613 (0,402-0,825), was not significant. (see Figure 4) Based on the ROC curve, the cut-off points for CT scores were established at seven (7), while for ferritin at 883 ng/ml.

For the CT score cut-off point, PCR was considered as positive if it was ≥ 7; otherwise, PCR was considered negative, resulting in a sensitivity of 93.33%, specificity 53.33%, PPV 66.67% (positive predictive value: likelihood of disease if a positive test result is obtained), NPV 88.89%(negative predictive value: the probability that a person with a negative test result is healthy), accuracy 73.33%. Besides, an odds ratio suggests that patients with CT score ≥ 7 are 16 times more likely to have a positive PCR result for COVID-19 than those reporting CT score <7.

On the other hand, the ferritin cut-off point was considered as PCR positive if this was ≥ 883; otherwise, it was deemed to be negative. Sensitivity obtained was 93.33%, specificity 66.67%, PPV 73.68%, NPV 90.91%, accuracy 80%, the odds ratio at cut-off point was significant. This indicates that patients with ferritin ≥ 883 ng/ml are 28 times more likely to have a positive PCR result for COVID-19 as compared to patients with ferritin <883 ng/ml.

Through logistic regression, the multivariant relationship and predictive model for PCR positive COVID-19 were determined, based on the CT score cut-off points and ferritin.

The results showed that the CT score cut-off points p-value 0,008 and ferritin p-value 0,003 were positive PCR predictors for COVID-19, where CT score values ≥7 and ferritin ≥ 883 were 53,51 and 80,18 times more likely to present positive PCR for COVID-19.

The logistic regression equation based on the β i coefficients and the cut-off points of the CT score and ferritin, as well as the constant of the model, allowed to predict the group membership, i.e. positive or negative PCR for COVID-19, where the concordance of results was obtained in 90%.

The mathematical model would be the following:

$$P(X = PCR+) = \frac{1}{1 + e^{-(-5{,}786 + 3{,}980x_1 + 4{,}384x_2)}}$$

Classifying as:

$$\{PCR\ positive\ if\ \ P(X = PCR+) \geq 0{,}5\ PCR\ negative\ if\ P(X = PCR+) < 0{,}5$$

Where:

$$\{x_1: CT\ Score, range\ (0\ if < 7;\ \ 1\ if\ \geq 7)\ x_2: Ferritin, range\ (0\ if < 883\frac{ng}{ml};\ 1 \geq 883\frac{ng}{ml})$$

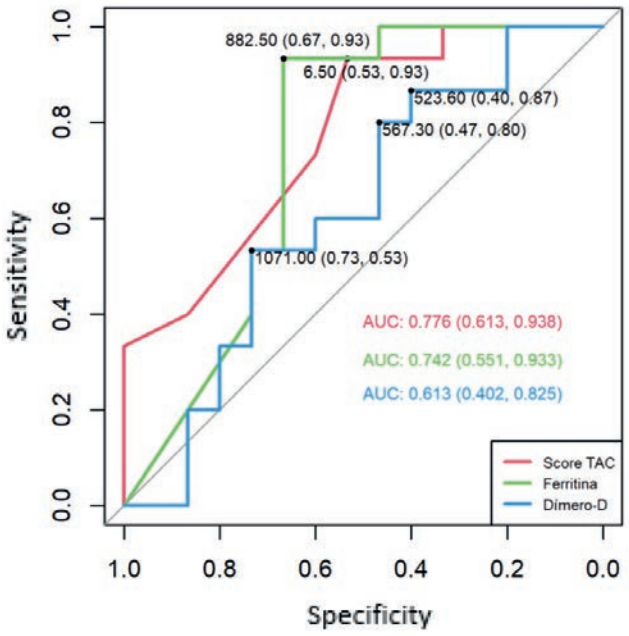

Figure 4. ROC curve to predict positive PCR for COVID-19, based on CAT score, ferritin, and D-dimer.

Table 2. Diagnostic test parameters for positive PCR results for COVID-19, based on CT score cut-off points and ferritin.

Parameters	CT Score	Ferritin
Cut-off points	7	883
Sensitivity	93,33%	93,33%
Specificity	53,33%	66,67%
PPV	66,67%	73,68%
NPV	88,89%	90,91%
Accuracy	73,33%	80,00%
OR (CI-95%)	16* (1,66 - 154,60)	28* (2,82 - 277,96)
Note: PPV= positive predictive value, NPV= negative predictive value; * Odds Ratio (OR) significant risk factor for PCR+		

Variables	B	Wald	p-value	OR	CI-OR 95%		% of correct classification
					Lim inf	Lim sup	
CT Score ≥7	3,980	6,93	0,008*	53,51**	3	1036	90,00
Ferritin ≥ 883 ng/ml	4,384	8,71	0,003*	80,18**	4	1475	
Constant	-5,786	9,89	0,002*				
Note: Based on chi-square test; * significant variable p-value<0,05, ** OR=significant odds ratio Li >1; based on logical regression							

Table 3. Logistical regression to predict positive PCR for COVID-19.

Parameters	Classification Regression model P (X=PCR+)
Sensitivity	86,67%
Specificity	93,33%
PPV	92,86%
NPV	87,50%
Accuracy	90,00%
Note: PPV= positive predictive value, NPV= negative predictive value;	

Table 4. Diagnostic test parameters for positive PCR COVID-19 based on the logistic regression model.

The prognosis or classification, based on the regression model, resulted in a sensitivity of 86.67%, specificity 93.33%, PPV 92.86%, NPV 87.50%, accuracy 90%.

Discussion

In the current SARS COV 2 pandemic, around 80% of infected patients have mild disease symptoms and recover after 2-3 weeks. In severe patients, lung impact develops between days 7 and 10; the severity of the disease is mainly due to cytokine release inflammatory syndrome ('cytokine storm'). This is where typical tomographic findings, established as patterns for diagnosing COVID 19 disease, are evidenced. Once infected patients progress to acute respiratory distress syndrome (ARDS), more than 10% of them worsen within a short period and die of multiple organ failure.

Severe cases of COVID-19 are presented primarily in males over the age of 50. In our study, we replicate this data with a predominance of the male sex and an average age of 52. The comorbid factors associated with severe disease are arterial hypertension, diabetes mellitus, pneumopathy, and obesity - factors found in the population studied in our series[7].

The gold standard diagnostic test for COVID-19 is the RT-PCR, which was taken as a comparator of the CT image score, built for the study. Typical image characteristics include interstitial pattern, extensive consolidation with multifocal ground glass images, bilateral involvement, peripheral or subpleural distribution, rear, and lower lobe predilection, and multiple lesions. Based on these patterns, we set a score for the diagnostic imaging of this disease[8].

As for imaging scales, the CO-RADS scale, used by medical imaging specialists, assesses COVID-19 pulmonary involvement with the help of chest CT and provides good predictive performance in patients with moderate to severe symptoms. But as clinicians, we have found it imperative to present a different way to score image findings simply, in real-time and without the strict necessity for a physician specializing in imaging; the tool, which allows to have diagnostic certainty and to make clinical-therapeutic decisions and the one that has results adequately correlated with the RT-PCR test, providing an additional instrument for the clinical physician in charge of the first-line care in the current pandemic[9].

The CT score cut-off point was determined to be ≥7, with an odds ratio of 16, i.e., patients who achieve this score are 16 times more likely to have a positive PCR for COVID-19 than those with lower values, with high sensitivity values (93.3%) and negative predictive value (88.89%). This data correlates with international studies such as Ai *et al.* and Fang *et al.*, which demonstrated in 1014 and 51 patients respectively, the usefulness of CT concerning RT-PCR with high sensitivities of 97% and 98%[10,11].

There are patients with typical COVID 19 tomographic patterns, with negative PCR tests; if the clinic is reliable, this could correspond to false-negative results, and it could be explained by the variety of types of tests on the market available for the detection of this virus, the variation in the detection rate by different manufacturers, and a low viral load on the patient. Considering that in most cases, patients go to ED when the disease presents symptoms of pulmonary involvement; this happens when viral load is sometimes undetectable in the upper respiratory tract. Another inconvenience could be an inadequate clinical sample, since, as well as many other tests; this one is also centered around the dependent operator framework.

In this context, obtaining a CT scan will help us support early diagnosis and faster patient classification, even if the RT-PCR test is not reported or available or when the PCR result is negative and clinical suspicion is high[12].

As for diagnostic biomarkers and laboratory forecasts, ferritin is the predictor of the hyperinflammatory state given by the cytokine storm, and the D-dimer is the marker for identifying the procoagulant state of the blood system in infected patients.

In our research, the cut-off point found for ferritin was ≥ 883 ng/ml, the odds ratio being at 28 at the significant cut-off point, which implies that patients with these ferritin values are 28 times more likely to have a positive PCR for COVID-19 as compared to the ones with ferritin <883 ng/ml; high sensitivity (93.33%) and negative predictive value (90.91%).

In two studies conducted in China by Wang et al. and Sun *et al.*[13,14], severe patients showed serum ferritin values > 800 µg/L, reporting significant differences between mild and too severe groups. Besides, high levels of D-dimer were found in severe and too severe patients. To sum up, these studies showed a correlation between gravity and high inflammatory biomarkers.

Our data reveal correspondence comparing them to the studies mentioned above regarding ferritin cutting values, with a very similar cut-off point. However, concerning the D-dimer, they differ with the other findings since we did not find any statistical association between the RT-PCR and the D-dimer.

Finally, employing logistic regression, the multivariate relationship was determined with the cut-off points of the CT score (≥7) and ferritin (≥ 883 ng/ml), which determine the OR of 53.51 and 80.18 respectively, the high value of OR can be explained by the small sample. In the predictive model, generated by the logistic regression equation, the model-based classification yielded a sensitivity of 86.67%, specificity 93.33%, PPV 92.86%, NPV 87.50%, accuracy 90%, i.e., the two tests give a high diagnostic probability of COVID-19, turning the finding into a tool of high diagnostic value.

The limitation of our work, being a pilot study, was the size of the sample, but this analysis may be the starting point for new studies on this subject with a broader sample that could analyze other variables and healthy outcomes, such as mortality.

Conclusions

The tomographic score, created for this pilot study, yielded promising results; it provided an excellent diagnostic correlation with the RT-PCR with a cut-off point greater than or equal to 7 and, being augmented with the ferritin biomarker with values equal to or greater than 883 ng/ml, and thus reached a predictive diagnostic level.

It becomes mandatory to expand the sample of this study to verify if the results are replicated. For the time being, we will add the score to our hospital's diagnostic arsenal to facilitate the diagnosis and treatment of this disease.

Bibliographic references

1. Mcintosh, K. UpToDate. [Online]. Available from: https://www.uptodate.com/contents/coronavirus-disease-2019-covid-19-clinical-features?search=covid&source=search_result&selectedTitle=1~150&usage_type=default&display_rank=1 [Accessed 17 August 2020].

2. Salehi, S, Abedi, A, Sudheer, B, Gholamrezanezhad, A. Coronavirus Disease 2019 (COVID-19): A Systematic Review of Imaging Findings in 919 Patients Read More: https://wwwajronlineorg/doi/102214/AJR2023034. American Journal of Roentgenology. [Online] 2020;215(1): 87-93. Available from: https://doi.org/10.2214/ajr.20.23034 [Accessed 17 August 2020].
3. Farias Lucas de Pádua Gomes de, Strabelli Daniel Giunchetti, Fonseca Eduardo Kaiser Ururahy Nunes, Loureiro Bruna Melo Coelho, Nomura Cesar Higa, Sawamura Márcio Valente Yamada. Thoracic tomographic manifestations in symptomatic respiratory patients with COVID-19. Radiol Bras [Internet]. 2020 Aug [cited 2020 Aug 17] ; 53(4): 255-261. Available from: http://www.scielo.br/scielo.php?script=sci_arttext&pid=S0100-39842020000400255&lng=en. Epub July 15, 2020. https://doi.org/10.1590/0100-3984.2020.0030.
4. Yang, Z, Tao, A, Hou, H, Zhan, C.H, Chen, C.H. Correlation of Chest CT an RT-PCR Testing for Coronavirus Disease 2019 (COVID-19) in China: A Report of 1014 Cases. Radiology. 2020;296(2): 32-40. Available from: https://doi.org/10.1148/radiol.2020200642 [Accessed 16 August 2020].
5. Xie, X, Zhong, Z, Zhao, W, Zheng, C.H, Wang, F. Chest CT for Typical Coronavirus Disease 2019 (COVID-19) Pneumonia: Relationship to Negative RT-PCR Testing. Radiology. [Online] 2020;296(2): 41-45. Available from: https://doi.org/10.1148/radiol.2020200343 [Accessed 17 August 2020].
6. Sana Salehi, Aidin Abedi, Sudheer Balakrishnan, and Ali Gholamrezanezhad. Coronavirus Disease 2019 (COVID-19): A Systematic Review of Imaging Findings in 919 Patients. American Journal of Roentgenology 2020 215:1, 87-93. Available from: https://www.ajronline.org/doi/full/10.2214/AJR.20.23034
7. Chen G, Wu D, Guo W, Cao Y, Huang D, Wang H, et al. Clinical and immunological features of severe and moderate coronavirus disease 2019. J Clin Invest. 1 de mayo de 2020;130(5):2620-9.
8. Zu ZY, Jiang MD, Xu PP, Chen W, Ni QQ, Lu GM, et al. Coronavirus Disease 2019 (COVID-19): A Perspective from China. Radiology. 2020;296(2):E15-25.
9. Prokop M, van Everdingen W, van Rees Vellinga T, Quarles van Ufford H, Stöger L, Beenen L, et al. CO-RADS: A Categorical CT Assessment Scheme for Patients Suspected of Having COVID-19-Definition and Evaluation. Radiology. 2020;296(2):E97-104.
10. Ai T, Yang Z, Hou H, Zhan C, Chen C, Lv W, et al. Correlation of Chest CT and RT-PCR Testing for Coronavirus Disease 2019 (COVID-19) in China: A Report of 1014 Cases. Radiology. 2020;296(2):E32-40.
11. 10. Fang Y, Zhang H, Xie J, Lin M, Ying L, Pang P, et al. Sensitivity of Chest CT for COVID-19: Comparison to RT-PCR. Radiology. 19 de febrero de 2020;296(2):E115-7.
12. Rubin GD, Ryerson CJ, Haramati LB, Sverzellati N, Kanne JP, Raoof S, et al. The Role of Chest Imaging in Patient Management during the COVID-19 Pandemic: A Multinational Consensus Statement from the Fleischner Society. Radiology. 7 de abril de 2020;296(1):172-80.
13. Wang F, Hou H, Luo Y, Tang G, Wu S, Huang M, et al. The laboratory tests and host immunity of COVID-19 patients with different severity of illness. JCI Insight. 21 de 2020;5(10).
14. Sun Y, Dong Y, Wang L, Xie H, Li B, Chang C, et al. Characteristics and prognostic factors of disease severity in patients with COVID-19: The Beijing experience. J Autoimmun. 1 de agosto de 2020;112:102473.

Received: 20 August 2020
Accepted: 28 September 2020

RESEARCH / INVESTIGACIÓN

Treatment of SARS-CoV-2 (COVID-19) cases by the oral administration of montelukast tablets

Ameneh Norouzi
DOI. 10.21931/RB/2020.05.04.5

Abstract: According to the hypothesis, montelukast may have therapeutic action against severe acute respiratory syndrome (SARS) occurred by coronavirus 2 (CoV-19). The research was aimed to evaluate the therapeutic effects of montelukast tablet on coronavirus infectious disease (COVID-19) patients. A total of 20 COVID-19 confirmed patients were included in this study. The presence of COVID-19 infections in all patients was confirmed using real-time polymerase chain reaction (PCR) and computerized tomography (CT) scan. Confirmed cases were treated with oral administration of montelukast (10 mg) tablet for 10 days. The study population was included 18 to 82 years old patients (10 males and 10 females). The mean age of studied men and women individuals were 44.7±17 and 41±17.45 years, respectively. Frequency of respiratory distress, cough, abdominal cramps/diarrhea, fever, and odor disorder clinical signs amongst the examined patients were 85%, 90%, 20%, 70%, and 65%, respectively. Our findings revealed that all patients who were received 10 days of oral administration of montelukast tablets (10 mg) were recovered from the COVID-19 disease. Additionally, all of the clinical signs of COVID-19 patients, including respiratory distress, cough, and odor disorder, were gradually disappeared. Our findings revealed that widespread oral administration of montelukast tablets (10 mg) is a potential treatment for COVID-19 disease. However, several double-blind and multifactorial clinical trials should perform to determine the other clinical aspects of the treatment of COVID-19 patients by oral administration of montelukast.

Key words: SARS-COVID-19, Treatment, Montelukast.

Introduction

Infectious diseases remain a threatening issue for human health despite the high development of medical sciences[1,18,30,35,36]. Severe Acute Respiratory Syndrome (SARS)-Corona Virus Diseases-19 (CoVID-19) (SARS-CoVID-19) which also known as SARS-CoV-2, is the essential threatening disease in 2019 and 2020 years all around the world[57].

Coronaviruses (CoVs) belong to the family of Coronaviridae, the order Nidovirales, and the genus Coronavirus, with a positive sense, single-stranded RNA genome. Human coronaviruses (HCoVs), are documented as respiratory pathogens related to respiratory and intestinal infections with various severities from the usual cold to pneumonia and bronchiolitis to death. COVID-19, as a deadly disease is occurred owing to the activity of SARS-CoV-2, accounted as a global public health concern[31,43].

Rendering the World Health Organization's (WHO)' report, the epidemic of COVID-19 so far registered 26,763,217 cases and 876,616 deaths worldwide (9) WHO showed that the highest numbers of COVID-19 new cases had been reported from Iraq, Iran, Morocco, Saudi Arabia, Kuwait[34]. In Iran, several cumulative cases and also cumulative death of Covid-19 were 384,666 and 22,154, respectively[34].

Despite the worldwide spread, there were no definitive treatments for the COVID-19[38]. Thus, there was a large demand to introduce a novel therapeutic option for the treatment of the cases of COVID-19.

It has been theorized that Montelukast, an antagonist of the cysteinyl leukotriene (cysLT) receptor with potential antioxidant and anti-inflammatory effects, may reduce the development of the COVID-19 infection[16]. Montelukast has an effect on events developing with Angiotensin-converting enzyme (ACE) receptors, and also has an anti-inflammatory effect with bradykinin and leukotriene antagonism; Because of COVID-19 has entry into the cell through ACE receptors and caused mortality due to excessive inflammatory processes, it was thought that montelukast might have a therapeutic effect on the progression of COVID-19 infection[20].

According to the high importance of COVID-19, the absence of effective treatment, and the probable effect of the montelukast, the present research was done to assess the effects of oral administration of montelukast as a therapeutic agent for the treatment of SARS-CoV-2 patients.

Materials and methods

Ethics and consents

The present survey was conducted on volunteer patients who suffered from SARS-COVID-19 disease. Informed consent was obtained from the patients or their parents involved in this survey. Additionally, all the identity and personal information of the patients participating in this study remained secret. Ethical principles of patient care and sampling were also observed. Serious efforts were made to reduce patients' pain and anxiety during the research process.

Study population

A total of 20 male and female ≥18 years old patients with clinical signs of COVID-19 disease were confirmed by the computerized tomography (CT)-scan and Real-Time Polymerase Chain Reaction (PCR) were included in this study.

Inclusion and exclusion criteria

All patients confirmed to be infected with the COVID-19 virus through the nucleic acid detection by the Real-Time PCR assay, and positive outcomes of chest CT-scan were included in the study. Additionally, clinical signs of the disease were considered. If both chest CT-scan and Real-Time PCR test showed negative findings of COVID-19 disease for any patients,

Master of Cellular and Molecular Biology, Division of Biochemistry, Iran.

Corresponding author: Amen.norouzi@yahoo.com.

they were excluded from the study. Additionally, patients who died during the study and also those who used from other therapeutic options against SARS-COVID-19 were excluded from the research. Furthermore, patients with progressive and autoimmune diseases were excluded from the study.

COVID-19 virus detection and diseases confirmation in the study population

Patients were confirmed by Reverse transcription-Real-Time PCR (RT-Real-Time PCR) using throat swab specimens from the upper respiratory tract or clinically diagnosed based on lung imaging features, specially Chest CT scan ground glass pathognomonic features consistent with coronavirus pneumonia, depending on the physician's orders.

The presence of the COVID-19 virus was examined using the RT-Real-Time PCR method. For this purpose, the method described previously was used[47]. Throat swab samples were used for RNA extraction. Lesser than 37 cycle threshold values (Ct-value) were considered as a positive, while those of higher than 40 were recognized as negative. Additionally, a chest CT scan was performed, and its results were analyzed according to lung involvements, density (ground-glass and consolidations), and central to peripheral distribution[52].

Treatment protocol

Confirmed patients with CT-scan and RT-Real-Time PCR were subjected to oral administration of montelukast tablets (10 mg, Dr. Abidi Co, Tehran, Iran) for about 10 days. Patients were used two montelukast tablets on the first day of the experiment and then only one table from days 2 to 10 of the experiment. Routine cares of COVID-19 were addressed for all patients[24,44].

Statistical analysis

All data collected from the study were transferred to Microsoft Excel software (Microsoft Corp., Redmond, WA, USA). Statistical analyses were performed using SPSS 21.0 (Statistical Package for the Social Sciences) software (SPSS Inc., Chicago, IL, USA). Variables were defined as frequencies and percentages. A comparison of the differences was conducted using the Chi-square test. *P*-value<0.05 was considered statistically significant.

Results

COVID-19 identification

The present survey was performed to assess the therapeutic effects of oral administration of montelukast tablet (10 mg) in patients suffered from COVID-19 disease. Figure 1 represents the pattern of lung CT-scan in some of the examined COVID-19 patients. As shown, multi-lobar and bilateral groundβ glass opacities are seen in both lungs, mostly in mid to lower lungs, although all lobes are affected, with a peripheral subpleural distribution. Additionally, the presence of the COVID-19 virus was identified by the Real-Time PCR method in all examined patients.

Study population

Table 1 represents the characters of the study population of COVID-19 patients. The study population consisted of 18 to 82 years old male and female patients. The total distribution of male and female individuals amongst all 20 examined COVID-19 patients were 50% (10/20) and 50% (10/20),

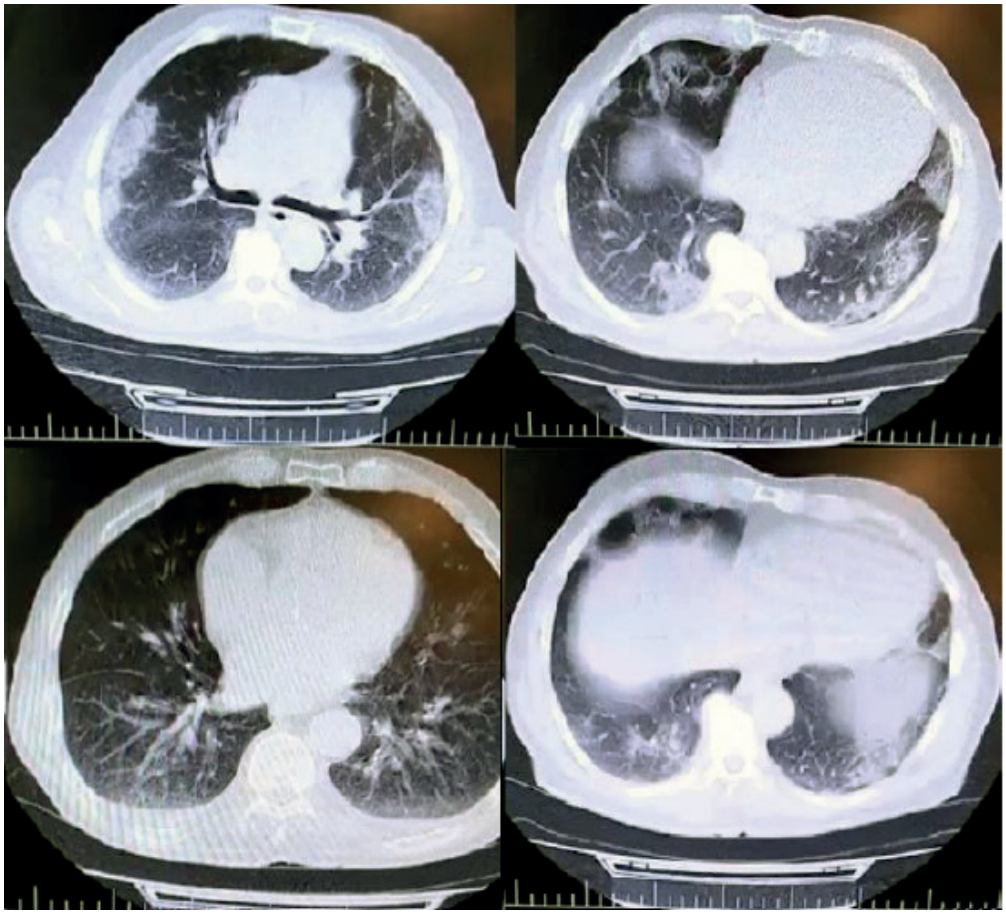

Figure 1. The pattern of lung CT-scan in some of the examined COVID-19 patients.

respectively. The mean age of male and female patients was 44.7±17 and 41±17.45 years, respectively. Total distribution of respiratory distress, cough, abdominal cramps/diarrhea, fever, and odor disorders amongst all examined patients were 85%, 90%, 20%, 70%, and 65%, respectively. However, there were no statistically significant differences between and within population-based data presented in this study (P <0.05). No deaths and also progressive and autoimmune diseases were found in the study population. Additionally, none of the patients were received any other anti-viral or other therapeutic options.

Patients	Number of examined	Age (year)				Clinical signs (%)					P-value
		Mean	SD	Min	Max	Respiratory distress	Cough	Abdominal cramps/diarrhea	Fever	Odor disorder	
Male	10	44.7	17	19	80	9 (45)	9 (45)	2 (10)	7 (35)	6 (30)	ns
Female	10	41	17.45	18	82	8 (40)	9 (45)	2 (10)	7 (35)	7 (35)	ns
Total	20	42.85	17.80	18	82	17 (85)	18 (90)	4 (20)	14 (70)	13(65)	ns

Table 1. Characters of the study population in the patients suffered from COVID-19.

Treatment outcomes

Our findings revealed that all of the COVID-19 patients who were treated with 10 days of oral administration of montelukast tablets (10 mg) were recovered from the COVID-19 disease. Findings revealed that all of the clinical signs of the COVID-19, including respiratory distress, cough, and odor disorder, were gradually disappeared. Respiratory distress and cough were the first clinical signs that disappeared after the montelukast administration. However, cramps and diarrhea continued for about a few days after the study experiment. Patients' odor appeared one to two days after the end of the study experiment. There were no detectable side effects after 10 days of oral administration of montelukast tablets in examined patients.

Discussion

From the first days of the occurrence of COVID-19 disease, diverse kinds of therapeutic options have been presented to patients[38]. However, none of them weren't introduced as definitive and affected treatment[46]. Otherwise, no specific anti-viral option has been established as an effective agent against COVID-19 virus[26]. Despite the significant anti-viral effects of remdesivir[50], teicoplanin[55], nelfinavir[53], colistin, valrubicin, icatibant, bepotastine, epirubicin, epoprostenol, vapreotide, aprepitant, caspofungin, and perphenazine[28], rupintrivir and lopinavir[42], ebselen[23], beclabuvir and saquinavir[41], indinavir, cobicistat, caspofungin acetate, and atazanavir[15], carfilzomib, eravacycline, valrubicin, elbasvir, and streptomycin[48], thymopentin, carfilzomib, and saquinavir[49], ledipasvir and velpatasvir[14], atazanavir, efavirenz, ritonavir, and dolutegravir[5], mycophenolic acid, grazoprevir, telaprevir, and boceprevir[19], formoterol and chloroquine[4], eriodictyol, isoniazid pyruvate, nitrofurantoin, cepharanthine, ergoloid, and hypericin[45], ikarugamycin and molsidomine[27], baricitinib[37], and lithium[33] drugs, none of them weren't introduced as the definitive treatment of COVID-19 disease. Thus, it is essential to work on other therapeutic candidates for the treatment of lethal COVID-19 disease.

The present survey disclosed that the oral administration of montelukast tablets (10 mg) for about 10 days could decrease the risk of death in COVID-19 patients. Additionally, findings revealed that all of the clinical signs of COVID-19 patients were gradually disappeared after treatment. Thus, this is the report of the potential of treatment of COVID-19 patients by the oral administration of montelukast tablets (10 mg) for about 10 days.

Diverse researches have focused on the impact of montelukast as a probable candidate for the treatment of COVID-19[6,20]. Montelukast is initially and typically used for the treatment of asthma, but it has some anti-viral activities, which have been assessed in some surveys but not approved well[17,21,22,25]. Bozek *et al.*[9] surveyed elderly patients who suffered from asthma who were treated with montelukast. They found that montelukast administration provided benefits and improved asthma control, while other drugs did not lead to a comprehensive healing of asthma. Then, they performed a retrospective observational survey as an extension of the above project with the same patients on morbidity due to COVID-19[10]. They found a significant reduction in SARS-CoV-2 infection in the group of elderly asthmatic patients treated with montelukast. Nowak, J.K. & Walkowiak, J.[33] reported that the administration of antiallergic medications such as montelukast and levocetirizine, and their combination could be effective against COVID-19. In keeping with this, the high safety of montelukast administration for the treatment of viral and respiratory diseases has been reported previously[2,7,11,12]. Mansour, S. *et al.*[29] surveyed computational docking to assess the effects of montelukast on COVID-19 protease catalytic site. They showed a possible inhibitory portion of montelukast in binding to the *Mpro* catalytic site of the COVID-19 virus, which may modulate and inhibit the viral replication.

Reports indicated that ACE receptors are an essential target of the entrance of COVID-19 into the cell, which causes severe pneumonia and subsequently increases in the mortality rate[13,40]. The cough that can progress by ACE inhibition is caused by increased bradykinin and its bronchoconstrictor result, and montelukast, an antagonist of leukotriene D4 (LTD4), has a repressive effect on hypersensitivity of the airway induced by bradykinin[8,32]. Respiratory failures and acute respiratory distress syndrome (ARDS) are the most causes of death in the COVID-19 patients[39,56]. ARDS is mainly caused severe lung injuries with a high inflammatory response with an increase in the levels of Interleukin-6 (IL-6), IL-8, and IL-1 and tumor necrosis factor (TNF) in an initial phase and other pro-inflammatory cytokines in the later phase of the disease[13]. These procedures increased leukocyte migration to the affected region, which causes leukocytes accumulation, reactive oxygen secretion, and protease production with severe damages to capillary endothelium and alveolar epithelium[40]. Surveys revealed that the application of montelukast caused a severe reduction in the levels of TNF-α, IL-6, and IL-1[32]. Additionally, the inhibitory effect of montelukast toward tracheal contraction induced by bradykinin has also been established[8,13,32,40].

Furthermore, it has been established that the montelukast decreases the levels of oxidative stress in cells[39]. Investigations described that high doses and intravenous (IV) administration of montelukast caused a significant decrease in the expression of IL-4, IL-5, IL-13 proteins in the lungs, and anti-inflammatory activities by the T-helper type-2 cytokines suppression[51,56]. Moreover, montelukast administration caused significant decrease in the frequency and severity of wheezing in patients with an upper respiratory tract infection caused by coronavirus, adenovirus, metapneumovirus, and influenza[3,8,11].

Thus, montelukast has an effect on events developing with ACE receptors, and also has an anti-inflammatory effect with bradykinin and leukotriene antagonism; Because of COVID-19 has entry into the cell through ACE receptors and caused mortality due to excessive inflammatory processes, it was thought that montelukast may have a limiting effect on the progression of the disease on COVID-19 infection. Anti-COVID-19 activities of montelukast were confirmed in the present survey.

According to our hypothesis, montelukast caused healing effects and prevented from cough, respiratory distress, congestion, and suffocation of patients suffered from COVID-19 and provided more time for the immune system to fight the virus.

The author of the present study guesses that the COVID-19 virus causes immunodeficiency reactions by disrupting the complement system, and lung damage is not the direct function of the virus[54]. Thus, patients faced with immunodeficiency reactions caused severe damages to lung and consequent death. Proof of this hypothesis offers practical approaches to develop new drug therapies against COVID-19 disease. Otherwise, the COVID-19 virus is probably caused severe disorders in the immune system of patients and caused subsequent disturbances in the complement and cytokines systems, which resulted in the appearance of clinical signs and death in patients. This is the possible reason for the lack of anti-viral options used for the treatment of disease. However, the establishment of this hypothesis needs further researches.

Our observations are limited by the small group of patients and lack of some other supplementary tests, which may be partly due to avoid wasting time in the publication of the valuable results of this research to scientists around the world and saving millions of lives. Additionally, this is a preliminary work due to the size of the sample, the high dispersion in the age group, and the absence of a control group. However, the author potentially recommended oral administration of montelukast (10 mg) as a potential therapeutic option for the treatment of COVID-18 disease all-around the world.

Conclusions

According to the results of the present survey and also those of other review articles, montelukast is the potential treatment for COVID-19 disease. Our finding revealed that all of the COVID-19 patients were treated after 10 days of oral administration of montelukast tablets (10 mg) for about 10 days. Thus, the general oral administration of montelukast tablets (10 mg) is potentially suggested as a potential treatment for COVID-19 disease—this a preliminary study on the effect of montelukast as a potential treatment for COVID-19 infections. Thus, several double-blind and multifactorial clinical trials should perform to determine the other clinical aspects of the treatment of COVID-19 disease by oral administration of montelukast.

Acknowledgments

The author applied all coordination, work, and costs. There was no funding information and also no conflict of interest to the state.

Bibliographic references

1. Abdolmaleki, Z., Mashak, Z., & Dehkordi, F.S. Phenotypic and genotypic characterization of antibiotic resistance in the methicillin-resistant Staphylococcus aureus strains isolated from hospital cockroaches. Antimicrob. Resist. Infect. Control. 8, Page (2019).
2. Ahmad, A., Waseem, T., Butt, N.F., Randhawa, F.A., Malik, U., & Shakoori, T.A. Montelukast reduces the risk of dengue shock syndrome in dengue patients. Trop. Biomed. 35, Page (2018).
3. Andra, I.S. et al. Assertion for montelukast in the covid-19 pandemics? Farmacia. 68, Page (2020).
4. Arya, R., Das, A., Prashar, V., & Kumar, M. Potential inhibitors against papain-like protease of novel coronavirus (SARS-CoV-2) from FDA approved drugs. (2020).
5. Beck, B.R., Shin, B., Choi, Y., Park, S., & Kang, K. Predicting commercially available anti-viral drugs that may act on the novel coronavirus (SARS-CoV-2) through a drug-target interaction deep learning model. Comput. Structural, Biotech. J. (2020).
6. Bhattacharyya, D. Reposition of montelukast either alone or in combination with levocetirizine against SARS-CoV-2. Med. Hypoth.144, Page (2020).
7. Bisgaard, H. et al. Study of montelukast for the treatment of respiratory symptoms of post–respiratory syncytial virus bronchiolitis in children. Am. J. Respir. Crit. Care. Med. 178, Page (2008).
8. Bisgaard, H., Flores-Nunez, A., Goh, A., Azimi, P., Halkas, A., & Malice, M.P. Study of montelukast for the treatment of respiratory symptoms of post-respiratory syncytial virus bronchiolitis in children. Am. J. Respir. Critical. Care. Med. 178, Page (2008).
9. Bozek, A., Warkocka-Szoltysek, B., Filipowska-Gronska, A., & Jarzab, J. Montelukast as an add-on therapy to inhaled corticosteroids in the treatment of severe asthma in elderly patients. J. Asthma. 49, Page (2012).
10. Bozek, A., & Winterstein, J. Montelukast's ability to fight COVID-19 infection. J. Asthma. 2020, Page (2020).
11. Brodlie, M., Gupta, A., Rodriguez-Martinez, C.E., Castro-Rodriguez, J.A., Ducharme, F.M., & McKean, M.C. Leukotriene receptor antagonists as maintenance and intermittent therapy for episodic viral wheeze in children. Cochr. Database. Syst. Rev. (2015).
12. Bruce Chandler, Publication no. . Levocetirizine and montelukast for the treatment of influenza, common cold and inflammation, European. Patent. office. (17 Oct., 2018).
13. Chen, X., Zhang, X., & Pan, J. Medical science monitor: Effect of Montelukast on Bronchopulmonary Dysplasia (BPD) and Related Mechanisms. Int. Med. J. Exp. Clin. Res. 13, Page (2019).
14. Chen, Y.W., Yiu, C.-P., & Wong, K.-Y. Prediction of the 2019-nCoV 3C-like protease (3CLpro) structure: virtual screening reveals velpatasvir, ledipasvir, and other drug repurposing candidates. ChemRxiv. (2020).
15. Contini, A. Virtual screening of an FDA approved drugs database on two COVID-19 coronavirus proteins. (2020).
16. Copertino, D.C., Duarte, R.R., Powell, T.R., de Mulder Rougvie, M., & Nixon, D.F. Montelukast drug activity and potential against severe acute respiratory syndrome coronavirus 2 (SARSβ CoVβ 2). J. Med. Virol. (2020).
17. Crimi, N. et al. Inhibitory effect of a leukotriene receptor antagonist (montelukast) on neurokinin A-induced bronchoconstriction. J. Allergy. Clin. Immunol. 111, Page (2003).
18. Dehkordi, F.S., Gandomi, H., Basti, A.A., Misaghi, A., & Rahimi, E. Phenotypic and genotypic characterization of antibiotic resistance of methicillin-resistant Staphylococcus aureus isolated from hospital food. Antimicrob. Resist. Infect.Control. 6, Page (2017).
19. Elfiky, A., & Ibrahim, N.S. Anti-SARS and anti-HCV drugs repurposing against the Papain-like protease of the newly emerged coronavirus (2019-nCoV). (2020).
20. Fidan, C., & Aydoğdu, A. As a potential treatment of COVID-19: Montelukast. Med. Hypothes. 142, Page (2020).
21. Fitzgerald, D.A., & Mellis, C.M. Leukotriene receptor antagonists in virus-induced wheezing. Treatments in respiratory medicine. 5, Page (2006).
22. Han, J. et al. Montelukast during primary infection prevents airway hyperresponsiveness and inflammation after reinfection with respiratory syncytial virus. American. J.Respirat. Critical. Med. 182, Page (2010).
23. Jin, Z. et al. Structure-based drug design, virtual screening and high-throughput screening rapidly identify anti-viral leads targeting COVID-19. BioRxiv. (2020).

24. Kang, C., Yang, S., Yuan, J., Xu, L., Zhao, X., & Yang, J. Patients with chronic illness urgently need integrated physical and psychological care during the COVID-19 outbreak. Asian. J. Psychiatry. 51, Page (2020).
25. Kloepfer, K.M. et al. Effects of montelukast on patients with asthma after experimental inoculation with human rhinovirus 16. Annals of Allergy, Asthma. Immunol. 106, Page (2011).
26. Kouznetsov, V.V. COVID-19 treatment: Much research and testing, but far, few magic bullets against SARS-CoV-2 coronavirus. European. J. Med. Chem. 203, Page (2020).
27. Li, Z., Bai, T., Yang, L., & Hou, X. Discovery of potential drugs for COVID-19 based on the connectivity map. (2020).
28. Liu, X., & Wang, X.-J. Potential inhibitors against 2019-nCoV coronavirus M protease from clinically approved medicines. J. Gen. Genom. 47, Page (2020).
29. Mansour, S. et al. A Case for Montelukast in COVID-19: "The use of Computational Docking to estimate the effects of Montelukast on potential viral main protease catalytic site. Molecular. Biol. Virol. (2020).
30. Mashak, Z., Jafariaskari, S., Alavi, I., Shahreza, M.S., & Dehkordi, F.S. Phenotypic and Genotypic Assessment of Antibiotic Resistance and Genotyping of vacA, cagA, iceA, oipA, cagE, and babA2 Alleles of Helicobacter pylori Bacteria Isolated from Raw Meat. Infect. Drug. Resist. 13, Page (2020).
31. Mirzaie, A., Halaji, M., Dehkordi, F.S., Ranjbar, R., & Noorbazargan, H. A narrative literature review on traditional medicine options for treatment of corona virus disease 2019 (COVID-19). Complementary. Therap. Clin. Practice. (2020).
32. Noor, A., Najmi, M.H., & Bukhtiar, S. Effect of Montelukast on bradykinin-induced contraction of isolated tracheal smooth muscle of guinea pig. Indian J Pharmacol. 43, Page (2011).
33. Nowak, J.K., & Walkowiak, J. Is lithium a potential treatment for the novel Wuhan (2019-nCoV) coronavirus? A scoping review. F1000Research. 9, Page (2020).
34. Organization, W.H. Coronavirus disease (β β COVID-19)β β : weekly epidemiological update. (2020).
35. Rahi, A., Kazemeini, H., Jafariaskari, S., Seif, A., Hosseini, S., & Dehkordi, F.S. Genotypic and Phenotypic-Based Assessment of Antibiotic Resistance and Profile of Staphylococcal Cassette Chromosome mec in the Methicillin-Resistant Staphylococcus aureus Recovered from Raw Milk. Infect. Drug. Resist. 13, Page (2020).
36. Ranjbar, R., Farsani, F.Y., & Dehkordi, F.S. Phenotypic analysis of antibiotic resistance and genotypic study of the vacA, cagA, iceA, oipA and babA genotypes of the Helicobacter pylori strains isolated from raw milk. Antimicrobial Resistance & Infection Control. 7, Page (2018).
37. Richardson, P. et al. Baricitinib as potential treatment for 2019-nCoV acute respiratory disease. Lancet (London, England). 395, Page (2020).
38. Rismanbaf, A. Potential treatments for COVID-19; a narrative literature review. Arch. Academic. Emergency. Med. 8, Page (2020).
39. Rodriguez-Morales, A.J., Cardona-Ospina, J.A., Gutierrez-Ocampo, E., Villamizar-Pena, R., Holguin-Rivera, Y., & Escalera-Antezana, J.P. Clinical, laboratory and imaging features of COVID-19: A systematic review and meta-analysis. Travel. Med. Infect. Dis. (2020).
40. Sarzi-Puttini, P., Giorgi, V., Sirotti, S., Marotto, D., Ardizzone, S., & Rizzardini, G. COVID-19, cytokines and immunosuppression: what can we learn from severe acute respiratory syndrome? Clin Exp Rheumatol. 38, Page (2020).
41. Sekhar, T. Virtual Screening based prediction of potential drugs for COVID-19. Preprints. (2020).
42. Shang, J. et al. The treatment and outcomes of patients with COVID-19 in Hubei, China: a multi-centered, retrospective, observational study. (2020).
43. Sheikhshahrokh, A. et al. Frontier therapeutics and vaccine strategies for sars-cov-2 (COVID-19): A review. Iranian. J. Public. Health. 49, Page (2020).
44. Shih, H.-I., Wu, C.-J., Tu, Y.-F., & Chi, C.-Y. Fighting COVID-19: a quick review of diagnoses, therapies, and vaccines. Biomed. J. (2020).
45. Smith, M., & Smith, J.C. Repurposing therapeutics for COVID-19: supercomputer-based docking to the SARS-CoV-2 viral spike protein and viral spike protein-human ACE2 interface. (2020).
46. Tu, Y.-F. et al. A review of SARS-CoV-2 and the ongoing clinical trials. Int. J. Molecul. Sci. 21, Page (2020).
47. Wang, D. et al. Clinical characteristics of 138 hospitalized patients with 2019 novel coronavirus–infected pneumonia in Wuhan, China. Jama. 323, Page (2020).
48. Wang, J. Fast identification of possible drug treatment of coronavirus disease-19 (COVID-19) through computational drug repurposing study. J. Chem. Inform. Model. (2020).
49. Wang, Q., Zhao, Y., Chen, X., & Hong, A. Virtual screening of approved clinic drugs with main protease (3CLpro) reveals potential inhibitory effects on SARS-CoV-2. J. Biomolecul. Dynamics. (2020).
50. Wang, Y. et al. Remdesivir in adults with severe COVID-19: a randomised, double-blind, placebo-controlled, multicentre trial. The Lancet. 395, Page (2020).
51. Wu, A.Y., Chik, S.C., Chan, A.W., Li, Z., Tsang, K.W., & Li, W. Anti-inflammatory effects of high-dose montelukast in an animal model of acute asthma. Clin Exp Allergy. 33, Page (2003).
52. Xia, X. et al. Analyzing the Early CT findings and Clinical Features of 12 Patients with 2019 Novel Coronavirus Disease (COVID-19) in China. Iranian. Red. Crescent. Med. J. 22, Page (2020).
53. Xu, Z. et al. Nelfinavir was predicted to be a potential inhibitor of 2019-nCov main protease by an integrative approach combining homology modelling, molecular docking and binding free energy calculation. BioRxiv. (2020).
54. Yazdanpanah, F., Hamblin, M.R., & Rezaei, N. The immune system and COVID-19: Friend or foe? Life Science. 256:117900 (2020).
55. Zhang, J. et al. Teicoplanin potently blocks the cell entry of 2019-nCoV. BioRxiv. (2020).
56. Zhang, J.J., Dong, X., Cao, Y.Y., Yuan, Y.D., Yang, Y.B., & Yan, Y.Q. Clinical characteristics of 140 patients infected with SARS-CoV-2 in Wuhan, China. Allergy. (2020).
57. Zheng, J. SARS-CoV-2: an emerging coronavirus that causes a global threat. Int. J. Biol. Sci. 16, Page (2020).

Received: 26 Aug. 2020
Accepted: 28 Sept. 2020

RESEARCH / INVESTIGACIÓN

Asociación entre la hipertensión arterial y factores de riesgo modificables en sujetos de la población de "La bota" Quito, 2017

Association between arterial hypertension and modificable risk factors in subjects of the "la Bota" population Quito, 2017

Yadira Pilataxi, Martha Fors

DOI. 10.21931/RB/2020.05.04.6

Resumen: En el Ecuador la hipertensión arterial ocupa el cuarto lugar de mortalidad por enfermedades conocidas con una tasa del 22,09%. Este estudio es de tipo observacional, descriptivo y transversal, y tuvo como objetivo de cuantificar la prevalencia y estudiar la asociación entre la hipertensión arterial y los diferentes factores de riesgo: índice de masa corporal (IMC), frecuencia de actividad física, consumo de alcohol y tabaquismo. Para estudiar esta asociación se realizó una regresión logística bivariada. Se calcularon los odds ratios y sus IC al 95% de confianza. Se incluyeron 208 individuos, el 22,6% con Hipertensión arterial y el 55,8% de ellos con sobrepeso u obesidad. Existen más posibilidades de que se presente HTA a mayor edad del sujeto y una probabilidad 4.56 veces mayor de presentar HTA si el paciente tiene sobrepeso/obesidad con respecto al que no lo presenta. El perímetro de cadera igualmente esta correlacionado significativamente con todas las variables de una forma escasa con edad y presión diastólica y moderadas con peso e IMC. El sobrepeso u obesidad y la edad mayor a 40 años constituyen factores de riego para desarrollar HTA y la modifican en función exponencial, en la medida que aumenta el sobrepeso y la edad aumenta el riesgo de HTA

Palabras clave: Factores de riesgo, Hipertensión arterial, Obesidad, Prevalencia.

Abstract: In Ecuador, arterial hypertension occupies the fourth place of mortality due to known diseases with a rate of 22.09%. This study is observational, descriptive and transversal, and aimed to quantify the prevalence and study the association between high blood pressure and the different risk factors: body mass index (BMI), frequency of physical activity, consumption of alcohol and smoking. To study this association, a bivariate logistic regression was performed. Odds ratios and their 95% CI confidence were calculated. 208 individuals were included, 22.6% with arterial hypertension and 55.8% of them with overweight or obesity. There are more chances of presenting hypertension at a higher age of the subject and a 4.56 times greater probability of presenting hypertension if the patient is overweight / obese compared to the one who does not. The hip perimeter is also significantly correlated with all the variables in a scarce way with age and diastolic pressure and moderate with weight and BMI. Overweight or obesity and the age over 40 years constitute risk factors to develop this disease and modify it exponentially, as overweight and age increases the risk of HT.

Key words: Risk factors, Hypertension, Obesity, Prevalence, Physical activity.

Introducción

La hipertensión arterial es una enfermedad crónica que afecta a un gran número de personas a nivel mundial, según datos de la Organización Mundial de la Salud (OMS), uno de cada tres individuos adultos sufre de esta patología, siendo este el principal determinante de riesgo para padecer infartos de miocardio, insuficiencia renal y accidentes cerebrovasculares[1].

Según la Asociación Americana del Corazón (AHA) en el año 2017 en su nueva guía de hipertensión define como: "presión arterial elevada, una presión sistólica entre 120 y 129 mmHg y una diastólica con cifras menores a 80 mmHg e Hipertensión en etapa 1 cifras de 130 a 139 mmHg en la presión sistólica, y 80 a 89 mmHg en la diastólica[2].

El sobrepeso y la obesidad se da por un aumento excesivo de tejido adiposo y son factores que influyen en la hipertensión arterial. En la población adulta el tener un índice de masa corporal superior a 30 mg/kg^2, se interpreta como sobrepeso; mientras que con cifras mayores a 35mg/ kg^2 son categorizadas como obesidad, a mayor cantidad de índice de masa corporal mayor grado de obesidad, debido a que son directamente proporcionales[3].

En el Ecuador la hipertensión arterial ocupa el cuarto lugar de mortalidad por enfermedades conocidas según los datos del Instituto Nacional de Estadísticas y Censos (INEC) del año 2014 con una tasa del 22,09%[4], mientras que la prevalencia de obesidad y sobrepeso es del 62,8% en personas de 20 a 59 años, teniendo un predominio el sexo femenino, encontrándose de manera predominante en la cuarta y quinta década de la vida con cifras mayores al 73%[5].

En la Encuesta Nacional de Salud y Nutrición (ENSANUT) publicada en el año 2013 se reportó un consumo de alcohol del 41,3% en ecuatorianos de 20 a 59 años en el último mes con prevalencia del sexo masculino[5].

El tabaquismo es considerado un factor de riesgo en la hipertensión arterial, el consumo de tabaco disminuye los niveles de colesterol bueno o HDL en el cuerpo; la personas que inician este hábito en la adolescencia tienen un aumento, tres veces mayor de mortalidad en comparación con no fumadores. Se ha demostrado una asociación entre distintos factores de riesgo que incluyen el ser fumadores y una lesión aterosclerótica[6].

En relación con el consumo de tabaco los ecuatorianos entre los 20 y 59 años tienen una frecuencia diaria del 25,9%

Universidad de Las Américas, Quito, Pichincha, Ecuador.

Corresponding author: martha.fors@udlanet.ec

sin dominio de sexo, aumentándose esta práctica conforme avanza la edad, destacando el grupo de 50 a 59 años con una prevalencia del 50,8%[5].

El barrio "La Bota" se encuentra ubicado en la parroquia del Comité del Pueblo identificada como la zona 9 del Distrito Metropolitano de Quito perteneciente a la provincia de Pichincha, cantón Quito[7]. Cuenta con un centro de salud tipo 1 a cargo del Ministerio de Salud Pública (MSP) en el distrito 17 D 03 y según este tiene una población de 13172 de moradores en el sector[8].

Materiales y métodos

Este estudio es de tipo observacional, descriptivo y transversal, con el objetivo de cuantificar la prevalencia y estudiar la asociación entre la hipertensión arterial y los diferentes factores de riesgo: índice de masa corporal (IMC), frecuencia de actividad física, consumo de alcohol y tabaquismo.

Adultos mayores de 18 años que asistieron a la feria de salud organizada por la Universidad de las Américas, los días 7, 8 y 9 de septiembre de 2017.

Criterios de inclusión

- Género femenino o masculino.
- Adultos que hayan firmado el consentimiento informado para participar en la investigación.

Criterios de exclusión

- Personas con información incompleta.

Se incluyó un total de 208 participantes.

Análisis estadístico

Para las variables cualitativas se calcularon frecuencias absolutas y relativas. Para las variables cuantitativas, se calcularon media, o y desviación estándar. Se calculó la prevalencia de obesidad (medida a través del IMC), frecuencia de actividad física, consumo de alcohol y tabaquismo. También se tuvieron en cuentas otras variables como hábitos tóxicos, grupos de edad y sexo. Se calcularon razón de prevalencias y sus intervalos de confianza al 95% para los factores de riesgo seleccionados. Se realizaron comparaciones de proporciones (obesos-no obesos, sedentarios-no sedentarios, consumo de cigarros y alcohol-no consumo) en caso de variables cualitativas (Chi cuadrado) para conocer si existen diferencias significativas entre estos grupos. Para variables cuantitativas (t de Student) para conocer diferencias en edad e índice de masa corporal entre los diferentes grupos según sexo, y grados de obesidad y nivel de sedentarismo.

Para estudiar la asociación entre la hipertensión arterial y los factores de riesgo seleccionados se realizó una regresión logística bivariada. Se calcularon los odds ratios y sus IC al 95% de confianza. Se considerará un valor de $p < 0.05$ como estadísticamente significativo. Se calculó además el Coeficiente de correlación de Pearson y se clasificó la asociación según lo siguiente:

0,2 a 0,39: Correlación positiva baja
0,4 a 0,69: Correlación positiva moderada
0,9 a 0,99: Correlación positiva muy alta
0,7 a 0,89: Correlación positiva alta

Aspectos éticos

Se diseñó un documento para el consentimiento informado con el fin solicitar la participación de los sujetos en la investigación. Los datos recolectados se han mantenido de forma confidencial para lo que se utilizaron códigos numéricos para identificación de los sujetos. En todo momento se protegió la identidad de los sujetos, su dignidad y derechos, así como su privacidad. El proyecto de investigación no necesitó ser sometido a la consideración del Comité de Ética de Investigación en Seres Humanos (CEISH) de la Universidad de Las Américas ya que este proyecto es de riesgo mínimo para sus participantes.

Resultados

El total de participantes de la investigación fue 208 individuos, los resultados del análisis descriptivo señalan que la edad mínima de los participantes fue de 18 años y la máxima 91 años, con una Media de 51 y Desviación estándar (DE) de 19.6 años; el IMC mínimo fue de 15 y máximo de 53, con una Media de 27.5 y DE 5.4; en cuanto a la presión sistólica mínima registrada fue de 85mmHg y máxima de 200mmHg, con una media de 118.0mmHg y DE 16.5; la presión diastólica presentó como mínima cifra registrada 50mmHg y máxima 160mmHg, con una Media de 76.5mmHg y DE 11.7. (Tabla 1)

Los registros de obesidad según IMC se presentaron con mayor frecuenta los pacientes con sobrepeso en el 48.6% (n=101) de los casos, seguidos de Normal con 24% (n=50) participantes y luego Obesidad I registró el 16.8% (n=15). La suma de sobrepeso con el total de obesidad agrupa el 75% (n=156) de los participantes. (Tabla 2)

Se relacionó el antecedente de hipertensión arterial con los factores de riesgo registrados para verificar la asociación entre las variables, logrando establecer que las variables género, grupo etario y Sobrepeso + Obesidad, presentaron una relación estadísticamente significativa con valor de *p* menor a 0.05; sin embargo, esta relación no se evidenció entre hipertensión arterial y el consumo de alcohol, donde el valor de *p* fue mayor a 0.05. (Tabla 3)

Se estudió la relación entre hipertensión arterial y factores de riesgo registrados para verificar la estimación del riesgo, logrando establecer que el género femenino según el OR (0.10 a 0.75) constituye un factor protector. El grupo etario presenta según el OR (4.412 – 243.672) refiere que existen más posibilidades de que se presente HTA a mayor edad del sujeto. Entre hipertensión arterial y Sobrepeso + Obesidad la relación representa un factor de riesgo según el valor de OR (1.553–13.43) con una probabilidad 4.56 veces mayor de presentar HTA si el paciente tiene sobrepeso/obesidad con respecto al que no lo presenta. Al realizar los cálculos de OR ajustados se confirma que el género femenino no representa riesgo para desarrollar HTA y la variable Sobrepeso + Obesidad se mantiene como factor de riesgo para el desarrollo de la misma. (Tabla 4)

Para estudiar la relación existente entre las variables cuantitativas seleccionadas se realizó el cálculo del Coeficiente de correlación de Pearson demostrándose que existe una correlación positiva significativa baja entre las variables presión arterial diastólica y edad (0.23), peso (0.20), IMC (0.24) y perímetro de la cadera (0.21). También se evidenció correlación muy baja entre edad e IMC; no se evidenció correlación entre edad y peso.

Respecto al peso, una buena correlación con el perímetro de cadera y escasa con la presión diastólica. El perímetro de cadera igualmente esta correlacionado significativamente con todas las variables de una forma débil con edad y presión.

	Mínimo	Máximo	Media	Desviación estándar
Edad	18	91	51.0	19.6
IMC	15	53	27.5	5.4
Presión Sistólica	85	200	118.0	16.5
Presión Diastólica	50	160	76.5	11.7

Tabla 1. Estadísticos descriptivos.

	Frecuencia	Porcentaje
Bajo Peso (menor a 18.5)	2	1.0
Normal (18.5-24.9)	50	24.0
Sobrepeso (25-29.9)	101	48.6
Obesidad I (30-34.9)	35	16.8
Obesidad II (35-39.9)	15	7.2
Obesidad III (mayor a 40)	5	2.4
Total	208	100.0

Tabla 2. Distribución según Índice de Masa Corporal.

Características	Hipertensión arterial				
	Si (n =47) 22,6%		No (n =161) 77,4%		Valor p*
	No.	%	No.	%	
Género					
Masculino	5	2.4	48	23.0	0.005
Femenino	42	20.2	113	54.0	
Grupo etario					
Adolesc +Adulto Joven	1	0.5	67	32.0	0.000
Adultez + adulto Mayor	46	22.0	94	45.0	
Sobrepeso + Obesidad					
Ausente	4	1.9	48	23.0	0.002
Presente	43	21.0	113	54.0	
Consumo de alcohol					
Ausente	44	21.0	158	76.0	0.130
Presente	3	1.4	3	1.4	

Tabla 3. Relación entre las HTA y características demográficas.

Discusión

En base a lo establecido por la Asociación Americana del Corazón y otras instituciones internacionales, quienes a través de "la Guía para la prevención, detección, evaluación y desarrollo de la hipertensión arterial en adultos"[9], se tomaron en cuenta las cifras de 130/80 como para agrupar a los pacientes con hipertensión arterial, en este caso se logró evidenciar una prevalencia de 22.6% de casos con antecedente de HTA, cifras cercanas a las reportadas a nivel mundial que oscilan entre el 20 al 25% según Borges, Cruz y Moura[10], y por encima de las registradas en Ecuador que según la Encuesta Nacional de Salud y Nutrición es de 9,3% para la población adulta[5].

En cuanto a los factores asociados, en este estudio se evidenció una mayor prevalencia en las mujeres con un 74.5% de los participantes, por encima de lo estimado a nivel nacional que señala un mayor predominio de hombres hipertensos, en otros países como Brasil el predominio se presenta en mujeres[5]. El 75% de los participantes tenía sobrepeso u obesidad, cifra muy cercana a lo encontrado a nivel nacional, 73%[5].

	Hipertensión arterial			
	Sin ajustar		Ajustado	
	OR (95% IC)	*p*	OR (95% IC)	*P*
Genero				
Masculino	**Referencia**		**Referencia**	
Femenino	0.28 (0.10-0.75)	0.007	4.5(-2.26- -0.29)	0.009
Grupo etario				
Adolescente + Adulto joven	**Referencia**		**Referencia**	
Adultez + Adulto Mayor	32.78(4.4-243.7)	0.000	0.038(1.48-5.5)	0.002
Consumo de alcohol				
No	**Referencia**		**Referencia**	
Si	3.59(0.7-18.41)	0.130	0.114 (-0.35-2.9)	0.213
Sobrepeso + Obesidad				
Ausente	**Referencia**		**Referencia**	
Presente	4.56(1.55-13.43)	0.002	0.356 (0.44-2.6)	0.049

Tabla 4. Estimación de riesgo entre HTA y las variables del estudio.

La edad predominante en el estudio fue mayor de 40 años, se agruparon según OMS y la suma de adultez y adulto mayor abarca el 67% de la muestra, rango de edad donde hay mayor predomino de hipertensión, en concordancia con los estudios de Ortiz y otros[11].

El consumo de alcohol se registró en un 2.9%, por debajo de lo demostrado a nivel nacional, donde la población de mayor consumo es la que presenta edades comprendidas entre los 19 a 24 años de edad con un porcentaje de consumo del 12%, en este estudio la mayor población presentaba más de 40 años, edades donde se disminuye el consumo de alcohol, en quienes se registra un consumo del 7.4%, sin embargo, estuvo en concordancia con los niveles registrado para mayores de 65 años con 2.8%.

Respecto a la relación con los factores de riesgo se estableció una asociación estadísticamente significativa entre HTA y género, sin embargo, no se evidenció relación de riesgo con el sexo femenino que fue el predominante; concuerda con la investigación de Nogueira y otros[12], quienes igualmente encontraron mayor predominio de mujeres, sin embargo, no representan factor de riesgo sino de protección.

Se establece relación estadísticamente significativa con la edad, siendo un riesgo de 32.7 veces mayor para desarrollar HTA si se tiene más de 40 años, se relaciona con los resultados de Borges, Cruz y Moura[10], quien encontró valores de riesgo que se incrementaban con la edad, donde los pacientes de 35 a 44 años presentaron un riesgo de desarrollar HTA de 4.5 veces; de 45 a 54 años fue de 10.69, los pacientes de 55 a 69 años con riesgo de 12.92 y los mayores de 65 años el riesgo se elevó a 21.34 veces. (Tabla 5)

El sobrepeso evidenció una relación estadísticamente significativa con un riesgo de 4.56 veces mayor posibilidad de desarrollar HTA si se presenta esta condición, en concordancia con los hallazgos de Borges, Cruz y Moura[10], donde el riesgo de hipertensión aumentó con el peso tanto para hombres como para mujeres, presentando en esa investigación un valor de 6.33 veces mayor en los hombres obesos y 3.33 en las mujeres obesas en comparación con las personas sin esta condición. Otro estudio similar registra un riesgo de 1.71 para sobrepeso y de 3.13 para obesidad de presentar HTA si se reúnen estas condiciones[13].

Conclusiones

Se encontró mayor prevalencia de la Hipertensión arterial en mujeres, en personas de más de 40 años y en personas

	Edad	Peso	IMC	Presión Diastólica	Perímetro de Cadera
Edad	1	0.01	0.18**	0.23**	0.37**
Peso	0.01	1	0.77**	0.20**	0.60**
IMC	0.18**	0.77**	1	0.24**	0.68**
Presión arterial diastólica	0.23**	0.20**	0.24**	1	0.21**
Perímetro de cadera	0.37**	0.60**	0.68**	0.21**	1

**La correlación es muy significativa en el nivel 0,01 (2 colas).

Tabla 5. Correlaciones entre las variables.

con sobrepeso u obesidad; se debe tomar en cuenta la diferencia entre un hallazgo de hipertensión arterial que es una sola toma de presión arterial elevada mientras que un diagnóstico basa en cumplir con los criterios previamente descritos para categorizar a un paciente con hipertensión arterial. El sobrepeso u obesidad y la edad mayor a 40 años constituyen factores de riego para desarrollar HTA y la modifican en función exponencial, en la medida que aumenta el sobrepeso y la edad aumenta el riesgo de HTA. No se demostró que el consumo de alcohol sea un factor asociado a la HTA en la población estudiada. La presión arterial diastólica esta correlacionada positivamente con la edad, el IMC y el perímetro de la cadera.

Agradecimientos

Agradecemos a los participantes de este estudio y a la universidad de Las Américas por su apoyo en este estudio.

Conflictos de interés

Los autores declaran no tener conflictos de interés.

Referencias bibliográficas

1. OMS. [Online].; 2013 [cited 2018 02 20. Available from: http://www.who.int/campaigns/world-health-day/2013/es/.
2. American Heart Association. IntraMed. [Online].; 2017 [cited 2018 02 20. Available from: https://espanol.medscape.com/verarticulo/5902091.
3. Organización Mundial de la Salud. [Online].; 2016 [cited 2018 02 20. Available from: http://www.who.int/mediacentre/factsheets/fs311/es/.
4. Instituto Nacional de Estadisticas y Censos. Instituto Nacional de Estadisticas y Censos. [Online].; 2014 [cited 2018 02 20. Available from: http://www.ecuadorencifras.gob.ec/vdatos/.
5. Freire W, Larrea C, Larrea A, Montoya R, Ramírez M, Silva K. Encuesta Nacional de Salud y Nutrición del Ecuador. Quito:; 2013.
6. Rodríguez L, Díaz M, Ruiz V, Hernández H, Herrera V, Montero M. Factores de riesgo cardiovascular y su relación con la hipertensión arterial en adolescentes. Revista Cubana de Medicina. 2014; 53: p. 25-36.
7. Distrito Metropolitano de Quito. mapa de servicios socialesintegrados del distrito metropolitano de Quito. [Online].; 2013 [cited 2018 02 20. Available from: http://www.quito.gob.ec/mapas_servicios/Comite_Pueblo_mapa.pdf.
8. Ministerio de Salud Pública. [Online].; 2017 [cited 2018 02 20. Available from: https://geosalud.msp.gob.ec/geovisualizador/.
9. Whelton PK ea. 2017 ACC/AHA/AAPA/ABC/ACPM/AGS/APhA/ASH/ASPC/NMA/PCNA Guideline for the Prevention, Detection, Evaluation, and Management of High Blood Pressure in Adults. [Online].; 2017 [cited 2018 abril 01. Available from: http://hyper.ahajournals.org/content/hypertensionaha/early/2017/11/10/HYP.0000000000000065.full.pdf.
10. Borges H, Cruz N, Moura E. Association between hyertension and overweight in adults in Belém, state of Pará (Brazil). Arquivos Brasileiros de Cardiologia. 2008; 91(2): p. 110-118.
11. Ortiz , Torres M, Peña S, Alcántara V, Supliguicha M, Vasquez Procel X, et al. Factores de riesgo asociados a hipertensión arterial en la población rural de Quingeo. Revista Latinoamericana de Hipertensión. 2017;(3): p. 95-103.
12. Nogueira y otros. Nueva Guía de HTA 2017 AHA/ACC. [Online].; 2017. Available from: https://espanol.medscape.com/verarticulo/5902091.
13. Nascente FMN JPPMdRMEBWMHea. Hipertensión arterial y su asociación con índices antropométricos en adultos de una ciudad de pequeño porte del interior de Brasil. Asociación Medica de Brasil. 2009; 55(6): p. 716-722.

Received: 23 septiembre 2020
Accepted: 20 octubre 2020

RESEARCH / INVESTIGACIÓN

Modeling of the spatial distribution of the vector *Aedes Aegypti*, transmitter of the Zika Virus in continental Ecuador by the application of GIS tools

Mario Bolivar Balseca Carrera, Oswaldo Padilla Almeida and Theofilos Toulkeridis
DOI. 10.21931/RB/2020.05.04.7

Abstract: In recent years Ecuador has suffered from the Zika virus. Geo-software and statistical software allowed the probabilistic identification of suitable ecological niche species, such as the vector *Aedes aegypti*, which is the leading cause of the Zika virus transmission, depending on the dependent and independent variables. These models require pre-weighted input, normalized, and rasterized inputs to continue the validation process to estimate their predictive performance through several statistics such as the confusion matrix or the Receiver Operating Characteristic Curve (ROC). It resulted that the Maxent method has been with the higher predictive performance with a value of Area Under Curve (AUC) = 0.998, which describes the areas of Zika with a greater probability of the transmission vector resembling the actual distribution of the species as a function of the presence data and the predictor variables. A large part of the Ecuadorian coastal territory yielded a statistical-based, probabilistic presence of the vector, being the most vulnerable before a possible epidemiological risk.

Key words: Ecological niche model, GIS, *Aedes Aegypti*, Zika, Ecuador.

Introduction

The vector *Aedes aegypti* is the leading cause of the Dengue, Chikungunya, and Zika viruses, transmitted by the bites of transmission of infected females[1,2]. In 1947, the virus was determined for the first time in Uganda, particularly in the forests of Zika[3]. It has been discovered in a Rhesus monkey during a study about the transmission of yellow fever in the jungle. In 2007, the first significant outbreak of Zika virus infection occurred in Yap Island (Micronesia), in which 185 suspected cases were reported[4,5]. Subsequently, an outbreak was recorded in French Polynesia, which began at the end of October 2013[6,7]. There were around 10,000 cases where approximately 70 cases have been severe, with neurological complications (Guillain Barré syndrome, meningoencephalitis) or autoimmune (thrombocytic purpura, leukopenia). In 2014, cases were also recorded in New Caledonia and the Cook Islands[8,9]. In February 2014, the Chilean public health authorities confirmed a case of autochthonous transmission of Zika virus infection on Easter Island[10]. This appearance coincided with other transmission sources in islands of the Pacific, like French Polynesia, New Caledonia, and the Cook Islands. The Pan-American (PAHO) and World Health Organization (WHO), as well as the Network of Arbovirus Diagnostic Laboratories (RELDA) of the Americas, agreed on new guidelines to identify and confirm suspected cases of Zika in the affected countries. At the same time, the WHO and the scientific community seek to develop more precise tests[11,12].

Vector diseases represent 17% of the estimated global burden of infectious diseases and, even in some cases, lethal[13,14]. In Ecuador, there is an endemic presence of the *Aedes aegypti* mosquito that has been closely related to climatic phenomena (temperature and humidity), causing direct and indirect economic losses that mainly affect the lower strata of society[15-19]. The Ministry of Public Health of Ecuador (MSP) has issued the mandatory epidemiological alert for health establishments of the Comprehensive Public Health Network and the Complementary Network, including all public and private establishments, which will allow the timely detection of all patients with suspicious symptoms, such as fever below 38.5°C, inflammation of the joints in hands and feet, red spots on the skin, conjunctivitis. Fever less than 38.5°C and the possible presence of conjunctivitis differentiate Zika fever symptoms from the symptoms of dengue and chikungunya[15]. Therefore, the National System of Vigilance and Early Warning for the control of the vector of dengue and yellow fever has proposed a project that proposes obtaining climatological, socio-economic, and biological information of the *Aedes aegypti* mosquito to deploy it with Geographic Information Systems (GIS) to develop an Early Warning System for the Control of the Vector of Dengue and Yellow Fever, developing predictive mathematical models for dengue based on the relationship between entomological, epidemiological, socio-economic and climatological data[15].

These models generate predictions regarding the species' distribution and environmental requirements, enable the identification of the variables that best predict favorable habitats, allow ecological testing hypotheses about the distribution of organisms, and evaluate the impacts of possible environmental changes. This type of ecological distribution modeling (Maximum Entropy, Logistic Regression, etc.) has been used in the current study to identify suitable areas for the development and proliferation of *Aedes aegypti*, the transmitter of the parasite that causes the Zika virus[20].

Methodology

Methods for Ecological Niche Modeling

Currently, there is a wide variety of methodologies to perform ecological niche modeling by using mathematical algorithms and automatic learning methods that require biological data of the species and the application of environmental variables[21-26]. Mainly these methodologies are based on three statistical classification techniques, namely discriminant, descriptive, and mixed. In the discriminant techniques, the species' biological data are needed being presence and absence to build the statistic. Among them are classification trees (CART), artificial neural networks (AN), generalized linear mo-

Universidad de las Fuerzas Armadas ESPE, Sangolquí, Ecuador.

Corresponding author: ttoulkeridis@espe.edu.ec

dels (GLMs), generalized additive models (GAMs), maximum entropy models (MAXENT), multivariate adaptive regression splines (MARS) among several others[27-32]. Descriptive techniques require biological data of the species with presence only. Examples of such techniques include BIOCLIM, BIOMAP, and Ecological Niche Factor Analysis-Biomapper (ENFA), among others[33-36]. Mixed techniques use both descriptive and discriminating techniques, making their pseudo-absences. Among them are Desktop-GARP and OM-GARP, among others[37-39].

In some cases, the algorithms have been implemented in a friendly way for the user through software packages that allow describing the relationship between the environment and the species, which are generally available for free to later integrate it into a GIS to obtain cartographic products[40].

Information collection

To model the spatial distribution of a species, it has been necessary to have two types of information: the dependent variables (presence, absence, or pseudo-absence data) and independent variables (predictors). Furthermore, we needed a series of ecological modeling techniques that have been used, such as Maxent, MARS, SPSS, that emulate or demonstrate the research result through statistical modeling, thus determining the suitability of the habitat for the development of the species. The ArcGis version 9.x software has also been used to collect, organize, manage, generate, and analyze the necessary supplies for each model used. As generated, all the collected information has been handled with the WGS84 Reference System with UTM projection, zone 17 South.

a) Dependent Variables

The records of the presence of the vector *Aedes aegypti* have been obtained from periodical publications (Gazettes) issued by the Ecuadorian Undersecretary of Public Health Surveillance through the National Directorate of Epidemiological Surveillance specialized in Diseases Transmitted by Vectors, which since the end of 2015 (weeks epidemiological studies 52-53) began to publish them. The data for modeling the species' distribution has been taken until the report issued on September 14, 2016 (epidemiological weeks 1-36).

As the vector usually transmits the Zika virus, *Aedes aegypti*, therefore, only the localities where there are confirmed autochthonous cases of the virus have been georeferenced (42 records), which according to the WHO, are local epidemiological contagion records[11], meaning that there is the presence of the vector in situ. Table 1 and Figure 1 summarize the provinces with their respective cantons, where the confirmed autochthonous and imported cases of Zika Virus (ZikaV) have been encountered in continental Ecuador.

Data of absence or pseudo-absence of Aedes aegypti

The data of absence are fundamental in the species' distribution models; however, currently, there are no scientific investigations that determine areas not suitable for the reproduction of the vector because it adapts easily to any environment. Therefore, pseudo-absences have been created that are absences estimated from the vector's biological, ecological, and historical data. The pseudo-absences for the present study have been generated based on the presence data as suggested by several authors, who state that from them, a radius of 30 km has been established in which the environmental, topographic, and landscape conditions stabilize, that is, there is a probability of the presence of the vector within this area. This delimitation has been conducted with the ArcGis buffer

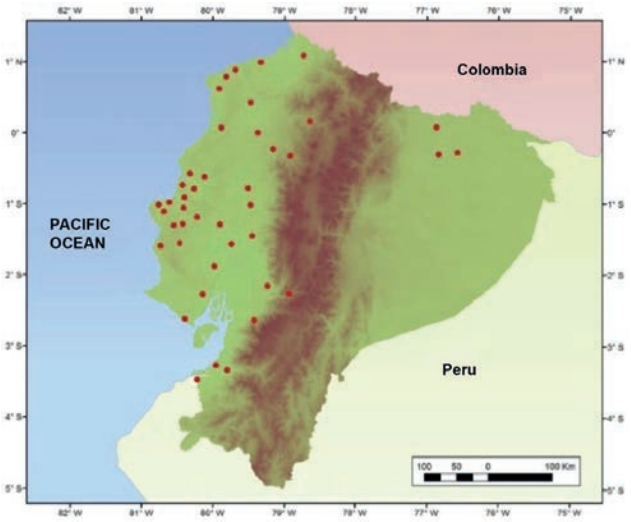

Figure 1. Presence of the Vector *Aedes aegypti* in continental Ecuador[41].

Province	Canton	Autochtone	Imported	Total
AZUAY	Cuenca	1		1
CHIMBORAZO	Chunchi	1		1
EL ORO	Huaquillas	1		1
	Machala	6		6
	Pasaje	1		1
ESMERALDAS	Atacames	1		1
	Esmeraldas	106		106
	Muisne	1		1
	Quininde	13		13
	Rioverde	1		1
	San Lorenzo	54		54
GALAPAGOS	Santa Cruz	2		2
GUAYAS	Balzar	2		2
	Daule	2		2
	Gnral.	1		1
	Antonio	98	1	99
	Guayaquil	1		1
	Playas			
LOS RÍOS	Buena Fe	2		2
	Quevedo	3		3
	Ventanas	10		10
	Vinces		1	1
MANABI	24 de Mayo	1		1
	Chone	2		2
	Jaramijo	19		19
	Jipijapa	92		92
	Manta	827	1	828
	Montecristi	110		110
	Pajan	1		1
	Pedernales	2		2
	Portoviejo	638	1	639
	Puerto Lopez	4		4
	Rocafuerte	3	1	3
	San Vicente	3		3
	Santa Ana	5		5
	Sucre	52		52
	Tosagua	1		1
ORELLANA	La Joya de los Sacha	1		1
PICHINCHA	Mejia	1		1
	Quito	16	15	31
SANTO DOMINGO	La Concordia	8		8
	Santo Domingo	6	1	7
SUCUMBIOS	Lago Agrio	1		1
	Shushufindi	2		2
Total		2.102	21	2.123

Table 1. Confirmed cases of autochthonous and imported Zika Virus[41].

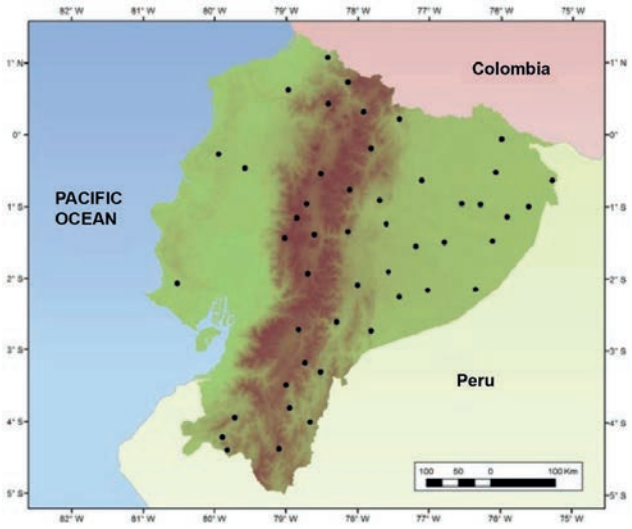

Figure 2. Pseudo-absence of the Vector *Aedes aegypti* in the mainland of Ecuador.

not the same, then the points are discarded that are less than 30 km (again) from the points of presence.

b) Independent Variables

The 19 iboclimatic variables have been taken from the Worldclim Website (http://www.worldclim.org/), which brings together a set of global climate data with a 30-second spatial resolution that is approximately 1km^2 on the Equator line. This portal's offered layers have been created by interpolating the averages of monthly, quarterly, and annual climatic data for each station. The variables that have been included in the model are average annual temperature, an average of the day range, isothermality, seasonal temperature, maximum temperature of the hottest month, minimum temperature of the coldest month, annual temperature range, the average temperature of the wettest quarter, average temperature of the driest quarter, average temperature of the warmest quarter, average of the coldest quarter temperature, annual precipitation, precipitation of the wettest month, precipitation of the driest month, seasonal precipitation (Coefficient of variation), precipitation for the quarter wettest, precipitation of the driest quarter, precipitation of the hottest quarter and precipitation of the coldest quarter.

The layers are worldwide in .grid format; therefore, all the used variables have been cut to the size of the study area (Ecuadorian mainland) with the same pixel size (1000x1000) meters and in the same way, the same number of rows and columns (650x721) with the ArcGis "Extract by Mask" tool (Figure.3a-e).

Geographic Variables

The geographical variables that have been used to perform the modeling have been part of the base cartography with a scale of 1: 50000, which has been included in the Geoportal of the National Information System SNI (http://sni.gob.ec/inicio), except for the altitude. We realized a previous process to each variable, is described below, before becoming part of each model.

a) Altitude

The information corresponding to the altitude has been compiled from the Worldclim Web Site, which relied on the Topographic Radar Shuttle Mission (SRTM) driven by the NASA. At this moment, a digital model of the Earth's surface has been developed based on the information collected from space. Like the environmental variables, the resolution and the size of the pixel have been cut and adjusted to the study area with the ArcGIS Extract by Mask tool.

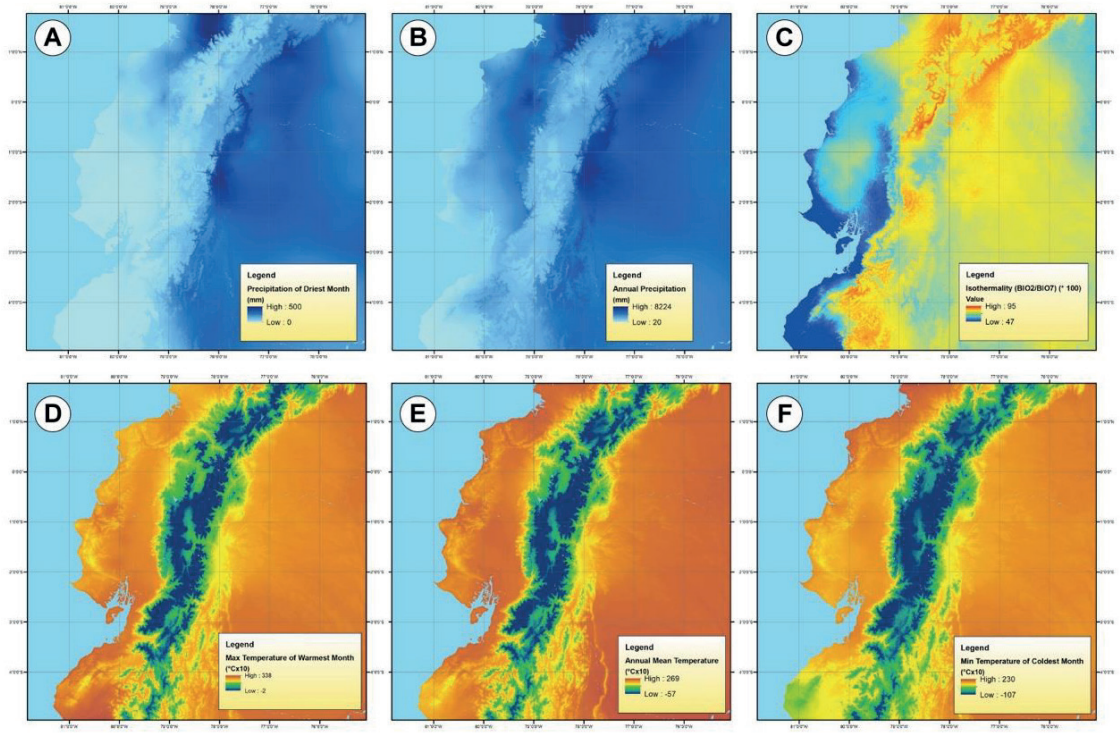

Figure 3. Examples of the bioclimatic variables for modeling the *Aedes aegypti* in the Ecuadorian mainland, as taken from the Worldclim Website (see text). A) precipitation of the driest month; B) annual rainfall; C) isothermality: D) maximum temperature of the warmest month; E) central annual temperature; F) minimum temperature of the coldest month.

b) Areas susceptible to flooding

The raw information of this variable has been in vector format, therefore the ArcGis "Euclidean distance" tool has been used, which, when rasterized, provided the distance from each cell to the nearest source of the areas susceptible to flooding (Figure.4b).

c) Populated centers

Like the previous variable, the raw information has been treated in the identical form and followed the same procedure (Figure.4c).

d) Land use

For the land-use variable, Saaty's Analytical method has been used, which has been based on hierarchizing the components or variables by means of numerical values for the preference judgments, thus determining which variable has the highest priority[42,43]. In table 2, the land use at the national level has been weighted according to the percentage of presences (Figure.5) and the characteristics that result in them more apt to become the vector's habitat. Later the information has been rasterized using the tool ArcGis "Feature to Raster" based on a new field called "weights" where the range of values has been between 0 and 1 (Figure.6).

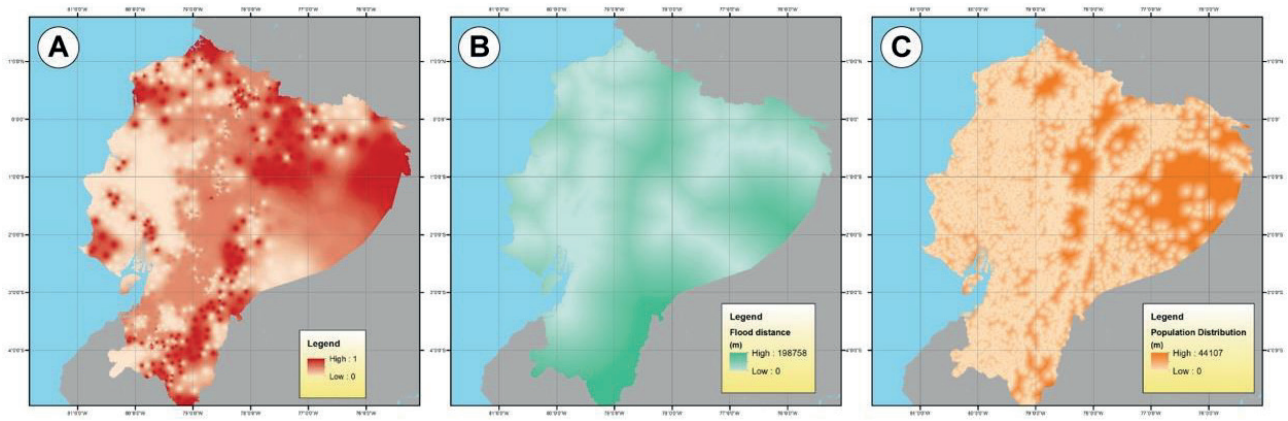

Figure 4. Modeling of *Aedes aegypti* with different variables: A) Poverty Index; B) Flood distances C) Populated Centers.

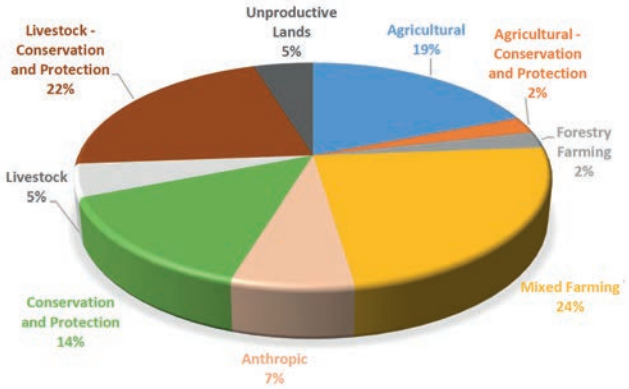

Figure 5. Presence of *Aedes aegypti* in the function of Land use.

Variables	V	V1	V2	V3	V4	V5	V6	V7	V8	V9	V10	V11	W	C	Weight	Weighing
Water body	V1	**1.00**	1.00	0.50	0.50	0.33	0.33	0.25	0.20	0.17	0.14	0.13	0.32	0.02	1	**0.024**
Forest	V2	1.00	**1.00**	0.50	0.50	0.33	0.33	0.25	0.20	0.17	0.14	0.13	0.32	0.02	1	**0.024**
Forestry Farming	V3	2.00	2.00	**1.00**	1.00	0.67	0.67	0.50	0.40	0.33	0.29	0.25	0.65	0.05	2	**0.048**
Agricultural - Conservation and Protection	V4	2.00	2.00	1.00	**1.00**	0.67	0.67	0.50	0.40	0.33	0.29	0.25	0.65	0.05	2	**0.048**
Livestock	V5	3.00	3.00	1.50	1.50	**1.00**	1.00	0.75	0.60	0.50	0.43	0.38	0.97	0.07	3	**0.071**
Unproductive Lands	V6	3.00	3.00	1.50	1.50	1.00	**1.00**	0.75	0.60	0.50	0.43	0.38	0.97	0.07	3	**0.071**
Anthropic	V7	4.00	4.00	2.00	2.00	1.33	1.33	**1.00**	0.80	0.67	0.57	0.50	1.30	0.10	4	**0.095**
Conservation and Protection	V8	5.00	5.00	2.50	2.50	1.67	1.67	1.25	**1.00**	0.83	0.71	0.63	1.62	0.12	5	**0.119**
Agricultural	V9	6.00	6.00	3.00	3.00	2.00	2.00	1.50	1.20	**1.00**	0.86	0.75	1.94	0.14	6	**0.143**
Livestock - Conservation and Protection	V10	7.00	7.00	3.50	3.50	2.33	2.33	1.75	1.40	1.17	**1.00**	0.88	2.27	0.17	7	**0.167**
Mixed Farming	V11	8.00	8.00	4.00	4.00	2.67	2.67	2.00	1.60	1.33	1.14	**1.00**	2.59	0.19	8	**0.190**

Table 2. Matrix of Saaty about the land use[42,43].

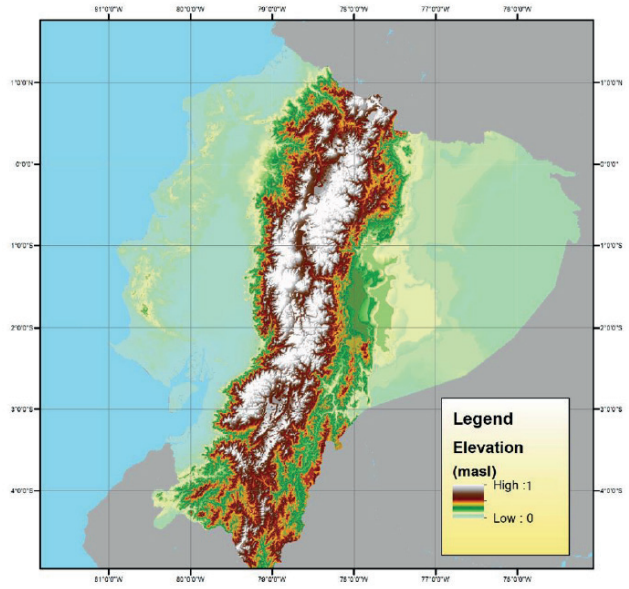

Figure 6. Reclassification of Variable values.

Socio-economic variables

As stated above, the variable about the Poverty Index has been linked to the quality of life in the socio-economic environment. That is, if the quality of life has been low, there will be houses without access to potable water through a water network, in addition to not having drainage systems, so the population is forced to store water in internal or external tanks, which favors the proliferation of the *Aedes aegypti* vector. In the Geoportal of the National Institute of Statistics and Censuses (http://www.ecuadorencifras.gob.ec/geoportal/) this information has been in vector format has been rasterized using the ArcGis "IDW" interpolation tool. This process calculated each of the cells' values through a linearly weighted combination based on a given field. In the present study, the percentage of the poverty index through the centroids of all the parishes nationwide has been considered as illustrated in Figure 4a. The same has been done about the flood distances and the populated centers (Figure.4b and Figure.4c). Hereby, it is about the variables taken in the model, being predictor variables. The summary of the predictor variables that have been used for the *Aedes aegypti* vector modeling has been listed in Table 3.

Normalization of the variables

Most distribution models of species require the homologation of the values of both dependent and independent variables; therefore, the information has been dimensioned and referenced within the same scale. That is, in a range of [0,1] where it has been considered that there has been a greater probability of the presence of the vector when the values have been closer to "1". Within the study area, the maximum and mi-

Variables	Description	Type
Bio_1	Average annual temperature	Bioclimatic
Bio_2	Average of the day range (Average monthly (max temp - min temp))	Bioclimatic
Bio_3	Isothermality (BIO2/BIO7) (* 100)	Bioclimatic
Bio_4	Seasonal temperature (Standard deviation * 100)	Bioclimatic
Bio_5	Max temperature of hottest month	Bioclimatic
Bio_6	Min temperature of coolest month	Bioclimatic
Bio_7	Annual Temperature Range (BIO5-BIO6)	Bioclimatic
Bio_8	Average temperature of the wettest quarter	Bioclimatic
Bio_9	Average temperature of the driest quarter	Bioclimatic
Bio_10	Average temperature of the hottest quarter	Bioclimatic
Bio_11	Average temperature of the coldest quarter	Bioclimatic
Bio_12	Annual precipitation (rainfall)	Bioclimatic
Bio_13	Precipitation of the wettest month	Bioclimatic
Bio_14	Precipitation of the driest month	Bioclimatic
Bio_15	Seasonal precipitation (Coefficient of variation)	Bioclimatic
Bio_16	Precipitation of the wettest quarter	Bioclimatic
Bio_17	Precipitation of the driest quarter	Bioclimatic
Bio_18	Precipitation of the hottest quarter	Bioclimatic
Bio_19	Precipitation of the coldest quarter	Bioclimatic
Altitude	Height referred to the Mean Sea Level	Geographic
Flooding	Distance to areas susceptible to flooding	Geographic
Land use	Current state of the distribution of vegetation	Geographic
Population	Distance to populated centers	Geographic
Poverty	Areas with the highest Poverty Index	Socio-economic

Table 3. Predictor variables for the modeling of *Aedes aegypti*.
Not all of the above-described variables contributed in the same way to each model, which includes that even dispense with any of them has been possible due to the statistic performed by each modeling method.

Variables	General		Presence	
	Minimum	Maximum	Minimum	Maximum
Bio_1	-61	261	170	258
Bio_2	45	152	60	111
Bio_3	47	95	65	88
Bio_4	72	1743	170	1449
Bio_5	-6	331	237	321
Bio_6	-112	220	106	217
Bio_7	75	172	79	139
Bio_8	-60	269	170	267
Bio_9	-66	266	168	254
Bio_10	-59	270	171	269
Bio_11	-66	258	167	254
Bio_12	104	5092	202	3499
Bio_13	36	729	59	553
Bio_14	0	310	1	218
Bio_15	9	189	15	140
Bio_16	84	2012	155	1483
Bio_17	0	1047	3	747
Bio_18	10	1995	125	1483
Bio_19	0	1519	6	1010
Altitude	-17	6169	3	1550
Poverty Index	0	97	39	85
Distance to populated centers	0	43705	0	3344
Distance to Flood Areas	0	199517	0	61320

Table 4. Maximum and minimum values of the Independent Variables.

nimum values have been determined with the presence of the vector of each one of the variables, using the ArcGis "Extract Multi Values to Points" tool, with which the extreme conditions for vector survival have been able to be established and in turn excluding the zones with the absence of it, as evidenced in Table 4. Using the ArcGis "Reclassify" tool, the excluded ranges of the raster that has the data of the particular variable have been assigned to a value of "0".

Once the maximum and minimum values with the presence of a vector have been obtained, the formula (1) to normalize has been used for each of the variables:

$$X_n = \frac{X_i - X_{min}}{X_{max} - X_{min}} \qquad (1)$$

Where X_n is the normalized variable, X_i is the variable, X_{min} and X_{max} represent the minimum and maximum values, respectively. The land-use variable did not perform this process because it has been previously normalized by applying the Saaty method[42,43].

Distribution Models of the species

In the current study, several statistical models have been applied to determine which of them is the most optimal to predict the spatial distribution of the *Aedes aegypti* mosquito vector of the Zika virus. The used models have been Maxent, ROC Curve Analysis, Fuzzy Logic, Logistic Regression, and Multivariate Adaptive Regression Splines (MARS).

a) Maxent (Maximum Entropy)

For the application of maximum entropy model or Maxent, free software with the same name MaxEnt has been used[31]. This statistic is discriminant and requires presence and absence data. However, Maxent provides its absences, called "background". Additionally, this virtual platform does not require that the predictor variables be normalized because this statistical process is carried out internally by the program. Maxent is a software used to calculate geographic distribution models, in which the relationship of the presence data of a species and different predictive spatial variables are analyzed. The model itself can be spatialized and can represent the probability of the localization of the species.

b) Receiver Operating Characteristic analysis (ROC)

The ROC curve (Receiver Operating Characteristic analysis), is a statistic that graphically represents the discriminative capacity of any model for all its possible cut points. It needs the data to be evaluated to be of presence/absence to define the threshold or criteria necessary for predicting the species[44]. The ROC curve is obtained by relating the sensitivity that is the fraction of true positives (y-axis), with the "1- specificity" which is the fraction of false positives (x-axis), for ease of calculation is used the expression "1- specificity" so that sensitivity and specificity vary in the same direction when the threshold is defined[45].

The derived statistic is the area under the ROC curve, or Area Under Curve (AUC), which provides a full measure of the predictive capacity as well as assessing the best fit in ecological niche models, defined by (45) as:

$$AUC = \int_0^1 ROC(p)dp \qquad (2)$$

The AUC is calculated by adding the area under the ROC curve and takes values from 0 to 1, where values less than 0.5 indicate that the model is naughty since it classifies erroneously more cases than chance. AUC values of 0.5 to 0.7 are considered a low performance of the model, while values between 0.7 to 0.9 presume a moderate model's moderate performance. Values greater than 0.9 estimates a high level of the model, indicating that all cases have been classified correctly[46]. The AUC values are not affected by changes in the prevalence of the species, and therefore it is a reliable statistic in the comparison of models. Some studies have demonstrated that AUC does not decrease with increasing species prevalence[47]. Among the advantages that the AUC calculation provides is the possibility of comparing several methods, whatever the type of output values, because it only needs the distributions of these values[48].

c) Diffuse Logic or Fuzzy Logic

The main application of Fuzzy Logic is to represent quantitative values (numerical values between 0 and 1) through qualitative linguistic inputs, employing managing domains that are not within the scope of classical logic[49]. For Fuzzy Logic, the functions that are applied are the Sine and the Cosine because the range in which one works is between 0 and 1. The methodology that fuzzy Logic manages consists of determining the interaction of each variable that is part of the model with the probability of the presence of the species within three possible scenarios or cases. We analyzed how the predictor variables react with respect to the probability of the presence of the species to determine which of the cases raised in the Fuzzy methodology will be applied (table 5).

For the land-use variable, it has not been necessary to determine Fuzzy's corresponding case because previously, this process was performed using the Saaty method.

Once the normalization process has been applied and the corresponding scenarios (cases) of the fuzzy Logic have been identified, the value of the variables has been transformed to radians using the following formule:

$$R = X_n * V \qquad (3)$$

Where *R* is the value of the variable in radians, X_n is the normalized variable and *V* is the value of "π"or "π/2" according to the range corresponding to each scenario.

In order to analyze the probability of occurrence of each variable it has been necessary to use the following equation:

$$P = Sen(R) \wedge P = Cos(R) \qquad (4)$$

The trigonometric functions that have been used were the sine and the cosine because after performing the analysis of scenarios proposed by Fuzzy, it has been determined that the model has all three cases.

Finally, we averaged the probabilities of all the variables using the ArcGis "Raster Calculator" tool by applying the equation described below (Formula 5):

$$Y = (P_{Bio_1} + P_{Bio_2} + P_{Bio_3} + P_{Bio_4} + P_{Bio_5} + P_{Bio_6} + P_{Bio_7} + P_{Bio_8} + P_{Bio_9} + P_{Bio_{10}} + P_{Bio_{11}} + P_{Bio_{12}} + P_{Bio_{13}} + P_{Bio_{14}} + P_{Bio_{15}} + P_{Bio_{16}} + P_{Bio_{17}} + P_{Bio_{18}} + P_{Bio_{19}} + P_{altitude} + P_{poverty} + P_{flooding} + P_{populated} + Land\_use)/24$$

Where *Y* is the probability of the model

d) Logistic regression

For the application of the Logistic Regression method, we used a statistical software called Statistical Package for Social Sciences (SPSS), which is very often used to perform analytical processes to conduct research and make better decisions. Within this statistical package, the element of binary logistic regression is necessary to calculate the constant and the coefficients that best fit the functional expression of the variables. The logistic regression method is discriminant; therefore, it is necessary to have the needed inputs such as predictor variables, presence, and pseudo-absence data that have been previously generated.

To perform the corresponding statistical analyzes in the SPSS 23 program, it is necessary to generate a matrix with all the predictor variables' values already normalized according to the points of absence and presence. This information has been obtained through the ArcGis "Extract Multi Values to Points" tool. The type of regression that has been chosen for the current study has been binary logistic, because the values of the inputs are dichotomous, being within the range [0,1] which are optimally fitting this statistic to the model. Afterward, we configured which are the dependent and independent variables (covariables).

Several statistics have been obtained from the execution of the program that evaluates the reliability of the results, such as classification tables for the variables, omnibus tests, correlation matrix and, mainly, the coefficient table needed to generate the model (β_0, β_1, β_2,... β_p) , as indicated in Figure.7.

In this way, the values of the constants have been multiplied by each variable with the help of the ArcGis "Raster Calculator" tool, following the formula of the logistic regression:

Where Y is the probability of the model.

e) Multivariate Adaptive Regression Splines (MARS)

The MARS program with other statistical products such as classification and regression tree (CART), TreeNet, and Random Forests, are all focused on elaborating predictive and descriptive models to analyze databases of any size and of different complexity[32,50,51]. The MARS method proposes a complete analysis of the variables according to the importance of each of them for the prediction of the event, adjusting the model not only to a predictive curve but rather dividing it into zones (base functions) through nodes or the so-called inflection points, which improves the results. Like the previous models, the inputs needed to apply the model are the predictor variables, presence, and pseudo-absence data.

MARS generates an internal process of iterations called "forward" on the original predictor variables' base functions.

$$y = \frac{1}{1 + (Exp\,(-1 * \,(Constant + \beta_1 * Bio\_1 + \beta_2 * Bio\_2 + \beta_3 * Bio\_3 \ldots + \beta_P * Altitude\,))}$$

Formula 6.

	bio_6n 2,312	**bio_7n** 1,162	**bio_5n** -10,328	**bio_4n** ,530	**use_soiln** 1,357	**bio_13n** -7,843
	bio_14n ,919	**bio_15n** 4,253	**bio_16n** 7,521	**bio_17n** 1,017	**bio_3n** ,359	**poverty_n** -,195
Constant -4,089	**bio_12n** 1,746	**bio_2n** ,281	**populated_n** ,366	**bio_11n** -,877	**bio_1n** -,583	**flooding_n** -,533
	bio_10n -1,205	**bio_19n** -1,471	**bio_9n** -489	**elevation_n** ,122	**bio_18n** -1,393	**bio_8n** 11,341

Figure 7. Example of a table with coefficients of the variables.

Variables	Description	Fuzzy Case
Bioclimatics	The extreme weather conditions are generally able to deteriorate the habitat of the species. Therefore, the non-extreme conditions represent an appropriate condition for life.	Case 1 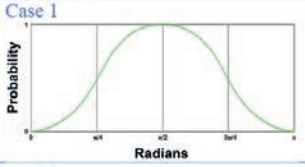
Altitude	The *Aedes aegypti* has its habitat within a range of elevations. When leaving this range, either by higher or lower elevation, the species dwindles or disappears.	Case 1 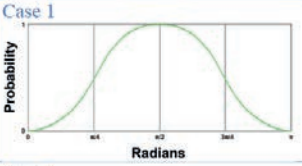
Poverty Index	Certain conditions linked to poverty mean that people with scarce resources are more exposed to the mosquito and its diseases.	Case 3 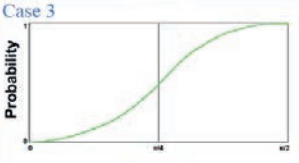
Distance to Populated Centers	*Aedes aegypti* has a flight range of approximately 3500 meters to population centers. Outside of this range, the species disappears as the female feeds on human blood.	Case 1 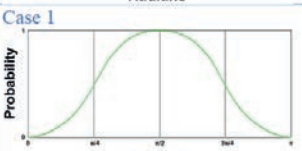
Distance to Flood Areas	Natural deposits of water formed by floods favor the proliferation of the vector *Aedes aegypti*, because the females deposit there their eggs.	Case 2 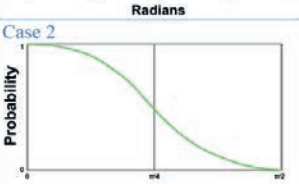

Table 5. Analisis of the variables.

Subsequently, the program will discard those that least fit the model through another process called "backward", which converts the original variable *X* into a new variable defined as: max (0, X-c) or max (c-X), where c is the threshold established by the nodes, as shown below.

BF2 = max(0, 0.416 - [bio_15n])

BF3 = max(0, [flooding _n] - 0.015118)

BF4 = max(0, 0.015118 - [flooding_n])

BF5 = max(0, [poverty_n] - 0.723404)

BF6 = max(0, 0.723404 - [pobreza_n])

BF7 = max(0, [populated_n] - 0.392163)

BF8 = max(0, 0.392163 - [populated _n])

BF9 = max(0, [bio_8n] + 5.96046e-008)

BF11 = max(0, 0.72619 - [bio_5n])

BF12 = max(0, [bio_12n] - 0.863209)

BF14 = max(0, [bio_2n] - 0.764706)

Finally, MARS creates a final predictive equation that is defined by the generated base functions, which in turn are multiplied by the coefficients that best fit the model, by using the ArcGis "Raster Calculator" tool.

Where *Y* is the probability of the model.

Standard Deviation and Adjustment of Models

The standard deviation is a set of data or a measure of dispersion that indicates how far the obtained values may be moved away from the average. That means that this statistic's importance is based on the probability that an event will occur or not. The values of the standard deviations of the models applied have been described in Table 6 in addition to their maximum, minimum, and arithmetic mean values.

The adjustment has been conducted on the previously normalized final models within a range of [0,1], depending on the standard deviation, applying the following equation:

N = Measured Value – Calculated Value (4)

Where *N* is the adjustment value, the Measured Value is the maximum value at which the models could arrive, that is to say, "1" (probability of presence), and the Calculated Value is the value of the standard deviation of the averages of probabilities of the different models.

Table 7 lists the standard deviations of the models and the adjustment made to each of them.

$$Y = -0.630691 - 1.29024 * BF2 - 0.26154 * BF3 - 18.1487 * BF4 - 1.46987 * BF5 - 0.283358 * BF6 - 0.480713 * BF7 - 0.583341 * BF8 + 2.07942 * BF9 + 2.0564 * BF11 + 3.74046 * BF12 + 1.33308 * BF14$$

Formula 7.

	Minimum	Maximum	Average	Standard deviation
Maxent	0	0.970063	0.104460	0.173263
Diffuse Logic	0	0.844170	0.104500	0.221607
Logistic Regression	0	0.999995	0.347007	0.302110
Mars	0	1	0.361043	0.105743

Table 6. Standard Deviation of Models.

Results

To select the model with a more excellent predictive performance of the spatial distribution of the vector *Aedes aegypti* within the Ecuadorian mainland, several analyzes and comparisons have been performed, both statistics and graphs of the four applied models.

a) Analysis of the adjustment of the models

By analyzing the adjustment of the previously normalized models (Table 8), it has been observed that the MARS method with an adjustment of 0.894 has been the closest to the value of one, demonstrating a low dispersion of its data concerning the mean, which means that the prediction has been significant. Next are the methods of Maxent and Fuzzy Logic with adjusted values within an acceptable range of 0.821 and 0.737, respectively. Finally, the logistic regression method with the adjusted value of 0.653, describes a low predictive performance.

b) Analysis of the AUC Curve of the models

The predictive capacity of the models has been validated by the AUC statistical analysis from the ROC curve, whose main function has been to calculate the sensitivity and specificity of the values of the occurrences of the species by intersecting the presences with the layers (raster) of each of the obtained models. The ROC curve has been based on the union of different cutting points, corresponding on the Y-axis to the "sensitivity" and the X-axis to the "1-specificity". The two axes contain values between 0 and 1 (0% to 100%), while the confidence interval that has been used for the analysis has been of about 95%.

The graphs of the ROC curves have been superimposed in Figure 9, illustrating satisfactory predictive results> 0.9 of the AUC in all models, which means that within the confusion matrix environment, there have been predictions with authentic presences and true absences. However, the model that has been closest to "1" is the Maxent Model (Figure.8a) with a value of AUC = 0.998. Then the MARS Model (Figure.8d) with a value of AUC = 0.996 and finally with a similar value the models of Fuzzy Logic (Figure.8b) and Logistic Regression (Figure.8c) of AUC = 0.986.

c) Graphic Analysis of the models

As a result of the comparison of the used models for the prediction of the spatial distribution of the *Aedes aegypti* vector, it has been evidenced that both the Maxent models (Figure.10a) and the Fuzzy Logic models (Figure.10b) conform to the real distribution of the vector because the areas most likely predicted by these models have been close to the points of presence. Additionally, these zones must meet the zones with biological parameters essential for the survival of the vector such as low altitudes, being not higher than 1600 meters above sea level, and distances to population centers that do not exceed 4000 meters since the females need to have enough blood as a source of proteins to multiply for the production of their eggs. The models of Logistic Regression (Figure.10c) and MARS (Figure.10d) predict a high probability of the vector's presence in almost the entire coastal region without discriminating zones where absences may exist due to climatic, topographic, and other factors.

d) Logistic Regression Model

After having performed several analyzes and comparisons, both statistics and graphs of the four applied models in the present investigation, we concluded that the Maxent model has a better predictive performance of the spatial distribution of the vector *Aedes aegypti*, since it represents a satisfactory performance in the analysis of ROC curve, with a value AUC = 0.998, and with an adjustment of the standard deviation 0.821390 (Table 8), only below the MARS model. In addition, it visually describes the areas with the most significant probability of the vector, which conveniently resembles reality according to the present data and the predictor variables.

Model	*Maxent*	*Diffuse Logic*	*Logistic Regression*	*MARS*
Average	0.107683	0.123790	0.347000	0.361043
Standard deviation	0.178610	0.262514	0.347000	0.105743
Adjustment	**0.821390**	**0.737486**	**0.653000**	**0.894257**

Table 7. Adjustment of the Models.

Model	*Maxent*	*Diffuse Logic*	*Logistic Regression*	*MARS*
General standard deviation	0.178610	0.262514	0.347000	0.105743
Normalized standard deviation	0.173263	0.221607	0.302110	0.105743
Difference	0.005347	0.040907	0.044890	0
Adjustment	**0.821390**	**0.737486**	**0.653000**	**0.894257**

Table 8. Analysis of the Adjustment of the Models.

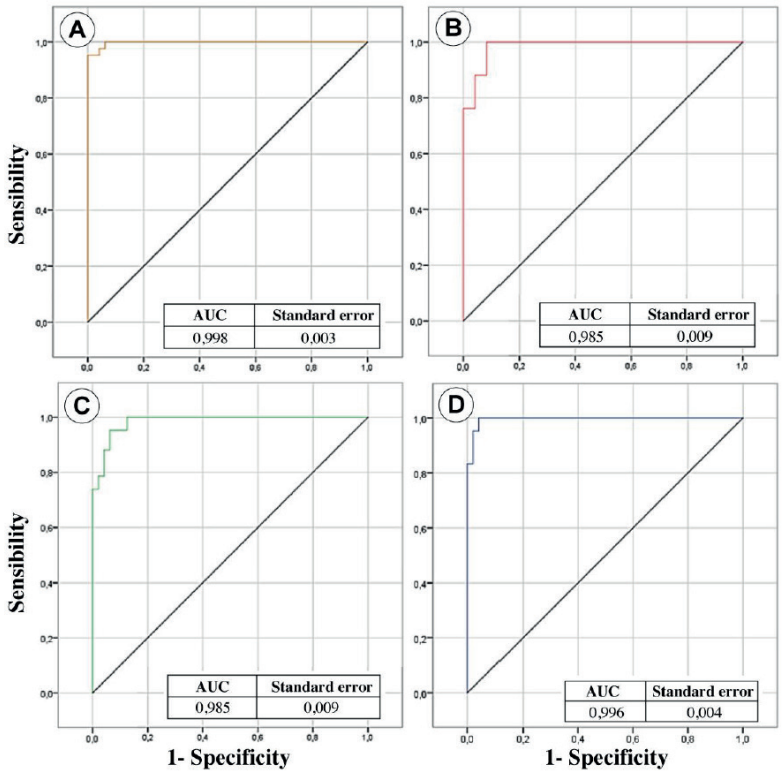

Figure 8. Analysis of the ROC Curve, a) Model Maxent; b) Fuzzy Logic Model; c) Logistic Regression Model; d) MARS model (4.1-4.4)

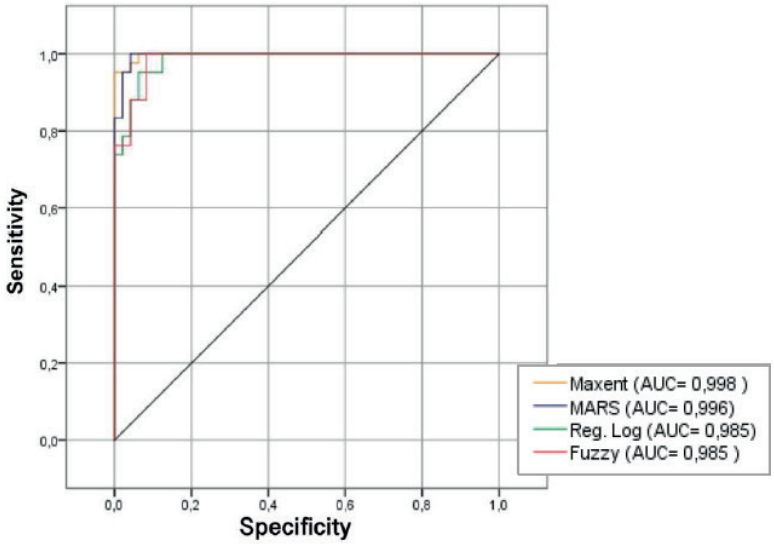

Figure 9. Analysis of the ROC Curve of all four models.

Discussion

Methods used

Maxent has been established as the model with the highest predictive performance after several statistical validations. Besides, it visually describes the zones with the highest probability of the vector's presence, which also resembles the vector's real distribution according to the present data and the predictor variables. The Fuzzy or Fuzzy Logic methodology determines quite good predictions with a predictive performance scarcely inferior to the Maxent method, which constructs its model based on the generation of background due to the necessity that its algorithm requires, sometimes causing an over the adjustment of the model. Unlike Fuzzy, which makes its predictions based on the predictor variables, presence, pseudo-absence data, and improvement if the model will include absence data sampled in the field. The logistic regression methods and MARS registered good values in the statistical analyzes. However, graphically they register a high probability of the vector in almost all the coastal regions without discriminating zones in which there could be absences of the same due to climatic, topographic factors, among others.

Delimitation of suitable zones for the presence of the vector

The estimation of the areas with the highest probability of

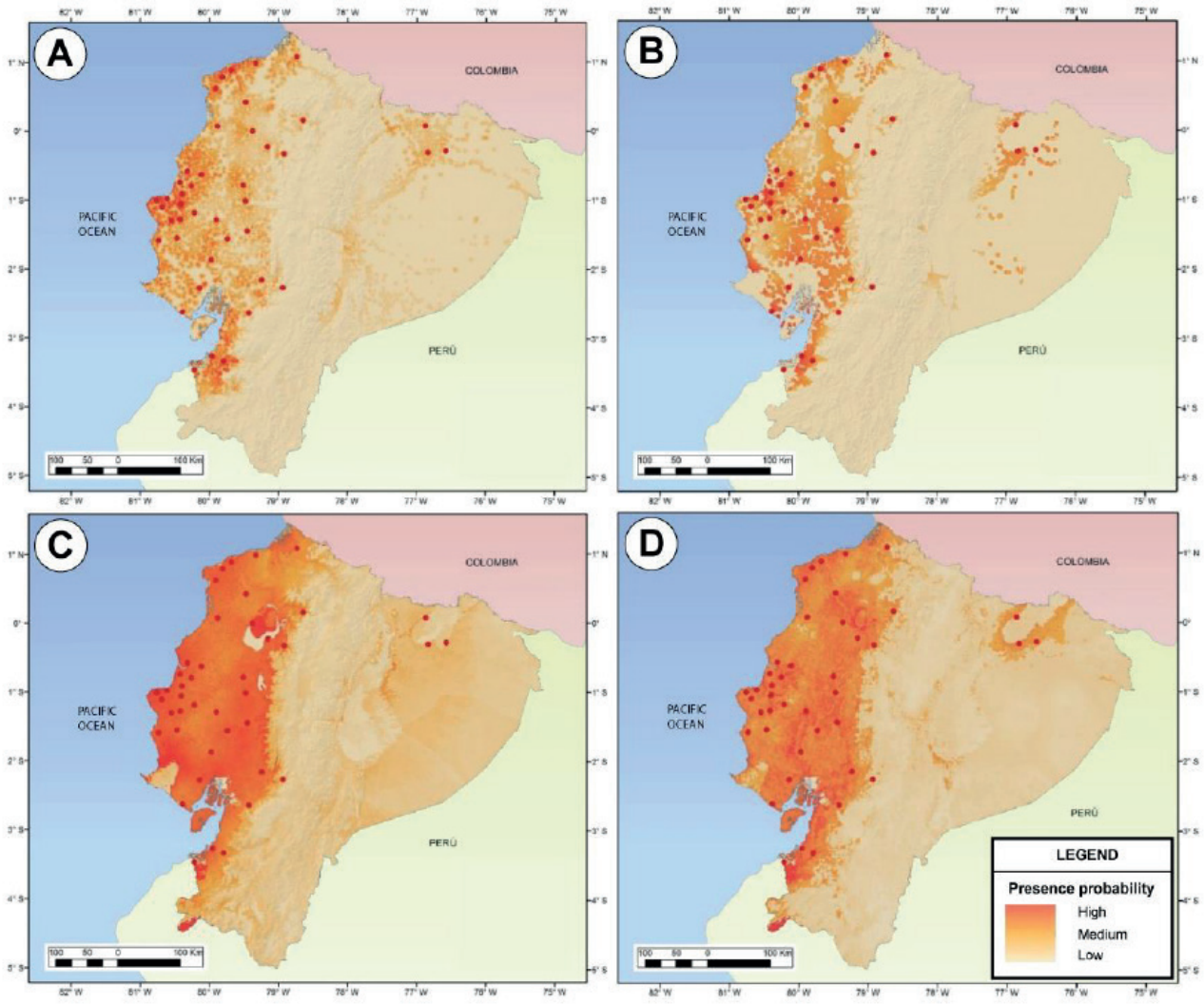

Figure 10. Distribution of *Aedes aegypti*: A) Model Maxent; B) Fuzzy Logic Model; C) Logistic Regression Model; D) MARS model.

the presence of the *Aedes aegypti* vector has been determined by analyzing their frequency within the study area, resulting in the histogram of Figure 11. It illustrates that the lowest number of frequencies is in a range of (0-30%) with only 4 presences, an intermediate frequency with a value of 18 presences in a range of (30-60%) and half of the presence data with a value of 22 in the range of (60-100%).

Figure 12 graphically illustrates the range of probabilities that have been previously determined, which clearly shows that the coastal region is the most suitable for the vector's existence.

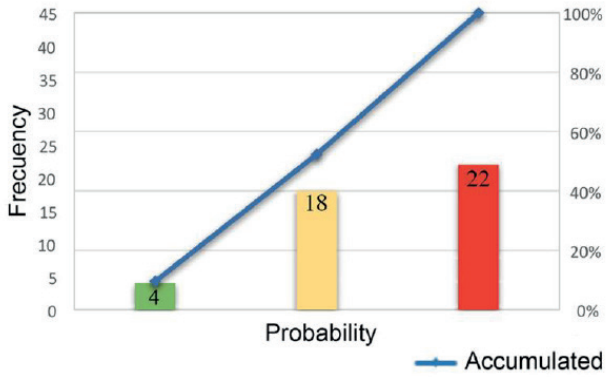

Figure 11. Probability Histogram.

According to the frequency analysis of the vector within the study area that has been previously performed, it has been estimated that the zones with the highest probability of the presence of the vector are within the range (60-100%) that is proportional to the epidemiological risk. Subsequently, only areas with a high probability of the presence of the vector have been reclassified, as documented in Figure 13.

The ideal zones for the Aedes aegypti vector's presence cover an area of 7806 km^2, representing 3.15% of the territory of the Ecuadorian mainland. This area is divided into 16 provinces (111 cantons). There is a high presence in the coastal region in important localities such as Guayaquil, Machala, Babahoyo, Portoviejo, Salinas, and others, a low presence in the Amazon region and absence entirely in the Highlands region (Table 9).

Characterization of the areas with the highest epidemiological risk

There are several zones along the Ecuadorian coast that have been suitable for the characterization of epidemiological risk, as the probability of the vector's presence is very high. However, the provinces of Manabí and El Oro have been considered for this study because more than 15% of their territorial areas have been exposed to a vector's possible spatial distribution. The province of Manabí has 22 cantons, of which 21 determine a possible presence of the vector, while the province

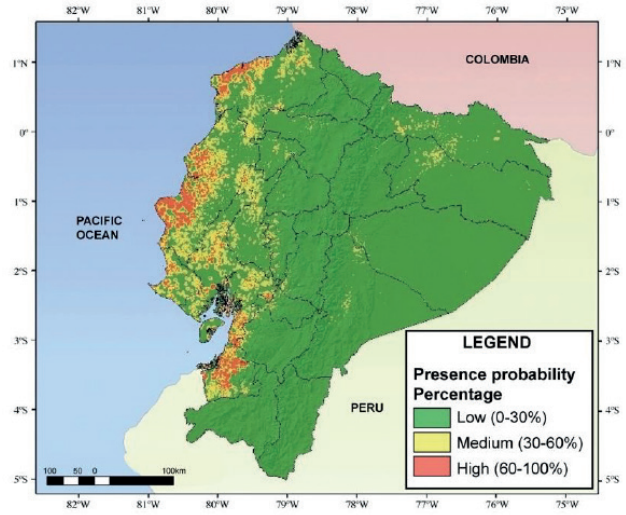

Figure 12. Probabilities of the presence of the vector *Aedes aegypti*.

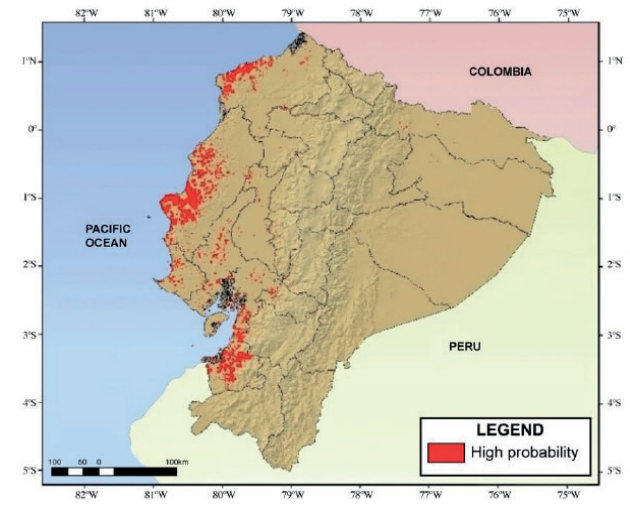

Figure 13. Suitable areas for the presence of vector *Aedes aegypti*.

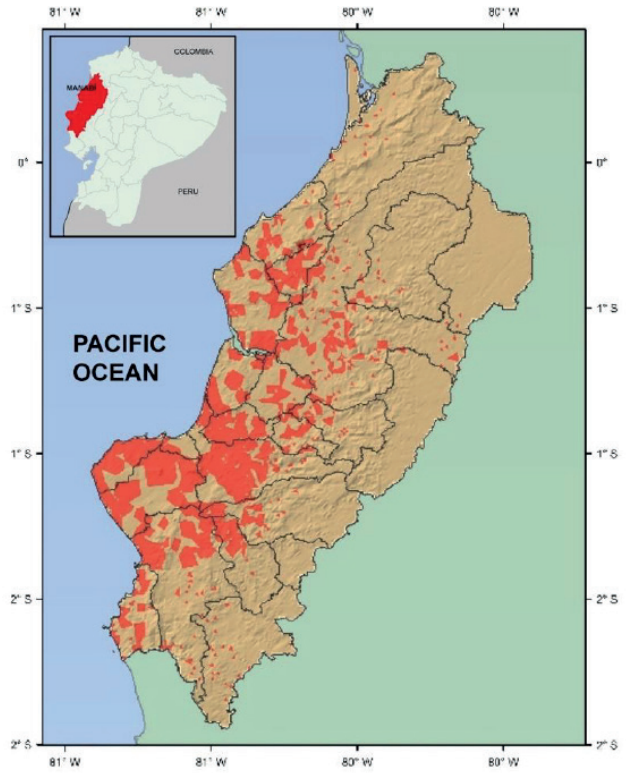

Figure 14. Manabí province with suitable areas for the presence of vector *Aedes aegypti*.

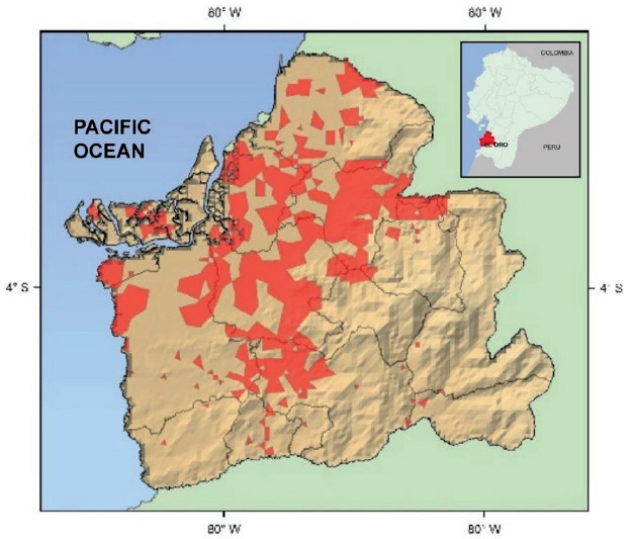

Figure 15. El Oro province with suitable areas for the presence of vector *Aedes aegypti*.

of El Oro has a territorial expansion on a smaller scale compared to Manabí, with 14 cantons of which all show the presence of the vector.

The province of Manabi has about 18,400 km^2, about 1.369.780 inhabitants, with a poverty rate of about 39.8%. The precipitation has a range of 500 to 1000 mm per year, an average temperature of 25°C, and a dry subtropical climate to tropical humid. Manabí has approximately 350 km of maritime coastline, with important geographical and climate features[52]. Certain areas of the province are predisposed to flooding in the winter seasons with higher rainfall[53,54]. There is a predominance of 51.3% cultivated pastures representing little more than half of the used provincial area. The mountains and forests with 21.5% and the permanent crops with 13.2% added to the grassland areas document the existence of protected areas and areas suitable for livestock[55]. The most extensive parts of the province have high deficit rates in essential residential services (water, wastewater disposal, electricity supply) with 80% and 61.20%, respectively[54].

The province of El Oro, has an area of about 5767 km^2, about 648,316 inhabitants with a poverty rate of about 23.4%. The precipitation has a range of 200 to 1500 mm per year, an average temperature of 25°C and a dry coastal climate, tropical Savanna, and rainy winters. This province is divided into two areas, to the northwest, the foothills that descend to the Gulf of Guayaquil are the plains, where banana is grown, and the southeast mountainous area that is crossed by the Western Cordillera of the Andes, where the temperature decrea-

Province	Area Km²	Percentage (%)
El Oro	1334	23.22
Manabí	3402	17.96
Santa Elena	331	8.94
Esmeraldas	1301	8.06
Guayas	1103	7.43
Los Ríos	112	1.46
Azuay	102	1.22
Bolívar	31	0.79
Cañar	15	0.47
Santo Domingo de los Tsáchilas	8	0.23
Sucumbíos	37	0.21
Chimborazo	12	0.18
Pichincha	4	0.04
Orellana	6	0.03
Morona Santiago	5	0.02
Pastaza	3	0.01
Seven more provinces	0	0

Table 9. Provinces with higher epidemiological risk.

ses according to the height[54]. The area of land occupied by agricultural activity is 457,025 ha, distributed as follows: 2.17% of transitory crops; 53.56% pastures (cultivable and natural); 12.36% forests; 13.45% other uses, rest and páramos[55]. Some 79% of the total population of the province is concentrated in the urban area, while the residual 21% remain in the rural area[54].

Both provinces have a significant environmental and social problem where pollution and high demographic and poverty rates are the most representative.

Conclusions

Maxent has been established as the model with the highest predictive performance after several statistical validations. In addition, it visually describes the zones with the highest probability of the presence of the vector, which additionally resembles the real distribution of the vector according to the present data and the predictor variables.

The Fuzzy or Fuzzy Logic methodology determines good predictions with a predictive performance scarcely inferior to the Maxent method, which constructs its model based on the generation of background due to the necessity that its algorithm requires, sometimes causing an over the adjustment of the model. Unlike Fuzzy, which makes its predictions based on the predictor variables, presence, pseudo-absence data, and improvement, the model will include absence data sampled in the field.

The logistic regression methods and MARS registered good values in the statistical analyzes. However, graphically they register a high probability of the vector in almost all the coastal regions without discriminating zones in which there could be absences of the same due to climatic, topographic factors, among others.

The areas with the highest probability of the vector *Aedes aegypti* generally cover an area of 7806 km² distributed in 16 provinces, located almost exclusively in the coastal region. There, the provinces of Manabí and El Oro, due to their geographical, climatic, and even socio-economic characteristics, such as altitude, temperature, precipitation, and environments, associated with human life conditions, establish favorable sites with a greater probability of the presence of the *Aedes aegypti* vector.

The spatial distribution model of the *Aedes Aegypti* allowed the characterization of the zones with a greater probability of the presence of the vector. This way, we have been able to define the ecological dynamics of transmission of ZIKA, the evaluation of the epidemiological-economic impact, and the intervention strategies that should be taken before a possible epidemiological risk in Ecuador.

Bibliographic references

1. Foy, B. D., Kobylinski, K. C., Foy, J. L. C., Blitvich, B. J., da Rosa, A. T., Haddow, A. D., Lanciotti, R.S. and Tesh, R. B. (2011). Probable non–vector-borne transmission of Zika virus, Colorado, USA. Emerging infectious diseases, 17(5), 880.
2. Ioos, S., Mallet, H. P., Goffart, I. L., Gauthier, V., Cardoso, T., & Herida, M. (2014). Current Zika virus epidemiology and recent epidemics. Medecine et maladies infectieuses, 44(7), 302-307.
3. Dick GW, Kitchen SF, Haddow AJ (1952) Zika virus. I. Isolations and serological specificity. Trans R Soc Trop Med Hyg 46: 509-520.
4. Lanciotti, R. S., Kosoy, O. L., Laven, J. J., Velez, J. O., Lambert, A. J., Johnson, A. J., Stanfield, S.M. & Duffy, M. R. (2008). Genetic and serologic properties of Zika virus associated with an epidemic, Yap State, Micronesia, 2007. Emerging infectious diseases, 14(8), 1232.
5. Duffy, M. R., Chen, T. H., Hancock, W. T., Powers, A. M., Kool, J. L., Lanciotti, R. S., Pretrick, M., Marfel, M., Holzbauer, S., Dubray, C. and Guillaumot, L. (2009). Zika virus outbreak on Yap Island, federated states of Micronesia. New England Journal of Medicine, 360(24), 2536-2543.
6. Cao-Lormeau, V. M., Roche, C., Teissier, A., Robin, E., Berry, A. L., Mallet, H. P., Sall, A.A. and Musso, D. (2014). Zika virus, French polynesia, South pacific, 2013. Emerging infectious diseases, 20(6), 1085.
7. Cauchemez, S., Besnard, M., Bompard, P., Dub, T., Guillemette-Artur, P., Eyrolle-Guignot, D., Salje, H., Van Kerkhove, M.D., Abadie, V., Garel, C. and Fontanet, A. (2016). Association between Zika virus and microcephaly in French Polynesia, 2013–15: a retrospective study. The Lancet, 387(10033), 2125-2132.
8. Musso, D., Nilles, E. J., & Caoβ Lormeau, V. M. (2014). Rapid spread of emerging Zika virus in the Pacific area. Clinical Microbiology and Infection, 20(10).
9. Dupont-Rouzeyrol, M., O'Connor, O., Calvez, E., Daures, M., John, M., Grangeon, J. P., & Gourinat, A. C. (2015). Co-infection with Zika and dengue viruses in 2 patients, New Caledonia, 2014. Emerging infectious diseases, 21(2), 381.
10. Tognarelli, J., Ulloa, S., Villagra, E., Lagos, J., Aguayo, C., Fasce, R., Parra, B., Mora, J., Becerra, N., Lagos, N. and Vera, L. (2016). A report on the outbreak of Zika virus on Easter Island, South Pacific, 2014. Archives of virology, 161(3), 665-668.

11. WHO (World Health Organization), (2016a). Zika virus research agenda. Geneva, Switzerland: 19pp
12. WHO (World Health Organization), (2016b). Zika situation report: neurological syndrome and congenital anomalies. Geneva, Switzerland: 6pp
13. Bhatt, S., Gething, P. W., Brady, O. J., Messina, J. P., Farlow, A. W., Moyes, C. L., Drake, J.M., Brownstein, J.S., Hoen, A.G., Sankoh, O. and Myers, M. F. (2013). The global distribution and burden of dengue. Nature, 496(7446), 504.
14. Hotez, P. J., Alvarado, M., Basáñez, M. G., Bolliger, I., Bourne, R., Boussinesq, M., Brooker, S.J., Brown, A.S., Buckle, G., Budke, C.M. and Carabin, H. (2014). The global burden of disease study 2010: interpretation and implications for the neglected tropical diseases. PLoS neglected tropical diseases, 8(7), e2865.
15. MSP (Ministerio de Salud Pública del Ecuador), (2015). Alerta Epidemiológica: Ante La Posibilidad De Introducción Del Virus Zika En Ecuador. Quito: Ministerio de Salud Pública. http://www.salud.gob.ec/boletin-de-prensa-alerta-epidemiologica-ante-la-posibilidad-de-introduccion-del-virus-zika-en-ecuador/
16. Zambrano, H., Waggoner, J. J., Almeida, C., Rivera, L., Benjamin, J. Q., & Pinsky, B. A. (2016). Zika virus and chikungunya virus coinfections: a series of three cases from a single center in Ecuador. The American journal of tropical medicine and hygiene, 95(4), 894-896.
17. Padilla, O., Rosas, P., Moreno, W., & Toulkeridis, T. (2017). Modeling of the ecological niches of the anopheles spp in Ecuador by the use of geo-informatic tools. Spatial and spatio-temporal epidemiology, 21, 1-11.
18. Perugachy Kindler, J.T., Zapata, J., Ordoñez, E., Toulkeridis, T. and Zapata A. (2020). Ecological Niche Modeling of Vector Species of the American Trypanosomiasis Disease (Chagas), in Continental Ecuador. 7th International Conference on eDemocracy and eGovernment, ICEDEG 2020, 165-174.
19. Toulkeridis, T., Tamayo, E., Simón-Baile, D., Merizalde-Mora, M.J., Reyes –Yunga, D.F., Viera-Torres, M. and Heredia, M. (2020). Climate change according to Ecuadorian academics–Perceptions versus facts. La Granja, 31(1), 21-49
20. Rotela. (2014). Epidemiologìa panorámica: introducción al uso de herramientas geoespaciales aplicadas a la salud pública. Ciudad Autónoma de Buenos Aires: Comisión Nacional de Actividades Espaciales; Ministerio de Planificación Federal Inversión Pública y Servicios Ministerio de Salud de la Nación. 110pp
21. Soberón, J., & Nakamura, M. (2009). Niches and distributional areas: concepts, methods, and assumptions. Proceedings of the National Academy of Sciences, 106(Supplement 2), 19644-19650.
22. Soberón, J., & Peterson, A. (2005). Interpretation of models of fundamenta ecological niches and species distributional areas. Biodiversity Informatics , 1-10.
23. Owens, H. L., Campbell, L. P., Dornak, L. L., Saupe, E. E., Barve, N., Soberón, J., Ingenloff, K., Lira-Noriega, A., Hensz, C.M., Myers, C.E. and Peterson, A. T. (2013). Constraints on interpretation of ecological niche models by limited environmental ranges on calibration areas. Ecological Modelling, 263, 10-18.
24. Bentlage, B., Peterson, A. T., Barve, N., & Cartwright, P. (2013). Plumbing the depths: extending ecological niche modelling and species distribution modelling in three dimensions. Global Ecology and Biogeography, 22(8), 952-961.
25. Qiao, H., Soberón, J., & Peterson, A. T. (2015). No silver bullets in correlative ecological niche modelling: insights from testing among many potential algorithms for niche estimation. Methods in Ecology and Evolution, 6(10), 1126-1136.
26. Peterson, A. T., Papeş, M., & Soberón, J. (2015). Mechanistic and correlative models of ecological niches. European Journal of Ecology, 1(2), 28-38.
27. Timofeev, R. (2004). Classification and regression trees (CART) theory and applications. Humboldt University, Berlin. 40pp
28. Lek, S., & Guégan, J. F. (1999). Artificial neural networks as a tool in ecological modelling, an introduction. Ecological modelling, 120(2-3), 65-73.
29. Nelder, J. A., & Wedderburn, R. W. M. (1972). Generalized linear models. Journal of the Royal Statistical Society. Series A (General), Vol. 135, No. 3 (1972), pp. 370-384
30. Guisan, A., & Thuiller, W. (2005). Predicting species distribution: offerting more than simple habitat models. Ecol Let, 8(9): 993-1009.
31. Phillips, S. J., Anderson, R. P., & Schapire, R. E. (2006). Maximum entropy modeling of species geographic distributions. Ecological modelling, 190(3-4), 231-259.
32. Leathwick, J. R., Elith, J., & Hastie, T. (2006). Comparative performance of generalized additive models and multivariate adaptive regression splines for statistical modelling of species distributions. Ecological modelling, 199(2), 188-196.
33. Nix, H. A., & Busby, J. (1986). BIOCLIM, a bioclimatic analysis and prediction system. Annual report CSIRO. CSIRO Division of Water and Land Resources, Canberra, Australia.
34. Booth, T. H., Nix, H. A., Busby, J. R., & Hutchinson, M. F. (2014). BIOCLIM: the first species distribution modelling package, its early applications and relevance to most current MAXENT studies. Diversity and Distributions, 20(1), 1-9.
35. Segurado, P., & Araujo, M. B. (2004). An evaluation of methods for modelling species distributions. Journal of Biogeography, 31(10), 1555-1568.
36. Tole, L. (2006). Choosing reserve sites probabilistically: A Colombian Amazon case study. Ecological Modelling, 194(4), 344-356.
37. Townsend Peterson, A., Papeş, M., & Eaton, M. (2007). Transferability and model evaluation in ecological niche modeling: a comparison of GARP and Maxent. Ecography, 30(4), 550-560.
38. Giovanelli, J. G., de Siqueira, M. F., Haddad, C. F., & Alexandrino, J. (2010). Modeling a spatially restricted distribution in the Neotropics: How the size of calibration area affects the performance of five presence-only methods. Ecological Modelling, 221(2), 215-224.
39. Elith, J., Graham, C. H., Anderson, R. P., Dudík, M., Ferrier, S., Guisan, A., Hijmans, R.J., Huettmann, F., Leathwick, J.R., Lehmann, A. and Li, J. (2006). Novel methods improve prediction of species' distributions from occurrence data. Ecography, 129-151.
40. Miller, J. (2010). Species Distribution Modeling. Geography Compss, No.46, 490-509.
41. de la Salud SD. Pública, Dirección Nacional de Vigilancia Epidemiológica, Subsistema de vigilancia epidemiológica. Muerte evitable. Gac Epidemiol Semanal. 2015, No. 40: 40-45.
42. Saaty, T. (1980a). Fundamentals of Decision Making and Priority Theory. McGrawHill.
43. Saaty, T. (1980b). The Analytic Hierarchy Process. New York: McGraw-Hill.
44. Stockwell, D., & Peterson, A. (2002). Effects of sample size on accuracy of species distribution models. Ecological Modelling, 148: 1-13.
45. Pearson, R. (2008). Modelling species distributions in Britain: a hierarchical integration of climate and land-cover data. Ecography (27), 285-298.
46. Muñoz, J., & Felicisimo, A. (2012). Modelos de distribución de especies: Una revisión sintética. Universidad de Castilla-La Mancha, España, 4-8.
47. Franklin J. Mapping species distributions: spatial inference and prediction. Cambridge University Press; 2010 January 7.
48. Ghaham, C. (2012). Modelos de distribución de las especies y el desafío de pronosticar distribuciones futuras. Cambio Climático y la Biodiversidad de los Andes Tropicales, 147-186.
49. Zadeh, L.A., 1965: Fuzzy sets. Inf. Control 8: 338–352.
50. Friedman, J. (1991). Multivariate Adaptive Regression Splines (with discussion). The Annals of Statistics , 1-141.
51. Lee, T. S., Chiu, C. C., Chou, Y. C., & Lu, C. J. (2006). Mining the customer credit using classification and regression tree and multivariate adaptive regression splines. Computational Statistics & Data Analysis, 50(4), 1113-1130.
52. Mato, F. and Toulkeridis, T., 2017: The missing Link in El Niño's phenomenon generation. Science of tsunami hazards, 36: 128-144.
53. SNI (Sistema Nacional de Información), (2011). Plan de Ordenamiento Territorial del Gobierno Provincial de Manabí. Quito: Sistema Nacional de Información.
54. SNI (Sistema Nacional de Información), (2014). Plan de Ordenamiento Territorial del Gobierno Provincial de El Oro. Quito: Sistema Nacional de Información.
55. INEC (Instituto Nacional de Estadistica y Censos), (2012). Encuesta de Superficie y Producción Agropecuaria Continua 2012. Quito: Instituto Nacional de Estadística y Censos. http://www.ecuadorencifras.gob.ec/institucional/home/

Received: June 14 2020
Accepted: September 25 2020

RESEARCH / INVESTIGACIÓN

mRNA level of genes related to apoptosis in a colitis model in rats treated with epidermal growth factor

Juan Roca, Hanlet Camacho, Ana Aguilera, Isabel Guillen, Yuneisy Delgado, Yiliam Bermudez, Dania Bacardí, José Suarez Alba, Daniel Palenzuela.

DOI. 10.21931/RB/2020.05.04.8

Abstract: The deregulation of cell death pathways in intestinal epithelial cells could involve the pathogenesis of Inflammatory Bowel Diseases. An increase in apoptosis has been observed in patients who have Ulcerative Colitis. Previous experiments have demonstrated the efficacy of EGF in the healing of ulcerative Colitis and other gastrointestinal mucosa lesions. However, there are not many reports on the molecular characterization of EGF's positive effect on the gastrointestinal mucosa. This work aims to deepen the transcriptional changes induced by EGF in the intestinal epithelium in a colitis model in rats. Samples from the distal colon of an EGF-treated colitis model were collect, followed by an analysis by quantitative PCR of the mRNA of 23 genes related to apoptosis. 57% of the genes analyzed presented statistically significant changes in their mRNA level. Of these, two anti-apoptotic genes increased their mRNA level, while the genes that decreased their mRNA level were pro-apoptotic genes and genes related to the TNFα signal transmission path. Changes in the transcription profile of the genes analyzed could suggest a reduction of apoptosis, which could favor the integrity of the Intestinal Epithelium.

Key words: Animal model, apoptosis, epidermal growth factor, mRNA level, qPCR, Ulcerative Colitis.

Introduction

Inflammatory bowel disease (IBD) is a term that includes two primary forms of the chronic inflammatory intestinal disorder: Crohn's Disease (CD) and Ulcerative Colitis (UC), both of these with prevalence and incidence rates increasing worldwide[1]. IBD is considered a multifactorial disease whose pathogenesis is not fully deciphered. Some hypotheses propose that they result from a deregulation of the intestinal barrier, followed by a pathological activation of the Immune System, leading to chronic inflammation and oxidative stress (OS) of the colon mucosa[2].

The intestinal epithelium (IE) acts as a physical barrier that prevents microorganisms' passage to the lamina propria[3]. The IE is continuously being renewed, and its integrity is conditioned by a balance between the formation of new intestinal epithelial cells (IEC) and senescent IEC's death. On the one hand, the intestinal stem cells (ISC) resident in the crypt of the intestinal epithelium proliferate and differentiate, giving rise to the adult cells that make up the IE, and at the same time, there is cell death and detachment of the IEC that occurs predominantly at the tip of the villi in the Small Intestine or on the luminal surface of the Large Intestine[4].

An increase in cell death in the IE is sufficient to cause intestinal inflammation in the animal model, suggesting that deregulation of cell death pathways in IEC might be involved in IBD's pathogenesis[5,6]. In correspondence with this hypothesis, many apoptotic bodies have been found in biopsies taken from patients suffering from active UC[7].

In mammalian cells, apoptosis is activated by two pathways, intrinsic or mitochondrial and extrinsic or receptor-mediated[8,9].

Proteins of the BcL2 family control the mitochondrial pathway. There are 2 groups of genes within this family. The pro-apoptotic proteins promote apoptogenic factors, such as cytochrome C protein, from the intermembrane space of the mitochondrion into the cytoplasm, triggering apoptosis. The anti-apoptotic proteins block the release of cytochrome C, avoiding apoptosis[8].

Cell death receptors mediate the external pathway. One of the best-studied models is the TNFR1 (TNFα receptor 1); the receptor's union with its ligand initiates a signaling pathway that can lead to inflammation or apoptosis. This route begins with the recruitment of TRADD (TNF Receptor –associated death domain) and RIPK1 (Interacting Kinase Receptor 1) adapter proteins, which form a membrane-bound complex. CIAPs 1 and 2 (cellular inhibitor of apoptosis1 and 2) and TRAF2 or 5 (TNF receptor-associated factor 2 or 5) proteins bind to this complex and polyubiquitinate RIPK1, forming the Complex I that activates the NFKB transcriptional factor, which leads to inflammation and survival. On the contrary, TNFAIP3 (Tumor necrosis factor-alpha-induced protein 3, also known as A20) and CYLD (Cylindromatosis) remove the RIPK ubiquitin tail. The non-ubiquitinate RPK1 bind to FADD (Fas-associated death domain) and procaspase 8, forming complex II that promotes the activation of apoptosis[9,10].

Epidermal Growth Factor (EGF) in enemas has been used successfully in the treatment of distal UC. The healing effect of the EGF in gastrointestinal lesions by oral route has also been demonstrated, but in none of the cases the molecular characterization of the effects of the EGF in the gastrointestinal mucosa has been deepened, and the mechanism that mediates these positive effects of the EGF in UC is not fully clarified[11,12].

To explore the mechanism of action of the healing effect of EGF in UC, the transcription profile of 23 genes related to apoptosis was evaluated in a dextran sulfate sodium salt (DSS) induced colitis animal model treated with human recombinant Epidermal Growth Factor (hrEGF) in a pellet formulation (patent: EP2533758B1).

Although gene expression can be controlled at various levels, it is widely accepted that it generally happens in DNA transcription, and evidence of the degree of a gene's transcription can be observed by measuring the quantity of messenger RNA corresponding to the gene's DNA[13,14]. To study gene transcription variation, real-time PCR is routinely used in molecular

Center for Genetic Engineering and Biotechnology, Cuba.

Corresponding author: juan.roca@cigb.edu.cu

biology to amplify products transcribed from messenger RNA. Quantification of such variation may be relative (based on target gene transcription relative to that of a reference gene (RG)) or absolute (based on an internal or external calibration curve). With relative quantification, RNA transcription change is shown as the factor of regulation between two sample groups using normalization. This process compares the degree of transcription of the genes being studied with two or more RG that have unchanging transcription levels, regardless of cell type and treatment being investigated[15].

Materials and methods

Experimental design

The bio model of DSS-induced Colitis in rats was performed as reported in the literature, following the recommendations implemented in the guide for the use and care of laboratory animals.16,17 Briefly, the experiment consisted of 2 phases. In the first phase, Colitis was induced in all groups (except group I), by administering 8% DSS in drinking water, ad libitum. In a second phase, the DSS administration was interrupted, and the treatment was applied orally with pellet-placebo or pellet-hrEGF in different doses, depending on the group. Biopsies for histopathological evaluation were taken after 5 days of DSS administration in group II and its control group (group I). In groups III, IV, V, and VI treated with pellet-rhEGF or pellet-placebo, samples were taken after 7 days of treatment. Additionally, in treated groups, samples for RNA extraction were also collected.

Male Wistar rats weighing approximately 300-400gr were used. Animals were randomly assigned to the following experimental groups:

Group I: Healthy animals. Five animals were sacrificed on day 6 to obtain excisional biopsies of the distal colon.

Group II: Bio model of Colitis induced with 8% DSS for 6 days. Untreated animals, 5 animals were sacrificed on day 6 to obtain excisional biopsies of the distal colon.

Group III: Bio model of Colitis induced with 8% DSS for 6 days. Afterward, animals were treated with pellet-placebo for 7 days, 5 animals were sacrificed on day 14 to obtain the distal colon's excisional biopsies.

Group IV: Biomodel of Colitis induced with 8% DSS for 6 days. Afterward, animal were treated with pellet-hrEGF 125 µg / capsule / day was administered for 7 days and 5 animals were sacrificed on day 14 to obtain excicional biopsies of distal colon.

Group V: Biomodel of Colitis induced with 8% DSS for 6 days. Afterward, animal were treated with hrEGF 250 µg / capsule/day was administered for 7 days, and 5 animals were sacrificed on day 14 to obtain excisional biopsies of the distal colon.

Group VI: Bio model of Colitis induced with 8% DSS for 6 days. Afterward, animals were treated with- hrEGF 500 µg / capsule/day was administered for 7 days, and 5 animals were sacrificed on day 14 to obtain excisional biopsies of the distal colon.

RNA extraction

Colon biopsies for RNA extraction were stored in AmbionRNAlater (AppliedBiosystems, USA) at –20°C until used. Fragments of approximately 30 mg of colon samples were processed in the Tissue Lyser equipment (Qiagen, Hilden, Germany), and the total RNA was purified with the RNeasy® Plus reagent kit (QIAGEN GmbH, Germany) using the Qiacube platform. RNA performance and quality were determined with the NanoDrop spectrophotometer (NanoDrop Technologies, USA) and the Bioanalyzer Bioanalyzer (Agilent, 2100, USA).

Synthesis of the complementary DNA chain

The complementary DNA (cDNA) chain was synthesized from 1 µg of total RNA, using the Superscript III First-Strand Synthesis Supermix for RT-PCR reagent kit (Invitrogen Technologies, Carlsbad, California, USA), according to manufacturer instructions.

A) Verification of the absence of genomic DNA (gDNA) in the cDNAs by quantitative PCR (qPCR)

Two reactions were performed: one using the cDNAs, diluted 1:10, and the other one with the corresponding RNAs diluted to an equivalent concentration. The same reaction conditions were followed in 20 µL as described in the qPCR section. The primers used in this case amplify a segment of the gene that encodes the protein Catalase (CAT) (table1). Two technical replicas were used for each condition (RNA or cDNA) in each sample. The difference between the Ct (ΔCt), from the average Ct of the RNAs amplification, replicates, and the average Ct of the cDNAs amplification replicates were calculated.

B) Verification by qPCR of the absence of inhibitors in the cDNAs

The qPCRs were performed for the amplification of a calibrator (pGEM-T Vector), using specific primers. The reaction was prepared in a final volume of 20 µL, with 2 µL of cDNA(1:25) or H2O, and 18 µL of a mix, containg10 µL of LightCycler 480 SYBR Green I Master 2x, 8 µL of pGEM-T Vector primer mix(300nM final concentration) and pGEM®-T Vector (2,56 x103 copies per reaction). Negative control reactions were prepared in the same condition, but without adding the pGEM-T Vector.

qPCR and Bioinformatic tool

The Primer3 website application was used to design the qPCR primers with a size of 22 bases, TM= 62 °C, and an average G + C content of 50% (Table 1)[18].

To determine the RG, the geNorm program was used[19]. The housekeeping genes (HSKG) evaluated were: PPIA, MAPK6, MAP2k5, GAPDH YWHAZ, and RPL13A.

The LingReg program (version 11.3, 2009, Amsterdam, Netherlands) was used to estimate the efficiency of qPCR

The qPCR reactions were prepared in a volume of 20 µl, containing 10 µl of the PCR TM Absolute QPCR SYBR Green (Thermo Scientific), 6 µl of primers (70 nM), and 4 µl of cDNA (diluted in a factor of 25).

The reactions were incubated at 95 ° C for 15 min, followed by 40 cycles of 95 ° C for 15 s, 60 ° C for 30 s and 72 ° C for 30 s. On the CapitalBio RT-Cycler001 equipment (CapitalBio Co., Ltd., Beijing, China) and qPCR data analysis was performed using the CapitalBio RT-Cycler Version 2.001 program (CapitalBio Co., Ltd., Beijing, China).

In all cases, qPCR used 3 technical replicas for each biological replica. A total of 23 genes related to apoptosis were evaluated. (Table 1)

The mRNA transcription ratios were calculated using the statistical model "Pair Wise Fixed Reallocation Randomisation Test" implemented in the REST software 2009 v2.0.13 program (Qiagen GmbH, Germany), according to a report by Ptaffl *et al.*; in 2002. For up-regulation, the factor of regulation is equal to the given value in the Randomisation results. In the

Gene Name	Accession No.	Sense Primer 5'-3'	Antisense Primer 5'-3'	Biological function
BAD	NM_022698.1	GACAGGCAGCCAATAACAGTCA	AAGGGCTAAGCTCCTCCTCCAT	Proapoptotic gene
BAX	NM_017059.2	AGAACCATCATGGGCTGGAC	AGATGGTCACTGTCTGCCATGT	Proapoptotic gene
BAK	NM_053812.1	GACGATATTAATCGGCGCTACG	CAGCTGATGCCGCTCTTAAATA	Proapoptotic gene
BID	NM_022684.1	CAGGTGATGAACTGGACCACAG	GGAAGGATGTCTTCACCTCGTC	Proapoptotic gene
BIM	NM_171988.2	GATCGGAGACGAGTTCAATGAG	TTCTCCAGACCAGACGGAAGAT	Proapoptotic gene
BIK	NM_053704.1	ATTTCATGAGGTGCCTGGAGAG	CAGCAAGTCTGTGCATAGCAATC	Proapoptotic gene
NOXA	NM_001008385.1	GTGGAGTGCACCGGACATAACT	TGATCACACTCGTCCTTCAGGT	Proapoptotic gene
TNFAIP3	XM_017589829.1	CGACAGTCAGCACTTTGTACCC	CAGGGTCTGTCAAAAAGTGAACC	Proapoptotic gene
CYLD	NM_001017380.1	ATGACTCTGCCTGGCTCTTCTT	GCAGGTCCTCCAGAGACATCTT	Proapoptotic gene
Pell	NM_001100565.1	CCCAGACAGTGGTGGTTGAATA	ACTGCGTGTCGGAATTACTCTG	Proapoptotic gene
BCL2	NM_016993.1	ACAACATCGCTCTGTGGATGAC	CAGAGACAGCCAGGAGAAATCA	Antiapoptotic gene
cIAP1	NM_021752.2	GCCACTGGTGAGAACTACAGGA	TCCGAATCAATGACAAGTCACC	Antiapoptotic gene
cIAP2	NM_023987.3	AGCGACCTCATTCAGAAACTCC	TGTTCTTCCATCGGTAGAGCTG	Antiapoptotic gene
Xiap	NM_022231.2	TAACCCATTCACTTGGGGAATC	CCTTGAAGTTGAATCCCATTCG	Antiapoptotic gene
BIRC5	NM_022274.1	CTGCGCCTTCCTTACAGTCAA	GGGTCTCCTCGAACTCTTTCTG	Antiapoptotic gene
Cflip	NM_001033864.2	TATAGGGTGCTGCTGATGGAGA	CAGTTCAATCACCAGGTCCAAG	Antiapoptotic gene
TNFR1	NM_013091.1	GCCACGCAGGATTCTTTCTAAG	AGTACCTGAGTCCTGGGGGTTT	Receptor TNFα
FASR	NM_139194.2	TCTTTGCACCTGCACTTGGTAT	TGGGCAGACACGACCTACTG	Receptor FAS
TRADD	NM_001100480.1	CCCAAGAAGAAAGTGGCAATCT	CAGAAACGCAACTGAACGATG	TNFα signaling pathway gene
RIPK1	NM_001107350.1	GAGTCAACTTCCAGGCATCAAG	AGACTCAGTGAAGCCCAGCTTT	TNFα signaling pathway gene
TRAF2	NM_001107815.2	GACCATGTCAGAACGTGCAGTA	CAGCAGTAGGGCCAGATGTTC	TNFα signaling pathway gene
CASP8	NM_022277.1	GGGAGGACATACCCAAACTCAG	TTGACTTGCTGTGCAATCACTG	Initiator Caspase
CASP7	NM_022260.3	CGGTGGAAGCTGACTTTCTCTT	CTGCATGATCTCCAGGTCCTT	Efector Caspase
GAPDH	NM_001256799.2	CAAGTTCAACGGCACAGTCAAGG	ACCAGCATCATCACCCCATTTGATCTTG	Reference gen
MAP2K5	NM_001206804.1	TTGTAAACACAAGCGGACAGGT	CTTTCGGGTGCCATATAAGCAT	Reference gen
MAPK6	NM_002748.3	TTAGTCGGGAAGCACTGGATTT	CCGTTGGGAAAGAGTAGATGCT	Reference gen
RPL13A	NM_001270491.1	TCCGAGCCCCAAGCCGCATTTT	AGCAGGGACCACCATCCGCTTT	Reference gen
YWHAZ	NM_001135699.1	TTGGTGTGTGCTGGCGGGGAAT	TGTGCACGCAGACACACGGTCT	Reference gen
CAT		AAGCGCTTCAACAGTGCTAATG	AGCTGAGCATCTTTCAGGTGGT	Catalase gene Used in the cDNA quality control (absence of gDNA).
pGEM-T Vector		AGCGGATAACAATTTCACACAGGA	GCCAGGGTTTTCCCAGTCACGAC	Used in the cDNA quality control (absence of PCR inhibitors)

Table 1. Sequence of primers used in the qPCR analysis.

case of down-regulation, the regulation factor is illustrated as (-1/factor of regulation). Statistically significant changes were considered those associated with a p-value of less than 0.05[15].

Results and Discussion

Characterization of DSS-induced Colitis in rats and the histological improvement induced by rhEGF treatment

During treatment with 8% DSS, rats in all groups, except those in group I (colitis control group), experienced clinical signs indicating the presence of Colitis such as diarrhea, rectal bleeding, and weight loss (manuscript in preparation).

After sacrificing the animals, the total histopathological score(THS) of mucosa damage was calculated, as previously described, to confirm that the colitis model was established and secondly: the effect of Pellet-rhEGF on the colonic IE[20].

When comparing THS between group II vs group I, an increase in histological damage was detected, confirming the colitis model's reproduction, comparing groups IV, V, and VI (treated with different doses of rhEGF) vs. group III (treated with placebo), shows the effect of rhEGF, at different doses, on the colon mucosa damage. Group IV (dose of 125µg / capsule/ day) did not present significant THS differences concerning group III. However, Groups V and VI (doses of 250 and 500 µg / capsule/day, respectively) did show a significant decrease in histological damage, concerning group III, indicating an improvement of the colon mucosa damage. Additionally, no significant differences were observed between the doses of 250 and 500 µg / capsule/day; therefore, both groups were united to determine the differential transcription profile of genes between the treated group responding to pellet-rhEGF vs. the placebo group[21].

Diferential transcription study

Differential transcription studies by qPCR require a rigorous control in each step of the process, such as the Quality Control of the extracted RNA sand of the synthesized cDNAs, as well as a normalization of the qPCR with RG that ensures that the variation of the levels of mRNA found to respond to real variations in transcription induced by EGF and are not artifacts due to errors made in the workflow. The results of each of these controls are described below:

Quality Control of total RNA purified from distal colon samples

The concentration obtained was in all RNAs greater than 100 ng / µL. The OD 260/280 ratio (protein contamination) was within the established parameters (1.7-2.2). The samples' quality was also examined by microcapillary electrophoresis, whose program established by the Agilent company includes the calculation of the RNA integrity number (RIN). A RIN value greater than 7 was obtained in all RNAs, indicating that they can be used in a qPCR[22]. (table 2, fig.1 supplementary)

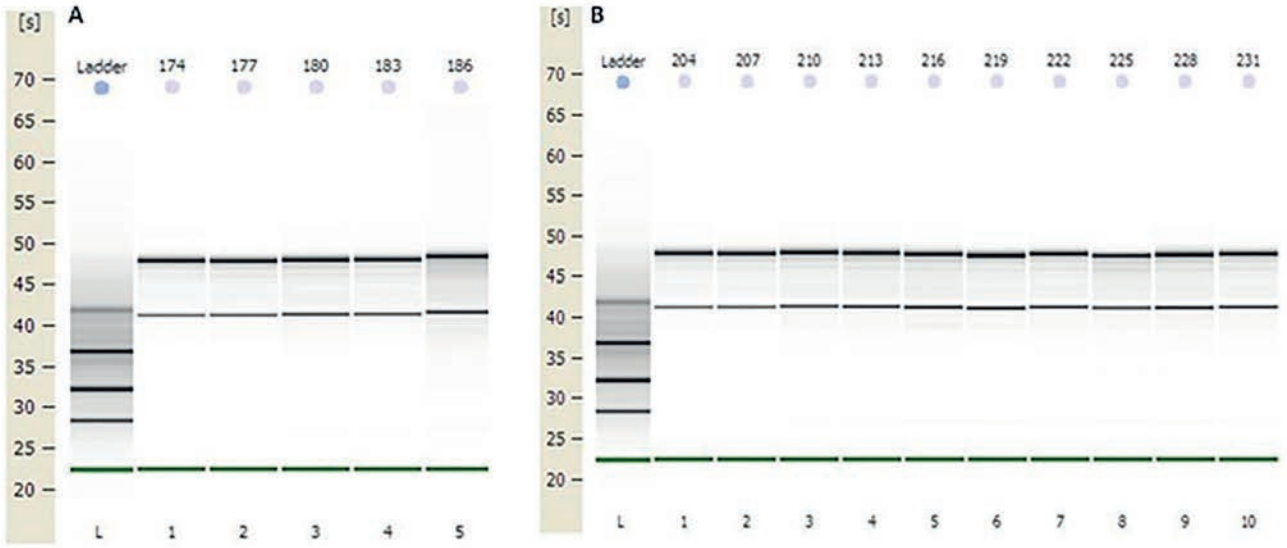

Figure 1. Capillary electrophoresis of total RNA obtained from distal colon tissue. First lane: molecular weight standard (MW ladder). The remaining lanes show the bands corresponding to the 28S and 18S rRNA subunits (retention times of 48 s and 43 s, approximately) of the total RNA of the samples. A) Total RNA from samples: 174, 177, 180, 183, and 186 (Group III). B) Total RNA from samples: 204, 207, 210, 213, 216, 219, 222, 225, 228 and 231 (Groups V and VI).

Group	Code	Conc ng/uL	260/280	260/230	RIN
III (DSS+Pellet Control)	174	1444,98	2,11	2,16	10
	177	569,95	2,13	2,19	10
	180	1663,03	2,01	2,26	9,5
	183	1072,95	2,11	2,23	9,4
	186	719,8	2,13	2,02	9,5
V DSS+ Pellet EGF 250 mg/Kg	204*	166,44	2,08	2,07	9,7
	207	1458,5	2,08	2,16	7,6
	210*	297,2	2,01	2,53	9,8
	213	1211,42	2,1	2,27	9,6
	216	1161,54	2,1	2,23	9,8
VI DSS+ Pellet EGF 500 mg/Kg	219	1242,7	2,14	2,45	9,2
	222	490,14	2,24	2,29	9,8
	225	1030,15	2,16	2,43	9,6
	228	958,21	2,16	2,46	9,4
	231	1084,65	2,14	2,3	10

Table 2. Results of the quality control of the total RNA extraction. The observed values correspond, from left to right, to: identification number of the samples, the concentration in ng / µL, the OD 260/280, 260/230 ratio and the RIN value (RNA integrity) of each one. of the samples. * means that for their total amount of RNA, they were depleted in previous studies.

Quality control of cDNA obtained from total RNAs

To standardize qPCR's initial conditions, it is necessary to determine several parameters such as the absence of gDNA and qPCR inhibitors in the synthesized cDNAs.

A) Verification of absence of gDNA in samples of complementary DNA by qPCR

To verify that the cDNAs met this condition, qPCRs were performed with both RNAs extractions and their corresponding cDNAs, using a set of primers that amplifies a segment of CAT gene. Hybridization of these primers in the same exon of CAT gene makes it possible to efficiently amplify the gene, both in the cDNA samples and the contaminating gDNA, if it exists, obtaining in both cases a product with the same amplification profile. The modular value of the ΔCt was more than 7 in all cases, which ensures that the gDNA if it exists, will not interfere with the Qpcr[23]. (table 3, supplementary).

B) Verification by qPCR of the absence of inhibitors in the cDNAs

To verify the absence of inhibitors in the cDNA samples, qPCRs were performed using a calibrator. The amplification of this calibrator is produced with high efficiency and reproducibility of the Ct values. Therefore, a decrease in the qPCR Ct of the calibrator "contaminated" with cDNA would indicate inhibitors' presence.

The modular value of ΔCt of the reactions containing cDNA (amplification reaction of the pGEM®-T Vector "contaminated" with cDNA) and those containing H2O (amplification reaction of the pGEM®-T Vector "not contaminated") is less than 1 in all cases (table 4, supplementary). Therefore, it can be stated that there is no presence of inhibitors in any of the analyzed cDNAs[23].

Selection of RG

The mean expression stability values (M) of an RG must be less than 1.5 for its expression could be considered stable[19]. The six HKGs evaluated showed M values less than 0.78. The 3 most stable genes (GAPDH, MAPK6, and MAP2K5) were selected as RGs.16 (fig. 2 supplementary)

Figure 2. Graphic of the stability analysis in the expression of the HKGs. The most stable genes are located to the right.

Transcription profile

As explained in materials and methods, the mRNA transcription ratios were calculated using the statistical model "Pair

Sample name	Sample content	Average Ct replicas	l ΔCl t (Ct ARN- Ct ADNc)
174	RNA y Oligo CAT	36.81	10.96
177	RNA y Oligo CAT	36.04	10.54
180	RNA y Oligo CAT	36.31	8.05
183	RNA y Oligo CAT	36.02	10.07
186	RNA y Oligo CAT	36.90	7.99
207	RNA y Oligo CAT	40	12.82
213	RNA y Oligo CAT	40	15.64
216	RNA y Oligo CAT	36.48	10.04
219	RNA y Oligo CAT	35.19	7.92
222	RNA y Oligo CAT	40	15.35
225	RNA y Oligo CAT	33.45	7.28
228	RNA y Oligo CAT	40	16.85
231	RNA y Oligo CAT	33.36	8.4
174	cDNA y Oligo CAT	25.85	
177	cDNA y Oligo CAT	25.50	
180	cDNA y Oligo CAT	28.27	
183	cDNA y Oligo CAT	25.95	
186	cDNA y Oligo CAT	28.92	
207	cDNA y Oligo CAT	27.19	
213	cDNA y Oligo CAT	24.37	
216	cDNA y Oligo CAT	26.45	
219	cDNA y Oligo CAT	27.27	
222	cDNA y Oligo CAT	24.66	
225	cDNA y Oligo CAT	26.18	
228	cDNA y Oligo CAT	23.16	
231	cDNA y Oligo CAT	24.96	

Table 3. Check for absence of gDNA by qPCR. The Ct values correspond to the amplification from the cDNA or from the total RNAs (diluted to a concentration equivalent to that present in the cDNAs) of each sample. The ΔCt are the difference between the average Ct obtained from the replications of the reactions prepared with RNA and the average Ct resulting from the replications of the reactions prepared with RNA with the corresponding cDNAs.

Wise Fixed Reallocation Randomisation Test" implemented in REST software. REST© allows a comparison of target genes with reference genes in two experimental groups. Relative quantification of a target transcript is based on the mean CP deviation of control and sample group, normalized by a reference transcript.

The Randomisation test is a useful alternative to standard parametric tests for analyzing the experimental data. It's results allow us to determine if the specific mRNA in the sample group in comparison with the control group is up- or down-regulated and illustrates the factor of regulation and if this up- or down-regulation is significantly different or not[24].

In the comparison of transcription profile found in EGF treated rats that respond to EGF (Group V + VI) vs. placebo (group III), the following change was observed:

Of the genes analyzed (Table 1), nine pro-apoptotic genes showed a statistically significant decrease in mRNA level including, both those related to mitochondrial apoptosis: BAD (Bcl2-associated death promoter), BAX (Bcl2-associated X protein), BAK (BCL2-antagonist / killer 1), BCL211 (BCL2 like 11, also known as BIM), BIK (Bcl-2-interacting killer), BID (BH3 interacting domain death agonist,), NOXA (NADPH oxidase activator), as with external apoptosis: A20 and CYLD (fig.3).

Figure 3. mRNA regulation factor in colon biopsies of apoptosis related genes evaluated by qPCR. Data are represented as regulation factor of mRNA level of animal model treated with pellet-hrEGF vs animal model treated with pellets-placebo (normalized with the selected RGs), obtained with a Pair Wise Fixed Reallocation Randomization Test implemented in REST software 2009 v2.0.13 (Qiagen GmbH, Germany). For up-regulation, the factor of regulation is equal to the given value in the Randomization results. In the case of down-regulation, the regulation factor is illustrated as (-1/ factor of regulation). * mean statistically significant variations in mRNA levels

The balance between pro-apoptotic and anti-apoptotic proteins is what determines whether mitochondrial apoptosis occurs or not. The decrease mRNA level of 7 pro-apoptotic

Sample name	Sample content	Average Ct replicates	ΔCt (Ct C + - Ct samples)
174	cDNA and Calibrator	22.87	0.225
177	cDNA and Calibrator	22.85	0.205
180	cDNA and Calibrator	22.81	0.165
183	cDNA and Calibrator	22.82	0.225
186	cDNA and Calibrator	22.825	0.18
207	cDNA and Calibrator	22.89	0.245
213	cDNA and Calibrator	22.89	0.245
216	cDNA and Calibrator	22.98	0.335
219	cDNA and Calibrator	22.86	0.215
222	cDNA and Calibrator	22.945	0.3
225	cDNA and Calibrator	22.935	0.29
228	cDNA and Calibrator	22.955	0.31
231	cDNA and Calibrator	23	0.355
C- ADNc	C- cDNA and Calibrator	22.84	0.195
C + Calibrator	H_2O and Calibrator	22.645	0

Table 4. Values of Ct and ΔCt, obtained in the check of inhibitors by qPCR. In column three: the average Ct values of the positive control "contaminated" with the samples and the calibrator. In column four: Modular value of the difference in average Ct of the positive control and the control "contaminated" with the cDNAs (ΔCt = ł (Ct (calibrator) -Ct (calibrator cDNA) ł).

genes of mitochondrial apoptosis might suggest a shift in the balance of apoptosis regulation, favoring the decrease in mitochondrial apoptosis[25,26].

The RPK1 protein acts at the crossing of the pathways towards apoptosis or inflammation. Its degree of ubiquitination determines whether inflammation or apoptosis takes place. The non-ubiquitinate form induces apoptosis[9,10]. Therefore, the decrease in the TNFAIP3 and CYLD genes that code for enzymes that remove the ubiquitin tail from RIPK1 suggests a decrease in external apoptosis. Likewise, the statistically significant decrease of the TNFR1 and RPK1 genes involved in transmitting the TNFα signal argue for a decrease in both inflammation and external apoptosis.

The significant increase of the mRNA level of XIAP (X-linked apoptosis inhibitor) and BIRC5 (baculoviral inhibitor of repeat-containing apoptosis 5, also known as survivin), could also contribute to a reduction of apoptosis. Proteins codes by these anti-apoptotic genes can inhibit the catalytic activity of the effector caspases 3, 7 and the initiator caspase 9 (fig. 3)[27,28].

Healing of the intestinal mucosa is a marker of remission and a predictor of long-term positive IBD results[29]. Despite this, medications currently approved for the treatment of IBD can inhibit the repair of the IE ulcers[30]. The development of biological therapies such as growth factors that accelerate the healing process of ulcers of the intestinal epithelium, then constitute an attractive therapeutic objective. On the other hand, growth factors have been associated with cancer, and this has caused concern that its use could increase the risk of Colitis associated cancer(CAC), which has limited the progress of UC therapy with the EGF[31]. It is also reported that decreased apoptosis is an essential mechanism in carcinogenesis and the cancer resistance to chemotherapy[32].

However, the main mechanism that links inflammation to preneoplastic genetic alterations is the chronic OS, which constitutes a constant danger of damage to the IE, causing mutations in DNA as well as damage to cellular proteins and lipids[33]. Consequently, it has been shown that direct or indirect inhibition of OS avoid DNA damage and decreases the development of intestinal tumors[34].

A group of genes associated with the development of CAC, such as cytokines: IL-6, IL-1b, TNFα, and transcription factors NFKB and STAT3, are reported[34]. Our group has recently reported that these genes, as well as other genes associated with inflammation and OS, significantly decrease their transcription in colon biopsies of this colitis model treated with hrEGF[21]. Therefore, a decrease in IEC apoptosis, far from assuming an increased risk of CAC, could reduce this cancer risk. This is consistent with other studies in animals that indicate that activating the EGF pathway could reduce CAC's long-term risk in UC[35]. All these changes in the transcription profile of the analyzed genes could suggest a decrease of apoptosis in the IEC, which could favor IE's integrity and, therefore, reduce inflammation, supporting the use of EGF for the treatment of UC in its initial stage. (Fig. 4)

Figure 4. Scheme on the effect in apoptosis of hrEGF in the treatment of ulcerative Colitis in an induced model in rats with DSS.

Despite these results observed in a model of Colitis in rats, for the use in humans of therapies of this type, it would always be necessary to deepen the question of drug biosecurity.

A limitation of this gene transcription analysis in this study in experimental Colitis is that at the moment, the results of proteomics studies that support these results are not available. Despite this, our results constitute a snapshot of the EGF-induced transcriptional activity in genes related to apoptosis.

Conclusions

In this colitis model in rats, hrEGF induces the IEC a decrease in the mRNA level of pro-apoptotic genes and an increase in the mRNA level of anti-apoptotic genes. This could reduce apoptosis in the intestinal epithelium, favoring the healing of typical colitis ulcers. The previous mechanism could at least partly explain the previous reports of the positive effect of EGF in ulcerative colitis therapy.

Bibliographic references

1. M'Koma AE. Inflammatory Bowel Disease: An Expanding Global Health Problem. Clinical Medicine Insights: Gastroenterology 2013, vol6: 33–47. DOI: 10.4137/CGast.S12731
2. Katsanos KH and Papadakis A. Inflammatory Bowel Disease: Updates on Molecular Targets for Biologics. Gut and Liver. 2017, Vol. 11(4): 455-463. https://doi.org/10.5009/gnl16308
3. Okamoto, R. and Watanabe, M. Role of epithelial cells in the pathogenesis and treatment of inflammatory bowel disease. J Gastroenterol (2016) 51(1): 11-21. DOI 10.1007/s00535-015-1098-4.2)
4. Van der Flier LG and Clevers H. Stem Cells, Self-Renewal, and Differentiation in the Intestinal Epithelium. Annu. Rev. Physiol. 2009. 71:241–60. DOI: 0.1146/annurev.physiol.010908.163145
5. Delgado ME, Grabinger T and Brunner T. Cell death at the intestinal epithelial front line. FEBS Journal 2016 vol 283: 2701–2719. doi:10.1111/febs.13575
6. Blander JM: Death in the intestinal epithelium-basic biology and implications for inflammatory bowel disease. The FEBS Journal, 2016, vol 283: 2720–2730. doi:10.1111/fe bs.13771
7. Hagiwara C, Tanaka M, and Kudo H, "Increase in colorectal epithelial apoptotic cells in patients with ulcerative colitis ultimately requiring surgery," Journal of Gastroenterology and Hepatology, 2002, vol. 17 (7): 758–764.
8. Duprez L, Wirawan E, Vanden Berghe T and Vandenabeele P. Major cell death pathways at a glance. Microbes and Infection 2009, vol 11: 1050-1062. doi:10.1016/j.micinf.2009.08.013
9. Declercq W, Vanden Berghe T and Vandenabeele P." RIP Kinases at the Crossroads of Cell Death and Survival ". Cell 2009. Vol 138:229-232. DOI 10.1016/j.cell.2009.07.006
10. Vanden Berghe T, Kaiser WJ, Bertrand MJM, and Vandenabeele P. Molecular crosstalk between apoptosis,necroptosis, and survival signaling.Molecular & Cellular Oncology. 2015. Vol 2(4): e975093-1- e975093-12. http://dx.doi.org/10.4161/23723556.2014.975093
11. Atul Sinha A, Nightingale J, West KP, Berlanga J and Playford RJ. "Epidermal Growth Factor Enemas with Oral Mesalamine for Mild-to-Moderate Left-Sided Ulcerative Colitis or Proctitis". Engl J Med 2003; 349:350-357
12. Kuwahara Y, Sunagawa Y, Imoto Y and Okabe S. "Effects of Orally Administered Human Epidermal Growth Factor on Natural and Delayed Healing of Acetic Acid-Induced Gastric Ulcers in Rats". The Japanese Journal of Pharmacology. 1990; 52(1): 164-166
13. Lodish H, Berk A, Matsudaira P, Kaiser C. Molecular Cell Biology. 5th ed. New York: W. H.Freeman; 2003 Aug 1. 973 p.
14. Berg JM, Tymoczko JL, Stryer L. Biochemistry. 5th ed. New York: W. H. Freeman; 2002 Feb 15.1100 p.
15. Michael W. Pfaffl, Graham W. Horgan, Leo Dempfle. Relative expression software tool (REST©) for group-wise comparison and statistical analysis of relative expression results in real-time PCR. Nucleic Acids Research. 2002, Volume 30, Issue 9. https://doi.org/10.1093/nar/30.9.e36
16. Solomon L, Mansor S,Mallon P, Donnelly E, Hoper M, Loughrey M, et al. "The dextran sulphate sodium (DSS) model of colitis: an overview". Comp Clin Pathol.2010; 19:235–9.DOI 10.1007/s00580-010-0979-4.

17. Programa para el Uso y Manejo del Animal de Laboratorio con fines Experimentales y para el Control de Productos Biotecnológicos del Centro de Ingeniería Genética y Biotecnología de la Habana, Cuba. 2016.
18. Rozen S, Skaletsky HJ. "Primer3". 1998; Code available at http://www-genome.wi.mit.edu/genome_software/other/primer3.htm
19. Vandesompele J, De Preter K, Pattyn F, Pope B, Van Roy N, De Paepe et al. "Accurate normalization of real-time quantitative RT-PCR data by geometric averaging of multiple internal control genes". Genome Biologt. 2002; vol3(7): 0034.1-11.
20. FitzGerald AJ, Puc M, Marchbank T, Westley BR, Mayc FEB, Boyle J, et al. "Synergistic effects of systemic trefoil factor family 1 (TFF1) peptide and epidermal growth factor in a rat model of colitis". Peptides 25.2004, vol2004: 793–801. DOI:10.1016/j.peptides.2003.12.022
21. Roca J, Camacho H, Guillen IA, Aguilera A, Bermudez Y, Palenzuela DO, et al. Pharmacogenomic study of EGF treatment in a rat DSS-induced colitis animal model. Biotecnol Apl. 2019;vol 36(3):3211.
22. Fleige, S., Pfaffl M.W. (2006). "RNA integrity and the effect on the real-time qRT-PCR performance". Mol Aspects Med, 2006; vol27(2–3),126–39.
23. Bustin, S., Benes, V., Garson, J., Hellemans, J., Huggett, J., Kubista, M., Mueller, R., Nolan, T., Pfaffl, M., Shipley, G., Vandesompele, J. y Wittwer, C. "The MIQE Guidelines: Minimum Information for Publication of Quantitative Real-Time PCR Experiments". Clinical Chemistry. 2009; vol 55(4): 611–622
24. Horgan,G.W. and Rouault,J. Introduction to Randomisation Tests. 2000 Biomathematics and Statistics Scotland.
25. Hengartner, M.O. "Biochemistry of apoptosis" Nature. 2000; vol 407: 770-776. DOI:10.1038/35037710
26. Sharma HP., Jain P. and Amit P." APOPTOSIS (PROGRAMMED CELL DEATH) - A REVIEW". World Journal of Pharmaceutical Research. 2014; vol3(4): 1854-1872.
27. Laurence DD, Dupoux A and Cartier J. IAPS: More than just inhibitors of apoptosis proteins. Cell Cycle. 2008, vol7(8): 1036-1046, DOI: 10.4161/cc.7.8.5783.
28. Owens TW, Gilmore AP, Streuli CH, Foster FM "Inhibitor of Apoptosis Proteins: Promising Targets for Cancer Therapy". J Carcinogene Mutagene 2013;S14: 004. doi:10.4172/2157-2518.S14-004.
29. Neurath, M. F. & Travis, S. P. L. Mucosal healing in inflammatory bowel diseases: a systematic review. Gut 61, 1619–1635 (2012). DOI: 10.1136/gutjnl-2012-302830.
30. Jung, S., Fehr, S., Harder-d'Heureuse, J., Wiedenmann, B. & Dignass, A. U. Corticosteroids impair intestinal epithelial wound repair mechanisms in vitro. Scand. J. Gastroenterol. 36, 963–970 (2001).
31. Garrido JB, Hernández-Calleros J, I García-Juárez I, Yamamoto-Furusho JK." Growth Factors as Treatment for Inflammatory Bowel Disease: A Concise Review of the Evidence Toward Their Potential". The Saudi Journal of Gastroenterology. 2009; vol. 15(3): 208-12. DOI: 10.4103/1319-3767.54742.
32. Chen L, Zeng Y and Zhou SF "Role of Apoptosis in Cancer Resistance to Chemotherapy", 2018. DOI: 10.5772/intechopen.80056
33. Foersch S, Neurath MF." Colitis associated neoplasia: molecular basis and clinical Translation". Cell. Mol. Life Sci. 2014; vol71: 3523–35. DOI 10.1007/s00018-014-1636-x.
34. Ferguson LR. "Chronic inflammation and mutagenesis". Mutat Res 2010; vol 690:3–11. doi:10.1016/j.mrfmmm.2010.03.007
35. Dube PE, Liu CY, Girish N, Washington MK, Polk DB. Pharmacological activation of epidermal growth factor receptor signaling inhibits colitis-associated cancer in mice. Sci Rep. 2018; 8(1):9119

Received: Aug 22 2020
Accepted: Sept 20 2020

RESEARCH / INVESTIGACIÓN

Exploración de la actividad antibacteriana de Metformina frente a *Escherichia coli*, *Staphylococcus aureus* y *Pseudomonas aeruginosa*

Exploration of the antibacterial activity of Metformin against *Escherichia coli*, *Staphylococcus aureus* and *Pseudomonas aeruginosa*

Pool Marcos-Carbajal[1,2], Christian Allca-Muñoz[2,3], Ángel Urbano-Niño[2], Alberto Salazar-Granara[2,4]
DOI. 10.21931/RB/2020.05.04.9

Resumen: El objetivo del estudio es determinar la actividad antibacteriana de Metformina frente a *Escherichia coli*, *Staphylococcus aureus* y *Pseudomonas aeruginosa*. Se evaluó la actividad antibacteriana mediante la técnica de Kirby Bauer. Se utilizó cepas de *Escherichia coli* (ATCC 25922), *Staphylococcus aureus* (ATCC 25923) y *Pseudomonas aeruginosa* (ATCC 27853), las cuales se expusieron a Metformina en concentraciones de 250 mg y 500 mg, Ciprofloxacino (CIP) 5 µg, Imipenem (IPM) 10 µg, y Cefoxitin (FOX) 30 µg. Frente a *Escherichia coli*, *Staphylococcus aureus* y *Pseudomonas aeruginosa* se presentó un halo de inhibición de 6 mm. para Metformina 250 mg, 6 mm. para Metformina 500 mg, y un halo de inhibición >25 mm. con el uso de Ciprofloxacino 5 µg, Cefoxitin 30 µg, e Imipenem 10 µg respectivamente. En conclusion, *In vitro* Metformina a dosis de 250 y 500 mg, no presentó efecto antibacteriano frente a *Escherichia coli*, *Staphylococcus aureus* y *Pseudomonas aeruginosa*.

Palabras clave: Antibacterianos, Metformina, prueba de sensibilidad microbiana.

Abstract: The aim of this study was to determine the antibacterial activity of Metformin against *Escherichia coli*, *Staphylococcus aureus*, and *Pseudomonas aeruginosa*. Antibacterial activity was evaluated using the Kirby Bauer technique. Strains of *Escherichia coli* (ATCC 25922), *Staphylococcus aureus* (ATCC 25923), and *Pseudomonas aeruginosa* (ATCC 27853) were used, which were exposed to Metformin at a concentration of 250 mg and 500 mg, Ciprofloxacin (CIP) 5 µg, Imipenem (IPM) 10 µg, and Cefoxitin (FOX) 30 µg. Regarding *Escherichia coli*, *Staphylococcus aureus*, and *Pseudomonas aeruginosa*, an inhibition halo of 6 mm was presented for Metformin 250 mg, 6 mm. for Metformin 500 mg, and an inhibition halo> 25 mm. with the use of Ciprofloxacin 5 µg, Cefoxitin 30 µg, and Imipenem 10 µg respectively. In conclusion, *in vitro*, Metformin at doses of 250 and 500 mg had no antibacterial effect against *Escherichia coli*, *Staphylococcus aureus*, and *Pseudomonas aeruginosa*.

Key words: Antibacterial, metformin, microbial sensitivity test.

Introducción

Uno de los grandes descubrimientos del siglo XIX fue la terapia antibacteriana descubierta por Alexander Fleming en el año 1928[1]. Así es como se iniciaría su uso en la clínica para diferentes intervenciones importantes para evitar enfermedades infecciosas. Sin embargo, aún en el siglo XXI muchas de estas enfermedades infecciosas siguen siendo causa de muerte en el mundo[2]. Para el 2016 se identificó que las enfermedades infecciosas respiratorias encabezan la lista como la enfermedad transmisible con mayor letalidad en el mundo, seguida por enfermedades diarreicas[3].

En el campo de los antibióticos, con la aparición de la resistencia a la actualidad, este representa un problema clínico considerable, debido a que las bacterias desarrollan la capacidad para sobrevivir en concentraciones de antibiótico que inhiben/matan a otras de la misma especie[4]. Capacidades como la resistencia a β-lactámicos en las bacterias Gram-negativos por la producción de β-lactamasas, y Gram-positivos desarrollaron resistencia por medio de modificaciones al sitio de acción de Proteínas Fijadoras de Penicilina (PBP)[5].

Hoy en día una gran mayoría de cepas de *Staphylococcus aureus* han desarrollado resistencia a la Meticilina, en España cerca del 25% de los aislamientos de hemocultivos presentan resistencia. Asimismo, *Pseudomonas aeruginosa* ha adquirido resistencia a una amplia gama de antibióticos como Piperacilina, Tazobactam, fluoroquinolonas, aminoglucósidos, entre otros[6].

Para el año 2017 patógenos como *Enterobacterias* y *Pseudomonas aeruginosa* fueron clasificadas en el nivel de prioridad crítico para la búsqueda de nuevas drogas antibacterianas, al igual con *Staphylococcus aureus*, *Helicobacter pylori*, *Campylobacter*, *Salmonella* y *Neisseria gonorrhoeae* con un nivel de prioridad alto[7].

Todo esto resulta un grave problema, debido a que las industrias farmacéuticas poco a poco van dejando los proyectos propuestos como el desarrollo de nuevos fármacos contra bacterias resistentes o le dedican una escasa cantidad de recursos a la investigación de nuevos antibióticos. Esto se debe a que existe una baja rentabilidad de estos fármacos en comparación con otros fármacos que atacan enfermedades de mayor índice mundial como la diabetes[8].

Actualmente, solo 5 laboratorios se dedican al estudio de nuevos fármacos antibacterianos[9]. En 1998 había en el mercado mundial de 20 nuevos antibióticos y en el 2011 había únicamente 4, es decir una disminución de un 75% en la disponibilidad de nuevos antibióticos[10]. Sin embargo, la resistencia a cada antibiótico utilizado en la práctica clínica se ha incrementado, con independencia de la clase química molecular de la droga[11].

Una estrategia para la búsqueda de nuevos antibióticos, es buscar el efecto pleiotrópico de drogas conocidas y en actual uso clínico terapéutico. Es el caso de la Metformina, un medicamento común utilizado en primera línea en el tratamiento de

[1] Universidad Peruana Unión, Escuela Profesional de Medicina Humana, Laboratorio de Investigación en Biología Molecular, Perú.
[2] Universidad San Martin de Porres, Facultad de Medicina Humana, Centro de Investigación de Medicina Tradicional y Farmacología, Perú.
[3] Universidad San Martin de Porres, Facultad de Medicina Humana, Centro de Investigación de Medicina Tradicional y Farmacología, Perú.
[4] Sociedad Peruana de Farmacología y Terapéutica Experimental - SOPFARTEX.
Corresponding author: poolmarcos@upeu.edu.pe

la Diabetes Mellitus tipo II. Resulta interesante el antecedente de un estudio de medicina traslacional que prueba cómo la Metformina actúa inhibiendo un factor de resistencia de *Mycobacterium tuberculosis*, proponiéndose un potencial efecto contra este patógeno[12,13].

El propósito del presente trabajo fue investigar la actividad antibacteriana de la Metformina sobre cepas ATCC de *Escherichia coli*, *Staphylococcus aureus* y *Pseudomonas aeruginosa*.

Materiales y métodos

Diseño y población de estudio

Estudio es de tipo experimental *in vitro*. El Estándar de clorhidrato de Metformina (material de referencia certificado) fue adquirido por la empresa Sigma-Aldrich con certificado de análisis (Producto número: PHR 1084) y proporcionado por el Centro de Investigación en Medicina Tradicional y Farmacología). La parte microbiología fue realizada en los Laboratorios de Investigación en Biología Molecular de la Escuela Profesional de Medicina Humana de la Universidad Peruana Unión. Se utilizaron cepas bacterianas ATCC (American Type Culture Collection, Microbiologics, St. Cloud, Minnesota USA) *Escherichia coli* 25922, *Staphylococcus aureus* 25923 y *Pseudomonas aeruginosa* 27853. Se utilizó los siguientes discos de antibióticos (Bioanalyse, İvedik Osb/Yenimahalle, Turquía), Ciprofloxacino (CIP) 5 µg, Imipenem (IPM) 10 µg y Cefoxitin (FOX) 30 µg.

Resuspensión del Estándar de Metformina

Se pesó con precisión 12.5 mg y 25 mg de Metformina (fármaco crudo) y se disolvieron en 0,5 ml de metanol para obtener la concentración de 250 µg / 10 µl y 500 µg / 10 µl.

Fase microbiológica

Se verificó la viabilidad de cada uno de los microorganismos a ensayar, para la preparación del inóculo se partió de un cultivo de 18 a 24 h en ATS (Agar Tripticasa Soya) para bacterias a 37°C. A partir de estos cultivos en crecimiento activo, se tocan tres a cinco colonias y se resuspenden en 5 mL de solución salina estéril (NaCl 0,85%). El resultado de la suspensión se homogeneizó durante 15 segundos y su turbidez se ajustó a 0,5 de la escala Mc Farland (1.5 x 108 ufc/ml). La técnica está basada en el método originalmente descrito por Bauer *et al.*[14]. Se procedió a impregnar cada papel-disco estéril de 6 mm de diámetro (papel filtro Whatman #4) con 10 µL de cada concentración de 250 µg y 500 µg de Metformina. El estándar de Metformina y se dejó secar el papel-disco para permitir su evaporación.

Se sembraron en placas de Petri con Agar Müeller-Hinton (AMH) sobre la superficie de las cepas de *Pseudomonas aeruginosa* ATCC 27853, *Staphylococcus aureus* ATCC 25923 y *Escherichia coli* ATCC 25922 respectivamente. Se hisoparon uniformemente y se incubaron en una estufa a 37 °C de temperatura durante 24 horas. Además, se colocó como control negativo un disco de papel Whatman #4 con 10 µL de agua destilada y como control positivo se usó imipenem en concentración de 10 mcg, cefoxitina en concentración de 10 mcg y ciprofloxacino en concentración de 5 mcg[12].

Al final del período, las zonas de inhibición formadas se midieron en milímetros usando el vernier. Las zonas de inhibición de menos de 12 mm de diámetro no se consideraron para el análisis de la actividad antibacteriana. Para cada concentración, se realizaron 6 réplicas.

Análisis estadísticos

Se presenta los resultados mediante gráficos de barras, expresados mediante valores absolutos. Se empleó como soporte informático el programa Microsoft Excel Versión 2010.

Resultados

En este estudio se utilizó como parámetro de medición el diámetro de la zona de inhibición (mm) para evaluar la propiedad antimicrobiana del medicamento Metformina. La dilución del estándar de Metformina fue enfrentada contra *Escherichia coli* ATCC 25922, *Staphylococcus aureus* ATCC 25923 y *Pseudomonas aeruginosa* ATCC 27853. La zona de inhibición fue de 6 mm (resistente) para todas cepas bacterianas y para el control negativo. También se utilizaron controles positivos que produjeron un halo de inhibición de > 25 mm (sensible) para cada ensayo con 6 repeticiones de cada uno de ellos (Ver Figuras 1, 2, 3). El fármaco Metformina no mostró actividad antimicrobiana a 250 ug/ µL y 500 ug/ µL.

Discusión

Entre los principales patógenos que destaca la OMS para la investigación de nuevos antibióticos para combatir esta enfermedad, están la *Pseudomonas aeruginosa*, *Staphylococcus aureus* y enterobacterias multidrogoresistentes[7]. Hoy en día existen laboratorios aun investigando nuevos antibióticos, pero solo dos de estos presentan una actividad frente a bacterias Gramnegativas multirresistentes y otras se encuentran aún en la fase clínica uno, categorizada como "posible agente activo"[15]. Después de la aparición de estos patógenos resistentes a múltiples drogas, la investigación de nuevas alternativas de antibioticoterapia ha llevado al reconocimiento del potencial de drogas antibacterianas conocidas como por ejemplo para el tratamiento de pacientes con diabetes que es la Metformina[12,16].

Es así como surge evidencia científica que logra demostrar que la Metformina podría presentar un efecto sobre el desarrollo de una mejoría en la inmunidad innata[17]. Diferentes tipos de bacterias afectan las vías respiratorias, sin embargo, el uso de Metformina logró disminuir la hiperglucemia inducida por *Pseudomonas aeruginosa*18. Aumentando la resistencia eléctrica transepitelial, es otro mecanismo como la Metformina logra disminuir la hiperglucemia inducida por *Staphylococcus aureus*, ya que esta como principal función tiende a disminuir la resistencia eléctrica transepitelial para lograr el eflujo de glucosa paracelular[19].

Por otra parte, diferentes estudios demostraron que el uso de Metformina en dosis de 250 mg, 300 mg, 400 mg y 500 mg reveló tener un efecto contra las diferentes cepas de *Escherichia coli*, *Staphylococcus aureus*, *Pseudomonas aeruginosa*, *Saccharomyces cerevisiae*, *Candida albicans* y *Aspergillus niger*[20-22] (Tabla 1).

Estudios adicionales han demostrado también lograr una inhibición del crecimiento bacteriano induciendo la inactivación de receptores como LasR y rhlR que desencadenan a la producción de piocianina, hemolisina, proteasas y elastasas que confieren a la *Pseudomonas aeruginosa* su capacidad de motilidad y resistencia frente al estrés oxidativo[23]. Incluso el uso de nanotubos de carbono en adición con metformina logró presentar una actividad inhibitoria frente a *Escherichia coli*[24].

Sin embargo, los resultados del presente estudio demostraron que el estándar de Metformina en concentraciones de 250 mg y 500 mg no mostró una actividad antibacteriana con-

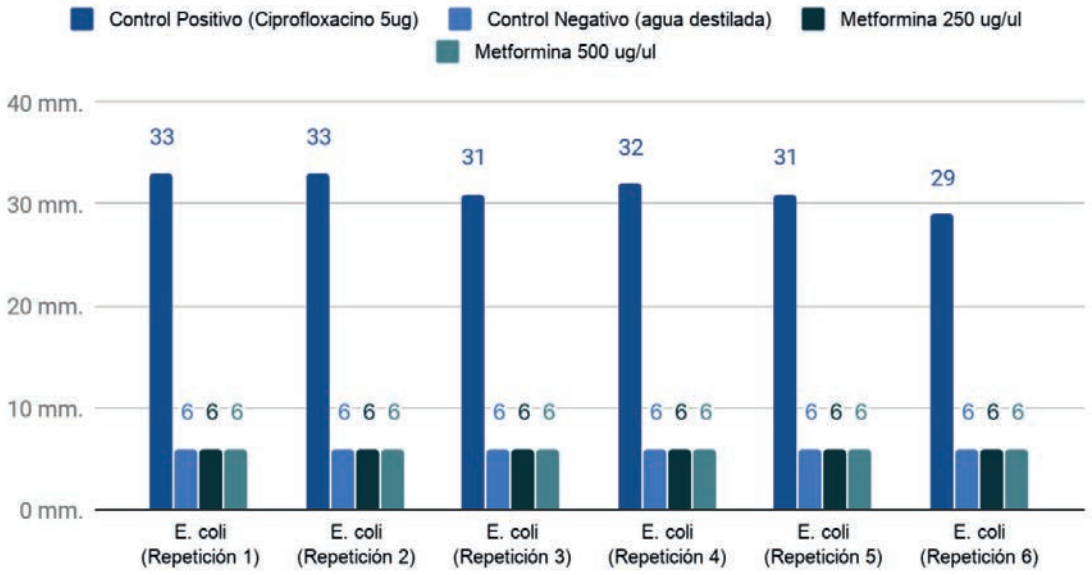

Figura 1. Actividad antibacteriana obtenida de estándar de Metformina frente a cepa de *Escherichia coli* ATCC25922.

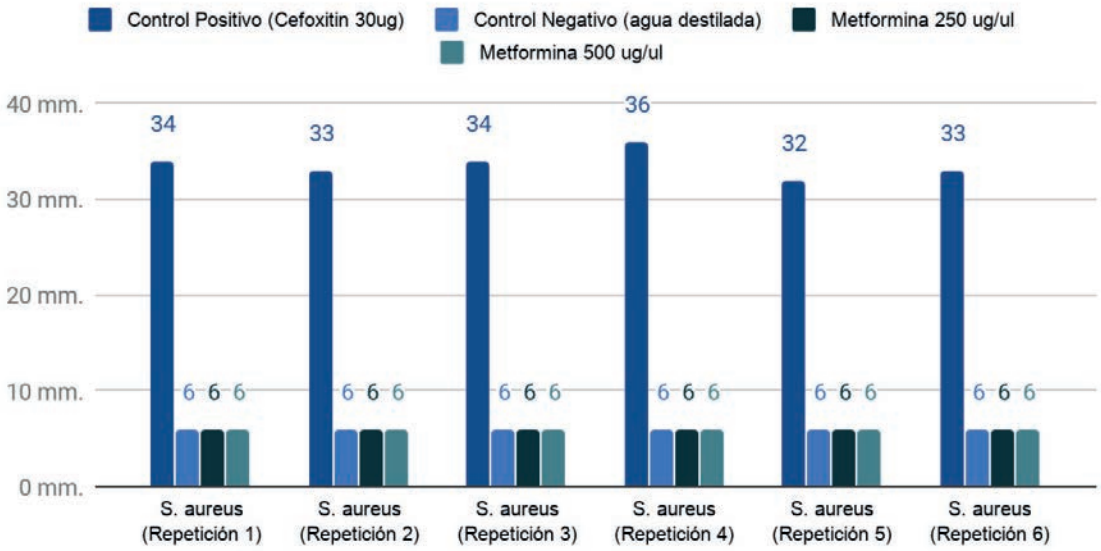

Figura 2. Actividad antibacteriana obtenida de estándar de Metformina frente a cepa de *Staphylococcus aureus* ATCC25923.

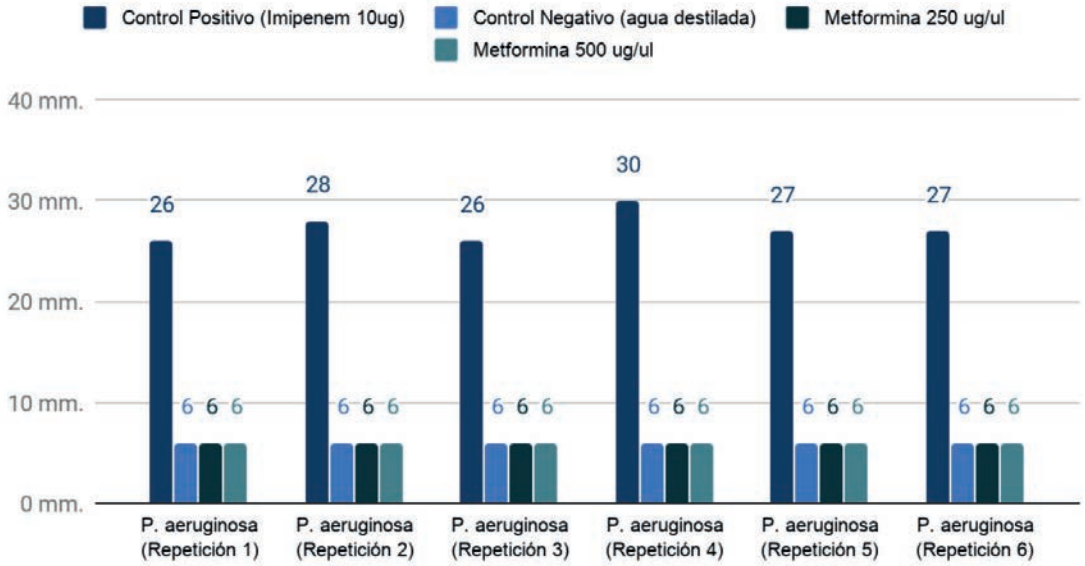

Figura 3. Actividad antibacteriana obtenida de estándar de Metformina frente a cepa de *Pseudomona aeruginosa* ATCC27853.

Metformina	En este estudio		Nasrin et al.[20]		Meherumisa et al.[21]		Dash et al.[22]	
	250mg	500mg	250mg	500mg	250mg	500mg	300mg	400mg
Escherichia coli	6 mm.	6 mm.	13 mm.	15 mm.	13 mm.	15 mm.	5 mm.	11 mm.
Pseudomonas aeruginosa	6 mm.	6 mm.	11 mm.	13 mm.	11 mm	13 mm.	9 mm.	12 mm.
Staphylococcus aureus	6 mm.	6 mm.	9 mm.	12 mm.	9 mm.	12 mm.	6 mm.	7 mm.
Saccharomyces cerevisiae	-	-	11 mm.	13 mm.	-	-	-	-
Candida albicans	-	-	12 mm.	14 mm.	12 mm.	14 mm.	-	-
Aspergillus niger	-	-	14 mm.	17 mm.	14 mm.	17 mm.	-	-

Tabla 1. Actividad antibacteriana de Metformina frente a diferentes patógenos.

tra las cepas de *Escherichia coli* ATCC 25922, *Staphylococcus aureus* ATCC 25923 y *Pseudomonas aeruginosa* ATCC 27853 y por lo tanto no tendría acción inhibitoria contra diferentes organismos que se sabe que son resistentes a múltiples fármacos.

Los estudios citados arriba no describen el uso de cepas ATCC (solo se mencionan nombre de especies bacterianas y fúngicas) en sus procedimientos de trabajo. Es posible que los resultados obtenidos en nuestro estudio difieren con tales publicaciones por el uso de cepas no catalogadas como cepas ATCC.

Estos hallazgos son importantes, porque categóricamente se descarta el efecto bactericida de la Metformina, y aunque los antecedentes son favorables para un potencial efecto antibacteriano, ante la evidencia, puede ser más sensato el dilucidar su uso como un fármaco coadyuvante con la terapia antibiótica. Los efectos pleiotrópicos de Metformina al modular la inmunidad (estimulación)[25,26], y la actividad antiinflamatoria[25,27], ambos mecanismos (inmunosupresión e inflamación) son fisiopatológicamente favorables para la progresión de la patogenicidad de las bacterias como, *Trichinella spiralis*[28], *Caenorhabditis elegans*[29,30], *hepatitis B virus*[31], *hepatitis C virus*[32,33], *M. tuberculosis*[13,34]. Por ello una gran iniciativa es contribuir aún más en la investigación de drogas de segundo uso o la elaboración de nuevos fármacos que puedan tener la capacidad de inhibir o destruir las bacterias que cuentan con una mayor tasa de resistencia y lograr reducir la letalidad a nivel mundial.

Limitaciones

Entre las limitaciones del estudio está solo la exposición a las 3 bacterias ATCC ensayadas, no incluyendo a otras bacterias y hongos no ATCC, siendo este estudio como base para investigaciones posteriores que utilicen cepas bacterianas resistentes hospitalarias. También el tipo de procedimiento no detallado usado por diversos autores para obtener el estándar de metformina.

Conclusiones

En la presente investigación, se demuestra que Metformina en concentraciones de 250 mg y 500 mg no presentó efecto bactericida frente a *Escherichia coli* (ATCC 25922), *Staphylococcus aureus* (ATCC 25923) y *Pseudomonas aeruginosa* (ATCC 27853).

Agradecimientos

Los autores agradecen al Centro de Investigación en Medicina Tradicional y Farmacología (CIMTFAR) de la Facultad de M[h1] edicina Humana Universidad San Martin de Porres (USMP) por proporcionar el estándar de Metformina. Al Laboratorio de Investigación en Biología Molecular (LIBM) de la Escuela Profesional de Medicina Humana la Universidad Peruana Unión (UPeU) por permitir la parte experimental con la metodología de Kirby Bauer con las cepas bacterianas ATCC. A las autoridades de ambas instituciones Dr. Frank Lizaraso Caparó y Dr. Roger Albornoz Esteban por el apoyo y licencias para el desarrollo de la investigación.

Contribuciones de autoría

P. Marcos, A. Salazar han participado en la concepción y diseño del artículo. Los procedimientos y resultados fueron realizados por P. Marcos y A. Urbano. Los análisis y discusiones fueron realizados por P. Marcos, Allca C., A. Salazar. La redacción del artículo estuvo a P. Marcos, A. Salazar. La revisión crítica la realizó A. Salazar. La versión final estuvo a cargo de P. Marcos, A. Salazar.

Fuentes de financiamiento

Facultad de Medicina Humana de la Universidad San Martin de Porres (USMP) / Escuela Profesional de Medicina Humana de la Universidad Peruana Unión (UPeU).

Conflicto de interés

Los autores declaran no tener conflicto de interés.

Referencias bibliográficas

1. Acuña L Guillermo. Evolución de la terapia antimicrobiana: lo que era, lo que es y lo que será. Rev. chil. infectol. [Internet]. 2003 [citado 2020 Mayo 19] ; 20(Suppl 1): 7-10. Disponible en: https://scielo.conicyt.cl/scielo.php?script=sci_arttext&pid=S0716-10182003020100001&lng=es.
2. Basak S, Kumar K, Ramalingam M. Design and release characteristics of sustained release tablet containing metformin HCl. Revista Brasileira de Ciências Farmacêuticas Brazilian Journal of Pharmaceutical Sciences. 2008. vol. 44, n. 3, jul./set.
3. OMS [internet]. USA: World Health of Organization ; 24 de Mayo de 2018; [acceso 19 de Mayo de 2020]. Disponible en: https://www.who.int/es/news-room/fact-sheets/detail/the-top-10-causes-of-death
4. Andrews JM. Determination of minimum inhibitory concentrations. J Antimicrob Chemother. 2001 Jul; 48 Suppl 1:5-16.
5. Munita JM, Arias CA. Mechanisms of Antibiotic Resistance. Microbiol Spectr. 2016 Apr;4(2):10.1128/microbiolspec.VMBF-0016-2015. doi: 10.1128/microbiolspec.VMBF-0016-2015. PMID: 27227291; PMCID: PMC4888801.
6. Katz M, Mueller L, Polyakov M, Weinstock S. Where have all the antibiotic patents gone? 2006. Nature Biotechnology volume 24 number 12 december
7. WHO [internet]. GENEVA: World Health of Organization; 27 de febrero 2017; [acceso 19 de mayo de 2020]. Disponible en: https://www.who.int/news-room/detail/27-02-2017-who-publishes-list-of-bacteria-for-which-new-antibiotics-are-urgently-needed

8. Huacuja F, Gomez M, Ortiz J, Soberanes B, Arevalo V, Morales E, Sanchez-Reyes L, Fanghanell G. Efecto de las estatinas más allá del colesterol. Revista de Endocrinología y Nutrición. 2006. Vol. 14, No. 2 abril-Junio pp 73-88
9. Ragnar S, Nord CE, Finch R. Lack of development of new antimicrobial drugs: a potential serious threat to public health. Lancet Infect Dis. 2005; 5: 115–19
10. Moncayo A. La resistencia a los antibióticos y la falta de interés de la industria farmacéutica. Infectio. 2014. 18(2): 35-36
11. Keiser M, Setola V, Irwin J, Laggner C, Abbas A, Hufeisen S, Jensen N, Kuijer M, Matos R, Tran T, Whaley R, Glennon R, Hert J, Kelan, Thomas K, Edwards D, Shoichet B. and Roth B. Predicting new molecular targets for known drugs. Nature. 2009 November 12; 462(7270): 175–181. doi: 10.1038/nature08506.
12. Vashisht R and Brahmachari K. Metformin as a potential combination therapy with existing front-line antibiotics for Tuberculosis. Journal of Translational Medicine201513:83 DOI: 10.1186/s12967-015-0443-y
13. Restrepo BI. Metformin: Candidate host-directed therapy for tuberculosis in diabetes and non-diabetes patients. Tuberculosis (Edinb). 2016 Dec;101S:S69-S72.
14. CLSI. Clinical and Laboratory Standards Institute. http://clsi.org/blog/2015/01/08/clsi-publishes-new-antimicrobial-susceptibility-testing-standards/
15. WHO. Antibacterial Agents in Clinical Development. [internet].2017.11. Geneva. September 2017; [acceso 19 de mayo 2020]. Disponible en: https://apps.who.int/iris/bitstream/10665/258965/1/WHO-EMP-IAU-2017.11-eng.pdf?ua=1
16. Yew WW, Chang KC, Chan DP, Zhang Y. Metformin as a host-directed therapeutic in tuberculosis: Is there a promise? Tuberculosis (Edinb). 2019 Mar;115:76-80. doi: 10.1016/j.tube.2019.02.004. Epub 2019 Feb 13. PMID: 30948180.
17. Xiao Y, Liu F, Li S, et al. Metformin promotes innate immunity through a conserved PMK-1/p38 MAPK pathway. Virulence. 2020;11(1):39β 48. doi:10.1080/21505594.2019.1706305
18. Patkee WR, Carr G, Baker EH, Baines DL, Garnett JP. Metformin prevents the effects of Pseudomonas aeruginosa on airway epithelial tight junctions and restricts hyperglycaemia-induced bacterial growth. J Cell Mol Med. 2016;20(4):758β 764. doi:10.1111/jcmm.12784
19. Garnett JP, Baker EH, Naik S, et al. Metformin reduces airway glucose permeability and hyperglycaemia-induced Staphylococcus aureus load independently of effects on blood glucose. Thorax. 2013;68(9):835β 845. doi:10.1136/thoraxjnl-2012-203178
20. Nasrin F; et al. Study of Antimicrobial and Antioxidant potentiality of Anti-diabetic drug Metformin. 2014 Vol: 2 Issue:3 Page:220-224
21. Meherunisa; Sapna J; Vikas S. Study of Metformin Effect on Antimicrobial Property. International Archives of BioMedical And Clinical Research. 2018 Vol 4.Issue 3.July
22. Dash, Arun & Pattanaik, BirendraKumar & Behera, SangeetaRani & Palo, AmiteshKumar. (2011). Study of antimicrobial property of some hypoglycemic drugs. Chronicles of Young Scientists. 2. 219.
23. Abbas HA, Elsherbini AM, Shaldam MA. Repurposing metformin as a quorum sensing inhibitor in Pseudomonas aeruginosa. Afr Health Sci. 2017 Sep;17(3):808-819.
24. Azizian J; Hekmati M. Functionalization of multi-wall carbon nanotubes with Metformin derivatives and study of their antibacterial activities against E-Coli and S. aureus. Journal of Nanoanalysis No. 03, Issue 03 (2016) 76-85
25. Cameron AR, Morrison VL, Levin D, et al. Anti-Inflammatory Effects of Metformin Irrespective of Diabetes Status. Circ Res. 2016;119(5):652-665. doi:10.1161/CIRCRESAHA.116.308445
26. Cha JH, Yang WH, Xia W, et al. Metformin Promotes Antitumor Immunity via Endoplasmic-Reticulum-Associated Degradation of PD-L1. Mol Cell. 2018;71(4):606-620.e7. doi:10.1016/j.molcel.2018.07.030
27. Joseph Sánchez-Gavidia, Carlos Pante-Medina, Elmer Lujan-Carpio, Alberto Salazar-Granara. Efecto antinociceptivo y antiinflamatorio de la metformina en modelos experimentales en ratón. Horiz. Med. [Internet]. 2019 Jul [citado 2020 Jul 06];19(3):49-57. Disponibleen: http://www.scielo.org.pe/scielo.php?script=sci_arttext&pid=S1727-558X2019000300008&lng=es.
28. Othman AA, Abou Rayia DM, Ashour DS, et al. Atorvastatin and metformin administration modulates experimental Trichinella spiralis infection. Parasitol Int. 2016;65:105–112.
29. Onken B, Driscoll M.. Metformin induces a dietary restriction-like state and the oxidative stress response to extend C. elegans Healthspan via AMPK, LKB1, and SKN-1. PloS One. 2010;5:e8758
30. Chen J, Ou Y, Li Y, et al. Metformin extends C. elegans lifespan through lysosomal pathway. eLife. 2017;6:e31268.
31. Xun YH, Zhang YJ, Pan QC, et al. Metformin inhibits hepatitis B virus protein production and replication in human hepatoma cells. J Viral Hepat. 2014;21:597–603
32. Yu JW, Sun LJ, Liu W, et al. Hepatitis C virus core protein induces hepatic metabolism disorders through down-regulation of the SIRT1-AMPK signaling pathway. Int J Infect Dis. 2013;17:e539–45.
33. Hsu CS, Hsu SJ, Lin HH, et al. A pilot study of add-on oral hypoglycemic agents in treatment-naive genotype-1 chronic hepatitis C patients receiving peginterferon alfa-2b plus ribavirin. J Formos Med Assoc. 2014;113:716–721.
34. Zhang M, He JQ. Impacts of metformin on tuberculosis incidence and clinical outcomes in patients with diabetes: a systematic review and meta-analysis. Eur J Clin Pharmacol. 2020 Feb;76(2):149-159.

Received: 10 agosto 2020
Accepted: 20 septiembre 2020

RESEARCH / INVESTIGACIÓN

Successful *in-vivo* treatment of mice infected with *Candida glabrata* using silver nanoparticles

Teeba H. Mohammad[1], Mohsen H. Risan[1], Gamal A. El-Hiti[2*], Dina S. Ahmed[3], Emad Yousif[4]
DOI. 10.21931/RB/2020.05.04.10

Abstract: The current study describes the production of silver nanoparticles (AgNPs) to treat *Candida glabrata* infections. The method involved incubation of silver nitrate ($AgNO_3$) with *Aspergillus terreus* using a green and straightforward route. The production of AgNPs was confirmed through a color change from transparent yellow to brown as well as by ultraviolet-visible (UV-VIS) spectroscopy. The surface morphology of AgNPs was assessed using a scanning electron microscope. The antifungal activity of AgNPs against *C. glabrata* was investigated in the serum of 20 infected mice. The mice were divided into four groups, and the level of cytokines: IL-4 and IFN-γ were examined after 21 days. The atomic force microscopy confirmed that the average diameter of AgNPs was 25.1 nm, which is appropriate for delivering silver nanoparticles to treat animals' infection. The concentration of cytokines IL-4 and IFN-γ were significantly ($P < 0.05$) higher in the *C. glabrata*-infected group than in the control group. While the cytokines level remained close to average concentration in mice administrated with AgNPs, such a result was comparable with the fourth group of mice (Candida-treated *Aspergillus*) after treatment with AgNPs.

Key words: *Candida glabrata*, *Aspergillus terreus*, cytokines, silver nanoparticles, antifungal activity, surface morphology.

Introduction

Candida is a genus of ascomycetes, yeast containing approximately 150 species of which more than 20 have clinical importance[1]. *Candida species* (spp.) cause several fungal infections and are considered the fourth most common cause of bloodstream infections (BSIs) in the general population[2]. Candidemia is expected in the USA, where it poses a severe health risk[3]. However, *Candida albicans* and *Candida glabrata* remain the primary cause of aggressive candidiasis since they contribute to 50% of all cases of infections[4]. The most common risk factors associated with *Candida* BSI are malignancy, disruption of mucosal barriers, sustenance broad-spectrum antibiotics, immune suppression due to radiotherapy or chemotherapy, and urinary catheterization[5].

Candidemia causes various severe illnesses and is not susceptible to many antifungal agents. Four common types of antifungal drugs, azoles, polyenes, flucytosine, and echinocandins, are effective against candidiasis[6]. Nonetheless, in most cases, the infection poses a mortality risk, and treatment is expensive and therapeutic effectiveness brutal to achieve[7]. Therefore, discovering a novel antifungal treatment is a vital strategy to control the infection and overcome antifungal resistance[8]. In recent years, nanoparticles have received substantial attention as a novel approach in developing useful materials with unique chemical and physical properties[9]. Such materials can be used exclusively in various fields such as medicine, biology, chemistry, health care, food, and industry[10,11]. Several synthetic procedures have been used to produce nanoparticles in which the size and shape of particles can be controlled[12]. These methodologies are sustainable, eco-friendly, and involve the in-vivo use of eukaryotes[13,14].

Silver nanoparticles (AgNPs) have been widely used in the production of antimicrobial agents, drug delivery, medical devices, household-uses, cosmetics, optical sensors, and pharmaceuticals[15]. Various processes have been developed for the synthesis of AgNPs. However, most synthetic methods are expensive to run and involve the use or production of hazardous materials[16]. Nevertheless, researchers have given much attention and are investigating the biological process as an alternative to synthetic processes in synthesizing AgNPs[16]. Such biological processes are environment-friendly, simple, high-yielding, inexpensive to run, and does not produce or use poisonous chemicals. Besides, AgNPs produced biologically have high stability and solubility, well-defined morphology, and appropriate particle size[16].

Many plants, fungi, and bacteria have been involved in the biological synthesis of AgNPs. Various fungal species, such as ascomycete and basidiomycete, can stabilize and reducing agents in the biological synthesis of AgNPs, including the intracellular and extracellular formation of *Aspergillus terreus*[17–19]. Mycelium, mycelium broth, and fungi substrate are used mainly in the AgNPs biosynthetic methods[20]. The biosynthesis of AgNPs involves culturing a fungus on agar followed by transfer to a liquid medium to produce biomass. Silver nitrate ($AgNO_3$) is then incubated with fungus in a controlled environment to produce AgNPs[21]. Various AgNPs have been synthesized and used as antimicrobial agents. For example, AgNPs synthesized using *A. fumigatus* showed cytotoxic, antibacterial activities[22]. Also, *A. terreus* obtained from *Calotropis procera*, was used to synthesize AgNPs that act as an antibacterial against *Salmonella typhi*, *Staphylococcus aureus*, and *Escherichia coli*[23]. Similarly, *A. terreus* has been used to produce AgNPs with antimicrobial activities against *C. albicans*, *C. krusei*, *A. fumigates*, *A. niger*, *A. ochraceus*, and *S. aruras*[24]. The AgNPs synthesized using *Andrographis paniculata* were used as antimicrobial against *S. typhi* and *S. aureus*[25].

The effect of a mixture of AgNPs and an antifungal agent such as fluconazole has been investigated against several pathogenic fungi[26]. The development of distinct cytokines in mice is essential in stimulating the practical outcome of host-defense against a fungal infection[27]. Resistance to *Candida* BSI requires the harmonized action of innate and adaptive immunity. Candida's distinct feature is the morphological change to the

[1] Department of Molecular and Medical Biotechnology, College of Biotechnology, Al-Nahrain University, Baghdad, Iraq.
[2] Cornea Research Chair, Department of Optometry, College of Applied Medical Sciences, King Saud University, Riyadh, Saudi Arabia.
[3] Department of Medical Instrumentation Engineering, Al-Mansour University College, Baghdad, Iraq.
[4] Department of Chemistry, College of Science, Al-Nahrain University, Baghdad, Iraq.
Corresponding author: gelhiti@ksu.edu.sa

hyphal form, which is associated with virulence factors. Phagocytosis of the *Candida spp.* Induced mice dendritic cells to produce cytokines[28]. Previous work concentrated on the successful *in-vitro* use of AgNPs as antimicrobial agents. Therefore, the current study aims to produce AgNPs using *A. terreus* based on previous reports[18–20] and their use in the treatment of *C. glabrata* in an animal model. Candida BSI's effective treatment in infected mice with *C. glabrata* in which the level of cytokines: (interleukin-4) IL-4 and interferon-gamma (IFN-γ) were measured. The current work reported an efficient and successful *in-vivo* treatment of mice infected with *C. glabrata* with AgNPs in which serum cytokines level was monitored.

Methods

Preparation of biomass

A. terreus was isolated from soil and grew on Czapek Dox Agar for 72 h at 25 °C. The identification of pure isolates was based on color changes and microscopic and morphological observations. Biomass of *A. terreus* was grown aerobically in a liquid medium containing KH_2PO_4 (47 g), K_2HPO_4 (2 g), $MgSO_4$ $7H_2O$ (0.1 g), $(NH4)_2SO_4$ (1 g), yeast extract (0.6 g), and glucose (10 g) in one liter. The culture was kept in a sterile flask (250 mL) and inoculated at 25 °C. In another sterile flask, fresh biomass (20 g) was added to distilled water (200 mL) and kept for 72 h at 25 °C. The mycelia were harvested through filtration using a Whatman filter paper (GE Healthcare Life Science, Chicago, IL, USA) (grade 1). Mycelia were washed with sterilized distilled water to remove any residues from the medium.

Extracellular synthesis of AgNPs

The *A. terreus* filtrate (20 mL) was treated with $AgNO_3$ (200 mL; 100 mM), and the flask was incubated in the dark at 25 °C for 24 h. The fungal filtrate color change recognized the production of AgNPs from transparent yellow to brown. The AgNPs were centrifuged (10,000 rpm) for 10 min, and the process was repeated for two times to produce a pellet that dried for use. The AgNPs were collected and characterized. The pure fungal filtrate (without $AgNO_3$) was used as a positive control. While pure $AgNO_3$ (1 mM) was used as a negative control.

Characterization of AgNPs

The UV-VIS spectrum of AgNPs was recorded on a UV-Vis-NIR-V670 spectrophotometer (JASCO Corp., Tokyo, Japan). The external surface morphology and particle dimensions of the synthesized AgNPs were inspected by the AA3000 SPM system AFM (Shimadzu Co., Kyoto, Japan). Droplets of AgNPs on a glass slide were examined using a NTEGRAÒ SPECTRA II NT-MDT (Spectrum Instruments Ltd., Moscow, Russia) at room temperature. The surface of the synthesized AgNPs was inspected by the TESCAN VEGA3Ò SEM (TESCAN Analytics, Brno–Kohoutovice, Czech Republic). Species identification and antifungal susceptibility were performed using the APIÒ ID 32 C (bioMérieux Corp., Marcy-l'Étoile, France).

Experimental procedures

The VITEK 2 compact system (BioMerieux Inc., Durham, NC, USA) was used to identify *C. glabrata*. A group of mice consists of 20 healthy males (6-weeks-old) with a weight that ranged from 20 to 25 g. Mice were captured in stainless steel cages at a controlled temperature (22 ± 2 °C) and moisture (55 ± 10%). The mice were provided with nutrients and water daily for 21 days and divided into four groups (n = 5 in each group). The control group of mice received physiological saline solution (1 mL). The *Candida* (non-treated) group of mice was infected with *C. glabrata* (10^5, 0.2 mL). The third group of mice was provided with AgNPs synthesized with *A. terreus* only (10 µg). The fourth group (treated) of mice was infected with *C. glabrata* a week after AgNPs had treated them synthesized with *A. terreus* (10 mg), as a suspension. After 21 days of treatment, mice were killed using ketamine-xylazine anesthesia for 1–2 h. The anesthesia consists of ketamine (1.0 mL; 100 mg mL^{-1}) and xylazine (0.5 mL; 20 mg mL^{-1}). An intraperitoneal injection protocol was followed using a dose of 0.1 mL per 10 g of body weight.

Cytokine assay

Cytokine levels in mice's serum were measured using the IL-5 ELISA (Fisher Scientific, Fairlawn, NJ, USA). Commercially available kits (Endogen Inc., Cambridge, MA, USA) were used for the IFN-g and IL-4 measurements. The ELISA plates were covered with cytokine-specific detention antibody (Ab; 0.5 mg mL^{-1}) overnight at 4 °C. The plates were washed with a phosphate buffer saline (PBS; × 4), Tween-20 (0.05%), and incubated with PBS for 30 min followed by bovine serum albumin (BSA; 2%) at 37 °C. After washing, the supernatant fluids were added to the pits and incubated for 2 h at 37 °C or left overnight at 4 °C, and Ab concentration (0.5 mg mL^{-1}) was detected. The ELISA plates were developed and amplified using the VECTASTAIN ABC kit (Vector Laboratories, Burlingame, CA, USA) according to the manufacturer's protocol.

The experimental work and statistical analysis

The current study is a complete randomized design in which each test was performed four times for each parameter. The experimental work was carried out at the Central Laboratory at Al-Nahrain University and the Materials Research Department, Ministry of Science and Technology, Iraq. The current study was conducted between September 2018 and January 2019. Ethical approval has been obtained before the start of the work. The average was expressed mean ± standard deviation, and the significance of the difference was tested for $P < 0.05$. The SPSS® statistical package, version 22.0 (SPSS Inc., Chicago, IL, USA) for Windows®, was used.

Results

Biosynthesis of AgNPs with A. terreus

Initially, the biosynthesis of AgNPs using *A. terreus* was induced. *A. terreus* was cultured on Czapek Dox Agar (Sigma-Aldrich, St. Louis, MO, USA) at 25 °C for a week[29]. Silver nitrate was incubated with *A. terreus* in a controlled environment. Initially, the surface of the fungal colonies was light yellow. After the addition of $AgNO_3$ solution, the color shifts from transparent yellow to brown confirming the reduction of cationic silver into metallic silver; this indicates the successful production of AgNPs (Figures 1 and 2). Also, the formation of AgNPs was confirmed by ultraviolet-visible (UV-VIS) spectroscopy (JASCO Corp., Tokyo, Japan). The UV-VIS spectrum of AgNPs showed an absorption band at 439 nm as a result of the excitation of surface plasmon vibrations, which is consistent with the literature[30].

Atomic force microscopy (AFM)

The particle size of AgNPs synthesized with *A. terreus*

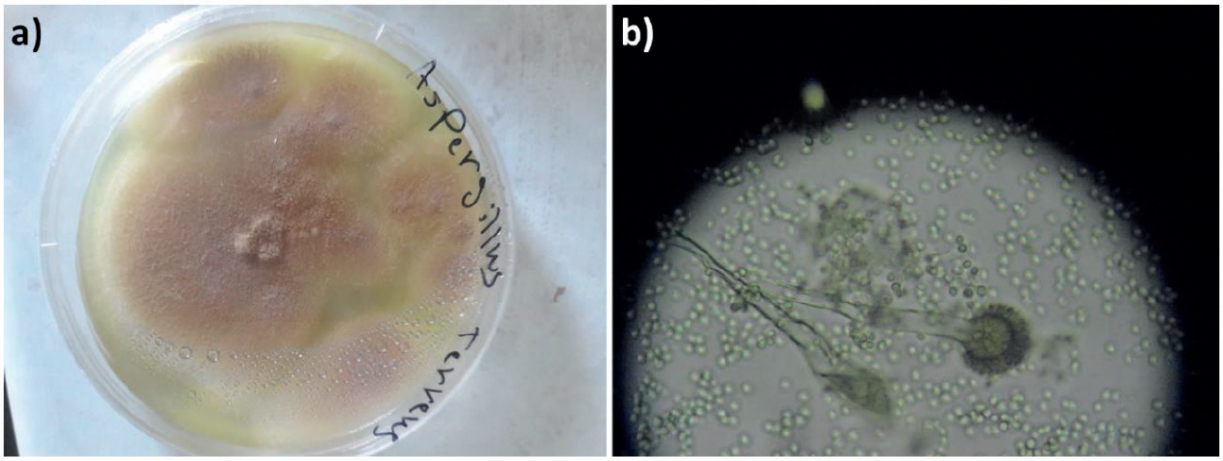

Figure 1. *A. terreus* cultured on Czapek Dox Agar at 25 ± 2 °C for a week: a) Colonies in a Petri dish with a diameter of 4 cm; b) Colonies under a light microscope (40×).

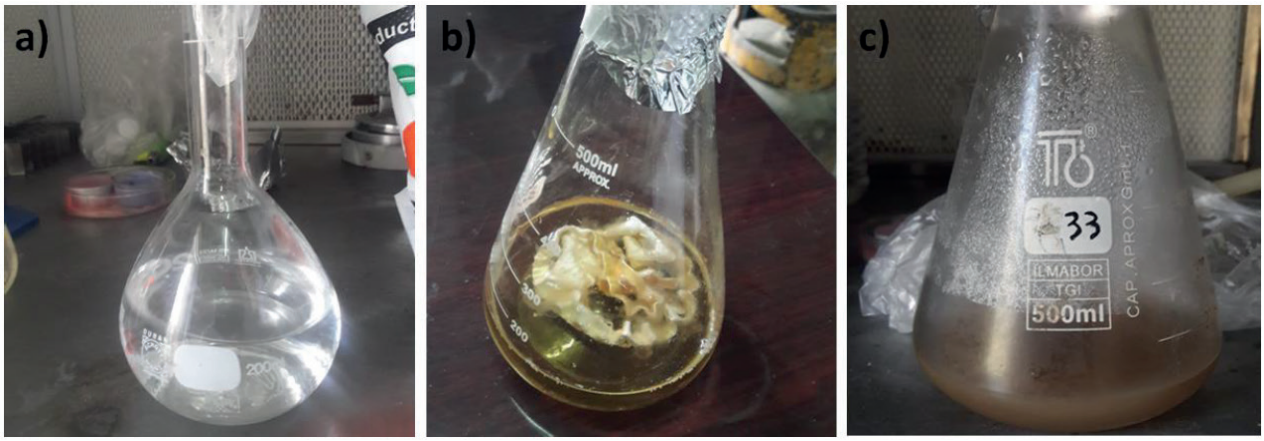

Figure 2. Synthesis of AgNPs: a) AgNO3 (1 mM) solution; b) *A. terreus* biomass (50 mL); c) Color alteration of filtrate after incubation in the dark.

was determined using the atomic force microscopy (AFM) (Hitachi High-Technologies, Minato City, Tokyo, Japan). The two- and three-dimensional AFM images (2 µm) of the synthesized AgNPs are shown in Figure 3. The AFM images showed the formation of nanoparticles that have a different particle size distribution (20–30 nm) with an average diameter of 25.1 nm. Such AgNPs particle size is appropriate for delivering silver nanoparticles to treat animals' infection with *Candida*[31]. The absorption band appeared at 332 nm in the UV-VIS spectra (Figures S1 and S2) due to the absorption of Ag+ or other elements in the culture medium.

Scanning electron microscopy (SEM)

The SEM can determine the external morphology of nanoparticles. Figure 4 shows the SEM images of the AgNPs synthesized with *A. terreus*. The images revealed that the particles displayed a distinctive morphology with a considerable variation in particle size and small numbers of aggregations. Also, they showed the formation of typically visually, small, and uniformly spherical-shape particles of multiple sizes.

Cytokines assay

The cytokines level: IL-4 and IFN-γ were measured four times in the serum of 20 mice, which had been divided into four groups (n = 5 within each group), and the averages were calculated. A blood sample was withdrawn from each mouse to obtain serum for cytokine level analysis after the 21 days trial. Table 1 shows the cytokine serum concentration among four different groups of mice that have been measured using the enzyme-linked immunosorbent assay (ELISA) plates. The level of cytokines: IL-4 and IFN-γ was significantly ($P < 0.05$) higher in the group of mice infected with *C. glabrata* (10^5, 0.2 mL) compared to those obtained within the control group (natural level). While the cytokines level remains close to the average concentration in mice administrated with AgNPs, such a result was comparable with that obtained in the fourth group of mice (*Candida*-treated *Aspergillus*) after treatment by AgNPs.

The blood of infected mice administered with AgNPs synthesized with *A. terreus* was observed to have an average cytokine level. Such results indicate that AgNPs do not disadvantageously affect the cytokine level. It is worth noting, the level of cytokine returned to its average concentration after treatment, except for the group that has been administrated with *Candida*.

Discussion

The synthesis of AgNPs with *A. terreus* was confirmed through an alteration in color from transparent yellow to brown after incubation in a dark room. Additionally, AgNPs synthesized with *A. terreus* was confirmed by UV-VIS spectroscopy[30,32]. *A. terreus*, which is unconventional mycobiosystem for synthesizing AgNPs, is cost-effective, highly-stable, and reproducible. Previous research has shown that nanoparticles can significantly inhibit fungi's mechanism of action,

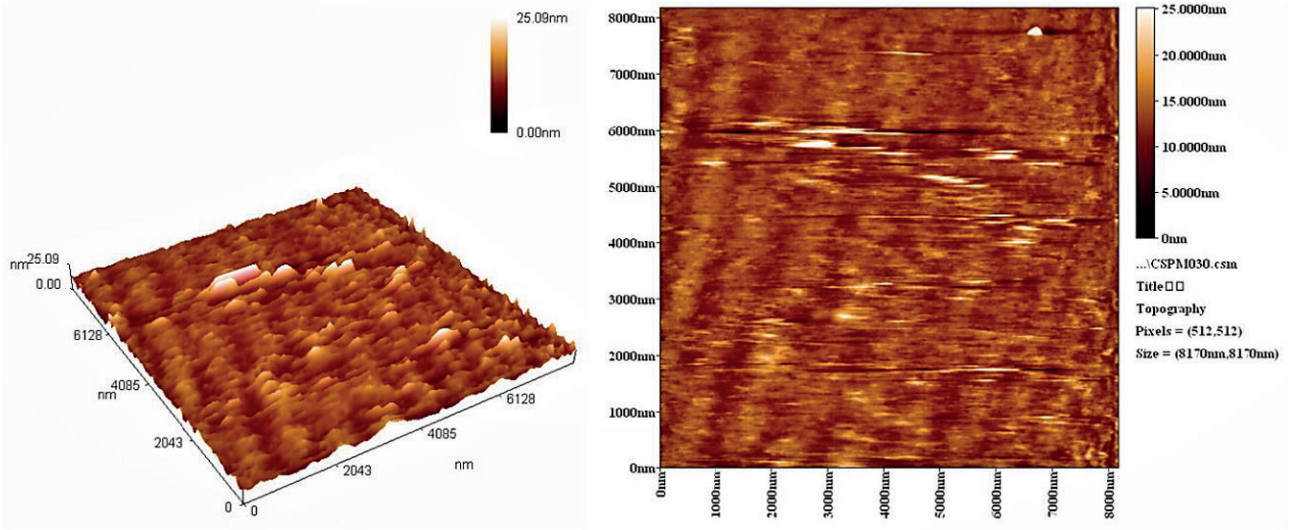

Figure 3. The 2- and 3-dimensional AFM images of AgNPs synthesized with *A. terreus*.

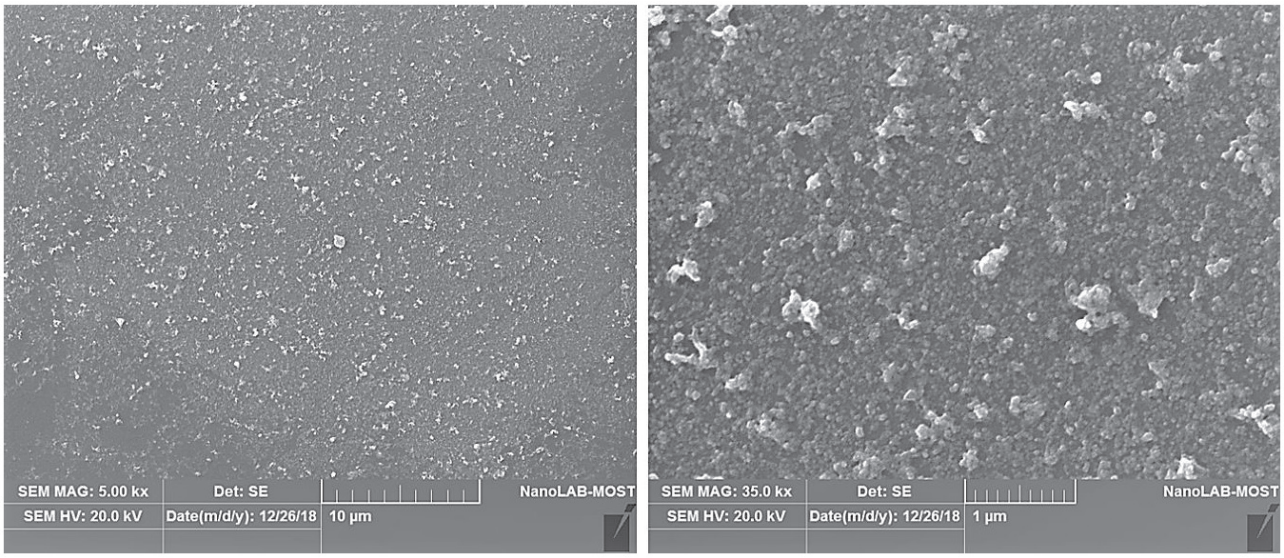

Figure 4. The SEM images for AgNPs synthesized with *A. terreus*.

Treatment/parameter	IL-4	INF-γ
Control	0.30 ± 0.01	0.38 ± 0.01
*Candida**	0.37 ± 0.00	0.45 ± 0.00
AgNPs	0.30 ± 0.01	0.37 ± 0.01
Candida treated *A. terreus*	0.33 ± 0.01	0.40 ± 0.01
LSD $P \leq 0.05$	0.02	0.02

* Statistically significant value at $P < 0.05$.

Table 1. Cytokine serum levels (pg mL^{-1}) among four different groups of mice.

which provides nanoparticles with unique characteristics in being potent broadband antifungal agents and active drug carriers[33]. The morphological AFM examination of some biologically synthesized AgNPs showed the presence of more than one distinctive particle[34]. The particle size distribution of AgNPs with *A. terreus* showed an average particle size of 25 nm, which is in agreement with the previous research[35]. The particle size of AgNPs biosynthesized using *Pseudomonas aeruginosa* showed multiple particle sizes that ranged from 33 to 300 nm. The majority of particles have a size of 50–100 nm[36]. Small-sized nanoparticles showed better antimicrobial activity than large-sized nanoparticles due to the particle's large surface area[37].

At times, no apparent changes were detected using the SEM within the AgNPs, since aggregated tiny particles were produced due to the coating agent[38]. The antimicrobial activity of AgNPs was found to be dependent on the concentration of nanoparticles used[39]. The AgNPs synthesized with *A. terreus* showed vigorous antifungal activity against pathogenic fungi such as *Candida albicans*[24]. Besides, AgNPs showed significant inhibition activity against three types of filamentous fungi that are resistant to antifungal agents such as fluconazole[40].

The cytokine levels in the serum of mice infected with *Candida spp.* revealed that the immune system response was diverse among different organs. Such an observation could have a critical effect on treatment strategy using immunomodulatory methods[41,42]. It has been established that resistance to candidiasis is related to the progress of the response that is based on IFN-γ secretion[43]. A fatal result is associated with the progress of response, which is based on IL-4, IL-13, and IL-10 secretion and IL-5 response[44]. The alteration in colonization patterns of *Candida spp.* in infection-resistant BALB/c mice and infection-prone mice after the infection is associated with the secretion of the cytokines: IFN-γ, IL-4, and IL-12[45]. In primary spread candidiasis, IL-4 may hinder *Candida* infection by promoting effector mediators of resistance; for example, IL-4 can promote the growth of a defensive Th1 response in candidiasis[41]. In another study, a detectable level of inspired IL-4 production was present in both the control and infected mice groups. The susceptibility of the infected mice group was higher than that for the control group concerning IL-4 production. Consistent with the current results, a high level of IL-4 was detected in mice infected with candidiasis[46]. Another study revealed that mice with low levels of IL-4 were more susceptible to infection than normal control group[47].

Conclusions

Silver nanoparticles using *Aspergillus terreus* were synthesized through a green, simple, fast, and eco-friendly process. This method has the potential to replace the traditional biochemical methods for the production of nanoparticles. The surface morphology of the synthesized nanoparticles was investigated using different techniques and showed an average particle diameter of 25 nm. Silver nanoparticles synthesized with *Aspergillus terreus* were used to investigate the response of cytokines, IL-4 and IFN-γ in mice infected with *Candida spp.* The cytokines: IL-4 and IFN-γ levels were significantly ($P < 0.05$) higher in mice infected with *C. glabrata* compared to the control group. The mice administered with AgNPs synthesized with *A. terreus* showed an average cytokine level: IL-4 and IFN-γ. The cytokines level returned to its normal range after treatment, except for the group that had been administrated with *Candida*.

Conflicts of Interest

The authors declare no conflict of interest.

Acknowledgements

The authors are grateful to the Deanship of Scientific Research, King Saud University, for funding through the Vice Deanship of Scientific Research Chairs. We thank Al-Nahrain and Al-Mansour Universities for their technical support.

Bibliographic references

1. Saikkonen K. Forest structure and fungal endophytes. Fungal Biol Rev 2007; 21(1–2): 67–74. doi:10.1016/j.fbr.2007.05.001.
2. Lia M-Y, Hsu J-F, Chu S-M, Wu I-H, Huang H-R, Chiang M-C, Fu R-H, Tsai M-H. Risk factors and outcomes of recurrent Candidemia in children: relapse or re-infection. J Clin Med 2019; 8(1): 99. doi:10.3390/jcm8010099.
3. Cleveland AA, Harrison LH, Farley MM, Hollick R, Stein B, Chiller TM, Lockhart SR, Park BJ. Declining incidence of candidemia and the shifting epidemiology of Candida resistance in two US metropolitan areas, 2008–2013: results from population-based surveillance. PLoS One 2015; 10(3): e0120452. doi:10.1371/journal.pone.0120452.
4. Lai C-C, Wang C-Y, Liu WL, Huang Y-T, Hsueh P-R. Time to positivity of blood cultures of different Candida species causing fungaemia. J Med Microbiol 2012; 61(Pt 5): 701–704. doi:10.1099/jmm.0.038166-0.
5. Giri S, Kindo AJ. A review of Candida species causing blood stream infection. Indian J Med Microbiol 2012; 30(3): 270–278. doi:10.4103/0255-0857.99484.
6. Pappas PG, Kauffman CA, Andes DR, Clancy CJ, Marr KA, Ostrosky-Zeichner L, Reboli AC, Schuster MG, Vazquez JA, Walsh TJ, Zaoutis TE, Sobel JD. Clinical practice guideline for the Management of Candidiasis: 2016 update by the Infectious Diseases Society of America. Clin Infect Dis 2016; 62(4): e1–e50. doi:10.1093/cid/civ933.
7. Colombo AL, Nucci M, Park BJ, Nouér SA, Arthington-Skaggs B, da Matta DA, Warnock D, Morgan J. Epidemiology of candidemia in Brazil: a nationwide sentinel surveillance of candidemia in eleven medical centers. J Clin Microbiol 2006; 44(8): 2816–2823. doi:10.1128/JCM.00773-06.
8. Lee W-J, Hsu J-F, Lai M-Y, Chiang M-C, Lin H-C, Huang H-R, Wu I-H, Chu S-M, Fu R-H, Tsai M-H. Factors and outcomes associated with candidemia caused by non-albicans Candida spp. versus Candida albicans in children. Am J Infect Control 2018; 46(12): 1387–1393. doi:10.1016/j.ajic.2018.05.015.
9. Han X, Xu K, Taratula O, Farsad K. Applications of nanoparticles in biomedical imaging. Nanoscale 2019; 11(3): 799–819. doi:10.1039/C8NR07769J.
10. Khan I, Saeed K, Khan I. Nanoparticles: properties, applications and toxicities. Arab J Chem 2019; 12(7): 908–931. doi:10.1016/j.arabjc.2017.05.011.
11. Alsaba MT, Al Dushaishi MF, Abbas AK. A comprehensive review of nanoparticles applications in the oil and gas industry. J Petrol Explor Prod Technol 2020; 10: 1389–1399. doi:10.1007/s13202-019-00825-z.
12. Dahoumane SA, Jeffryes C, Mechouet M, Agathos SN. Biosynthesis of inorganic nanoparticles: a fresh look at the control of shape, size and composition. Bioengineering 2017; 4(1): 14. doi:10.3390/bioengineering4010014.
13. Rahman A, Lin J, Jaramillo FE, Bazylinski DA, Jeffryes C, Dahoumane SA, In vivo biosynthesis of inorganic nanomaterials using eukaryotes—A review. Molecules 2020; 25(14): 3246. doi:10.3390/molecules25143246.
14. Menon S, Shanmugam R, Kumar VS. A review on biogenic synthesis of gold nanoparticles, characterization, and its applications. Resource-Efficient Technol 2017; 3(4): 516–527. doi:10.1016/j.reffit.2017.08.002.
15. Guzmán MG, Jean Dille J, Godet S. Synthesis of silver nanoparticles by chemical reduction method and their antibacterial activity. J Exp Nanosci 2016; 11(9): 714–721. doi:0.1080/17458080.2016.1139196.
16. Gurunathan S, Park JH, Han JW, Kim JH. Comparative assessment of the apoptotic potential of silver nanoparticles synthesized by Bacillus tequilensis and Calocybe indica in MDA-MB-231 human breast cancer cells: Targeting p53 for anticancer therapy. Int J Nanomed 2015; 10(1): 4203–4222. doi:10.2147/IJN.S83953.
17. Guilger-Casagrande M, de Lima R. Synthesis of silver nanoparticles mediated by fungi: a review. Front Bioeng Biotechnol 2019; 7: 287. doi:10.3389/fbioe.2019.00287.
18. Li G, He D, Qian Y, Guan B, Gao S, Cui Y, Yokoyama K, Wang L. Fungus-mediated green synthesis of silver nanoparticles using Aspergillus terreus. Int J Mol Sci 2012; 13(1): 466–476. doi:10.3390/ijms13010466.
19. Abd El-Aziz ARM, Al-Othman MR, Eifan SA, Mahmoud MA, Majrashi M. Green synthesis of silver nanoparticles using Aspergillus terreus (KC462061). Dig J Nanomater Bios 2013; 8(3): 1215–1225.
20. Verma VC, Kharwar RN, Gange AC. Biosynthesis of antimicrobial silver nanoparticles by the endophytic fungus Aspergillus clavatus. Nanomedicine (Lond) 2010; 5(1): 33–40. doi:10.2217/nnm.09.77.

21. Costa Silva LP, Oliveira JP, Keijok WJ, Silva AR, Aguiar AR, Guimarães MCC, Ferraz CM, Araújo,JV, Tobias FL, Braga FR. Extracellular biosynthesis of silver nanoparticles using the cell-free filtrate of nematophagus fungus Duddingtonia flagans. Int J Nanomedicine 2017; 12; 6373–6381. doi:10.2147/IJN.S137703.
22. Shahzad A, Saeed H, Iqtedar M, Hussain SZ, Naz S, Saleem F, Aihetasham A, Chaudhary A. Size-controlled production of silver nanoparticles by Aspergillus fumigatus BTCB10: likely antibacterial and cytotoxic effects. J Nanomater 2019; 2019: 5168698. doi:10.1155/2019/5168698.
23. Rani R, Sharma D, Chaturvedi M, J P Yadav. Green synthesis, characterization and antibacterial activity of silver nanoparticles of endophytic fungi Aspergillus terreus. J Nanomed Nanotechnol 2017; 8(4): 1000457. doi:10.4172/2157-7439.1000457.
24. Li G, He D, Qian Y, Guan B, Gao S, Cui Y, Yokoyama K, Wang L. Fungus-mediated green synthesis of silver nanoparticles using Aspergillus terreus. Int J Mol Sci 2012; 13(1): 466–476. doi:10.3390/ijms13010466.
25. Hossain MM, Polash SA, Takikawa M, Shubhra RD, Saha T, Islam Z, Hossain S, Hasan MA, Takeoka S, Sarker SR. Investigation of the antibacterial activity and in vivo cytotoxicity of biogenic silver nanoparticles as potent. Front. Bioeng. Biotechnol 2019; 7: 239. doi:10.3389/fbioe.2019.00239.
26. Ray S, Sarkar S, Kundu S. Extracellular biosynthesis of silver nanoparticles using the mycorrhizal mushroom Tricholoma crassum (Berk.) Sacc: its antimicrobial activity against pathogenic bacteria and fungus, including multidrug resistant plant and human bacteria. Dig J Nanomater Bios 2011; 6(3): 1289–1299.
27. Romani L. Immunity to fungal infections. Nat Rev Immunol 2004; 11(4): 275–288. doi:10.1038/nri2939.
28. Romani L, Mencacci A, Grohmann U, Mocci S, Mosci P, Puccetti P, Bistoni F. Neutralizing antibody to interleukin 4 induces systemic protection and T helper type 1-associated immunity in murine candidiasis. J Exp Med 1992; 176(1): 19–25. doi:10.1084/jem.176.1.19.
29. Arabatzis M, Velegraki A. Sexual reproduction in the opportunistic human pathogen Aspergillus terreus. Mycologia 2013; 105(1); 71–79. doi:10.3852/11-426.
30. Botcha S, Prattipati SD. Green synthesis of silver nanoparticles using Hyptis suaveolens (L.) Poit leaf extracts, their characterization and cytotoxicity evaluation against PC-3 and MDA-MB 231 cells. Biologia 2019; 74(7): 783–793. doi:10.2478/s11756-019-00222-1.
31. Abd El-Aziz ARM, Al-Othman MR, Al-Sohaibani SA, Mahmoud MA, Sayed SRM. Extracellular biosynthesis and characterization of silver nanoparticles using Aspergillus niger isolated from Saudi Arabia (strain ksu-12). Dig J Nanomater Bios 2012; 7(4): 1491–1499.
32. Ammar HAM, El-Desouky TA. Green synthesis of nanosilver particles by Aspergillus terreus HA1N and Penicillium expansum HA2N and its antifungal activity against mycotoxigenic fungi. J Appl Microbiol 2016; 121(1): 89–100. doi:10.1111/jam.13140.
33. Wang L, Hu C, Shao L. The antimicrobial activity of nanoparticles: present situation and prospects for the future. Int J Nanomedicine 2017; 12: 1227–1249. doi:10.2147/IJN.S121956.
34. Ishida K, Cipriano TF, Rocha GM, Weissmüller G, Gomes F, Miranda K, Rozental S. Silver nanoparticle production by the fungus Fusarium oxysporum: nanoparticle characterization and analysis of antifungal activity against pathogenic yeasts. Mem Inst Oswaldo Cruz 2014; 109(2): 220–228. doi:10.1590/0074-0276130269.
35. Lai C-C, Wang C-Y, Liu W-L, Huang Y-T, Liao C-H, Hsueh P-R. Time to positivity in blood cultures of staphylococci: clinical significance in bacteremia. J Infect 2011: 62(3); 249–251. doi:10.1016/j.jinf.2011.01.004.
36. Peiris MK, Gunasekara CP, Jayaweera PM, Arachchi NDH, Fernando N. Biosynthesized silver nanoparticles: are they effective antimicrobials? Mem Inst Oswaldo Cruz 2017; 112(8): 537–543. doi:10.1590/0074-02760170023.
37. Vanaja M, Annadurai G. Coleus aromaticus leaf extract mediated synthesis of silver nanoparticles and its bactericidal activity. Appl Nanosci 2013; 3(3): 217–23. doi:10.1007/s13204-012-0121-9.
38. Birla SS, Gaikwad SC, Gade AK, Rai MK. Rapid synthesis of silver nanoparticles from Fusarium oxysporum by optimizing physicocultural conditions. Sci World J 2013; 2013: 796018. doi:10.1155/2013/796018.
39. Khan SS, Mukherjee A, Chandrasekaran N. Studies on interaction of colloidal silver nanoparticles (SNPs) with five different bacterial species. Colloids Surf B Biointerfaces 2011; 87(1): 129–138. doi:10.1016/j.colsurfb.2011.05.012.
40. Espinel-Ingroff A, Chaturvedi V, Fothergill A, Rinaldi MG. Optimal testing conditions for determining MICs and minimum fungicidal concentrations of new and established antifungal agents for uncommon molds: NCCLS collaborative study. J Clin Microbiol 2002; 40(10): 3776–3781. doi:10.1128/jcm.40.10.3776-3781.2002.
41. Chin VK, Foong KJ, Maha A, Rusliza B, Norhafizah M, Chong PP. Multi-step pathogenesis and induction of local immune response by systemic Candida albicans infection in an intravenous challenge mouse model. Int J Mol Sci 2014; 15(8): 14848–14867. doi:10.3390/ijms150814848.
42. Thompson A, Griffiths JS, Walke L, da Fonseca DM, Lee KK, Taylor PR, Gow NAR, Orr SJ. Dependence on dectin-1 varies with multiple candida species. Front Microbiol 2019; 10: 1800. doi:10.3389/fmicb.2019.01800.
43. Ashman RB, Papadimitriou JM. Production and function of cytokines in natural and acquired immunity to Candida albicans infection. Microbiol Rev 1995; 59(4): 646–672.
44. Spellberg B, Ibrahim AS, Edwards JE Jr, Filler SG. Mice with disseminated candidiasis die of progressive sepsis. J Infect Dis 2005; 192(2): 336–343. doi:10.1086/430952.
45. Blobe GC, Schiemann WP, Lodish HF. Role of transforming growth factor beta in human disease. N Engl J Med 2000; 342(18): 1350–1358. doi:10.1056/NEJM200005043421807.
46. Káposzta R, Tree P, Maródi L, Gordon S. Characteristics of invasive candidiasis in gamma interferon and interleukin-4-deficient mice: role of macrophages in host defense against Candida albicans. Infect Immun 1998; 66(4): 1708–1717.
47. Laura LT, Roberta T, Roberta S, Elio S. Interleukin-4 and -10 exacerbate candidiasis in mice. Eur J Immunol 1995; 25: 1559–1565

Received: 14 August 2020
Accepted: 25 Spetember 2020

RESEARCH / INVESTIGACIÓN

Antimicrobial Activity of Herbal Mixture Extract Combination on Microorganisms Isolated from Urinary Tract infection

Risala H Allami[1], Raghad S. Mouhamad[2*], Sura A. Abdulateef[3], Khlood abedalelah al-Khafaji[4]
DOI. 10.21931/RB/2020.05.04.11

Abstract: Urinary tract infection (UTI) is the second most common infection after respiratory tract infection. Its prevalence is more in women as compared to men. Approximately 50% of women have an infection of the Urinary tract in their life-time. The bacterial infection is one of the most important bioactivity; using their ability to imitate evanish then distributes international fitness problems into the 21st centenary. Thus a recent study was undertaken to investigate the antibacterial activity of a mixture of three medicinal plants against UTI infectious isolates. The three considered plants were (*Aloe vera*, *Artemisia herba alba* and *Teucrium polium*), which were used in Iraqi medicine for many centuries. The effectiveness of this combination was investigated using *in vitro* well diffusion method. The extract was tested against four isolated pathogenic bacteria (*Staphylococcus aureus*, *Klebsiella spp*, and *Proteus spp*). The aqueous extract exhibited antibacterial activity against gram-positive and gram-negative bacteria. The mixture extract had the highest effect against *S. aureus* and *Proteus spp*, followed by a lower effect on *Klebsiella spp*. In conclusion, the antibacterial effect of the tested plant extracts confirmed a higher impact on Gram-positive bacteria as compared to Gram-negative bacteria. Therefore, it can be concluded that the usage of these plants as a traditional medicine form can be considered as a strong assistant to regular medicine drugs and treatments.

Key words: Urinary tract infection (UTI), Antimicrobial Activity, Herbal Mixture Extract.

Introduction

The herbal remedy is a developing sector of health care and demands attention[1]. Plants served as a valuable source of traditional treatment over the years[2]. World Health Organization (WHO) estimated that around 80% of the worldwide population remember at least one traditional remedy by extracting active components[3]. This, due to medicinal flora, bears various advantages (a low price or much fewer facet effects) compared to modern conventional drugs, as are expensive yet acknowledged in hazardous side effects[4].

The prevalence of Urinary tract infections (UTI) by bacteria is problematic worldwide and among all age range and gender. Several pathogens belong to gram-positive and gram-negative bacteria regard as a fundamental everyday health hazards[5] to cause UTI; the most pathogens for UTI infection include strains of uropathogenic *Escherichia coli*, *Klebsiella pneumonia*, *Enterococcus spp*, *Staphylococcus saprophyticus*, *St. aureus*, group B *Streptococcus*, *proteus mirabilis*[6-10] Among all bacterial species *E. coli* is known to be the most common in complicated and uncomplicated UTI especially in diabetic patients[6].

Treatment of UTI subordinate the severity of infection; it can be ranging from a single-dose antibiotic treatment to rescue nephrectomy for pyonephrosis in diabetic patients with septic shock[11]. Third-generation beta-lactam antibiotics such as ciprofloxacin, cefixime, and ceftriaxone are commonly used in UTI. Indiscriminate antibiotic use resulted in the development of resistance to one or multiple antibiotics that give a severe challenge upon disease treatment or even treatment failure[12] beside other adverse effects on the liver and bone marrow[13,14]. The tremendous use of antimicrobial has induced resistances among various bacterial kinds and, as much be counted concerning fact[1], the efficacy of these compounds is remarkably decreased. A long time put in appearances concerning antibiotic stopping pathogens has been a global problem in the latest. According to inquire, the undesirable facet consequences about half of antibiotics instituted us because of latter sources in conformity will combat these problems[15]. Literature cited that many strains of *E. coli* and *K. pneumoniae* isolated from UTI have extended-spectrum to Beta-lactam antibiotics, carbapenem-resistant, and polymyxin; moreover, the resist could be transferred to other infectious bacteria through horizontal gene transfer systems as transformation, transduction, and conjugation[16].

This necessitates relies on a safe and low-cost medicinal plant having antibacterial activities with a promising future. More than half a million plants worldwide have medical issues essential to treat or prevent many infections[17]. A variety of secondary metabolite produces in plant tissues with therapeutic values with less toxicity and side effects and could be a good substitute for traditional synthetic or semisynthetic chemical antibiotics and overcome multidrug-resistant bacteria[18]. Since several plant antimicrobial contains different functional groups, their antibacterial activity attributed to multiple mechanisms. Therefore, the prospect of developing resistance to plant constitutes is relatively smaller[19]. The antibiotic resistance phenomenon exhibited by the pathogenic microorganisms were not reported in medicinal flora because of their strong antimicrobial activity[20]. Phytochemical compounds and small secondary metabolites have a significant value for medicinal plants. The most important of these bioactive constituents are alkaloids, tannins, flavonoids, and phenol, all of which are accoutered for new antibacterial agents[21,22]. It is believed that crude extracts from some medicinal plants are more biologically active than isolated compounds due to their synergistic effects[23].

The researchers are showing interest in natural products with bactericidal activity[24-26]. Humans use plant extracts for a wide variety of diseases, of dense developing countries; it depends on traditional medical practitioners or their collections

[1] College of Biotechnology, Al-Nahrain University, Baghdad, Iraq.
[2] Ministry of Science and Technology, Baghdad, Iraq.
[3] Dept. of Applied Science, Division of Biotech, Univ. of Tech, Iraq.
[4] College of Biotechnology, Al-Nahrain University, Baghdad, Iraq.
Corresponding author: raghad1974@yahoo.com

regarding medicinal vegetation in conformity with treatment to them[27]. Herbals execute apply for an important position in conserving biodiversity. These plants are genuinely familiar to bucolic human beings anybody according to their scarcity yet their disappearance[28]. Indeed, medicinal plants lead the very necessary health ponderous position and then symbolize a giant source concerning profits for many families within the countryside and cities[29].

Urinary tract infection is the second most common infection after respiratory tract infection worldwide. Its prevalence is more in women than men[30]; approximately 50% of women have an infection of the Urinary tract in their life. The current s study focuses on discovering antibacterial outcomes regarding aqueous extracts of a natural combination of about 3 medicinal plants (*Aloe vera*, *Artemisia herba alba*, and *Teucrium polium*) against UTI causing bacteria.

Materials and methods

Isolation and identification of bacteria from UTI.

Twenty out samples of urine were collected from patients with suspicious clinical symptoms like dysuria, loin pain, fever, frequent urination, and need to urinate with an empty bladder[7]; patients were visited Ibn Al-Nafees Hospital/ Baghdad and asked about taken antibiotic prior visiting the hospital during last seven days. The ethical committee approved the study of the University.

All urine samples were cultured over blood agar, MacConkey agar, and mannitol salt agar. Bacterial characters were identified using Gram stain, urease test, oxidase, catalase, hemolysis of RBCs, and Indole Methyl red Vokes Proskauer (IMVC)[31].

Aqueous extraction of Plant Material

This research was conducted from January to February 2020. Plants of (*Aloe vera*, an Herbal (Sheh), and *Teucrium polium* (Algeada) toughness were obtained from the local Iraqi market and were identified at the College of Agriculture Engineering of Baghdad University - Iraq. The plants were kept at room temperature (20-25ºC) till usage. Equal weights of each force in (*Aloe vera*, *Artemisia herba alba* (sheh), and *Teucrium polium* (Algeada) were ground then mixed. The aqueous extract regarding that combination was prepared along with the useful resource; 2 g regarding mixture, including 200 ml of sterilized distilled water for 15 minutes, left overnight in a refrigerator. Meanwhile, the extract panel was filtered and refrigerated in a glass container as described (32) with modification.

Screening of the active compound

Many tests were applied to screen the different active compounds in the aqueous extract of plant mixture; these tests include the detection of each flavonoid, tannins, glycosides, saponin, and terpin and steroid. The procedures were briefly described below:

Flavonoids were detected in cold aqueous extract; the detecting solution composed of an equal volume of 50% ethanol and 1M KOH. About 5 ml of extract was mixed with 5 ml of detecting solution at 25C, and the color was changed to the yellow indicating presence of flavonoid[33].

The system below[34] was used to detect tannins; in its procedure, 50 ml of each ban was back in conformity withstand equally broken on couple conical flasks. For the first one, administration lead acetate (CH3COOPb) (1%; w/v) was once introduced to plant extract afterward; the jelly pellet was used following keep viewed a direct reaction. The second flask, ferric chloride ($FeCl_2$) (1%; w/v) was used for screening tannins. Navy-blue shade was involved in the emergence concerning tannins.

Glycosides

These techniques were once taken according to the method described by (35); non hydrolyzed extract: Equal aggregation concerning the bury recover was once as soon as blended with the Fehling test in the test tube; development of purple precipitate shows a quality result for glycosides.

Hydrolyzed extract

Few drops of HCl were added to 5ml of the aqueous extract of the plant since they were left at a water bath of 20 minutes, the acidity was once neutralized using NaOH solution, amount of aggregation respecting the Fehling test was added. The improvement concerning crimson precipitate suggests a positive result.

Saponins

This method was made under conformity with (35). Couple methods detected saponins:

The first method was applied by shaking the tube containing extract; the formation of foams standing indicates a first-rate result.

While the second method was done by adding five ml of plant extract over 1-3 ml of 3% ferric chloride solution, positive results were pointed out upon bright precipitate formation[33].

Terpenes and steroids

few drops of chloroform were drop wised to 1 ml of the, then a decline over acetic anhydride and a decline on sulfuric acid; brown precipitate appeared that represents the availability of terpenes. While dark blue color appeared after about five minutes, it suggests the availability of steroids[33].

Antibacterial activity of aqueous herbal extracts

Agar well diffusion approach on Mueller -Hinton agar was once used in imitation of the search for antibacterial activity[36]. Bacterial cultures were crashed out from the nutrient agar plate and were suspended in sterilized peptone water. Turbidity was evaluated and compared with McFarland standard tube number 1, which equivalents approximately to $1X10^8$ CFU/mL. The cotton swab was immersed in bacterial suspension and spread over Muller Hinton agar, which let for 10 minutes to ensure bacterial adherence. Meanwhile, the borer applicator was sterilized by flame, cooled, and pressed on the top of seeded Muller Hinton agar to make well with a 6 mm radius, let distance about 15 mm between wells the aspect of the plate. Each well was filled with 25, 50, 75, and 100 µl, plates were stand for 10 minutes and were incubated for 24 h at 37 °C. Three replicas of each plate were prepared, and the diameter of the inhibition zone was recorded from the edge of the well.

Results and Discussion

Isolation and identification of bacteria

The recent result of isolation and identification regarding bacterial isolates from patients with UTI symptoms showed the prevalence of *Klebsiella spp*, *Proteus*, and *S. aureus*; the characters of each isolate listed in the table (1). Although this

was a preliminary study with a small number of UTI patients, the study showed that G^{-ve} bacterial species were more prevalent than G^{+ve} bacteria. Many other researches referred to that different bacterial species might encounter with the UTI inpatients, and some of these bacteria develop antibiotic-resistant to one or more of the traditional and extended-spectrum of beta-lactam antibiotic[37] Mohamed H. Mourad and one of the most important reason is the recurrent uses of antibiotic even without a physician prescription. This following (38) found that 54.8% of isolates were gram-negative, while 45.2 % were gram-positive.

Bacterium spp	Blood agar	MacConky agar	Mannitol-salt agar	Nutrient agar or milk agar	Gram stain	Catalase test	Urease test
Klebsiella spp.	White colony, no hemolysis	Pink mucoid colony	*	White colony	G-ve rod	#	-
Proteus spp.	Swarming , no hemolysis	Pale colony NLF	*	White colony	G-ve rod	#	+ pink
S. aureus	B-hemolysis	*	Mannitol fermenter	White colony	G + grape like clusters	+ Bubbles	#

G-ve (Gram negative), G + (Gram positive), # (negative reaction),*(negative reaction), - (negative Results), + (positive results), NLF (Non Lactose Ferment).

Table 1. The morphological and characteristics of bacteria on different cultural media with some biochemical test.

Chemical analysis of the aqueous extract of plant mixture under study showed that a weight of 1.58g representing 5.95%, could achieve from 25g regarding the extracted plant material. Screening of bioactive components revealed that the extract contains some flavonoids, phenols, tannins, saponins, glycosides, and terpenes have been detected. Aqueous extracts were low in steroids (Table 2). *A. herba-alba* is a prosperous source of flavonoids certain as like hispidulin as well as cirsilineol. Flavonoids isolated out of some medicinal vegetation have been established in conformity with possessing anti-inflammatory effect[39].

Active compound	Quality result
Phenols	+
Tannins	+
Flavonoids	+
Terpenes	+
Saponins	+
glycosides	+
steroids	-

+ (Positive reaction), - (Negative reaction)

Table 2. Chemical analysis of active compounds in aqueous extract of a plant mixture.

Antibacterial activity

Each extract was tested against bacterial isolates (*S. aureus*, *Klebsilla.spp*, and *Proteus.spp*). The extracts' different concentrations illustrated increased effectiveness against the studied microorganisms represented by the increased inhibition zones in figure (1).

The measurement of the average diameter of inhibition zone indicated that highest bacterial inhibition reached with higher concentration of plant mixture extract for all bacterial isolates under study. Also, study found that *Staph. aureus* was more susceptible than other bacterial species followed by *Klebsiella spp.* (figure2).

An increase rate of re-emerging infections, has carried an inquire for instant and more safe natural antimicrobial compounds; however, these compound need more investigation for their effecting mechanism. Plants are valuable supply of pharmaceutical substances, due to the fact they have an almost limitless potential according to synthesize compounds including one of a kind antimicrobial endeavor against more than a few pathogenic as well as opportunistic microorganisms[40].

The essential factors up to expectation to antibacterial reactivity are the type of diffusion strategies of active substances used and the tendency to inter bacterial cell, pH, and temperature of the surroundings[41]. The pH may also result in the antibacterial inhibitory effect of *R. sativus* had an excellent antibacterial effect at acidic pH, which has declined by increasing pH toward alkaline. This might be because antibacterial compounds in cationic forms can also engage the negatively charged bacterial cells[42].

Successful extraction concerning bioactive compounds beside row material depends on the solvent back into the extraction procedure. The recent study's main success is using aqueous extract for three plant material that contained different active compounds with a synergistic effect in one preparation, a phenolic compound known to alter microbial cell permeability, leading to change damage the macromolecules inside the bacterial cell. Many enzymes responsible for either the bacterial reproduction and growth or virulence factor might lose their activity in response to phenolic compounds[43,44,45]. The saponin activity against monocrystalline sugar; reduces sugar within the bacteria reducing power intake to the bacterial cell, leading to growth decline and death[46]. The presence of tannins and flavonoids caused a toxic effect and an inhibition of different types of enzymes and transporter proteins found in the cell membrane and inside cell[47,48].

Many researchers observed that the extraction of the plant active ingredients and the organic solvents methanol, ethyl acetate, and chloroform resulted in a more substantial antibacterial effect, but aqueous extraction, cheaper and need less requirements to prepare 26=32. Gram-negative microorganisms are among the resistant organisms against chemotherapeutic antibiotics than gram-positive bacteria; a survey concerning currently observed antibacterial activity of herbal takes place, showing that >90% of herbal extracts lacked activity against *E. coli*, in compassion to gram-positive bacteria[49].

The mechanisms of bacterial resistance against antibiotic

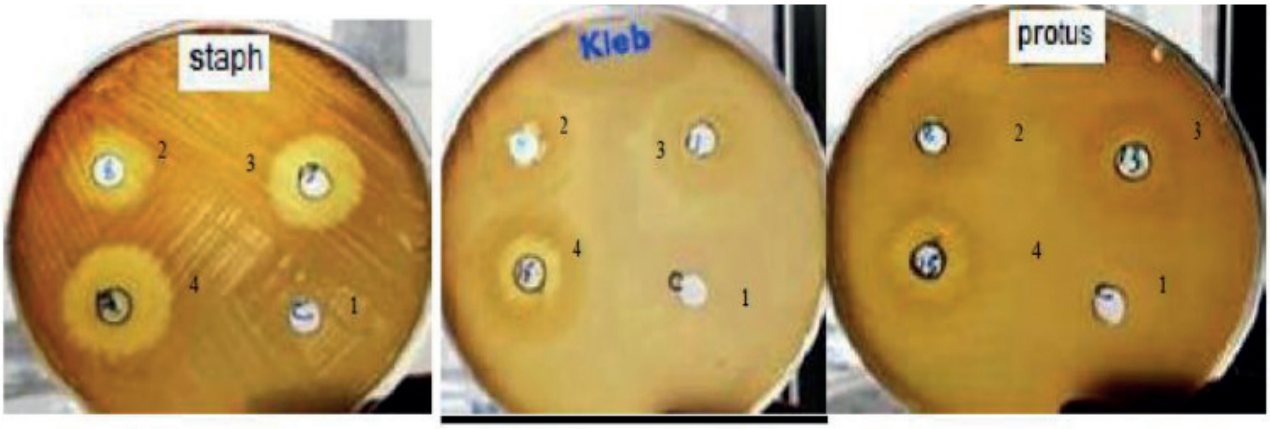

Figure 1. Bacterial inhibition zone with different concentration of aqueous plants extract (1= 25µl, 2= 50 µl, 3=75 µl, 4=100 µl): Muller Hinton agar.

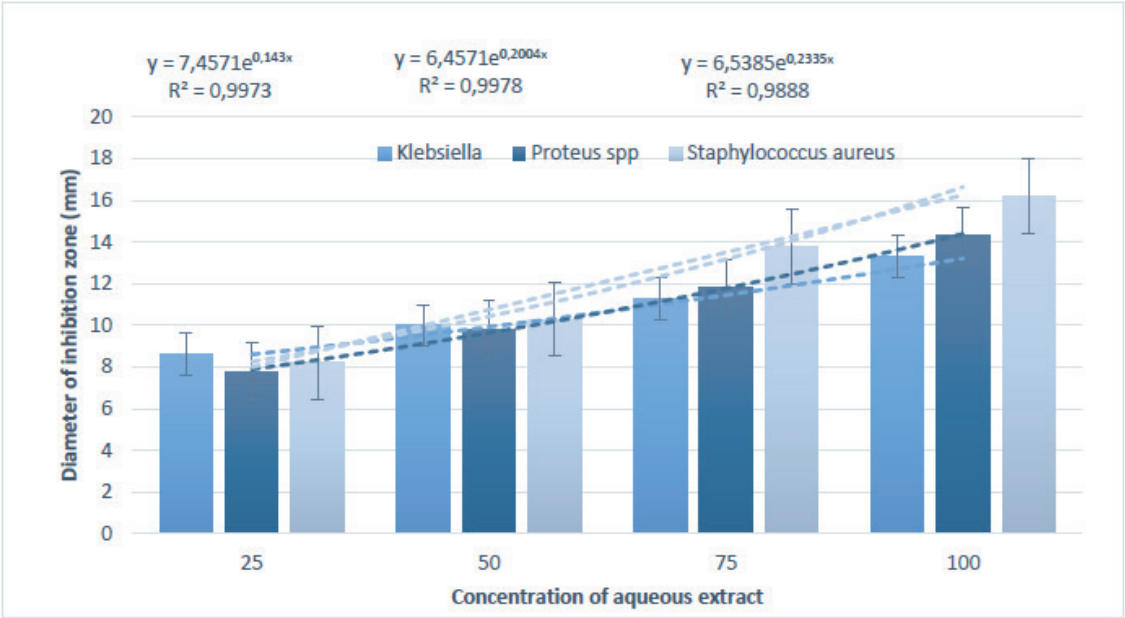

Figure 2. The differences in bacterial susceptibility in response to aqueous plant mixture extract

might be equipped through changing membrane permeability; drug molecules in accordance with a mobilephase can keep transferred through membrane via porins, diffusion through the bilayer then through self-uptake. The porin channels are located among OM (outer membrane) about Gram-negative bacteria. The little hydrophilic molecules (β-lactams then quinolones) can pass the OM only through porins. The minimize among quantity over porin channels leads to decreased access regarding β-lactam antibiotics between the cells, subsequently resistance[50]. G+ve microorganisms like Staphylococcus might harbor transmissible genetic element encoding for antibiotic resistance such as plasmids encoding the penicillinase genes, namely in collecting negative bacteria; conjugation is an essential mechanism regarding drug transfer and effect occur into supreme genera[50]. The main barrier for Gram-positive bacteria towards antibiotics is thick peptidoglycan that protects against osmotic rupture. The simple subunit over the peptidoglycan thing is a disaccharide monomer regarding N -acetylglucosamine (NAG) and N -acetylmuramic (NAM) pentapeptide. The pentapeptide consists of amino water brash residues alternating into L- and D-stereoisomers, then terminating within D-alanyl-D-alanine. A stem peptide regarding moving measure then contract is given to the third amino water brash over it pentapeptide. Pentapeptides are then same, including stem peptides, according to form a cross-link between polysaccharide chains. This reaction is catalyzed by a transpeptidase. This transpeptidation response is sensitive to prohibition via β-lactams. The penicillin-sensitive reactions are catalyzed by using a family of closely associated proteins, penicillin-binding proteins (PBPs). β-Lactam antibiotics out turn their lethal impact regarding bacteria through inactivation concerning more than one PBPs simultaneously, then for that reason inhibiting cell wall synthesis. The inhibition of PBPs additionally leads to imitation of breakdown on an ideal match, probably at the time over cell division. This agitated morphogenesis is hypothesized after provoking cell dying[51,52].

Conclusions

Different active compounds were detected in the aqueous mixed extract of the 3 medicinal vegetation (*Aloe vera*, *Artemisia herba alba* and *Teucrium polium*) permanency life, including phenols and flavonoids tannins, saponins, glycosides afterward terpenes. Aqueous extrusion concerning an herbal aggregate upon 3 medicinal vegetation (Aloe vera, Artemisia herba alba and Teucrium polium) undergo antibacterial effect

against positive but village Gram negative microorganism. Our consequences aid that the aqueous extract regarding this three plant combination well-known shows the synergistic effect as antibacterial activity compared to previous studies that examined each plant alone.

Bibliographic references

1. Ekor M. (2014). The growing use of herbal medicines: issues relating to adverse reactions and challenges in monitoring safety. Frontiers in pharmacology, 4: 177. https://doi.org/10.3389/fphar.2013.00177
2. Center for Substance Abuse Treatment. Substance Abuse Treatment for Persons with HIV/AIDS. Rockville (MD): Substance Abuse and Mental Health Services Administration (US); 2000. (Treatment Improvement Protocol (TIP) Series, No. 37.) Chapter 8—Ethical Issues. Available from: https://www.ncbi.nlm.nih.gov/books/NBK64933/
3. World Health Organization (WHO). 1992. Our planet, our health. Report of WHO Commission on Health and Environment. Geneva: World Health Organization. http://www.ciesin.org/docs/001-012/001-012.html
4. Sung, B., Chung, H. S., Kim, M., Kang, Y. J., Kim, D. H., Hwang, S. Y., Kim, M. J., Kim, C. M., Chung, H. Y. and Kim, N. D. (2015). Cytotoxic effects of solvent-extracted active components of Salvia miltiorrhiza Bunge on human cancer cell lines. Experimental and Therapeutic Medicine, 9(4): 1421–1428. https://doi.org/10.3892/etm.2015.2252
5. Flores-Mireles A. L., Walker J. N., Caparon M., and Hultgren S. J.(2015). Urinary tract infections: epidemiology, mechanisms of infection and treatment options. Nature Reviews Microbiology, 13(5): 269–284.
6. Foxman B. (2014). Urinary tract infection syndromes: occurrence, recurrence, bacteriology, risk factors, and disease burden. Infectious Disease Clinics of North America, 28(1): 1–13.
7. Kline K. A., Schwartz D. J., Lewis W. G., Hultgren S. J. and Lewis A. L.(2011). Immune activation and suppression by group B Streptococcus in a murine model of urinary tract infection. Infection and Immunity, 79(9): 3588–3595.
8. Nielubowicz G. R. and Mobley H. L.(2019). Host-pathogen interactions in urinary tract infection. Nature Reviews Urology, 7(8): 430.
9. Ronald A. (2003). Etiology of urinary tract infection: traditional and emerging pathogens. American Journal of Medicine, 113(1): 14–19.
10. Kang C. I., Chung D. R., Son J. S., Ko K. S,. Peck K. R. and Song J. H. (2011): Clinical significance of nosocomial acquisition in urinary tract-related bacteremia caused by gram-negative bacilli. Amer. J. Infection Control, 39(2): 135-140.
11. Foxman B.[2003], Epidemiology of urinary tract infections: incidence, morbidity and economic costs. Dis Mon.; 49:53-70.
12. Nicki R.Colledge et al. (2010). Davidson'S Principles and Practice of Medicine 21sted. Churchill Livingstone Elsevier publication; p-471-472
13. Vincent C., Boerlin P., Daignault D., Dozois C. M., Dutil L., Galanakis C., Reid-Smith R.J., Tellier P. P., Tellis P. A., Ziebell K. and Manges A. R. (2010). Food reservoir for Escherichia coli causing urinary tract infections. Emerg. Infect Dis. 16: 88-95.
14. Weam B., Abraham M., Doiphode S., Peters K., Ibrahim E., Sultan A., and Mohammed H. O. (2016). Foodborne Bacterial Pathogens Associated with the Risk of Gastroenteritis in the State of Qatar. International Journal of Health Sciences, 10(2), 197–207.
15. Liu Y.-Y., Wang Y., Walsh T. R. et al., (2016). Emergence of plasmid mediated colistin resistance mechanism mcr-1 in animals and human beings in China: a microbiological and molecular biological study. Lancet Infectious Diseases, 16(2): 161–168.
16. Hassan B. and Abdul R.(2012). Medicinal Plants (Importance and Uses)., Pharmaceut Anal Acta, 3: 1 .
17. Rath S., Dubey D., Sahu M.C., Debata N.K. and Padhy R.N. (2012). Antibacterial activity of 25 medicinal plants used by aborigines of India against six uropathogens with surveillance of multidrug resistance. Asian Pacif. J. Trop. Biomed. 2: S846-S854.
18. Tepe B., Daferera D., Sokmen N., Polissiou M. and Sokmen A. (2004). Invitro antimicrobial and antioxidant activities of the essential oils and various extracts of Thymus eigii Journal of Agricultural and Food Chemistry, 52: 1132-1137.
19. Shihata I.M. A pharmacological study of Anagallis arvensis. MD. Vet, Thesis, Cairo University (cited by Nehia Hussein, Noor A. Hanon).
20. Abubakar M.C., Ukwuani A.N. and Shehu RA (2008). Phytochemical screening and Antibacterial activity of Tamarindus indica pulp extract. Asian J. Biochem. 3(2):134-138.
21. Kalimuthu K., Vijayakumar S. and Senthilkumar R. (2010). Antimicrobial Activity of the Biodiesel Plant, Jatropha curcas L. International Journal of Pharma and Biosciences, 1(3):1-5.
22. Soković M., Glamočlija J., Marin P. D., Brkić D. D., van Griensven L. J. (2010). Antibacterial effects of the essential oils of commonly consumed medicinal herbs using an in vitro model. Molecules, 15 (11): 7532-7546.
23. Voon H. C., Bhat R., and Rusul G. (2012). Flower extracts and their essential oils as potential antimicrobial agents for food uses and pharmaceutical applications. Comprehensive Reviews in Food Science and Food Safety, 11(1): 34–55, 2012.
24. Kalwij J. M. (2012). Review of the Plant List, a working list of all plant species. Journal of Vegetation Science, 23(5): 998–1002.
25. Trinh P-C. , Thao T. Le-T., Ha H.-T.-Viet, and Nguyen T. (2020). DPPH-Scavenging and antimicrobial Activities of Asteraceae Medicinal Plants on Uropathogenic Bacteria Evidence-Based Complementary and Alternative Medicine, 2020: 1-9. ID 7807026, https://doi.org/10.1155/2020/7807026.
26. Chen S. L., Yu H., Luo H. M., Wu Q., Li C. F., and Steinmetz A. (2016). Conservation and sustainable use of medicinal plants: problems, progress, and prospects. Chinese Medicine, 11:37. https://doi.org/10.1186/s13020-016-0108-7
27. Sofowora A., Ogunbodede E., and Onayade A. (2013). The role and place of medicinal plants in the strategies for disease prevention. African journal of traditional, complementary, and alternative medicines : AJTCAM, 10(5): 210–229. https://doi.org/10.4314/ajtcam.v10i5.2
28. Scheunemann L. P., and White D. B. (2011). The ethics and reality of rationing in medicine. Chest, 140(6):1625–1632. https://doi.org/10.1378/chest.11-0622.
29. Najar M. S., Saldanha C. L., and Banday K. A. (2009). Approach to urinary tract infections. Indian Journal of Nephrology, 19(4): 129–139. https://doi.org/10.4103/0971-4065.59333
30. MacFaddin J. F.(2000). Biochemical tests for identification of medical bacteria, Williams and Wilkins. Philadelphia, PA, page 113.
31. Al- Khafaji K. A., Hammood S. A., Omran S. G., Hassan M.A., Yaseen H. J., Abood H., Ali S. G. (2014). Biological activity and protease inhibitor from watery extract of lentil (Lens culinaris) against some bacterial species. J. Baghdad Science, 2:781-788.
32. Harbone J. B. (Editor) (1984). Phytochemical Methods, 2nd Edition. Chapman and Hall, U.K., pp. 37-99
33. Lucera A., Costa C., Conte A. and Del Nobile M. A. (2012). Food applications of natural antimicrobial compounds. Frontiers in Microbiology, 3:287. https://doi. org/10.3389/fmicb. 2012. 00287
34. Barréro A., Herrador M. M., Arteaga P., Quitz J., Aksira M., Mellouki F. and Akkad S. (2005). Chemical composition of essential oils of leaves and wood of Tetraclinis articulata (Vahl) Masters. J. Essent. Oil Res. 17: 166-167.
35. Shaheen A. Y., Sheikh A. A., Rabbani M., Aslam A., Bibi T., Liaqat F., Muhammad J. and Rehmani S. F. (2015). Antibacterial activity of herbal extracts against multi-drug resistant Escherichia coli recovered from retail chicken meat. Pak. J. Pharm. Sci. 28 (4) :1295-1300.
36. Mourad M. H., Salih S. A-R. , Elaasser M. M., Safwat N. A. and Ibrahim M. Y..(2016). Antibacterial activity of certain medicinal plant and their essential oils on the isolated bacteria from UTI patients. Int. J. Adv. Res. 4(12): 1510-1530.
37. Ahmed M. E, Al-lami M. Q., and Abd Ali D. M. (2020). Evaluation of Antimicrobial Activity of Plants Extract Against Bacterial Pathogens Isolated from Urinary Tract Infection among Males Patients. Al-Anbar Medical Journal DOI: 10.33091/AMJ.0701622020/ http://doi.org/10.33091/AMJ.0701622020

38. Houari M., Ferchichi A. (2009). Essential oil composition of Artemisia herba-alba from southern Tunisia. Molecules, 14: 1585-1594.
39. Moghtader M. (2009). Chemical composition of the essential oil of Teucrium polium L. from Iran. Am Euras. J. Agric. Environ. Sci. 5, 843–846.
40. Nikaido H. and Vaara M. (1985). Molecular basis of bacterial outer membrane permeability. Microbiol Rev. 49:1–32.
41. C 1995. GC-MS analysis of Artemisia herba-alba Asso essential oils from Algeria. Dev Food Sci 37: 147-205.
42. Bajpai V.K., Rahman A., Dung N.T., Huh M.K. and Kang S.C. (2008). In vitro inhibition of food spoilage and foodborne pathogenic bacteria by essential oil and leaf extracts of Magnolia liliflora Desr. Journal of Food Science, 73:M314.
43. La Storia A., Ercolini D., Marinello F., di Pasqua R., Villani F. and Mauriello G. (2011). Atomic force microscopy analysis shows surface structure changes in carvacrol-treated bacterial cells. Res. Microbiol. 162: 164-172.
44. Tako M., Kerekes E. B.,Zambrano C., Kotogan A., Pap T., Krisch J.and Vagvolgyi C.(2020). Plant phenolic and phenolic enriched extract as antimicrobial agents against food- contaminating microorganisms. Antioxidants, 9: 165-186. Doi:10.3390/antiox9020165.
45. Saba T.H., Isam SH.H. and Manal AH (2013). Identification of quantitative chemical compounds of ethanolic extracts of Q.infectoria infectoria and studies its inhibitory effect in some bacteria. Indian Journal of Research, 2: 125-128.
46. Cowan M.M. (1999). Plant products as antimicrobial agent. Clin. Microbiol Review, 12(4): 564-582.
47. Ramanathan R., Tan C. and Das N. (1992).Cytotoxic effect of plant polyphenols and fat soluble vitamins on malignant human cultured cells. Cancer letters, 62: 217-224.
48. Ple' siat P. and Nikaido H. 91992). Outer membranes of gram-negative bacteria are permeable to steroid probes. Mol Microbiol. 6:1323–1333.
49. Rhodes P.L., Mitchell J.W., Wilson M.W. and Melton L.D. (2006). Antilisterial activity of grape juice and grape extracts derived from Vitis vinifera variety Ribier. Int J Food Microbiol. 107:281–286. doi: 10.1016/j.ijfoodmicro.2005.10.022.
50. Beevi S. S., Mangamoori L. N. and Anabrolu N. (2009). Comparative activity against pathogenic bacteria of the root, stem, and leaf of Raphanus sativus grown in India. World J. Microbiol. Biotechnol. 25:465–473.DOI 10.1007/s11274-008-9911-3.
51. Nejatzadel- Barandozi F. (2013). Antibacterial activities and antioxidant capacity of Aloe vera. NejatzadehBarandozi Organic and Medicinal Chemistry Letters, 3:, 5.

Received: 8 september 2020
Accepted: 10 october 2020

RESEARCH / INVESTIGACIÓN

Comparative study between ECL and ELISA to determine the reliable range of Estradiol in the treatment of infertility

Sadeghitabar Ali[1], Maleki Narges[2], Armand Maryam[2], Nasiri Reza[2*]

DOI. 10.21931/RB/2020.05.04.12

Abstract: Estradiol is one factor that can alter the outcome of the treatment of infertile couples following the application of in vitro fertilization techniques. Currently, the estradiol level is measured by two diagnostic methods Enzyme-Linked Immunosorbent Assay (ELISA) and Electrochemiluminescence (ECL). Accordingly, this study determines ELISA and ECL's sensitivity and consistency to measure different levels of estradiol and determine its reliable range and provide this information to laboratories and gynecologists. This study is performed on 250 patients of the Avicenna Fertility Center. The data of the study are analyzed in SPSS18 and MiniTab. Consent was obtained for experimentation with human subjects. Pearson correlation coefficient was used to investigate the relationship between these two methods. The results indicated a strong correlation between the two variables ECL and ELISA (r= 0.735, P-value<0.001). High numbers indicate that the decrease and increase of one variable are proportional to the other variable's fluctuation. This study shows that the results of estradiol obtained from both ECL and ELISA are similar. In the ELISA method, due to the linear values' limitation, samples with estradiol concentration above the highest standard level should be diluted and the dilution coefficient should then be applied.

Key words: Estradiol, estrogen, infertility, ELISA, ECL.

Introduction

Estradiol is a steroid hormone and is the most important sex hormone in women. It is the first type of estrogen and is produced in the ovaries. As the ovaries grow and develop, the egg follicles release estradiol to assist the onset and maintenance of the monthly cycle[1]. This hormone also affects other tissues such as bone, liver, blood vessels and reproductive tissues such as the uterus. Estradiol is one factor that can alter the outcome of the treatment of infertile couples following the application of in vitro fertilization techniques.

For this reason, in the infertility treatment cycles, the serum level of this hormone is used as a monitoring tool for ovulation induction, and the accuracy of IVF planning[2]. However, in the cycles following in vitro fertilization, the number of mature follicles is more due to the use of ovarian stimulating drugs, and hence the level of this hormone (estradiol) may be higher than its physiological range. This increase in estradiol level could raise concerns about luteal phase abnormalities, uterine tissue changes, and ovarian hyper-stimulation syndrome, a life-threatening complication of the ovulation induction cycle. Therefore, it is essential to measure the different levels of estradiol and its reliable ranges accurately[3]. Accordingly, the experience of some infertility centers suggests that by changing the method of estradiol measurement in the laboratory of an infertility center, the upper limit of this hormone, which poses the risk of OHSS, could be changed, and the state of not recognizing this level maintains the risk of consuming lower or higher doses of ovulation-stimulating drugs in infertile patients. In other words, if the physician is not informed of this change and the critical drug range, they would mistakenly increase or decrease the drug dosage due to the assumption of inadequate or excessive drug dose, which would ultimately lead to either OHSS or failure of the treatment cycle. Thus, it is essential to know that changing the method does not necessarily mean that high estradiol levels may be similar even by one unit of measurement, and this will be a critical point in the success and health of the treatment cycle.

During ovarian hyperstimulation for in vitro fertilization (IVF), serum estradiol concentrations are usually monitored daily for optimal timing of human chorionic gonadotropin (hCG) administration oocyte collection. The DRG Estradiol sensitive ELISA Kit is a solid phase enzyme-linked immunosorbent assay (ELISA), based on the competitive binding. The microtiter wells are coated with a polyclonal antibody directed towards an antigenic site on the Estradiol molecule. Endogenous Estradiol of a patient sample competes with an Estradiol horseradish peroxidase conjugate for binding to the coated antibody. After incubation, the unbound conjugate is washed off. The amount of bound peroxidase conjugate is reverse proportional to the concentration of estradiol in the sample. After adding the substrate solution, the intensity of color developed is reverse proportional to estradiol concentration in the patient sample[8].

Currently, diagnostic methods (ELISAs) and (ECLs) are used to measure estradiol levels; however, based on research studies, ECL has superiority in sensitivity, cost-effectiveness, and high precision over conventional colorimeter methods such as ELISA. On the other hand, quick and error-free answering is desirable in all situations, and to achieve this goal, changing the system from manual to machinery seems necessary. Therefore, although one of the most commonly used methods for measuring this hormone assay is ELISA, the ECL method's use is more rapid and accurate is prioritized[4,5].

Accordingly, one of the hypotheses raised in this study was that if the units of measurement were identical in the two methods, whether to obtain a standard concentration of serum estradiol level in the ECL method and to compare it with the ELISA method and to share this information with laboratories and gynecologists, is essential or not? And can the serum estradiol level measure in one person by 2 different (ELISA) methods and (ECL) be different under the same conditions? And finally, the measurement and prescription dosage of estradiol hormone should be based on the specific method (ELISA/ECL) which is used for assessing estradiol hormone.

[1] Monoclonal Antibody Research Center, Avicenna Research Institute, ACECR, Tehran, Iran.
[2] Avicenna infertility department, Avicenna Research Institute, ACECR, Tehran, Iran.

Corresponding author: jlvelez@uce.edu.ec

Based on the second hypothesis of this study, since estradiol results in high concentrations of this hormone by ELISA, which usually occurs during infertility treatment, it has no linear relationship with diluted hormone assays, therefore repeating the test with diluted samples from specified values above before reporting the result is essential. It is also crucial to specify a reliable reading range without the application of dilution. Given that assisted reproductive techniques' success is highly essential due to the financial costs and psychological problems following their failure, any studies that can increase these success rates are entirely critical. This study's main objective was to determine the sensitivity and consistency of ELISA and Electro Quantitative Luminescence (ECL) methods to measure different estradiol hormone levels and determine a reliable range to enhance assisted reproduction success and prevent complications which are dangerous and sometimes irreparable. Some other specific targets were considered to be evaluated in this paper, like determining the compatibility of two methods (ECL vs. ELISA) in measuring estradiol hormone and Determining the sensitivity of the ELISA method in measuring the high titers of estradiol and determining the reliable range for it. This study's hypothesis firstly entails some practical purposes such as changing the manual test method to an automatic one, Increasing the test's speed and accuracy, Increasing the sensitivity and specificity of the test, and increasing sensitivity and specificity of the test in high estradiol titers. This proposal's crux is to establish a satisfactory laboratory evaluation method for a clinical endocrinology hormone, estradiol.

Materials and methods

To start the practical process, inclusion criteria were established as follows. All patients with at least two previous unsuccessful IVF/ICSI cycles were admitted. After signing the informed consent and computer-generated randomization, the study was performed on 250 patients referred to specialized clinics of Avicenna infertility, and recurrent miscarriage treatment center referred to the medical diagnosis laboratory for estradiol testing. Consent was obtained for experimentation with human subjects. Out of the compilation, 250 samples were randomly selected with different concentrations and were analyzed and compared through both methods. Finally, the data were analyzed in SPSS18 and MiniTab.

$$\eta' = \left(\frac{Z_1 - \alpha\sigma}{d} \right)^2$$

$$\eta' \approx \left(\frac{(1.96)\,(200)}{25} \right)^2 = 2\,46 \approx 250$$

How to choose patients

All patients referred to the Medical Diagnostic Laboratory of specialized clinics of Avicenna Infertility and Repeated Abortion treatment center for estradiol testing during the project period were eligible for admission.

Sample size and calculation method

According to expert statistics for estimation of estradiol hormone level in Pg/ml, in two methods with 95% confidence and 25 Pg/ml, concerning standard deviation of estradiol in two methods equal to 200Pg/ml using the statistical method, approximately 250 cases who were randomly selected, were calculated.

The project started on 28 August 2018 after receiving the code of ethics: IR.ACECR.AVICENNA.REC.1397.006 from the Avicenna Ethics committee: www.ethics.research.ac.ir by Dr. Ali Sadeghi Tabar. Additionally, all applicants in this research received consent upon arrival to the program, and their information was used anonymously.

Data collection tools

Specimens were obtained from patients of the different specialized clinics referred to the Medical Diagnostic Laboratory for estradiol testing, and the results of ELISA and ECL tests were analyzed by SPSS software.

Results

Results were analyzed by the statistical expert and are as follows: Pierson correlation coefficient was used to investigate the relationship between these two methods. The results indicated a strong relationship between the two variables ECL and ELISA ($r=0.735$, P-value<0.001). High numbers mean that each variable's decrease and increase are proportional to the decrease and increase of the other variable. The distribution chart of the ECL and ELISA variables is as follows:

Discussion

Historically, quantitative methods for measuring E2 have been obtained by bioassay, mass spectrometry (MS), UV absorbance, and immunoassay. Up until now, applying any measurement method to biological specimens has required the isolation of steroids. The original immunological method for Estradiol evaluation was named RIA or indirect RIA[9]. Measurement of Estradiol in serum without its prior isolation is called direct RIA, like chromatography, as it is performed currently[10].

A group of scientists declared that estradiol must be measured at low concentrations to distinguish between suppressed levels of less than 1pg/mL and pretreatment levels[11].

Another paper suggests that the measurement of E2 should be reliable at levels of 3000pg/mL when testing performed in support of IVF programs, for ovulation induction and ovarian hyper-stimulation monitoring[12].

Several studies suggest concerns about the analytical performance in the measurement of E2 among different assays[13]. Sensitive assays for estradiol have been immunologically based, but it lacks specificity to satisfy all clinical and scientific requirements, up until recently, methods based on mass spectroscopy have been replaced[14].

ECL (ElectroChemiLuminescence) is Roche's technology for immunoassay detection of estradiol. Based on this technology, ECL delivers reliable results. The development of ECL immunoassays is based on the use of a ruthenium-complex and tripropylamine (TPA). The chemiluminescence reaction for detecting the reaction complex is initiated by applying a voltage to the sample solution resulting in a precisely controlled reaction[15].

In a study by Azim et al. (2015) on the mechanism and application of the ECL method, the results of the study showed that: different types of luminescence include quantum luminescence (cold radiation caused by a chemical reaction), bioluminescence (The biochemical reaction within an organism, such as a firefly), electroluminescence (passing electric current, such as LED lamps), electrochemical luminescence (electrochemical reaction), phosphorescence (such as lumi-

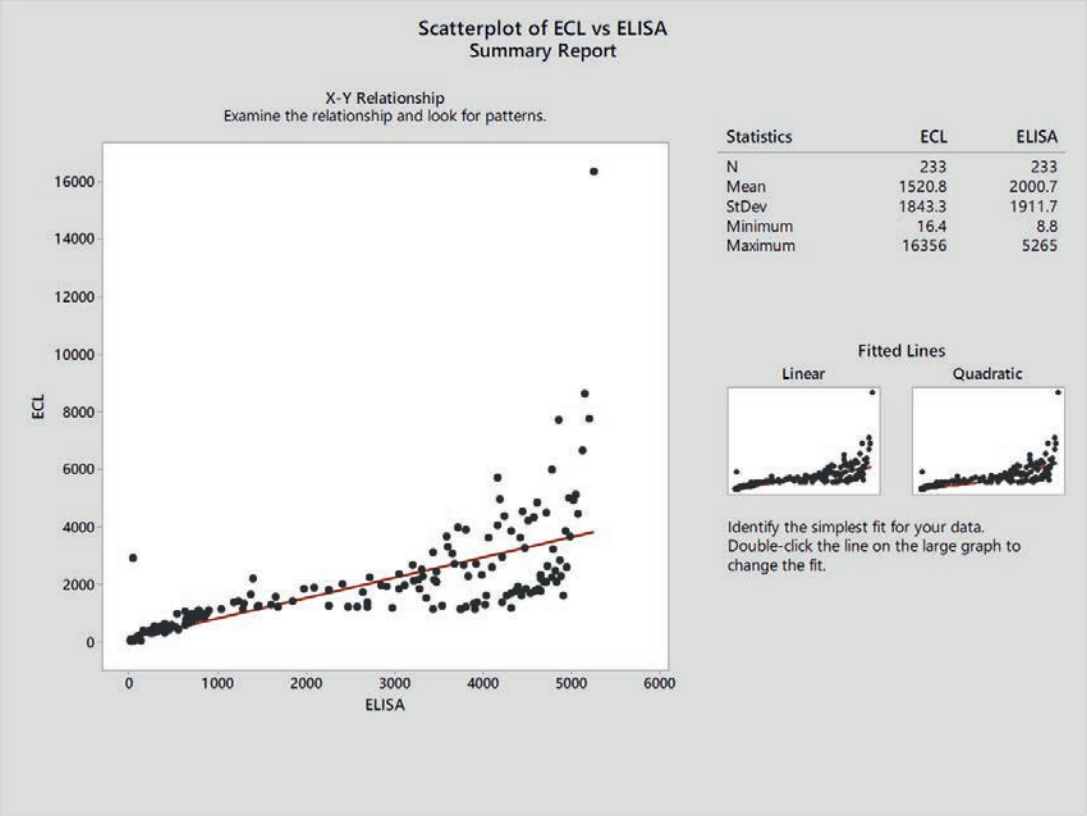

Figure 1. The distribution chart of the ECL and ELISA variables.

nous clock hands), and so on[6]. The source of radiation in ECL is often a polycyclic aromatic hydrocarbon, a metal complex, a quantum dot, or a nanoparticle. ECL's main advantage of ELISA methods is that it does not require light, and the analyte itself is the source of radiation. This small difference increases the test's sensitivity and specificity several times and makes the response or linearity of the radiation-dose curve in the ECL very wide and eliminating confounding factors in the majority of times. The concentration level of analytes in many laboratory methods is based on the light passing through the solution and its absorption rate. This process is illustrated by drawing a radiation-dose curve and that part of the curve, which has a linear correlation with the dose or concentration of the analyte of the test, can rely on[6].

In another study done by Nasiri et al. in 2013, Conducted to evaluate the compatibility of estradiol hormone levels with ELISA in two diluted and non-diluted serum of women treated by ovulation stimulation drugs concluded that in Serum estradiol level more fabulous than 2000 Pg/ml requires dilution of the samples and the results of the non-dilution assay will not be reliable. This should be taken into account in laboratories of infertility treatment centers or even other laboratories to determine the linearity of the methods used to dilute them when exposed to higher amounts[7].

Our study indicated that the estradiol results obtained from both ECL and ELISA were similar in the medical diagnostic laboratory and had a similar interpretation. It should be noted that in the ELISA method, due to the limitation of the linear values, samples with estradiol concentration above the highest standard level should be diluted, and then the dilution coefficient should be applied. This research's dilution coefficient was 1: 5, and 5µL of the sample was mixed with 20 µL of the diluent. Then the result was multiplied by 5 and compared with the ECL method.

Conclusions

As it is shown in the comparison chart of the distribution of ECL versus ELISA methods, at high concentrations of estradiol, the results of the two methods did not fit well with the low concentrations of estradiol. This means that at high concentrations of estradiol hormone, especially during infertility treatment that threatens the person with OHSS (ovarian hyper-stimulation syndrome), it is vital that the laboratory first interacts with the treatment team to allow the concentration of this hormone to be determined according to the method. Secondly, during the patients' treatment, method alternations should be avoided to evade misinterpretation of the results and overuse of ovulation induction drugs. This phenomenon is demonstrated in another way when interpreting the results of Beta-HCG concentrations in the study of pregnancy and follow-up of this molecule in infertility-treated individuals, including that it is crucial to perform the initial tests and subsequent titration in a single laboratory with a single measurement method to avoid the error of interpretation of the results due to the different specificity of the kits and different methods.

Acknowledgments

We are grateful to the respected personnel of Ebn Sina Infertility Treatment Laboratory for assisting us in this research.

Conflict of Interest

There was nothing detected as a conflict of interest by authors, and the authors have nothing to disclose.

The project started on 28 August 2018 after receiving the code of ethics: IR.ACECR.AVICENNA.REC.1397.006 from the Avicenna Ethics committee: www.ethics.research.ac.ir by Dr. Ali Sadeghi Tabar. The authors have nothing to disclose.

Abbreviations

ELISA: The enzyme-linked immunosorbent assay (analytical biochemistry assay)

ECL: Electrochemiluminescence (electrogenerated chemiluminescence)

Bibliographic references

1. Burke J. Gynecological (Novak) translators: AR monjmi, N. Khatibi. Tehran, the light of knowledge 2010; 2.
2. Gautam N, Allahbadia B, Rita B. The Art and Science of Assisted Reproductive Techniques (ART). London: Taylor & Francis: 2003.
3. Sperof L, Marc A. Clinical Gyn End & infertility: Translate by Ghazijahani B, Zonuzi A. Tehran, Iran 2005; 548-659.
4. Imai, A. Nishitani, H. Akimoto, Y. Tsukamoto, J. Biolumin. Chemilumin. 4 (1989) 500-504.
5. Yu. H., 1998a. Comparitives studies of magnetic particle-based solid-phase fluorogenic and electrochemiluminescence immunoassays. J. Immunol, Methods 218,1-8.
6. M. Azim, A. Nishitani, H. Mizanul. I. Hossain, N. Ansari. chemiluminescence immunoassay: basic mechanism and applications. J. Nucl. Med. 2015. 18 (2). 171-178.
7. R. Nasiri, H. Soltanghoraee, A. Mohammadzadeh,AM. Zarnani,M. Jeddi-Tehrani. A, SadeghitabarEvaluation ofcoordination between diluted and undiluted serum estradiol levels using ELISA method inwomenunder treatment with ovulation induction drugs. Razi Journal of Medical Sciences. 2013. 20 (111). 12-1. https://store.drg-international.com/shop/estradiol-sensitive-elisa.asp
8. Abraham GE, Odell WD. Solid-phase immunoassay for estradiol 17- ß: a semi-automated approach. In: Peron FG, Caldwell BV, eds. Immunologic methods in steroid determination. New York: Appelton-Century-Crofts;1970;87–112.
9. Laboratory instrumentation product guide: immunoassay analyzers. Northfiled, Illinois: College of American Pathologists; 2011;17–54.
10. Stanczyk FZ, Jurow J, Hsing AW. Limitations of direct immunoassays for measuring circulating estradiol levels in postmenopausal women and men in epidemiologic studies. Cancer Epidemiol Biomarkers Prev. 2010;19:903–906.
11. Demers LM. Testosterone and estradiol assays: current and future trends. Steroids. 2008;73:1333–1338.
12. Schioler V, Thode J. Six direct radioimmunoassays of estradiol evaluated. Clin Chem. 1988;34:949 –952.
13. Raff H, Sluss PM. Pre-analytical issues for testosterone and estradiol assays. Steroids. 2008;73:1297–1304.
14. Elecsys® Estradiol III package insert (2014). Roche Diagnostics Documentation, Basel. Roche Diagnostics International Ltd. CH-6343 Rotkreuz. Switzerland. www.cobas.com

Received: 23 August 2020
Accepted: 4 October 2020

RESEARCH / INVESTIGACIÓN

Obtención de un extracto rico en carotenoides con capacidad antioxidante a escala de banco a partir de residuos agroindustriales del tomate de árbol (*Solanum betaceum*)

Obtaining an extract rich in carotenoids with antioxidant capacity on a bank scale from agro-industrial residues of tree tomato (*Solanum betaceum*)

Walter Ramiro Urbina, Danae Fernández, Orestes Dario López, Antonio Iraizoz
DOI. 10.21931/RB/2020.05.04.13

Resumen: Los carotenoides son los compuestos químicos con mayor presencia en las cáscaras del tomate, son pigmentos naturales con capacidad antioxidante, estos se extraen utilizando solventes orgánicos como el etanol. En esta investigación se realizó una extracción de carotenoides utilizando etanol con una relación material vegetal/volumen de disolvente de 1/70 en los volúmenes de 0,5 L, 3 L y 5 L. Los extractos se caracterizaron físico químicamente y se compararon las medias obtenidas de cada ensayo para un nivel de significancia del 95% obteniendo para la escala de banco un extracto con un índice de refracción de 1,36, viscosidad cinemática de 2,09 $cSt.s^{-1}$, concentración de licopenos de 0,51 $mg.L^{-1}$ y una eficiencia del proceso de extracción de 34,34 $mg.k^{-1}$, no presentando diferencias significativas con las escalas de laboratorio (0,5 L y 3 L). Los valores de porcentaje de humedad y pH a la escala de banco fueron de 99,90% y 5,69 respectivamente, presentando diferencias significativas ente las tres escalas. Se microencapsuló mediante secado por aspersión el extracto obtenido a escala de banco con los polímeros maltodextrina y goma arábiga obteniendo un 99,39% de eficiencia de microencapsulación, mediante espectroscopía infrarrojo fue corroborado la presencia de carotenoides dentro de las microcápsulas. Se obtuvieron microcápsulas con un porcentaje de inhibición de DPPH del 21,72% equivalente a una concentración de Trolox de 142,72 $\mu mol.L^{-1}$.

Palabras clave: Actividad antioxidante equivalente de Trolox, extracto de carotenoides, microencapsulación de carotenoides.

Abstract: Carotenoids are the chemical compounds with the most significant presence in tomato peels; they are natural pigments with antioxidant capacity; these are extracted using organic solvents such as ethanol. In this research, a carotenoid extraction was carried out using ethanol with a plant material / solvent volume ratio of 1/70 in the volumes of 0.5 L, 3 L, and 5 L. The extracts were physically chemically characterized, and the means were compared obtained from each test for a significance level of 95%, obtaining for the bench-scale an extract with a refractive index of 1.36, the kinematic viscosity of 2.09 $cSt.s^{-1}$, lycopene concentration of 0.51 $mg.L^{-1}$ and efficiency of the extraction process of 34.34 $mg.k^{-1}$, showing no significant differences with the laboratory scales (0.5 L and 3 L). The values of the percentage of humidity and pH on the bench scale were 99.90% and 5.69, respectively, presenting significant differences between the three scales. The extract obtained on a bench scale with maltodextrin and gum Arabic polymers was microencapsulated by spray drying, obtaining a 99.39% microencapsulation efficiency, by infrared spectroscopy, the presence of carotenoids within the microcapsules was corroborated. Microcapsules were obtained with a DPPH inhibition percentage of 21.72%, equivalent to a Trolox concentration of 142.72 $\mu mol.\ L^{-1}$.

Key words: Trolox equivalent antioxidant activity, carotenoid extract, carotenoid microencapsulation.

Introducción

El tomate de árbol (*Solanum betaceum*) es una fruta originaria de Sudamérica y se cultiva en las regiones Andinas de países como Bolivia, Colombia, Ecuador y Perú. En Ecuador se cultivan en varias provincias de la Sierra, siendo Tungurahua la provincia de mayor producción a nivel nacional. El consumo es de forma tradicional en jugos y mermeladas. En el procesamiento industrial se generan desechos como las cáscaras y semillas llegando a alcanzar valores hasta un 5%[1].

Los carotenoides son los compuestos químicos con mayor presencia en las cáscaras de tomate, son pigmentos naturales con una estructura química de ocho unidades de isopreno, liposolubles y responsables de la coloración en el tomate de árbol[2]. El licopeno es uno de los carotenoides sintetizados por las plantas y microorganismos fotosintéticos, es el más abundante en el tomate, su estructura química es de un hidrocarburo alifático de cadena lineal constituido por 40 átomos de carbono con 13 enlaces carbono – carbono de los cuales 11 son conjugados y 56 átomos de hidrógeno. Participa en la desactivación de algunos radicales libres como el peróxido de hidrogeno, dióxido de nitrógeno, radicales sulfonilo y radicales hidroxilos, también es un intermediario de la biosíntesis de algunos carotenoides como el β-caroteno[3].

Los procesos de extracción desarrollados para la obtención de carotenoides de residuos agroindustriales del tomate a lo largo del tiempo han permitido obtener 36,5 mg de carotenoides por kilogramo de residuo seco del tomate de árbol con una mezcla de disolventes etilo – hexano, mientras que usando el solvente etanol se alcanzó una cantidad de 6,1 $mg.kg^{-1}$.[4]

La microencapsulación del extracto con alto contenido de licopeno es un proceso clave en la conservación de las propiedades funcionales y antioxidantes. Los efectos de la luz, pH, oxígeno y calor son causantes de la degradación de los carotenoides, además la microencapsulación permite mejorar las propiedades organolépticas del ingrediente activo. La tecnología de secado por pulverización permite la utilización de productos que se pueden incorporar como ingredientes activos

Facultad de Ciencia e Ingeniería en Alimentos y Biotecnología, Universidad Técnica de Ambato, Ecuador.

Corresponding author: da.fernandez@uta.edu.ec

en la preparación de alimentos funcionales o productos farmacéuticos de liberación controlada, aumentando su especificidad y disponibilidad[5].

Materiales y métodos

Obtención del material vegetal

La fruta del tomate de árbol se adquirió del Mercado Mayorista de Ambato y se trasladó a las instalaciones de los laboratorios de la Unidad Operativa de la Dirección de Investigación y Desarrollo (UODIDE-ICIA) de la Facultad de Ciencia e Ingeniería en Alimentos y Biotecnología, de la Universidad Técnica de Ambato, posteriormente se realizó el pelado de la fruta, las cáscaras se cortaron en pedazos pequeños de aproximadamente 2 cm y se sometieron a un proceso de secado en un horno de convección (GANDER MTN) a la temperatura de 50 °C por un tiempo de 55 horas. Se utilizó un molino de cuchillas (INOX-EQUIP) para obtener un tamaño de partículas finas y se preservó en fundas herméticas a la temperatura ambiente[4].

Obtención del extracto a nivel de laboratorio y de banco

Para obtener el extracto se utilizaron tres biorreactores con volúmenes de 0,5 L, 3 L y 5 L (Tabla 1).

Datos			
Volumen (V)	0,5 L	3 L	5 L
Diámetro del agitador (d)	0,025 m	0,05 m	0,062 m
Diámetro del reactor (D)	0,085 m	0,142 m	0,165 m

Tabla 1. Dimensiones de los biorreactores utilizados en la extracción.

Para extraer los carotenoides del material vegetal se utilizó el método descrito por (6) que utilizó una relación de material vegetal/volumen de disolvente 1:70, como disolvente orgánico etanol al 96%, un tiempo de extracción de 30 minutos a una temperatura de 50 °C. El proceso de extracción de carotenoides se realizó por triplicado en cada biorreactor.

Mediante la ecuación I se determinó la velocidad de agitación (n) para cada impelente, donde N es la potencia por unidad de volumen en watts, kn es igual a la constante 0,3 para el etanol, ρ es la densidad del etanol en $kg.m^{-3}$ y d^5 es el diámetro del impelente en metros elevado a la quinta potencia.

$$N = kn\ \rho\ n^3\ d^5 \qquad \text{(I)}$$

El número de potencia por unidad de volumen se determinó por el consumo de potencia (N) dividido por el volumen (V) del biorreactor.

La distancia mínima al fondo del biorreactor se calculó con la ecuación III donde Zi es la distancia entre el agitador con el fondo del biorreactor y D el diámetro del biorreactor.

$$Zi_{laboratorio} = \left(\frac{Zi_{industrial}}{D_{industrial}} * D_{laboratorio}\right) \qquad \text{(III)}$$

Para los factores de forma se utilizó relación de diámetro de impelente (d)/diámetro de tanque (D) constante.

Caracterización de los extractos vegetales

La caracterización físico-química se realizó a los extractos vegetales obtenidos en los tres volúmenes para los ensayos de: porcentaje de humedad, pH, índice de refracción, viscosidad, concentración de licopenos y eficiencia de extracción.

La determinación del porcentaje de humedad se realizó mediante la utilización de una balanza de humedad (KERN MLS 50-3) a través de energía infrarroja. Consistió en un método termogravimétrico, el principio es la determinación de la pérdida de peso por medio del secado, esto es pérdida de agua, sustancias volátiles como alcoholes, disolventes orgánicos, entre otros productos que se pueden descomponer por acción de la temperatura[7].

Se determinó el pH utilizando el método potenciométrico a través de un pH-metro (Thermo Scientific ORION VERSASTAR). El funcionamiento del pH-metro implica la medición de una diferencia de potencial entre un electrodo de referencia y un electrodo de vidrio que actúa como una membrana selectiva que permite el paso de hidrogeniones. Esta diferencia de potencial hace referencia a la ecuación de Nernst[8].

Para el índice de refracción se utilizó un refractómetro (ABBE NAR-2T) en un rango de medición de 1,30 a 1,70 de índice de refracción. El funcionamiento del equipo se fundamenta en la refracción de la luz de una sustancia que es igual al cociente entre la celeridad de la luz en el vacío y la celeridad de la luz en la sustancia analizada[9], relacionado con las propiedades físicas como la densidad.

Se determinó la viscosidad con un viscosímetro capilar (CANNON 150 Z285), este método consistió en pasar fluido a través de un capilar a temperatura constante, midiendo el tiempo requerido para que un volumen del líquido escurra desde una marca superior hasta una marca inferior grabada en el viscosímetro[10].

Se determinó la eficiencia de extracción a través de la relación entre la masa de licopenos extraída y la masa del residuo vegetal seco utilizado en el proceso de extracción.

La distancia mínima a la pared del biorreactor ($Ji_{laboratorio}$) se determinó a través de la ecuación II, donde es ($Ji_{industrial}$) es la distancia entre el agitador y la pared del biorreactor industrial y (D) es el diámetro del biorreactor.

$$Ji_{laboratorio} = \left(\frac{Ji_{industrial}}{D_{industrial}} * D_{laboratorio}\right) \text{(II)}$$

Ecuación 2.

El número de Reynolds se utilizó para conocer el comportamiento de los fluidos en movimiento. Se determinó mediante la ecuación IV, donde n corresponde a la velocidad de agitación en s^{-1}, ρ es la densidad en $kg.m^{-3}$, d^2 el diámetro del agitador en metros y μ corresponde a la viscosidad.

$$Re = \frac{n\ \rho\ d^2}{\mu} \qquad \text{(IV)}$$

Ecuación4.

La concentración de licopenos se realizó a través de un método espectrofotométrico con la utilización del espectrofotómetro (Fisher Scientific accuSkan GO) a una longitud de onda de 472 nm. Para el cálculo de la concentración de licopenos se utilizó la ecuación V donde $A_{\lambda max}$ es la absorbancia del extracto y $A_{1\ cm}^{1\%}$ es el coeficiente de absortividad del disolvente. La concentración de licopeno (C) es expresada en mg.L^{-1}. [5]

$$C = \frac{A_{\lambda max} 10^4}{A_{1\ cm}^{1\%}} \qquad (V)$$ **Ecuación 5.**

Microencapsulación del extracto mediante secado por aspersión

El extracto obtenido a escala de banco en el volumen de 5 L se concentró con la utilización del equipo rotavapor (IKA RV8) a una temperatura de 50 °C y una velocidad de agitación de 200 rpm[11]. Se preparó una emulsión a partir del extracto concentrado de licopeno utilizando un 15% de agua destilada y un 85% de maltodextrina/goma arábiga. Se utilizó el equipo mini spray dray (BUCHI-B290) a la temperatura de 120 °C y 80 °C para la entrada y salida respectivamente del equipo.

Determinación de la actividad antioxidante

Se realizo mediante el uso del reactivo 2,2-difenil-1-picril-hidracilo (DPPH), este radical reacciona con compuestos antioxidantes resultando en un cambio de coloración, el cual se determina utilizando un espectrofotómetro (Fisher Scientific accuSkan GO) a la longitud de onda de 515 nm[12]. Se realizó una curva de calibración con Trolox como antioxidante de referencia con concentraciones en el rango de 50 a 500 µmol.L^{-1}. Se determinó el porcentaje de inhibición del DPPH a través de la ecuación VI, donde Am es la absorbancia de la muestra y Ab la absorbancia del blanco reactivo. Se expresó la actividad antioxidante como equivalentes a µmol de Trolox/L.

$$\%\ Inhibición\ DPPH = \left(1 - \left(\frac{Am}{Ab}\right)\right) * 100 \qquad (VI)$$

Determinación del porcentaje de eficiencia de microencapsulación

Se calculó a través de la relación entre la concentración de licopeno obtenida al disolver el microencapsulado en agua (CA) y en etanol (CE) (ecuación VII).

$$E.M = \frac{CA_{agua} - CE_{etanol}}{CA_{agua}} * 100$$ **Ecuación 7.**

Espectroscopía infrarroja

Se realizó un análisis de espectroscopía infrarrojo por trasformadas de Fourier (FTIR) en una frecuencia de 400 a 4000 cm^{-1} a las muestras del extracto vegetal concentrado, microencapsulado y mezcla de polímeros utilizando un espectroscopio infrarrojo (Jasco FT/IR 4100).

Análisis estadístico

Se realizó un diseño completamente al azar, en el cual el factor de cambio fueron los volúmenes de extracción a nivel de laboratorio y banco con tres réplicas. Se utilizó el software Statgraphics Centurion (versión XVI.I) en el análisis ANOVA y para la comparación de medias entre los tres volúmenes para un nivel de significación del 95%.

Resultados y discusión

Obtención del extracto a nivel de laboratorio y de banco

En la tabla 2 se muestran los valores obtenidos de los parámetros analizados en el cambio de escala en los volúmenes de 0,5; 3 y 5 L.

Para la velocidad de agitación se da una disminución por efecto de las dimensiones de cada biorreactor con el agitador. El consumo de potencia es la disipación de la energía mecánica en el fluido a través del agitador que genera fricción entre las capas del fluido[13]. En efecto el consumo de potencia se relaciona de forma directa con el volumen del biorreactor, además el diámetro del agitador es la variable que más influye en la determinación de la velocidad de agitación. Entonces al incrementarse el volumen de 0,5 a 5 L se incrementó la potencia consumida, pero la velocidad de agitación fue menor porque el diámetro del impelente se incrementó.

En la relación diámetro del agitador con el diámetro del biorreactor se buscó la más cercana entre los tres biorreactores existiendo una diferencia de 0,081entre el de 0,5 L y el de 5 L, que se consideró como un valor poco significativo que no influyó en el número de potencia como mencionan García y Jáuregui[13] que si el valor de la relación d/D aumenta el número de potencia también aumenta.

Caracterización de los extractos vegetales

En la tabla 3 se muestran los resultados obtenidos en la caracterización físico química de los extractos obtenidos en las tres escalas.

Los resultados de porcentaje de humedad se encontraron en un intervalo de 99,85 a 99,9%, mediante un análisis estadístico ANOVA se identificó que existieron diferencias estadísticas significativas entre los tres volúmenes valor de p= 0,0488 (Tabla 4).

El resultado obtenido del diseño factorial para la variable respuesta pH indicó que existieron diferencias significativas entre los tres volúmenes de extracción valor de p= 0,0007 (Tabla 5). Los valores registrados se encuentran en el intervalo mínimo de 5,58 y un máximo de 5,68 considerando que la fruta del tomate de árbol se encuentra en un pH alrededor de 3,77 según manifiesta Carrasco y Encina[14] en su investigación y al estar en un medio con etanol se incrementa el pH.

Para el índice de refracción no se encontraron diferencias estadísticas significativas valor p= 0,7865 (Tabla 6). El etanol en los extractos se encuentra en un porcentaje mayoritario respecto a los carotenoides.

Los resultados para la viscosidad cinemática no mostraron diferencias estadísticas significativas obteniendo un valor de p= 0,8669 (Tabla 7). Según Aguado, Nuñez, Bela, Okulik y Bregni[15] para el extracto etanólico de *Aloysia polystachya* determinó la viscosidad cinemática a 37,8 °C obteniendo un valor de 1,037 cSt.s^{-1}. En contexto de que no existieron diferencias significativas en la escala de laboratorio y banco se puede atribuir a la realización del proceso de extracción a tiempo y temperatura constante. En un mayor tiempo a una temperatura determinada se incrementa la viscosidad y al no existir una variación de tiempo y temperatura los resultados no presentaron diferencias significativas.

El análisis estadístico indicó que no existió una diferencia

Volumen	0,5 L	3 L	5 L
Potencia consumida (N)	0,051 W	0,306 W	0,510 W
Velocidad de agitación (n)	26 s^{-1}	14,883 s^{-1}	12,329 s^{-1}
Distancia mínima a la pared (Ji)	0,0015 m	0,0025 m	0,0029 m
Distancia mínima al fondo (Zi)	0,0024 m	0,0041 m	0,0047 m
Diámetro del agitador/diámetro del biorreactor	0,294	0,352	0,375
Número de Reynolds	14979,050	34297,416	43685,986

Tabla 2. Resultados de los cálculos de desescalado.

Volumen (L)	*0,5*	*3*	*5*
% Humedad	99,849	99,882	99,905
pH	5,583	5,607	5,685
Índice de refracción	1,363	1,362	1,363
Viscosidad cinemática ($cSt.s^{-1}$)	2,105	2,073	2,086
Concentración de licopeno ($mg.L^{-1}$)	0,539	0,527	0,514
Rendimiento ($mg.kg^{-1}$)	35,47	35,34	34,34
% de inhibición del DPPH	55,72	53,65	50,80
Concentración equivalente de Trolox ($\mu mol.L^{-1}$)	496,82	475,24	445,54

Tabla 3. Resultados de la caracterización físico química de los extractos.

Fuente	*Suma de Cuadrados*	*Gl*	*Cuadrado Medio*	*Razón-F*	*Valor-P*
Entre grupos	0,00468867	2	0,00234433	5,21	0,0488
Intra grupos	0,00269933	6	0,000449889		
Total (Corr.)	0,007388	8			

Tabla 4. ANOVA para % de humedad por Volumen (L)

Fuente	*Suma de Cuadrados*	*Gl*	*Cuadrado Medio*	*Razón-F*	*Valor-P*
Entre grupos	0,0171842	2	0,00859211	30,38	0,0007
Intra grupos	0,00169667	6	0,000282778		
Total (Corr.)	0,0188809	8			

Tabla 5. ANOVA para pH por Volumen (L).

Fuente	Suma de Cuadrados	Gl	Cuadrado Medio	Razón-F	Valor-P
Entre grupos	2,22222E-7	2	1,11111E-7	0,25	0,7865
Intra grupos	0,00000266667	6	4,44444E-7		
Total (Corr.)	0,00000288889	8			

Tabla 6. ANOVA para Índice de refracción por Volumen (L).

Fuente	Suma de Cuadrados	Gl	Cuadrado Medio	Razón-F	Valor-P
Entre grupos	0,00152422	2	0,000762111	0,15	0,8669
Intra grupos	0,03127	6	0,00521167		
Total (Corr.)	0,0327942	8			

Tabla 7. ANOVA para Viscosidad Cinemática (cSt.s^{-1}) por Volumen (L)

Fuente	Suma de Cuadrados	Gl	Cuadrado Medio	Razón-F	Valor-P
Entre grupos	0,000940222	2	0,000470111	2,48	0,1639
Intra grupos	0,00113667	6	0,000189444		
Total (Corr.)	0,00207689	8			

Tabla 8. ANOVA para la concentración de licopenos (mg.L^{-1})

Fuente	Suma de Cuadrados	Gl	Cuadrado Medio	Razón-F	Valor-P
Entre grupos	2,31303	2	1,15651	1,39	0,3186
Intra grupos	4,98335	6	0,830558		
Total (Corr.)	7,29637	8			

Tabla 9. ANOVA para la Eficiencia de Extracción en mg.kg^{-1}.

significativa entre la concentración de licopenos en los tres volúmenes de extracción (valor p= 0,1639, (Tabla 8)), como consecuencia de que en la extracción se utilizó igual relación material vegetal/volumen de disolvente en los tres volúmenes lo que favorece a la no variabilidad de los resultados.

En el análisis de medias se obtuvo un valor p= 0,3186 (Tabla 9) lo que demuestra que no se encontraron diferencias estadísticas significativas en los tres volúmenes para la eficiencia de extracción, obteniendo el valor más elevado en el volumen de 0,5 L con 35,47 mg de licopenos en 100 kg de material vegetal (35,473 mg.kg^{-1}), encontrándose este valor dentro del rango reportado en literatura de 5 a 45 mg.kg^{-1} con temperaturas de extracción de 25 – 60 °C y tiempos de extracción de 30 min utilizando cáscaras de tomate[5]. Este valor se encuentra similar a otros reportados en bibliografía donde de una cantidad de 100 g de residuo vegetal se han logrado obtener alrededor de 4 mg de carotenos[14].

Microencapsulación del extracto mediante secado por aspersión

Se determinó la actividad antioxidante en el microencapsulado obtenido del extracto del volumen de 5 L alcanzando un valor de 21,73 % de inhibición del radical DPPH.

Se obtuvo la siguiente ecuación lineal (Ecuación VIII) con un coeficiente de correlación de 0,996 obteniendo una concentración equivalente a Trolox de 142,72 µmol.L^{-1}.

Se obtuvo un valor de 99,39% de porcentaje de eficiencia de microencapsulación (E.M) lo que demuestra que la re-

$$\%\ Inhibición = 8{,}02204 + 0{,}0960156 * Concentración\ (umol\ Trolox\ L\hat{}-1) \quad \text{(VIII)}$$

Ecuación 8.

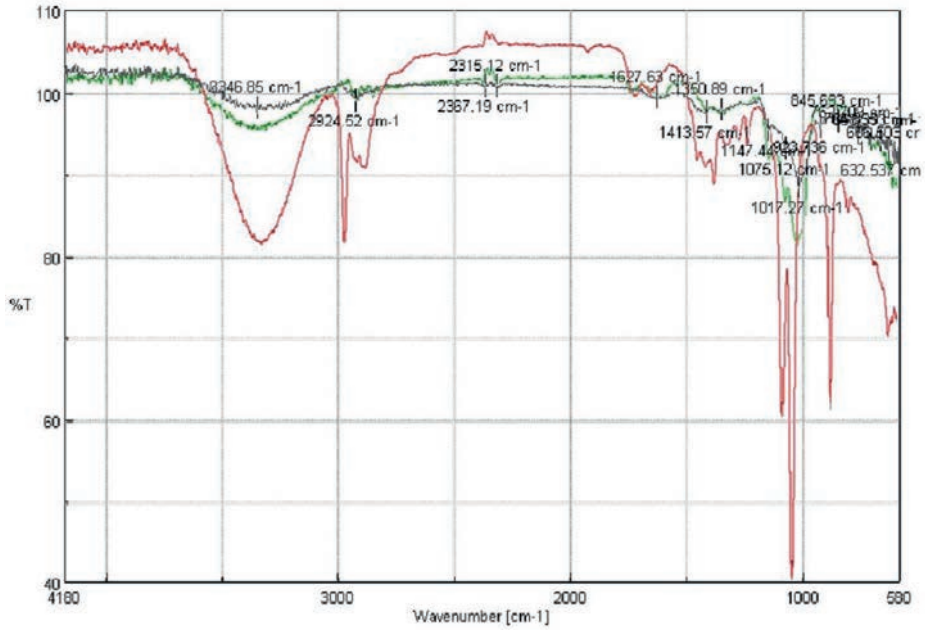

Figura 1. Espectros de resonancia infrarrojo de las muestras de extracto concentrado, microencapsulado y polímeros goma arábiga – maltodextrina.

lación polímeros y temperaturas utilizados en el proceso son óptimas. En comparación con datos bibliográficos de Pérez[6] el porcentaje de eficiencia de microencapsulación para el mismo compuesto activo es similar, en el cual obtuvo una eficiencia del 96,5% utilizando una mezcla de estos polímeros. Se corroboró este elevado porcentaje de eficiencia de la microencapsulación a través de espectroscopía infrarroja utilizando una frecuencia de absorción entre 580 – 4180 cm-1 y 40 – 110% de transmitancia (Figura 1). Se observó que el microencapsulado produjo un espectro infrarrojo muy similar que la mezcla de polímeros, confirmando que los licopenos se encuentran en el interior de las microcápsulas.

Conclusiones

Se extrajeron carotenoides a partir de los residuos agroindustriales del tomate de árbol, obteniendo a escala de banco (volumen de 5 L) una concentración de licopenos de 0,514 $mg.L^{-1}$ con un rendimiento del proceso de extracción de 34,34 $mg.kg^{-1}$.

Se caracterizó el ingrediente activo presente en el extracto y mediante el análisis estadístico ANOVA con un nivel de confianza del 95% se concluyó que no existieron diferencias estadísticas significativas de los resultados obtenidos entre los tres volúmenes para las variables de respuestas: índice de refracción, viscosidad cinemática, concentración de licopeno y eficiencia de extracción, mientras que para el porcentaje de humedad y pH si existieron diferencias significativas.

Se micro encapsuló el extracto obtenido en el volumen de 5 L registrando resultados del porcentaje de eficiencia de microencapsulación de 99,39% corroborado mediante espectroscopía infrarroja.

Referencias bibliográficas

1. Silva Y, Brooks MS-L, Ferreira TAPC, Caliari M, Borba BC, Reis MG, et al. Characterization of tomato processing by-product for use as a potential functional food ingredient: nutritional composition, antioxidant activity and bioactive compounds. Int J Food Sci Nutr [Internet]. 2018;70(2):150-60. Disponible en: https://doi.org/10.1080/09637486.2018.1489530
2. Silva Y, Ferreira T, Celli G, Brooks M. Optimization of Lycopene Extraction from Tomato Processing Waste Using an Eco-Friendly Ethyl Lactate – Ethyl Acetate Solvent : A Green Valorization Approach. Waste and Biomass Valorization [Internet]. 2018;0(0):0. Disponible en: http://dx.doi.org/10.1007/s12649-018-0317-7
3. Szabo K, Cătoi AF, Vodnar DC. Bioactive Compounds Extracted from Tomato Processing by-Products as a Source of Valuable Nutrients. Plant Foods Hum Nutr. 2018;73(4):268-77.
4. Cardona EM, Ríos LA, Restrepo GM. EXTRACCIÓN DEL CAROTENOIDE LICOPENO DEL TOMATE CHONTO (Lycopersicum esculentum). Rev la faculdad Química Farm [Internet]. 2006 [citado 10 de abril de 2019];13. Disponible en: http://www.scielo.org.co/pdf/vitae/v13n2/v13n2a06.pdf
5. Strati IF, Oreopoulou V. Effect of extraction parameters on the carotenoid recovery from tomato waste. Int J Food Sci Technol [Internet]. 2011;46(1):23-9. Disponible en: https://onlinelibrary.wiley.com/doi/epdf/10.1111/j.1365-2621.2010.02496.x
6. Pérez CF. Extracción y microencapsulación de licopenos provenientes de residuos agroindustriales del tomate de árbol (Solanum betaceum) [Internet]. Universidad Técnica de Ambato ; 2019 [citado 3 de abril de 2019]. Disponible en: http://repositorio.uta.edu.ec/bitstream/123456789/29416/1/BQ 178.pdf
7. PCE. Balanzas para medición de humedad [Internet]. 2019 [citado 4 de abril de 2019]. Disponible en: https://www.pce-iberica.es/instrumentos-de-medida/medidores/balanzas-humedad.htm
8. Macarulla JM, Goñi FM. Bioquímica humana : curso básico [Internet]. Reverté; 1994 [citado 4 de abril de 2019]. Disponible en: https://books.google.com.ec/books?id=4h_IosytGvkC&pg=PA33&dq=ph+metodo+potenciometrico&hl=es&sa=X&ved=0ahUKEwinnMfM6bbhAhUp1VkKHU6QABgQ6AEIJzAA#v=onepage&q=ph metodo potenciometrico&f=false
9. Cromer AH, Fernández J. Física en la ciencia y en la industria [Internet]. Reverté; 1998 [citado 4 de abril de 2019]. Disponible en: https://books.google.com.ec/books?id=egCFOg6V2j0C&pg=PA423&dq=indice+de+refraccion+de+una+sustancia&hl=es&sa=X&ved=0ahUKEwj1iZ-M-bbhAhUCtlkKHavnD_IQ6AEILTAB#v=onepage&q=indice de refraccion de una sustancia&f=false
10. Agudelo JC. Práctica 4. VISCOSIMETRO ROTACIONAL [Internet]. 2018 [citado 4 de abril de 2019]. Disponible en: https://www.academia.edu/36026224/Práctica_4._VISCOSIMETRO_ROTACIONAL

11. Corrêa L, Lourenço S, Duarte D, Moldão M, Alves V. Microencapsulation of Tomato (Solanum lycopersicum L.) Pomace Ethanolic Extract by Spray Drying: Optimization of Process Conditions. Appl Sci [Internet]. 2019;9(3):612. Disponible en: http://www.mdpi.com/2076-3417/9/3/612
12. Bobo G, Davidov G, Arroqui C, Vírseda P, Marín MR, Navarro M. Intra-laboratory validation of microplate methods for total phenolic content and antioxidant activity on polyphenolic extracts, and comparison with conventional spectrophotometric methods. J Sci Food Agric. 2015;95(1):204-9.
13. García D, Jáuregui U. Hidrodinámica en tanques agitados con turbinas de disco con paletas planas. Rev Fac Ing [Internet]. 2006 [citado 11 de septiembre de 2019];1:97-113. Disponible en: http://www.scielo.org.co/pdf/rfiua/n38/n38a09.pdf
14. Carrasco RR, Encina CR. Determinación de la capacidad antioxidante y compuestos bioactivos de frutas nativas peruanas. Revista de la Sociedad Química del Perú [Internet]. 2008 [citado 29 de mayo de 2019];74(2):108-24. Disponible en: http://www.scielo.org.pe/scielo.php?script=sci_arttext&pid=S1810-634X2008000200004
15. Aguado MI, Nuñez MB, Bela AJ, Okulik NB, Bregni C. Caracterización fisicoquímica y actividad antioxidante de un extracto etanólico de Aloysia polystachya (Griseb.) Mold. (Verbenaceae). Rev Mex Ciencias Farm. 2013;44(3):46-51.

Received: 15 junio 2020
Accepted: 20 septiembre 2020

RESEARCH / INVESTIGACIÓN

Composition and Occurrence of Fish Fauna from Thanbyuzayat Township, Mon Coastal Area

Zarni Ko Ko

DOI. 10.21931/RB/2020.05.04.14

Abstract: A total of 48 species of fish fauna were identified during the present study period. The dominant species of fish were found under order Perciformes in all study areas. The most species composition (40) was recorded in Setse fish landing area. The commercially important fish species were mostly found in Kyaikkhami area. Moreover, 17 species of fish were exported to other regions and foreign countries. Among the fish species, species such as Threadfin (*Polynemidae*), Croaker (*Sciaenidae*), Hilsa (*Clupeidae*), Bombay duck (*Harpadontidae*), Anchovy (*Engraulidae*), and Pomfret fish (*Stomateidae*) were the most economically important species. Bombay duck and Anchovy (especially *Coilia dussumieri*) were more abundant (70%) at the present study sites. *Harpodon nehereus* and Coilia species were the leading food employed as fresh and dried for local people in the present study areas.

Key words: Ichthyology, Taxonomy, Compositions, Occurrence, fish landing centers, Thanbyuzayat Township, Mon Coastal Areas.

Introduction

Myanmar is endowed with natural resources, including rich and various aquatic fauna and flora due to her diversified and the most favorable climate, topography, and habitats. Mon State is located between Latitude 15º 10' N and 17º 30' N and Longitude 96º 46' E and 98º15' E with a unique ecosystem. The Gulf of Mottama faced the Bay of Bengal on the East and the Andaman Sea in the south. This gulf is situated at the mouth of the Sittaung and the Thanlwin Rivers along with the two small rivers, the Gyine and the Attaran. This coastal area is characterized by the fluctuations of seawater flood and freshwater discharge. Mon State areas are covered with estuarine regions characterized by a variable salinity, a temperature range more significant than the sea, and turbid water and muddy bottom (Ohmar Min[1]). Economically, the fish component is a significant group of animals. Fish and fish products are an essential part of the diet in Mon State.

Both freshwater and marine fisheries are essential in Myanmar since the local people's livelihood from riverine areas, and the coastal areas depend on the fishes and fisheries. Fisheries are a critical commercial function and domestic or export role to South East Asia and worldwide to earn foreign currency (Ohmar Min[1]). Ish is one of the most critical animal protein resources in Myanmar. They can be utilized as food in many ways, such as dried, salted, smoked, paste, sauce, and fresh state locally and export to many other countries for commercial purposes. This study aims to determine fish species compositions and to analyze species distributed in Thanbyuzayat Township.

Materials and methods

Study areas

Fish samples were collected from the fish landing centers of Thanbyuzayat Township. The study areas were chosen at three sites, namely Kyaikkhami (Lat. 16° 03¢N, Long. 97° 33¢ E), Setse (Lat. 15° 56¢N, Long. 97° 37¢ E) and Sinpone (Lat. 16° 03¢N, Long. 97° 33¢ E). Kyaikkhami landing site was the main landing center along with the Thanbyuzayat Township. Moreover, in Setse and Sinpone, the bag net fishery was mainly conducted in this Township. The locations of fish landing sites were shown in Figure 1.

Sampling and identification of specimens

This study was conducted at Kyaikkhami, Siphone and Setse, situated at the of Thanlwin River mouth, from June 2019 to May 2020. Color patterns and measurements of the samples were recorded immediately after collections. The specimens were transported with icebox containing ice. The collected specimens were then preserved in 10% formaldehyde in seawater under room temperature within one week. The specimens examined visually were deposited in the Department of Marine Science, Mawlamyine University, Mawlamyine. The species' identification was based on external morphological characters followed by Carpenter, Krupp, Jories and Zajonz[2], Fischer and Bianchi[3], Day[4], Mya Than Tun[5], and Sann Aung[6].

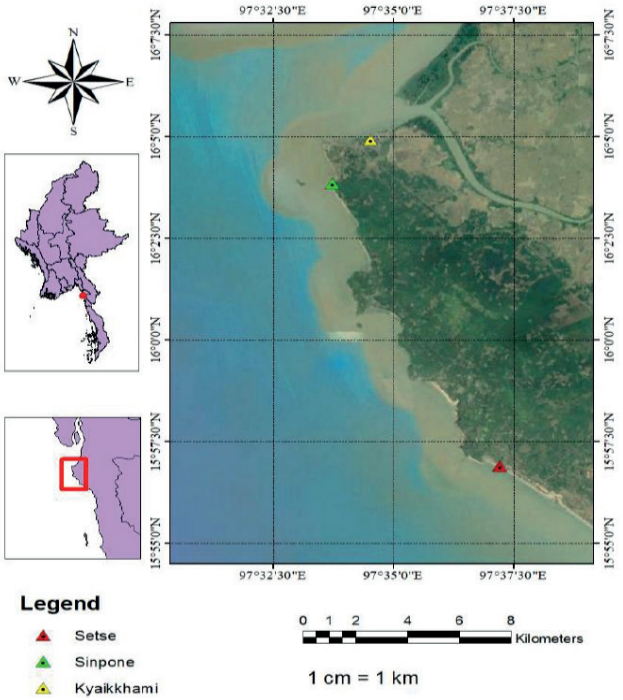

Figure 1. Map showing the fish landing centers during the present study.

[1] Lecturer, Department of Marine Science, Mawlamyine University, Mon State, Myanmar.

Corresponding author: jlvelez@uce.edu.ec

Results

Fish Composition and Occurrence

In the present study, the highest number of species (40) was found in Setse, followed by Kyaikkhami (35) and Sinpone (32) sites (Table 1 and Figure 2). The present study results revealed that 48 fish species' occurrence belongs to 12 orders, 31 families, and 42 genera (Figure 3). A list of fish species, including their order, family, species, common name, and local name, was recorded in the present investigation was given in Table 1. During the present study period, Order Perciformes was dominant represented 22 species with 45.83% contribution of the total species followed by Clupeiformes with 11 species (22.92%), Tetrodontiformes with 3 species (6.25%) and Mugiliformes, Pleuronectiformes and Siluriformes each with 2 (4.17%) species, Carcharhiniformes, Myliobatiformes, Torpediniformes, Anguilliformes, Beloniformes and Gadiformes each with 1 (2.08%) species (Table 2). Out of 42 genera reported, Perciformes contributed 47.62%, i.e., 20 followed by Clupeiformes with 8 (19.05%), Tetrodontiformes with 3 (7.19%), Mugiliformes and Siluriformes each with 2 (4.76%), Carcharhiniformes, Myliobatiformes, Torpediniformes, Anguilliformes, Beloniformes, Gadiformes and Pleuronectiformes each with 1 (2.38%) (Table 2). Out of 31 families recorded, order Perciformes contributed 15 (48.39%) families followed by Clupeiformes with 4 (12.90%) families, Siluriformes and Tetrodontiformes each with 2 (6.45%) families, Carcharhiniformes, Myliobatiformes, Torpediniformes, Anguilliformes, Beloniformes, Gadiformes, Mugiliformes and Pleuronectiformes each with 1 (3.23%) families (Table 2). In the present study, the species ranged from 32 and to 40. The previous study reported in Table 3 that it was similar to the present study areas.

Discussion

In the present study, 48 fish species belong to 12 orders, 31 families, and 42 genera were recorded. During the present study period, Perciformes was the most dominant order in all orders. In some previous studies from Myanmar Coastal Waters, Su Su Hlaing[7] reported 70 species to belong to 61 genera under 42 families of 15 orders from Thanlwin River mouth and the adjacent sea. Moreover, Cho Cho Latt[8] found 5 species of Anchovy (Family Engraulidae), and Thazin Aye[9] identified 6 species of Family Engraulidae, but only five species were recorded in the present study. *Setipinna wheeleri* and *Thryssa hamiltonii* was not found in the present study. Thu Ya Kyi Zin[10] 51 species from Thalwin River mouth, Zin Zin Zaw[11] 35 fish species in Asin Coastal areas. Min Ye Lwin Oo[12] observed *Chirocentrus nudus* and *C. dorab* in Zeephyuthaung; however, only *C. nudus* has occurred in the present study.

Thandar Aung[13] described 27 species of family Carangidae from Tha-baw-seik, Khin Myo Myo Tint[14] 47 species of fish from Ka-byar-wa area (Ye Township), Yin Yin Win[15] 61 species from Andin Village (Ye Township), Khin Myo Myo Tint[16] 69 fish species around Mein-ma-hla Island, Kaung Htet Hein[17] 25 species from Kadonebaw Village (Mudon Township). Wint Thuzar New[18] also reported 40 species along Attran ang Gyain River, and Su Su Hlaing[19] observed 96 species of fish belong to 71 genera under 48 families of 17 orders from Thanlwin River mouth and adjacent waters. (Figure 4)

In the present study, species ranged from 32 to 40. The fish species such as *Strongylura strongylura*, *Coilia dissumieri*, *C. ramcarati*, *Setipinna tenuifilis*, *Arius caelatus*, *A. maculatus*, *Hapadon nehereus*, *Polynemus indicus*, *P. paradiseus*, *Johinus coitor*, *Otoloithoides pama*, *Sillaginopsis panijus*, *Pampus argenteus*, *Therapon jarbua*, *Trichiurus lepturus*, *Cynoglossus bilineatus* and *C. lingual* were commonly found in present study areas. Su Su Haling[7] also reported that *Coilia dissumieri*, *C. ramcarati*, *Setipinna tenuifilis*, *Arius caelatus*, *A. maculatus*, and *Hapadon nehereus* were commonly found in Setse areas. In the present study, *T. lepturus* (Family- Trichiuridae) was found, but *L. savala* and *T. lepturus* were reported by Ei Ei Khaing[20]. In the present study, two species of *Atropus atroposa* and *Parastromateus niger* under Carangidae were found while 27 species of Carangidae were found in Tha-baw-seik, Longlone Township (Thandar Aung[13]). In the previous study, Su Su Hlaing[7] recorded 56 species in Setse and Kyaikkhami areas while 40 species in Setse and 35 species in Kyaikkhami areas during the present study period. Moreover, Su Su Hlaing[20] also reported 71 species in Kyaikkhami area and 69 species in Setse area, respectively.

Sekhara Ra, Simhachalam, and Sebastian Raju[21] reported Mystus vittatus and Clarias batrachus are of high economic importance in Andhra Pradesh, India M. vittatus was low economic value in present study areas. Mohanty *et al.*[22] reported 317 species (18 cartilaginous and 299 bony fishes) belonging to 207 genera, 88 families, and 23 orders in Chilika Lake, Odisha, India 1916-2014. In the present study, only 3 species of cartilaginous fish (*C. borneensis*, *H. imbricate* and *N. brunnea*) were found. Niloy Kundu *et al.*[23] also reported 31 species in the intertidal mudflats of Indian Sundarbans. In the present study, Bombay duck and Anchovy were more in abundance at all study sites. Among the anchovies' species, *C. dussumieri* and *H. nehereus* were the most abundant species in the catches of bag net fishery and popularly consumed in Mon State and exported to other regions dried product. Su Su Hlaing[20] also recorded *Coilia dussumieri* was the most abundant species in the catches of bag net fishery and popularly consumed in Mon State. In present study areas, some fishes such as *P. indicus*, *P. paradiseus*, *H. nehereus* and *C. dussumieri* were highly valued and favored by local people in Mon State. (Figures 5.6.7.8)

Otherwise, some economic species are considered value, abundance, and local demand and export. And the fishes were utilized as food in various ways such as fresh, dried, salted, smoked, and even some trash fishes can be made as fish paste and fish sauce. *H. nehereus* was the most popular fish food as fresh and production of dried fishes in Mon Coastal Region.

Conclusions

In the study, 48 species of fishes were recorded from the three fish landing centers located at the Thanbyuzayat Township, Mon State. The fish under the order Perciformes was found commonly in the study period. During the study, diverse species of commercial fish species; Croaker (Sciaenidae), Hilsa (Clupeidae), Bombay duck (Harpadontidae), and Anchovy (Engraulididae) were found commonly in the study period. They are essential for local people as food and support finance by exporting them to other areas and foreign countries. In all data collections, small fishable sizes were collected from large ones from all study areas.

Acknowledgments

I am indebted to Dr. Aung Myat Kyaw Sein, Rector of Mawlamyine University, and Dr. San San Aye, Pro-Rector, Mawlamyine University, for their encouragement and supports in preparing this work. I am very grateful to Dr. San Tha Tun,

Phylum: Chordata					
Class: Chondrichthyes (Cartilaginous)					
Order: Carcharhiniformes					
Family	Genus and Species	Local Name	Kyaikkhami	Sinpone	Setse
Carcharhinidae	*Carcharhinus borneensis*	Nga-mann	+	+	+
Order: Myliobatiformes					
Dasyatidae	*Himantura imbricata*	Nga-lake-kyauk	+	+	+
Order: Torpediniformes					
Narcinidae	*Narcine brunnea*	Nga-latt-htone	-	+	-
Class: Actinopterygii (Bony fish)					
Order: Anguilliformes					
Muraenesocidae	*Congresox talabon*	Nga-shwe	+	-	+
Order: Beloniformes					
Belonidae	*Strongylura strongylura*	Nga-hpaung-yoe	+	+	+
Order: Clupeiformes					
Chirountridae	*Chirocentrus nudus*	Nga-da-lwel	+	-	+
Clupeidae	*Anodontostoma chacunda*	Nga-wun-phyu	+	-	-
	Tenualosa ilisha	Nga-tha-lauk	+	+	+
	Tenualosa toli	Nga-tha-lauk-yout-pha	+	-	+
Engraulidae	*Coilia dissumieri*	Nga-kyan-ywat	+	+	+
	Coilia ramcarati	Nga-kyan-ywat	+	+	+
	Setipinna taty	Nga-byar	-	+	+
	Setipinna tenuifilis	Nga-byar	+	+	+
	Stolephorus baganensis	Nga-ni-du	+	+	+
Pristigasteridae	*Ilisha megaloptera*	Nga-zin-pyar	+	-	-
	Raconda russeliana	Nga-da-lar	-	+	+
Order: Gadiformes					
Bregmacerotidae	*Bregmaceros mcclellandi*	Nga-lone	-	+	+
Order: Mugiliformes					
Mugilidae	*Mugil cephalus*	Ka-be-lue	+	-	+
	Vaamugil georgii	Ka-be-lue	+	-	-
Order: Perciformes					
Ariidae	*Arius caelatus*	Shwe-nga-yaung	+	+	+
	Arius maculatus	Nga-yaung	+	+	+
Carangidae	*Atropus atropos*	Nga-da-ma	-	-	+
	Parastromateus niger	Nga-moat-mae	+	-	-
Centropomidae	*Lates calcarifer*	Ka-ka-tit	+	-	-
Gobiidae	*Gobioides buchanani*	Nga-yet-ni	-	+	+
	Taenioides gracilis	Ka-att	-	+	+
Harpadontidae	*Hapadon nehereus*	Nga-hnut	+	+	+
Leiognathidae	*Secutor ruconius*	Nga-waing	-	-	+
Polynemidae	*Eleutheronema tetradactylum*	Za-yaw-gyi	+	+	+
	Polynemus indicus	Ka-khu-yan	+	+	+
	Polynemus paradiseus	ga-pon-narr	+	+	+
Scatophagidae	*Scatophagus argus*	Nge-bee	-	+	+
Sciaenidae	*Johinus coitor*	Nga-byat-khone	+	+	+
	Otoloithoides pama	Nga-poat-thain	+	+	+
Scombridae	*Rasterlliger kanagurta*	Pa-lar-tue	+	-	-
	Scomberomorus guttatus	Nga-kon-shat	+	-	+
Siganidae	*Siganus canaliculatus*	unknown	-	+	+
Sillaginidae	*Sillaginopsis panijus*	nga-pa-lway	+	+	+
Stomateidae	*Pampus argenteus*	Nga-maot-phyu	+	+	+
Theraponidae	*Therapon jarbua*	Nga-goan-kyarr	+	+	+
Trichiuridae	*Trichiurus lepturus*	Nga-da-khon	+	+	+
Order: Pleuronectiformes					
Cynoglossidae	*Cynoglossus bilineatus*	Nga-khway-shar	+	+	+
	Cynoglossus lingual	Nga-khway-shar	+	+	+
Order: Siluriformes					
Clariidae	*Clarias batrachus*	Nga-khu	+	-	+
Bagridae	*Mystus vittatus*	Nga-zin-yaine	+	-	-
Order: Tetraodontiformes					
Tetraodontidae	*Lagocephalus lunaris*	Nga-pu-tinn	-	+	+
	Xenopterus naritus	Nga-pu-tinn	-	+	+
Triacanthide	*Triacanthus nieuhofii*	unknown	-	-	+
			35	32	40
Occurred (+), not occurred (-)					

Table 1. Classified list and Species composition of some fish from Fish landing centers during study period.

Professor, and Head of the Department of Marine Science, Mawlamyine University, for his valuable suggestions and constructive criticisms on this study. I also thank my colleagues, Dr. Naung Naung Oo, Lecturer, Department of Marine Science, Settwe University, and Daw Khin Myo Myo Tint, Assistant Lecturer Department of Marine Science, Mawlamyine University, for their help in field trips and advising and willing helper to me. I also grateful to my pupils, final students, Department of Marine Science, Mawlamyine University, for help in field trips and identified the fish specimens. Finally, my infinite thanks are to my beloved family for their kind and financial support throughout this study period.

Order	Families	Genus	Species	% of families in an order	% of genera in an order	% of species in an order
Carcharhiniformes	1	1	1	3.23	2.38	2.08
Myliobatiformes	1	1	1	3.23	2.38	2.08
Torpediniformes	1	1	1	3.23	2.38	2.08
Anguilliformes	1	1	1	3.23	2.38	2.08
Beloniformes	1	1	1	3.23	2.38	2.08
Clupeiformes	4	8	11	12.90	19.05	22.92
Gadiformes	1	1	1	3.23	2.38	2.08
Mugiliformes	1	2	2	3.23	4.76	4.17
Perciformes	15	20	22	48.39	47.62	45.83
Pleuronectiformes	1	1	2	3.23	2.38	4.17
Siluriformes	2	2	2	6.45	4.76	4.17
Tetraodontiformes	2	3	3	6.45	7.14	6.25
Total	31	42	48			

Table 2. Number and percent composition of families, genera, and species of fish under various orders.

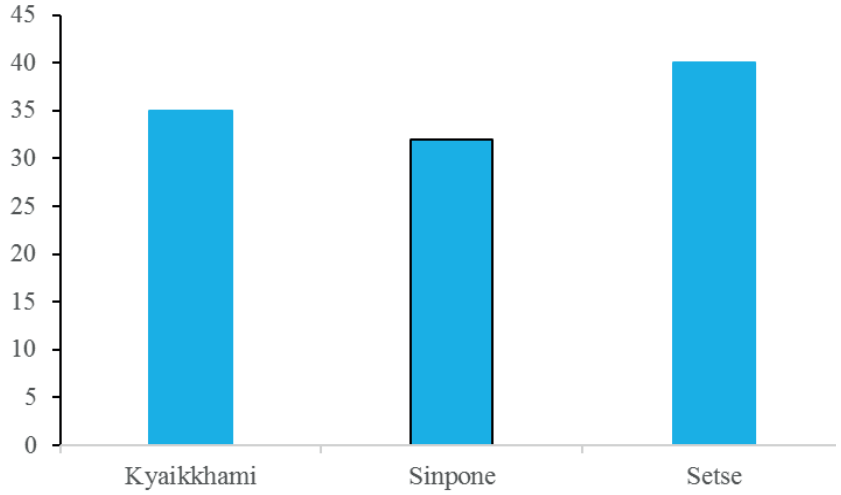

Figure 2. Fish species composition reported in Fish Landing Areas.

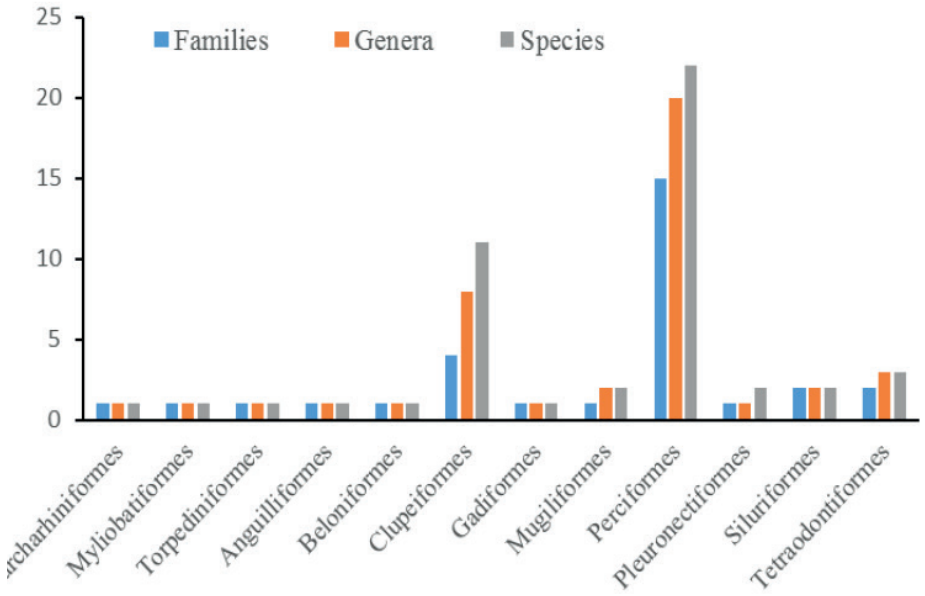

Figure 3. Composition of different fish taxa recorded from Kyaikkhami, Sinpone and Setse Fish Landing Areas.

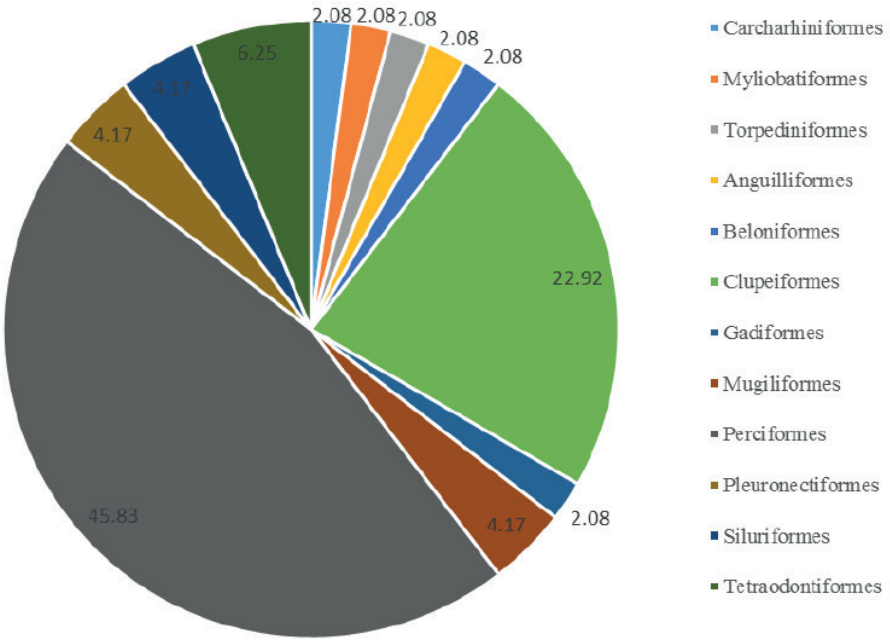

Figure 4. Percentage contributions of Species to the Orders.

Figure 5 (A-L). (A-L): A) *Carcharhinus borneensis*, B) *Himantura imbricate*, C) *Narcine brunnea*, D) *Congresox talabon*, E) *Strongylura strongylura*, F) *Chirocentrus nudus*, G) *Anodontostoma chacunda*, H) *Tenulosa ilisha*, I) *Tenulosa toli* J) *Coilia dussumieri*, K) *Coilia ramcarati* and L) *Setipinna taty* (Scale bar= 5cm)

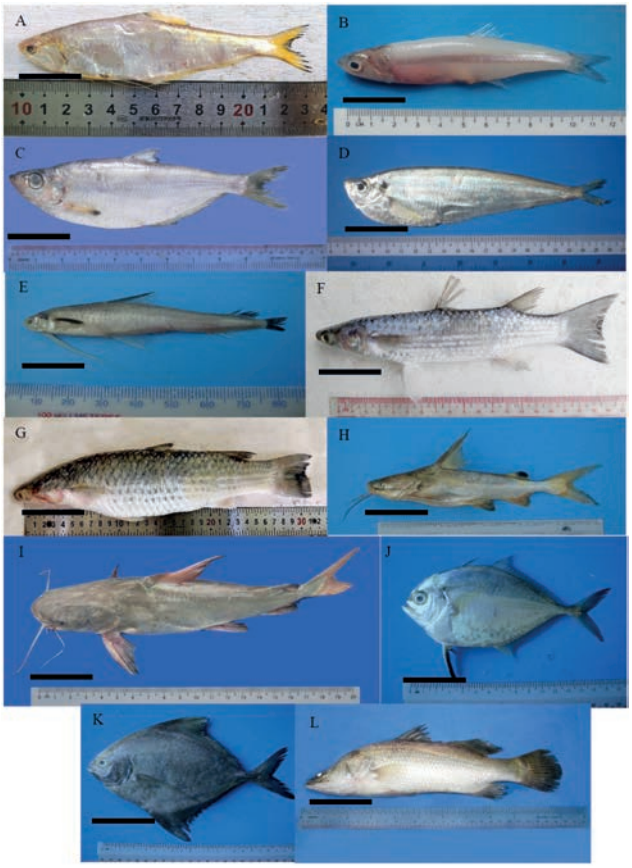

Figure 6 (A-L). A) *Setipinna tenuifilis*, B) *Stolephorus baganensis* C) *Ilisha megaloptera*, D) *Raconda russeliana*, E) *Bregmaceros sp*, F) *Mugil cephalus*, G) *Valamugil georgii*, H) *Arius caelatus*, I) *Arius maculatus*, J) *Atropus atropos*, K) *Parastromateus niger* and L) *Lates calcarifer* (Scale bar= 5cm)

No	Present record	Previous record*	Previous record**	Local consumption & Export
1	*Carcharhinus borneensis*	+	-	Local
2	*Himantura imbricata*	+	+	Local
3	*Narcine brunnea*	+	+	Local
4	*Congresox talabon*	-	-	Local/Export
5	*Strongylura strongylura*	-	-	Local
6	*Chirocentrus nudus*	+	+	Local/Export
7	*Anodontostoma chacunda*	-	+	Local
8	*Tenualosa ilisha*	+	+	Local/Export
9	*Tenualosa toli*	+	+	Local/Export
10	*Coilia dissumieri*	+	+	Local
11	*Coilia ramcarati*	+	+	Local
12	*Setipinna taty*	-	-	Local
13	*Setipinna tenuifilis*	+	+	Local
14	*Stolephorus baganensis*	-	+	Local
15	*Ilisha megaloptera*	-	-	Local
16	*Raconda russeliana*	+	+	Local
17	*Bregmaceros mcclellandi*	-	-	Local
18	*Mugil cephalus*	-	-	Local
19	*Valamugil georgii*	-	-	Local
20	*Arius caelatus*	+	+	Local
21	*Arius maculatus*	-	+	Local
22	*Atropus atropos*	+	+	Local
23	*Parastromateus niger*	+	+	Local/Export
24	*Lates calcarifer*	+	+	Local/Export
25	*Gobioides buchanani*	-	-	Local
26	*Taenioides gracilis*	-	-	Local
27	*Hapadon nehereus*	+	+	Local
28	*Secutor ruconius*	-	-	Local
29	*Eleutheronema tetradactylum*	+	+	Local/Export
30	*Polynemus indicus*	+	+	Local/Export
31	*Polynemus paradiseus*	+	+	Local/Export
32	*Scatophagus argus*	+	+	Local
33	*Johinus coitor*	+	+	Local/Export
34	*Otoloithoides pama*	+	+	Local/Export
35	*Rasterlliger kanagurta*	+	+	Local/Export
36	*Scomberomorus guttatus*	+	+	Local/Export
37	*Siganus canaliculatus*	-	-	Local
38	*Sillaginopsis panijus*	-	-	Local
39	*Pampus argenteus*	+	+	Local/Export
40	*Therapon jarbua*	+	+	Local
41	*Trichiurus lepturus*	-	-	Local/Export
42	*Cynoglossus bilineatus*	-	-	Local/Export
43	*Cynoglossus lingual*	-	-	Local/Export
44	*Clarias batrachus*	-	-	Local
45	*Mystus vittatus*	-	-	Local
46	*Lagocephalus lunaris*	+	+	Local
47	*Xenopterus naritus*	+	+	Local
48	*Triacanthus nieuhofii*	-	-	Local
* Su Su Hlaing (2010) & **Su Su Hlaing (2019)				

Table 3. A comparison of fish species' occurrence and their local consumption role and export during the present study.

Figure 7 (A-L). A) *Gobioides buchanani*, B) *Taenioides gracilis*, C) *Harpadon nehereus*, D) *Secutor ruconius*, E) *Eleutheronema tetradactylum*, F) *Polynemus indicus*, G) *Polynemus paradiseus*, H) *Scatophagus argus*, I) *Johnius coitor*, J) *Otoloithoides pama*, K) *Rastrelliger kanagurta*, L) *Scomberomorus guttatus* (Scale bar= 5cm)

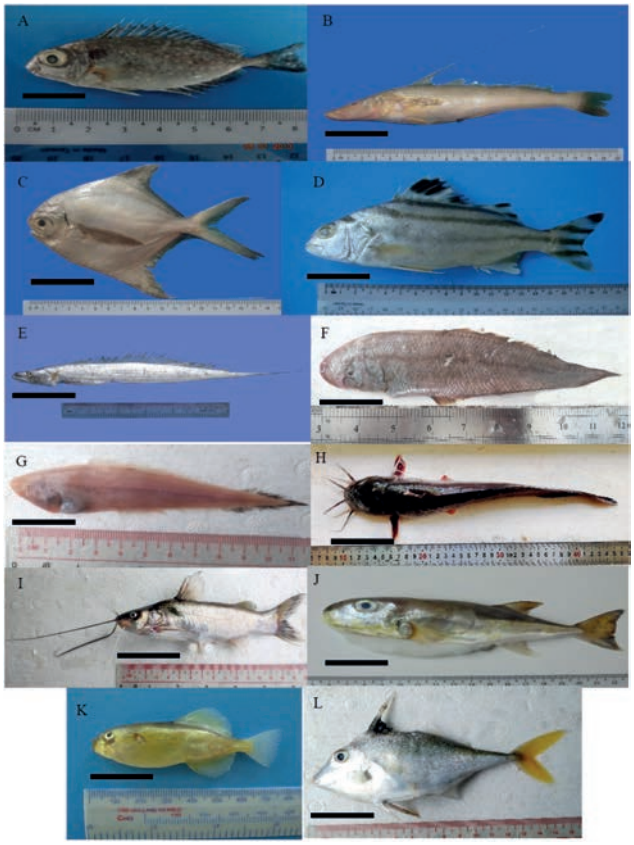

Figure 8 (A-L). A) *Siganus canaliculatus*, B) *Sillaginopsis panijus*, C) *Pampus argenteus*, D) *Therapon jarbua*, E) *Trichiurus lepturus*, F) *Cynoglossus bilinecatus*, G) *Cynoglossus lingua*, H) *Clarias batrachus*, I) *Mystus vittatus*, J) *Lagocephalus lunaris*, K) *Xenopterus naritus*, L) *Triacanthus nieuhofii* (Scale bar= 5cm)

Bibliographic references

1. Ohnmar Min (2013). Fishery Biology of Sciaenid fishes in Mon Coastal Waters. Unpublished PhD. Dissertation. Department of Marine Science, Mawlamyine University, Myanmar.
2. Carpenter, K. E., Krupp, F., Jories, D.A. and Zajonz, W. (1997). FAO species Identification guide for Fishery purposes. The marine living resources of Kuwiat, Eastern Saudi Arabia, Bahraian, Qatar, and the United Arab Emirates. Food and Agriculture Organization of the United Nations, Rome. 292 pp.
3. Fischer, W. and Bianchi, G. (1984). FAO species identification sheets for fishery purposes Western Indian Ocean (Fishing Area 51). Vol I-VI. Food and Agriculture Organization of the United Nations, Rome.
4. Day, F., F.L.S. & F.Z.S. (1878). The Fishes of India, being a natural history of fishes known to inhibits at the seas and freshwater of India, Burma and Ceylon. Vol. I (Text)-1-778 pp and Vol. II (Atlas), Today & Tomorrow Book Agency, New Delhi, 195 pp
5. Mya Than Tun (2001). Marine fishes of Myanmar (Pelagic and Demarsal). Marine Fisheries Resources Survey Unit. Department of Fisheries. Yangon: 276pp.
6. Sann Aung (2003). Commercial Fishes of Myanmar Seas. Myanmar Academy of Agricultural, Forestry, Livestock and Fishery Sciences: 111pp.
7. Su Su Hlaing (2010). Commercially important ichthyological fauna of the Thanlwin River mouth and Adjacent sea. Unpublished M.Res. Thesis. Department of Marine Science, Mawlamyine University, Myanmar.
8. Cho Cho Latt (2010). Observations on The Fisheries of Anchovies (Engraulidae) of Setse Coast. Unpublished MSc. Thesis. Department of Marine Science, Mawlamyine University, Myanmar.
9. Thu Ya Kyi Zin (2011). Base line data on the Artisanal Fishery of the Thanliwn River Mouth Areas. Unpublished MSc. Thesis. Department of Marine Science, Mawlamyine University, Myanmar.
10. Zin Zin Zaw (2014). A study on Fishery of some commercial fishes in Asin Coastal Areas, Ye Township, Mon State. Unpublished M.Res. Thesis. Department of Marine Science, Mawlamyine University, Myanmar.
11. Thazin Aye (2014). A study on some aspects of Biology of Anchovy Fishes (Family: Engraulidae) in Zeephyuthaung Coastal Areas. Unpublished MSc. Thesis. Department of Marine Science, Mawlamyine University, Myanmar.
12. Min Ye Lwin Oo (2014). A study on some aspects of Biology of Wolf-herring (Family: Chirocentridae) from Zeephuthaung Coastal Area. Unpublished MSc. Thesis. Department of Marine Science, Mawlamyine University, Myanmar.
13. Ei Ei Khaing (2014). A study on some aspects of Biology of Ribbon Fishes (Family: Trichiuridae) in Asin Coastal Area. Unpublished MSc. Thesis. Department of Marine Science, Mawlamyine University, Myanmar.
14. Thandar Aung (2015). A study on some aspects of Biology Status of Carangids (Family: Carangidae) from Tha-baw-seik Fish Landing Centre, Longlone Township, Taninthayi Region. Unpublished M.Res. Thesis. Department of Marine Science, Mawlamyine University, Myanmar.

15. Khin Myo Myo Tint (2015). A study on Ichthyofauna of Ka-byar-wa Coastal Waters, Ye Township, Mon State. Unpublished MSc. Thesis. Department of Marine Science, Mawlamyine University, Myanmar.
16. Yin Yin Win (2016). A study on some fish community in Andin Village, Ye Township, Mon State. Unpublished M.Res. Thesis. Department of Marine Science, Mawlamyine University, Myanmar.
17. Khin Myo Myo Tint (2016). Occurrence of Fish species around Mein Ma Hla Island in the Lower reaches of Bogalay river. Unpublished M.Res. Thesis. Department of Marine Science, Mawlamyine University, Myanmar.
18. Kaung Htet Hein (2017). Fishery Status of Kadonebaw Village in Mudon Township, Mon State. Unpublished M.Res. Thesis. Department of Marine Science, Mawlamyine University, Myanmar.
19. Wint Thuzar Nwe (2017). Fish and Fishery of lower Attran River and Gyaing River Areas. Unpublished M.Res. Thesis. Department of Marine Science, Mawlamyine University, Myanmar.
20. Su Su Hlaing (2019). Commercial fishes of the Thanlwin River mouth and Adjacent waters, Mon State, Myanmar. J. Myanmar Acad. Arts Sci. 17 (4):17-39.
21. Sekhara Ra. J.C., Simhachalam, G. and Sebastian Raju, Ch. (2013). Ornamental Fish Diversity of Lake Kolleru, the only Ramsar site in Andhra Pradesh, India. Bull. Env. Pharmacol. Life Sci., 2 (7): 48- 55.
22. Mohanty, S.K., Mishra, S.S., Khan, M., Mohanty, R.K., Mohapatra, A. and Pattnaik, A.K. (2015). Ichthyofaunal diversity of Chilika Lake, Odisha, India: an inventory, assessment of biodiversity status and comprehensive systematic checklist (1916–2014). The Journal of biodiversity data. 11 (6):1-19.
23. Niloy Kundu, Atreyee Chaudhuri, Sudeshna Mukherjee, Shilpa Sen and Sumit Homechaudhuri. (2012). Seasonal fish diversity under tidal influence in the intertidal mudflats of Indian Sundarbans. Indian J. Fish., 59(4) : 43-52.

Received: 22 June 2020
Accepted: 15 September 2020

RESEARCH / INVESTIGACIÓN

Microbial implications of beef fat and pork fat in the environment

Chinonye Medline Maduka[1*], Akuma Oji[2], Ugochi Queen Fineboy[3], Gideon Chijioke Okpokwasili[2]
DOI. 10.21931/RB/2020.05.04.15

Abstract: Developing countries are known to dispose of waste indiscriminately into their environment, off which fat is one of them. These fats release awful odor making passersby uncomfortable and also breeds microorganisms. Environmental factors such as rainfall, sunlight, and wind aid the migration of these fats to other sites, thereby leading to contamination. Total heterotrophic plate count of pork fat ranged from 4.0 x 10^5 cfu/g to 4.2 x 10^5 cfu/g and its total coliform plate count was from 3.8 x 10^5 cfu/g to 4.0 x10^5 cfu/g while the total heterotrophic plate count of beef fat ranged from 3.1 x 10^5 cfu/g to 3.5 x 10^5 cfu/g and its total coliform plate count was from 2.4 x 10^5 cfu/g to 2.8 x10^5 cfu/g. *E.coli* and *Salmonella sp.* were the highest occurring in both fats. Pork fat had more microbial count than beef fat. Fats can be converted to useful products, which will reduce waste in the environment. Statistical analysis showed a significant difference in mean counts of pork and beef fat samples at p≤0.05.

Key words: Pork fat, beef fat, microorganisms, environment, wastes.

Introduction

Environmental pollution is an issue that has been a threat to the world for many years and is presently a significant problem because of the rapid population growth in developing countries[1]. The burden of increasing waste and its control in urban areas of developing countries is an environmental concern. This situation grew worse due to the lack of technology to help reduce the heap of wastes[2]. Another global problem is soil pollution resulting from waste discharges freely dumped into the environment. The richest reservoir of microorganisms in the soil play a significant role in the ecosystem because its continuity depends mainly on it. If the soil becomes polluted, the ecosystem is tilted, and agricultural activities are disrupted[3,4]. A major problem of many urban areas in Nigeria is the low sanitary condition best described by Sule[5] as indiscriminate waste disposal and the ability to reduce it to the minimum and the low usage of laws for this waste disposal problem. These abnormal waste dumping methods have created many problems such as sanitation and environmental issues, an imbalance of groundwater, and soil pollution and water resources[6]. This pollution problem either on air, water, or land caused by man's day to day activities is rapidly growing to the point that it can no longer be managed and will be seen as a usual way of life. This issue hurts human health and well-being.

One of the by-products of animals is fat[7], and it can be edible or inedible depending on the animal and the animal's part it is gotten from. Cattle are a source of protein and fats[8]. Fat has an essential role in meat quality. Surface fat stops frequent cooling of the underlying muscle tissues, which lowers the tendency of cold-shortening and lowers weight loss due to chilling. The hardness or softness of fat directly impacts its processing efficiency also fat and adds to meat's beneficial properties. Physical properties to look out for in fat are color, hardness, and texture. The better the properties of fat, the higher the market value. It is known that 85% of fat tissue consists of triglycerides located in the fat cells; for every triglyceride, three molecular fatty acids are found in it. The other part of the fat tissue consists of approximately 12% moisture, and the connective tissue is approximately 3%. Different types of collagen and various cross-linking levels are crucial to the structure of fat tissue, and these affect the texture and strength of fat at any temperature, and it depends on the composition of its fatty acid and the molecules that constitute its triglycerides. Palmitic and stearic acids are saturated fatty acids with high melting points of about 65-70°C, and this account for hard fat, unlike palmitoleic and oleic acids, which are unsaturated fatty acids with low melting points of 0-15°C and contribute to softness. The temperature at which fat melts depends on the amount each fatty acid contributes. In Australia, prolonged grain feeding enhances fat color, leads to a uniform product, and a rise in the hardness of fat[9].

Mature Pigs are known to have fat. Feeding habits, the composition of animal feeds, breed diversity, animal age, and other factors are significant contributors to the quality of pork fat[10]. Pork's quality may increase or decrease as a result of nutrition, genetics, management, and pork-processing procedures. Pigs' lean genotype fed with diets high in unsaturated fat might possess thinner and soft fat at their bellies, which is of low quality[11]. This reduction in fat quality is related to their thinner bellies, which might negatively affect the processing, separation of tissue, and stability during storage. Several factors define Pork's quality, such as color, consistency, and keeping quality, and these are affected by the size of the fat deposits located in the pig and the composition of dietary fat. The fatty acid profile of pork fat represents the role played by each source of dietary fat[12,13,14].

Oleic and palmitic acids are the primary fatty acids in beef fat[15]. Many factors, such as the breed of Cattle, sex, diet, weight, age, fatness, and environmental conditions, including climate and season, are known to affect the composition of fat tissue in cattle. Although the factors do not apply to all cattle, the cattle known as Brahman are known for higher unsaturated fat content than a few other breeds. Brahman-cross cattle have softer fat when compared to purebred Hereford and various crossbreeds. Most likely, age plays a significant role in the unsaturation of fat; the older an animal becomes, the more unsaturated fat it is likely to have. Colder climates are known to have Cattles with softer subcutaneous fat. When a healthy cattle grazes green pasture, it utilizes the yellow pigments in these plants known as carotenoids, beta-carotene, which makes up a larger part of carotenoids and gives the fat

[1] World Bank Africa Centre of Excellence, Centre for Oilfield Chemicals Research, University of Port Harcourt, Port Harcourt, Nigeria.
[2] Department of Chemical Engineering, University of Port Harcourt, Port Harcourt, Nigeria.
[3] Department of Microbiology, Michael Okpara University of Agriculture Umudike, Umuahia, Abia State, Nigeria.

Corresponding author: madukachinonye@yahoo.com

its color. Most fats are known to have a cream or yellow color.

This research aims to identify the impact of fats in the environment and the microbial load.

Materials and methods

Fat samples were collected from slaughterhouses in Umuahia, Abia State, Nigeria. These samples were collected in sterile polythene bags and transported within 45 minutes for microbiological analysis (Figure 1). All laboratory procedures were done aseptically. One gram of each mashed sample was introduced into 9ml of distilled water, the conical flask was carefully shaken, and from it, ten-fold serial dilution was done[16]. The pour plate method was used to isolate microorganisms on MacConkey agar and Nutrient agar at 37oC for 24-48 hours. Pure isolates were identified and characterized. The other part of the fat that was not bought from slaughterhouses was discarded as waste.

Results and Discussion

A total of ten samples were used for this study. Five out of the ten samples were pork fat, while the other five samples were beef fat. Total heterotrophic plate count (THPC) and total coliform plate count (TCPC) of pork and beef fat samples are shown in Figure 2. These samples had higher counts for total heterotrophic plate count than total coliform plate count.

Figure 2 shows that pork fat has a higher bacterial load than beef fat. This could be as a result of the physical appearance of pork fat. Pork fat appeared wet with more oil content than beef fat. Research by Abdelwhab[17] revealed that beef fat had lesser fat content than mutton fat. This slimy nature of pork fat could be the reason behind its higher number of microbial load. Aymerich *et al.*[18] identified that meat with aw between 0.94-0.99 promoted microbial growth. Also, pork fat might have higher nutrients than beef fats, which makes microorganisms thrive more in it. Lulietto *et al.*[19] stated that meat has high protein, lipids, minerals, and vitamin contents

Figure 1. Area of Study. Umuahia, Abia State, Nigeria.

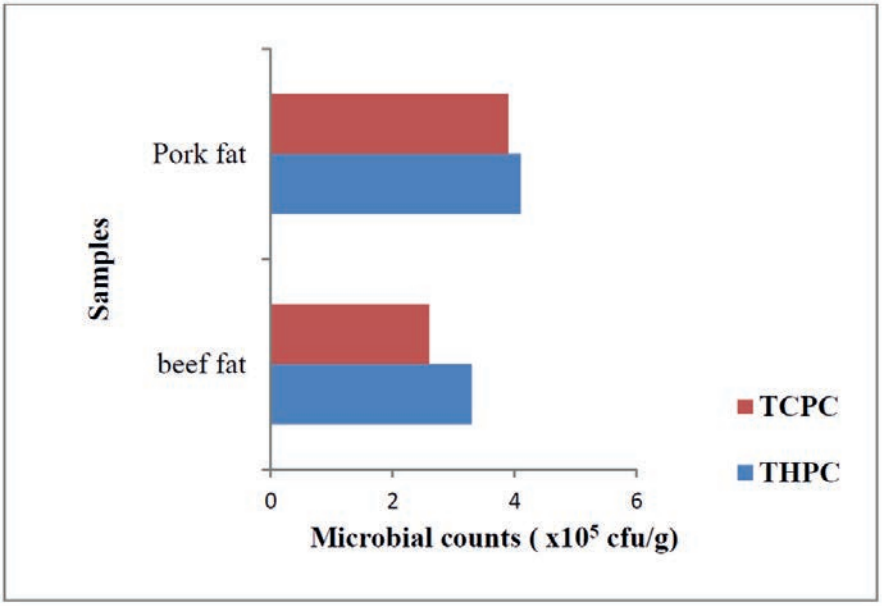

Figure 2. Mean bacterial counts of pork fat and beef fat.
THPC: Total heterotrophic plate count
TCPC: Total coliform plate count

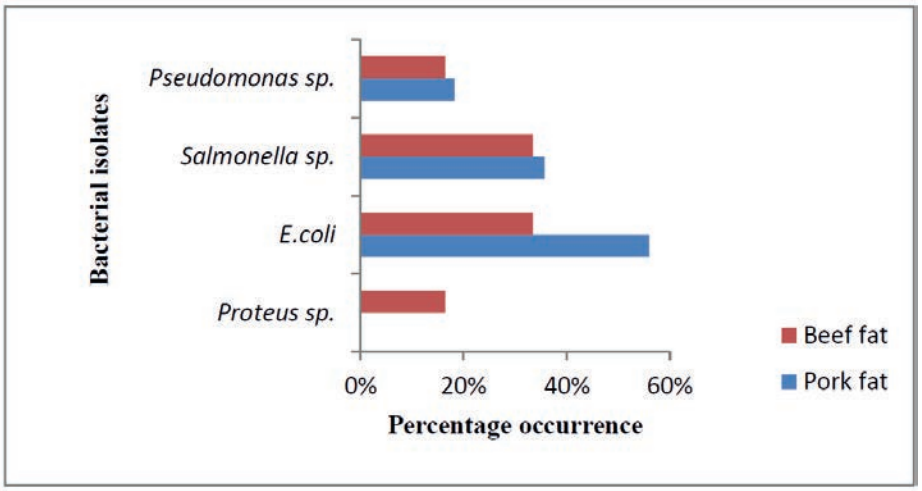

Figure 3. Percentage occurrence of bacterial isolates from pork fat and beef fat.

but low carbohydrate content, which allows some organisms to survive. Nychas *et al.*[20] recorded that meat spoilage results from some available substrates such as glucose, lactic acid, nitrogenous compounds, and free amino acids present in the meat.

Four bacterial isolates were identified from this study, and they are *Pseudomonas aeruginosa*, *E. coli*, *Salmonella sp.*, and *Proteus sp.* Odey[16] isolated seven bacterial isolates, and they include *Staphylococcus spp.*, *Streptococcus spp.*, *Escherichia coli*, *Salmonella spp.*, *Bacillus spp.*, *Pseudomonas sp.*, and *Proteus sp.* The microbial counts from nutrient agar from their sample was from 1.4 x 10^5 cfu/g to 3.5 x 10^5 cfu/g. Lamb[21] identified *Samonella sp.* in all fat and oil samples, including beef tallow and pig lard. Shaffer[22] stated that the common bacterial contaminants in Pork are *E. coli*, *Salmonella sp.*, *S. aureus*, and *Yersinia enterocolitica* and that the intrinsic properties of meat, such as pH and moisture promotes microbial growth, and also does the extrinsic factor such as temperature.

Results from percentage occurrence showed that *E. coli* and *Samonella sp.*, highly occurred in both samples, *Pseudomonas sp.* and *Proteus sp.*, were more in pork fat than beef fat. Yannick *et al.*[8] recorded 81.8% for *Staphyloccocus aureus*, 72.7% for *Klebsiella pneumonia*, 54.4% for *Escherichia coli*, 45.4% for *Salmonella spp.*, 27% for *Proteus vulgaris*, and 9% for *Shigella spp.* Figure 3 is a representation of the percentage occurrence of bacteria in both fats.

It could be possible that after processing these fats that the bacterial load of these fats will reduce as a result of heating or other techniques used on it. It could also be possible that the microorganisms in these fats are also released into the environment when dumped. When deposited as wastes into the environment, these fats begin to decay and release an offensive odor. The odor released could result from the action of the microorganisms already present in the fat, which most times begin the degradation process or the action of other microorganisms that find the fat as a source of energy. The delicate nature of these fats may have contributed to the easy access of these microorganisms, which, when broken down, will lead to more fat-loving microorganisms inhabiting these fats.

Environmental factors such as sunlight and rainfall further promote the migration of the degraded fats, and this could be beneficial or harmful depending on their quantity in the environment. When these fats are washed in small quantities into the environment, it is tolerated, but when in large quantities, they will either compete or work in synergy with the existing nutrients in such an environment. The oil released by these fats covers the surface (water or soil) they occupy, thereby preventing such environment and the microorganisms in the environment from getting the essential nutrients needed for their growth. This might be the reason for the awful odor given out by these wastes (fats). These decaying fats could trigger the degradation of other materials in the environment. The dumped fats and other wastes are not a sight to behold as it makes the environment look unhealthy. Ifeoluwa[23] stated that solid wastes lead to soil, air, and water contamination, which creates health challenges and is a significant problem to man and its environment, especially those who live closer to areas where these waste release offensive odors a result of decay.

Conclusions

I also wish to thank Africa Centre of Excellence, University of Port Harcourt for the great knowledge given to me Many thanks to Nweze, N.C.F of LinnC laboratory for his technical support. My sincere appreciation goes to Michael Okpara, the [h1] University of Agriculture Umudike[h2] , for making this research a success.

Acknowledgments

Many thanks to Nwoba Chinedu Frank Nweze of the LinnC laboratory for his technical support. My sincere appreciation goes to Michael Okpara, the University of Agriculture, for making this research a success.

Competing interest

The authors have no competing interests.

Bibliographic references

1. Ali, S.M., Pervaiz, A., Afzal, B., Hamid, N., and Yasmin, A. (2014). Open dumping of municipal solid waste and its hazardous impacts on soil and vegetation diversity at waste dumping sites of Islamabad city. Journal of King Saud University – Science, 26(1): 59 – 65.
2. Baum, B. and Parker, H.C. (1973). Solid waste disposal. Incinerations and landfill, 2nd Edition Ann Arbor Science Publishers Inc. Ann Arbor, Mich. United States. (vol.1) 636 pages.
3. Adedokun, O.M. and Ataga A.E. (2006). Effects of Crude Oil and Oil Products on Growth of Some Edible Mushrooms. Journal of Applied Science and Environmental Management, 10(2): 91 – 93.
4. Igwo-Ezikpe, M.N., Gbenle, O.G., Ilori, M.O., Okpuzor J., and Osuntoki, A.A. (2009). Evaluation of Alcaligenes faecalis Degradation of Chrysene and Diesel Oil with Concomitant Production of Biosurfactant. Research Journal of Environmental Toxicology, 3(4): 159-169.

5. Sule, A. B. (2011). Management of Environments in Africa: A Handbook and References, Lagos: Greenwood Publishing Group Inc, Lagos.
6. Ajibade, F. O., Adewumi, J. R. and Oguntuase, A.M. (2014). Sustainable Approach to Wastewater Management in the Federal University of Technology, Akure, Nigeria. Nigerian Journal of Technological Research, 9(2): 27-36.
7. Tarté, R. (2016). Composition, Functionality and Utilization of Pork Variety Meats. Animal Science Iowa State University. Novel Processing – Pork Variety Meat Workshop Ames. "Last accessed 14/5/2019". http://works.bepress.com/rodrigo_tarte/20/
8. Yannick, N., Rawlings, N. and Emmanuela, A. (2013). Assessment of bacteriological quality of cooked pork meat sold along the commercial streets of Nkwen through Bambili Metropolis, Cameroon. African Journal of Food Science. 7(12): 441-445.
9. Meat Technology Update (2006). Cutting edge technology for the meat processing industry. Food Science Australia. 1-5. "Last accessed 14/5/2019"; https://meatupdate.csiro.au//MeatQualityIndexPage.htm.
10. Pipek, P., Rohlík, B., Potůček, T. and Šimoniová, A. (2012). The composition of pork lard as a raw material in meat production. Journal of Food Science and Technology. 2: 115-119.
11. Gatlin, L.A., See, M.T., Hansen, J.A. and Odle, J. (2003). Hydrogenated dietary fat improves pork quality of pigs from two lean genotypes. Journal of Animal Science. 81(8): 1989 - 1997.
12. Seerley, R.W., Briscoe, J.P. and McCampbell, H.C. (1978). A comparison of poultry and animal fat on performance, body composition and tissue lipids of swine. Journal of Animal Science. 46: 1018–1023.
13. Miller, M. F., Shackelford, S.D., Hayden, K.D. and Regan, J.O. (1990). Determination of the alteration in fatty acid profiles, sensory characteristics and carcass traits of swine fed elevated levels of monounsaturated fats in the diet. Journal of Animal Science. 68: 1624–1631.
14. Madsen, A., Jakobsen, K. and Mortensen, H. (1992). Influence of dietary fat on carcass quality in pigs. A review. Acta Agriculturae Scandinavica Sect A Animal Science. 42(4): 220-225.
15. Nizar, N.N.A., Marikkar, N.M.J. and Hashim, D.M. (2013). Differentiation of Lard, Chicken fat, Beef fat and Mutton fat by GCMS and EA-IRMS Techniques. Journal of Oleo Science. 62 (7): 459-464.
16. Odey, M. O., Mboso, E. O., Ujong, U. P., Johnson, J. T., Gauje, B. and Ategwu, M. A. (2013). Microflora analysis of selected meat and meat products from Calabar, Cross River State-Nigeria. Archives of Applied Science Research. 5(3): 50-56.
17. Abdelwhab, S., Olish, E., Mohammed, S., Khatim, S.B.S., and Mohammed, H. (2017). A Comparative Study of Fat Content in Beef and Sheep Meat. International Journal of Research in Agriculture and Forestry. 4(2): 41-44.
18. Aymerich, M.T., Garriga, M., Costa, S., Monfort, J.M., Hugas, M. (2002). Prevention of ropiness in cooked Pork by bacteriocinogenic cultures. International Dairy Journal, 12(2/3): 239-246.
19. Lulietto, M. F., Sechi, P., Borgogni, E. and Cenci-Goga, B.T. (2015). Meat Spoilage: A critical Review of a Neglected Alteration Due to Ropy Slime Producing Bacteria. Italian Journal of Animal Science. 14(3): 315-326.
20. Nychas, G.J.E., Skandamis, P.N., Tassou, C.C., and Koutsoumanis, K.P. (2008). Meat spoilage during distribution. Meat Science. 78: 77-89.
21. Lamb, K.E. (2017). The survival of various pathogenic organisms in fats. Master of Science Thesis. University of Kentucky. Lexington, Kentucky.
22. Shaffer, C. (2019). Microbes in Raw Meat. 1-5. "Last accessed 14/5/2019". https://www.news-medical.net/lifesciences/Microbes-in-Raw-Meat.aspx
23. Ifeoluwa, O.B. (2019). Harmful Effects and Management of Indiscriminate Solid Waste Disposal on Human and its Environment in Nigeria: A Review. Global Journal of Research and Review, 6(1): 1- 4.

Received: 28 June 2020
Accepted: 26 September 2020

RESEARCH / INVESTIGACIÓN

Combinaciones estables en morfología y polaridad de las ondas electrocardiográficas P, QR y T en bovino, como referencia para el diagnóstico

Stable combinations in morphology and polarity of the electrocardiographic P, QR and T waves in cattle, as a reference for diagnosis

Alberto Pompa Núñez[1], Dania Yusimí Pompa Rodríguez[2]

DOI. 10.21931/RB/2020.05.04.16

Resumen: El objetivo de este trabajo fue determinar las combinaciones más estables en morfología y polaridad de las ondas electrocardiográficas P, QR y T obtenidas en varias derivaciones en el bovino, para su utilización diagnóstica. Se emplearon registros correspondientes a 100 bovinos Holstein, en 17 derivaciones, 7 bipolares y 10 monopolares. Las áreas donde se conectaron los electrodos fueron depiladas, frotadas con alcohol y se les aplicó pasta conductora de electricidad. El electrocardiógrafo fue calibrado con una señal de 1 mV/cm y una velocidad de corrida del papel de 25 mm/s. Como resultado, se encontró que los puntos de derivación que se sitúan hacia la base del corazón o hacia el ápice originan patrones de combinación P-QR-T con una gran constancia en la polaridad y poca diversidad morfológica. Las ondas R son positivas en la base y negativas en el ápice y las ondas P y T son en ambas regiones discordantes con la R, excepto en la derivación V_{H3}, en la que P es concordante Se concluye que en las porciones de la superficie corporal del bovino situadas por encima o por debajo de la línea que pasa por la derivación V_3 en la que se obtienen registros nulos para QR, existe una elevada estabilidad en las características morfológicas y de polaridad de las combinaciones de las ondas P-QR-T, por lo que las derivaciones monopolares en cada una de estas áreas o las bipolares registradas entre una y otra, son muy útiles para diagnosticar las alteraciones cardíacas.

Palabras clave: Morfología, polaridad, ondas electrocardiográficas, bovino.

Abstract: This work's objective was to determine the most stable combinations in morphology and polarity of the electrocardiographic P, QR, and T waves obtained in various leads in cattle for their diagnostic use. Records corresponding to 100 Holstein cattle were used in 17 leads, seven bipolar and ten monopolar. The areas where the electrodes were connected were depilated, rubbed with alcohol, and electrically conductive paste was applied. The electrocardiograph was calibrated with a signal of 1 mV/cm and a paper speed of 25 mm / s. As a result, it was found that the derivation points that are located towards the base of the heart or the apex originate P-QR-T combination patterns with a great constancy in polarity and little morphological diversity. The R waves are positive at the base and negative at the apex, and the P and T waves are in both regions discordant with the R, except in lead V_{H3}, in which P is concordant. It is concluded that in the portions of the bovine body surface located above or below the line that passes through lead V_3 in which null recordings are obtained for QR, there is a high stability in the morphological and polarity characteristics of the combinations of P-QR-T waves, so that the monopolar leads in each of these areas or the bipolar leads recorded between one and the other are very useful for diagnosing cardiac abnormalities.

Key words: Morphology, polarity, electrocardiographic waves, bovine.

Introducción

El empleo de las técnicas electrocardiográficas es muy útil, tanto en el hombre como en los animales. En su estudio y aplicación se valoran los fenómenos de excitación del corazón que anteceden y provocan la contracción. La lectura correcta y completa de un trazado electrocardiográfico es la mejor garantía de que se pueda hacer el diagnóstico adecuado[1]. El corazón para contraerse y ejercer su función de bomba tiene que ser objeto primero del proceso de despolarización y repolarización. Como consecuencia de esta actividad eléctrica se producen diferencias de potencial que pueden registrarse a nivel de la superficie corporal como un electrocardiograma (ECG).

El registro de la electrocardiografía convencional, se basa en la toma de las tres derivaciones bipolares de Einthoven, las tres aumentadas de Goldberger y las seis precordiales o del plano horizontal, lo cual hace un total de 12 derivaciones, distribuidas en la colocación de 10 electrodos[2]. A consecuencia de la diferente disposición anatómica del corazón en la cavidad torácica de los cuadrúpedos no es útil emplear los mismos puntos de derivación que en el hombre. En el caso particular del bovino, se ha establecido un conjunto de derivaciones estables, cuya utilización práctica tiene una gran importancia en las razas productoras de leche como la Holstein, debido a que estos animales están sometidos a una alta intensidad metabólica y expuestos a desbalances electrolíticos.

En las investigaciones iniciales que condujeron a la obtención del sistema de derivaciones que originan registros estables, en cuanto a la polaridad de la onda P, el complejo QR y la onda T del ECG en el bovino, no se detalló el comportamiento morfológico de cada una de ellas en los diferentes puntos de la superficie corporal. Sin embargo, es necesario contar con el registro más característico en cada derivación cuando se combinan los tres componentes entre sí, lo cual es un elemento muy importante para evaluar las lesiones y otras alteraciones cardíacas. Por eso, el objetivo de este trabajo fue determinar las combinaciones más estables en morfología y polaridad de las ondas electrocardiográficas P, QR y T obtenidas en varias derivaciones en el bovino, para su utilización diagnóstica.

[1] Profesor Titular de Biofísica y Fisiología (PhD), con Categoría Especial de Profesor Consultante de la Universidad Agraria de La Habana, Cuba.
[2] Especialista de primer grado en Medicina General Integral, especialista de primer grado en Anestesiología y Reanimación, Profesora instructor.

Corresponding author: albertopompa1949@gmail.com

Materiales y métodos

En esta investigación se registraron electrocardiogramas (ECG) a un total de 200 bovinos de la raza Holstein, clínicamente sanos y pertenecientes a diferentes grupos etarios de uno y de otro sexo empleando 20 derivaciones. Se seleccionaron, aleatoriamente, los registros correspondientes a 100 bovinos Holstein, en 17 derivaciones, 7 bipolares y 10 monopolares de: 10 terneros, 10 terneras, 20 novillas, 20 vacas lactantes, 20 sementales jóvenes y 20 adultos. La edad promedio de las 6 categorías estuvo comprendida entre 33 días y 7,8 años. Los terneros, las novillas y las vacas lactantes fueron procedentes del distrito de producción de la Universidad Agraria de la Habana (UNAH) y los sementales del Centro Nacional de Inseminación Artificial "ROSAFE SIGNET" ubicado en San José de Las Lajas, provincia Mayabeque. Durante el muestreo los animales se mantuvieron en un estado de correcto aplomo sobre sus extremidades y aislados del piso por medio de una manta de goma. A las áreas donde se colocaron los electrodos se les aplicó pasta conductora de electricidad, después de haber sido depiladas y despojadas de grasa al frotarlas con alcohol. El electrocardiógrafo fue calibrado con una señal de 1 mV/cm y una velocidad de corrida del papel de 25 mm/s.

En la figura 1, se ilustran los puntos en los que se conectaron los electrodos para registrar derivaciones monopolares pericordiales, en forma de una circunferencia que encierra el plano transversal. Con ellas, se exploró el corazón en toda su periferia desde el ápice hasta la base tanto por el lado izquierdo, con las derivaciones V_5, V_4, V_{3C}, V_{2C}, V_3, V_{3H} y V_{10}, como por el derecho, con V_{1C} y V_6 colocadas simétricas a V_{2C} y V_{3C}, respectivamente y V_{1H}, por delante del hombro derecho. Se empleó una derivación bipolar para medir la diferencia de potencial entre las regiones de la base y del ápice del corazón (BA), colocando el electrodo explorador en V_5 y el negativo en V_{10}. Las derivaciones bipolares estándares de extremidades DI, DII y DIII fueron registradas según se han establecido clásicamente. Para obtener las derivaciones bipolares IH, IIH y IIIH se desplazaron los dos electrodos, conectados inicialmente en los metacarpos para el registro de las derivaciones estándares, hasta la altura de la articulación escapulohumeral.

Para determinar la cantidad de combinaciones entre las ondas P, QR y T con diferentes morfologías y polaridad se realizó una codificación de cada una de ellas, con la asociación de un número (Tabla 1).

Análisis estadístico

El procesamiento estadístico consistió en determinar la frecuencia de las combinaciones de morfología y de polaridad de las ondas P, complejo QR y T del ECG en cada derivación, a partir la codificación establecida para cada una de ellas[3]. Se realizó la prueba de comparación de proporciones para determinar diferencias estadísticamente significativas entre derivaciones, con relación a la cantidad de combinaciones encontradas. Se empleó como criterio para seleccionar las derivaciones más útiles en el diagnóstico las que mostraran un porcentaje más elevado de una misma secuencia de la Polaridad de las ondas P, QR y T y el menor número de combinaciones con diferentes tipos de morfología.

Resultados y discusión

En el electrocardiograma normal del hombre y de otros mamíferos categorizados en el grupo A, con frecuencia el complejo QRS está formado por tres ondas separadas: la onda Q, la onda R y la onda S[4-7]. En los animales que se categorizan en el grupo B como los bovinos y los equinos sólo aparecen 2 ondas componentes, la onda Q y la R[8,9]. En todos los complejos de despolarización ventricular registrados en esta investigación aparecieron sólo estas dos ondas, independientemente del tipo de derivación utilizada. A partir de lo observado y de las comprobaciones eléctricas se pudo determinar que la primera onda corresponde a la Q y la segunda a la R. La onda Q es poco frecuente y de baja amplitud por lo que se tratarán en su conjunto como QR y la referencia a las combinaciones producidas entre todas las ondas del ECG será a través de la tríada P-QR-T. Otros autores han hecho referencia a esta categorización electrocardiográfica de los animales en un grupo B[10-13], pero se ha conservado hasta la actualidad la denominación clásica de complejo QRS[14-17].

Aunque se encontraron 13 formas de ondas P, 22 del complejo QR y 16 de la onda T que pueden originar muchas combinaciones, las detectadas con mayor frecuencia se reducen a 30 con morfologías diferentes. Al tener en consideración la codificación previa ilustrada en la tabla 1, se obtuvieron 3 tipos de combinaciones de polaridad P-QR-T (Fig 1): 1. Las ondas P y QR positivas y discordantes con T, para dar origen a un triplete +/+/-, 2. La onda QR positiva y la P y la T concordantes negativas, en una combinación del conjunto -/+/- y 3. La onda QR negativa con P y T concordantes positivas, por lo que la polaridad de la combinación fue de +/-/+. Otras combinaciones aparecieron en las derivaciones que no manifestaron estabilidad ni en su polaridad ni en su morfología y por tal causa carecen de valor para el diagnóstico (Tablas 2 y 3).

En la electrocardiografía es importante tener la habilidad de interpretar, además de confianza para lograr una definición certera en el diagnóstico y en el tratamiento[1,18-21], lo que tiene una gran relevancia para evaluar la fisiología cardiovascular, tanto bajo el efecto de medicamentos como en cualquier actividad física[22-25]. Al detectar los puntos que originan ondas electrocardiográficas con estabilidad en cuanto a su morfología y a su polaridad, así como en el tipo de combinación que se establece con más frecuencia entre ellas, se pueden caracterizar los registros normales en esas derivaciones y adoptarlos como referencia para su interpretación diagnóstica. Sobre esta base, fueron descritas las combinaciones P-QR-T que aparecen con mayor frecuencia en las derivaciones monopolares y en las bipolares (tabla 2 y 3).

Se encontraron diferencias estadísticamente significativas ($p<0,05$), tanto en la morfología como en la polaridad

MORFOLOGÍA DE LAS ONDAS DEL ECG EN BOVINOS

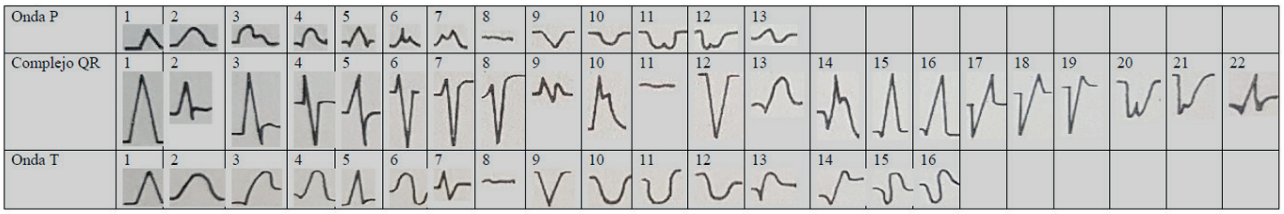

Tabla 1. Codificación de las ondas electrocardiográficas en el bovino, acorde a su morfología.

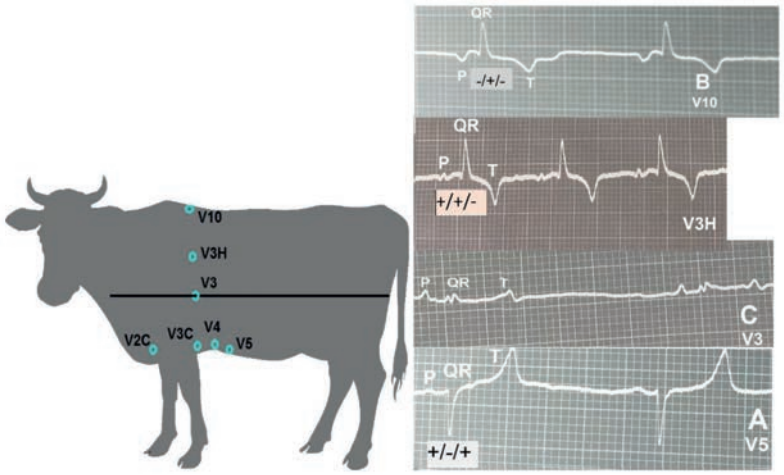

Figura 1. Puntos de colocación de los electrodos para registrar derivaciones monopolares. Registros monopolares en la base (B=»V_{10}), en el ápice (A=»V_5), en la línea isoeléctrica del corazón para QR (C=»V_3) y en un punto próximo V_{3H}.

	Cantidad de formas de onda:			Combinaciones morfológicas.		% de animales con polaridad combinada de P, QR y T:				
Derivaciones.	**P**	**QR**	**T**	**Total**	**Típica**	**+/+/-**	**+/-/+**	**-/+/-**	**Otras**	
Monopolares periscordiales									**+/+/+**	**Varias**
Basales.										
V10	**4**	**3**	**4**	**14**	**9.15.9**	--	--	**100**	--	--
V3H	**8**	**5**	**5**	**10**	**1.1.9**	**97**	--	--		**3**
V1H	**5**	**3**	**4**	**17**	**9.1.9**	--	--	**100**	--	--
Isoeléctrica para QR										
V3	**4**	**16**	**8**	**28**	**1.1.9**	**80**	--	--	--	**20**
Transición.										
V1C	**5**	**8**	**7**	**16**	**10.16.9**	--	--	**84**		**16**
V2C	**5**	**8**	**7**	**16**	**10.1.9**	--	--	**97**		**3**
V3C	**4**	**8**	**10**	**32**	**1.12.1**	--	**80**	--	--	**20**
V6	**7**	**5**	**8**	**40**	**8.6.1**		**84**			**16**
Apicales.										
V4	**4**	**5**	**6**	**17**	**2.12.1**		**100**			
V5	**3**	**5**	**6**	**15**	**2.6.1**		**100**			

Tabla 2. Combinaciones de diferentes forma y polaridad de ondas P, QR y T del ECG en bovinos en derivaciones monopolares (n = 100).

	Cantidad de formas de onda:			Combinaciones morfológicas.		% de animales con polaridad combinada de P, QR y T:				
Derivaciones bipolares:	**P**	**QR**	**T**	**Total**	**Típicas**	**+/+/-**	**+/-/+**	**-/+/-**	**Otras**	
Extremidades.									**+/+/+**	**Varias**
DI	**5**	**15**	**11**	**44**	**1.1.11**	**48**	**2**	--	**4**	**46**
DII	**4**	**16**	**12**	**50**	**1.12.1**	**11**	**50**	--	--	**29**
DIII	**6**	**16**	**13**	**53**	**1.12.1**	**23**	**47**	--	--	**30**
De hombros.										
IH	**6**	**5**	**4**	**24**	**10.15.9**	--	--	**96**	--	**4**
IIH	**3**	**6**	**7**	**16**	**2.12.1**	--	**100**	--	--	
IIIH	**4**	**4**	**6**	**16**	**2.6.1**	--	**100**	--	--	--
Base-Ápice (B-A).	**4**	**4**	**6**	**14**	**1.6.1**	--	**100**	--	--	--

Tabla 3. Combinaciones de diferentes forma y polaridad de ondas P, QR y T del ECG en bovinos en derivaciones bipolares (n = 100).

entre derivaciones basales, apicales y las próximas a la línea isoeléctrica que pasa por V_3 (Fig. 1). En la base (en V_{10}), QR es positiva, P y T son concordantes negativas para una polaridad de la combinación -/+/- y en el ápice (en V_5) QR es negativa, P y T son concordantes positivas formando un triplete +/-/+.

El registro isoeléctrico para el complejo QR, se obtiene en la derivación V_3 ubicada en el punto medio del segmento que une los puntos de las derivaciones V_{3C} y V_{3H}, con lo que se demuestra que durante la despolarización ventricular el corazón actúa como un dipolo dinámico. En el transcurso de dicho proceso, la recta que pasa por V_3 separa la región superior o basal del corazón, que es positiva, de la ventral o apical que es negativa. Este dipolo origina al vector que se dirige hacia la base y describe al complejo QR. Por esta causa, en todos los registros basales el complejo QR es positivo como se puede evaluar en las derivaciones V_{10}, V_{3H} y V_{1H} a los cuales corresponden, respectivamente, los patrones morfológicos, según la codificación (tabla 1), 9.15.9, 1.1.9 y 9.1.9 con la polaridad indicada en tabla 2. En la región apical, en V_4 y V_5, los registros para QR resultaron negativos y las combinaciones morfológicas, respectivas, fueron de: 2.12.1 y 2.6.1 con el mismo tipo de combinación de polaridad de P, QR y T equivalente a +/-/+.

En las derivaciones apicales próximas a la línea isoeléctrica para QR (Fig. 1 y Tabla 2), tales como V_{2C}, V_{3C}, V_{1C} y V_6 se obtienen registros con menor estabilidad ($p<0,05$), en cuanto a las combinaciones morfológicas y la polaridad. Por esta causa se pueden considerar derivaciones de transición, ya que están más influenciadas por los desplazamientos del corazón, los cuales en el bovino pueden ser notables por repleción del rumen, la gestación y otros factores.

Como el corazón se comporta como varios dipolos dinámicos, de acuerdo a la porción que se va despolarizando, aparece primero el correspondiente a la onda P, cuando el proceso de activación tiene lugar en las aurículas , a continuación se produce el que representa la despolarización ventricular constituido por el complejo QR y luego con la producción de la repolarización ventricular aparece el dipolo que caracteriza a la onda T[26,27]. El flujo de corriente producido en cada instante, del polo negativo al positivo, se representa por un vector, con su dirección, amplitud y sentido. Se ha comprobado que en los animales categorizados electrocardiográficamente en el grupo B los tres vectores difieren entre sí en dirección y sentido, el del mayor componente del complejo QR se dirige hacia la base del corazón y los correspondientes a P y T hacia el ápice[3,8,28]. En este sentido, debe recordarse que el electrocardiógrafo está diseñado de modo que cuando el vector que genera la onda se dirige hacia el electrodo positivo o explorador la deflexión es positiva y en caso contrario es negativa.

Tanto la evolución temporal del vector del dipolo como sus proyecciones en el cuerpo del sujeto están influenciados por las trayectorias de conducción eléctrica dentro del corazón, las características geométricas intrínsecas al propio corazón, su posición dentro del tórax y por la no homogeneidad del volumen conductor de los tejidos[29].

En la tabla 3, se muestran las características de las combinaciones P-QR-T en las derivaciones bipolares estándares de extremidades, de hombros y de BA. Entre los 1 700 registros realizados sólo se encontraron 4 en los que las combinaciones de las 3 ondas fueron concordantes positivas y fue en la derivación bipolar de extremidad DI, que mide la diferencia de potencial entre el metacarpo izquierdo y el derecho, ambos conectados eléctricamente a la zona de transición entre el ápice y la base del corazón (Fig. 1).

Las derivaciones DII y DIII también son de transición porque poseen la misma relación de proximidad a la línea isoeléctrica para QR que DI. En estas tres derivaciones se produce una elevada cantidad de combinaciones de P-QR-T morfológicamente diferentes y una gran dispersión en los tipos de polaridad. Las características descritas les confiere muy poco valor para ser empleadas en el diagnóstico de alteraciones cardíacas como las que se detectan en el hombre[30-33]. Sin embargo, han sido empleadas en Veterinaria para evaluar el estado del ritmo cardíaco al igual que en Medicina Humana, ya que estas alteraciones se reflejan de alguna forma en cualquier derivación[8,34-36].

Las derivaciones bipolares de hombro y la de base-ápice, que miden las diferencias de potencial eléctrico entre dos puntos alejados de la línea que pasa por el punto de la derivación V_3 resultaron de alta estabilidad, tanto en las combinaciones de la morfología como en las de la polaridad de las ondas P-QR-T. La colocación de los electrodos en la derivación IH se realiza de la misma forma que en DI, pero a nivel de los hombros y mide la diferencia de potencial entre dos puntos de la base del corazón. En las tres derivaciones restantes el electrodo explorador o positivo, amarillo para la derivación BA y verde para la IIH y la IIIH, se conectaron hacia la región del ápice y el negativo en la base. Dado que el vector QR se dirige hacia la base del corazón, se aleja del correspondiente electrodo explorador y da como resultado un registro negativo en las tres derivaciones, con una combinación P-QR-T de +/-/+ en el 100% de los animales, similar a la de V_4 y V_5 (Fig. 1). La onda P se origina a nivel del nódulo sinusal en la aurícula derecha y su vector se dirige hacia abajo[37,38]. Entretanto, el vector de la repolarización ventricular representado por la onda T, se inicia en la base de los ventrículos y también está dirigido hacia el ápice, al igual que en el hombre[3,39,40].

Las derivaciones que muestran mayor constancia en la polaridad de las combinaciones de P-QR-T poseen también el menor número de combinaciones morfológicas diferentes ($p<0,05$). Sobre este aspecto se han hecho pocas referencias en la literatura y se le ha atribuido al ECG bovino una extraordinaria variabilidad, tanto en el complejo QRS como en la onda T, la cual posee un valor diagnóstico relevante en el hombre[41,42]. La distribución de cargas opuestas entre la base y el ápice, es el factor que determina que una misma onda electrocardiográfica se pueda registrar en diferentes puntos de la superficie corporal positiva, negativa, bifásica o nula, tal como ocurre con la onda P en la derivación V_6 donde alcanza 71 valores nulos y para QR en V_3, con 8 valores equivalentes a cero.

Conclusiones

Se comprobó que en las porciones de la superficie corporal del bovino situadas por encima o por debajo de la línea isoeléctrica para QR, se obtienen ECG con mucha estabilidad en las características morfológicas y de polaridad de las combinaciones registradas en la tríada de las ondas P-QR-T, por lo que las derivaciones monopolares en cada una de estas áreas o las bipolares registradas entre una y otra, son muy útiles para diagnosticar las alteraciones producidas en la actividad cardíaca.

Referencias bibliográficas

1. Zavala VJA. Descripción del electrocardiograma normal y lectura del electrocardiograma. Taller: Electrocardiografía básica para anestesiólogos. 2017;40(1):210-213.
2. Avitia R, Avena G, Flores N, Reyna M, Nava M. Datos Fisiológicos de Baja California: PhysioBC. Resultados en Electrocardiografía. Revista Mexicana de Ingeniería Biomédica. 2017;38(1):372-381.

3. Pompa NA. Morfología y polaridad de la onda T del electrocardiograma en el bovino. Revista de Salud Animal. 2019;41(3):1-8.
4. Rivero I, Valdés E, Valdés FE. Detection of IM Points in Seismocardiogram and Possible Application. IEEE Latin America Transactions. 2018;16(1):25-30.
5. Vindas ZJD, Moya AA, Muñoz HP, Rojas MR. Interpretación práctica del electrocardiograma en el Servicio de Emergencias. Revista de Salud. Facultad de Medicina. 2016;1(1):9-22.
6. Aguirre RJC. Diagnóstico de las Arritmias en Atención Primaria. Revista Andaluza de Atención Primaria. 2016. Año 5;5:5-6.
7. Luna LR, Datino T. Electro-Reto. ECG de enero de 2020. Rev Esp Cardiol. 2020;73(1):87.
8. Matsui K, Sawasaki T, Oyama T, Kano Y. Changes in electrocardiographic parameters with growth in Holstein cows. Jpn. Adv. Anim. ECG. 1981;14:41-45.
9. Camejo ZM, Masot LD, Pompa NA, Morfología y polaridad de las ondas electrocardiográficas en caballos (Equus caballus) como base para el diagnóstico clínico. Revista de Salud Animal. 2019;41(2):1-8.
10. Hamlin R, Smith C. Categorization of common domestic mammals based upon their ventricular activation process. Ann. N. Y. Acad. Sci. 1965;127:195–203.
11. Hilwig W. ECG of the month, genesis of the electrocardiogram. J. Am. Vet. Med. Ass. 1976;169(10):1054-1055
12. Upadhyay RC, Sud SC, Joshi HC, Bagha HS. Electrocardiographic studies in Jersey cattle. Ind. Vet. J. 1976;53:953-961.
13. Illera JC, Illera M, Hamlin R. Unipolar thoracic electrocardiograms that induces QRS complexis of relative uniformity from male horses. Am. J. Vet. Res. 1987;48(12):1700–1702.
14. Baquero BLM, Quesada ACI. Bloqueo atrioventricular de primer grado asociado a bloqueo de rama derecha del haz de His. Revista Clínica de la Escuela de Medicina UCR-HSJD. 2018; (EKG 1-2018):1-3.
15. Fernández A, Pena JA, Mombelli A. COVID-19 con afectación cardiovascular. Reporte de un caso. Rev Urug Cardiol. 2020;35:1-3.
16. Maciel NKC, Hernández FMS. Canal atrioventricular transicional en un paciente conocido con síndrome de Ellis Van Creveld. Presentación de un caso clínico en el Centro Médico Puerta de Hierro, Zapopan, Jalisco, México. Archivos de CIENCIA. Revista en Ciencias de la Salud. 2020;12(1):143.
17. Astudillo TE, Aguayo EC, Ayala CC, Caguano CW, Cisneros ChD, Pavón BR, Pumarica TJ. Síndrome de Wolff Parkinson White en paciente gestante. MEDICIENCIAS UTA.2020;4 (2):108-114.
18. Sprockel DJ, González ML, Barón R. Escalas de riesgo en el diagnóstico de la angina inestable en pacientes con dolor torácico con electrocardiograma y biomarcadores negativos. Repert med cir. 2016;25(3):156–162.
19. Short H. Isquemia Miocárdica Perioperatoria en Cirugía no Cardíaca. Anestesia general Tutorial 2018; 375:1-8.
20. Suárez AM, Lemus Y, Dulce M, Otero M. Valor del electrocardiograma en el diagnóstico de hipertrofia ventricular izquierda de pacientes en hemodiálisis. CorSalud. 2018;10(1):21-31.
21. Olvera CHE, Nieto MAJF, Rocha MYF, Morales LS, Ortiz SAG, Díaz CFA. Mejora de habilidades en la interpretación del electrocardiograma mediante un taller con simulación clínica. EDUMECENTRO 2020;12(1):30-45.
22. Hellman T, Kiviniemi T, Vasankari T, Nuotio I, Biancari F, Bah A, Hartikainen, J, Mkrinen M, Airaksinen J. Prediction of ineffective elective cardioversion of atrial fibrillation: a retrospective multi-center patient cohort study. BMC Cardiovascular Disorders. 2017;17(33):3-5.
23. Ramognino F, Ferraro F, Salmon BE, Caruso N, Sánchez C, Bortman G. Hallazgos electrocardiográficos anormales en deportistas amateur: comparación de los criterios de Seattle 2013 y 2017. Rev Argent Cardiol. 2019;87:146-151.
24. León RML, García ÁY, Álvarez HR, Morales PC, Regal CVM, González LHD. Influencia del estrés psicológico y la actividad física moderada en la reactividad cardiovascular. Revista Finlay. 2018;8(3): 224-232.
25. Stocich KMG, Gomero CR. Estudio piloto de la variabilidad de la frecuencia cardiaca en trabajadoras no atletas durante tareas de limpieza, 2017. Rev Asoc Esp Med Trab. 2020;29(1):25-33
26. Pozas G, Valdés R, Ibarra C. Método de Grant, eje eléctrico de P, eje eléctrico de QRS, eje eléctrico de T, eje eléctrico espacial. Rev. Ciencias Clínicas. 2012;9(27):18-22.
27. Acoltzin VC, Rabling AE. Retraso de la rama descendente de la onda T en electrocardiogramas sin datos de riesgo aparente de muerte súbita. Gac Med Mex. 2018;154:198-201.
28. Szabuniewicz M, Ortega FV, Sosa FAJ, Gómez M, Gil CB. La electrocardiografía en clínica veterinaria. III parte: Análisis vectorial. Rev. Fac. Ciencs. Vet. U. C. Ven. 1980;28(1-8):107-112.
29. Rodríguez, A.A., Miranda, A.P.V., Sánchez, H.O.E., Rodríguez, A.M.E., Sánchez, T.B.I. Vectores de impedancia bioeléctrica para analizar la composición corporal de mujeres mexicanas embarazadas. Rev Esp Méd Quir. 2016;21(2):55-64.
30. Pérez RAR, de Abreu LC, Barbosa BR, Paixao AA. El síndrome del QT corto congénito: Avances en los últimos años. REVISTA CONAREC 2016;32(135):141-147.
31. Schafer S. Mutaciones que alteran el gen titin afectan a la función cardíaca también en población general. Revista de Genética Médica NEWS. 2017;4(67): 1-10.
32. Baquero L M, Quesada ACI. Infarto agudo al miocardio de cara inferior con posterior revascularización. Revista Clínica de la Escuela de Medicina UCR-HSJD. 2018;2:1-4
33. Borrayo SG, Rosas PM, Pérez RG, Ramírez AE, Almeida GE, Arriaga DJJ. Infarto agudo del miocardio con elevación del segmento ST: Código I. Rev Med Inst Mex Seguro Soc. 2018;56(1):26-37.
34. Morales A, Carrasco V, Martínez E. Toxicidad cardiaca por anestésicos locales, protocolo de estudio en un modelo experimental porcino. Revista Complutense de Ciencias Veterinarias 2017; 11(especial):120-125.
35. Soto RL, Garduño RM, Millán CK, Moreno LA, Valladares CB. Intoxicación por teobromina en perros. Una revision. REDVET Rev. Electrón. vet. 2018;19 (3):1-7.
36. Lobo M L, Cursack G, García B D, Echazarreta D, Perna E. Algoritmo de insuficiencia cardíaca aguda Manejo inicial: etapa prehospitalaria, departamento de emergencias, internación en unidad coronaria. Insuf Card. 2018;13(1):24-39.
37. Montoya AJA, Ponce VJ. Ritmos cardiacos normales en la cabra. Med. Vet (Espana).1986;3(4):227–231.
38. Rubio SJC. Actuación de enfermería ante una alteración electrocardiográfica. Eje, onda P y complejo QRS. Enferm Cardiol. 2016;23(67):58-65.
39. Abu-Suboh A, Abu-Suboh M. Abadia. Variantes normales en electrocardiografía. ABS Almenar-Alfarras. Lleida. Hospital Vall d'Hebron. Barcelona. [en línea] mayo 2015. Disponible en: http://www.elsevier.es. [Consultada: 11 de enero de 2020].
40. Lara, PJI. El electrocardiograma: una oportunidad de aprendizaje. Revista de la Facultad de Medicina de la UNAM. 2016;59(6):39-42.
41. Ortega DCI, Vintimilla GJF, Moreira VWX, Villa CEH, Mora C, Mishel L, Peralta MEY. Caso Clínico: Infarto Agudo de Miocardio sin Enfermedad Coronaria Aterosclerótica Obstructiva. Revista Médica HJCA 2016;8(3):263-267.
42. Nogara R, Ferrando CF, Ricca MR, Ferrando R, Marichal P. Distorsión morfológica isquémica de la onda T en la centellografía de perfusión miocárdica con estrés vasodilatador. MEDICINA (Buenos Aires). 2017;77:130-134.

Received: 28 agosto 2020
Accepted: 20 septiembre 2020

RESEARCH / INVESTIGACIÓN

Evaluación de la calidad del agua en el río Alambrado utilizando macroinvertebrados bentónicos como bioindicadores en la zona del embalse de la Laguna de la Mica

Assessment of water quality in the Alambrado River using benthic macroinvertebrates as bioindicators in Laguna de la Mica Reservoir

Christian García Rengifo, Alexandra Endara González

DOI. 10.21931/RB/2020.05.04.17

Resumen: Se evaluó la calidad del agua del río Alambrado usando macroinvertebrados bentónicos y parámetros físico-químicos. Se midieron los índices: Índice Multimétrico de estado ecológico de Ríos Altoandinos (IMEERA), Índice Ephemeroptera, Plecoptera y Trichoptera (EPT), Índice Biótico Andino (ABI) y el índice piloto Biological Monitoring Working Party / Ecuador (BMWP/ECU), Análisis de Componentes Principales (ACP) y Análisis de Correspondencia Canónica (ACC), durante tres meses (enero a marzo, 2019). Se colectaron 1993 individuos; la familia Chironomidae fue la más abundante (80%) y las menos abundantes fueron: Gerridae, Simulidae y Leptoceridae (0,05%). Más del 90% fueron macroinvertebrados colectores. El ACP y ACC determinó que los sólidos suspendidos totales tuvieron una mayor relación con la gran mayoría de taxones. Se determinó que la calidad del agua se encuentra en un rango de malo a moderado y los resultados de los índices biológicos son sensibles a los parámetros físico-químicos de oxígeno disuelto, Demanda Bioquímica de Oxígeno 5 (DBO5), Demanda Química de Oxígeno (DQO); los cuales varían según la temporada climática.

Palabras clave: Ríos altoandinos, entomofauna, índices bióticos, conservación.

Abstract: The water quality of the Alambrado River was evaluated using benthic macroinvertebrates and physical-chemical parameters. The following indices were measured: Multimetric Index of the Ecological Status of High Andean Rivers (IMEERA), Ephemeroptera, Plecoptera, and Trichoptera Index (EPT), Andean Biotic Index (ABI), and the pilot index Biological Monitoring working party / Ecuador (BMWP/ECU), Principal Component Analysis (PCA) and Canonical Correspondence Analysis (ACC), during three months (January to March 2019). 1993 individuals were collected; the Chironomidae family was the most abundant (80%), and the lesser abundant were Gerridae, Simulidae, and Leptoceridae (0.05%). More than 90% were collector's macroinvertebrates. PCA and ACC determined that total suspended solids had a more significant relationship with most taxa collected. Water quality was determined to be between bad to moderate, and the biological indices used were sensitive to dissolved oxygen, biochemical oxygen demand (DBO5), chemical oxygen demand (DQO). These parameters vary according to the climatic season.

Key words: High Andean Rivers, entomofauna, biotic indices, conservation.

Introducción

La conservación de los ríos dentro de las áreas protegidas del Ecuador ha adquirido mayor importancia para las autoridades ambientales que se encargan de dirigir cada una de estas áreas, debido a la falta de conciencia ambiental de las personas que visitan estos espacios, lo que tiende a generar impactos a los ecosistemas más vulnerables como son los ríos. Es por esto que la Reserva Ecológica Antisana (REA) en sus informes han notado una creciente visita de personas que no ingresan por los puntos autorizados para no ser controlados y con ello pescar de maneras incorrectas afectando a la calidad de los cuerpos hídricos que posee la REA.

Para el análisis ambiental de estos cuerpos de agua, se presenta por parte de la REA la necesidad de realizar un monitoreo biológico de uno de los principales ríos que tiene dentro de su territorio, el río Alambrado. La investigación se centra en determinar la calidad de agua del río Alambrado usando bioindicadores y parámetros físico – químicos, para poder tener un panorama más amplio de cómo se encuentra estructurada la biodiversidad de macroinvertebrados bentónicos y determinar los cambios que en ella se producen por las alteraciones de las características físico químicas del agua.

Materiales y métodos

Área de estudio

El estudio fue realizado en el río Alambrado a 1.169 metros desde la desembocadura del río con la laguna, con tres estaciones previamente seleccionadas con la metodología del Índice de Hábitat Fluvial, el cual califica diversas métricas de desarrollo de vida en ecosistemas acuáticos. (IHF)[1].

Muestreo y Análisis

Durante los meses de enero, febrero y marzo del 2019, se tomaron muestras con red Surber[2]. Estas se ubicaron en hábitats con corriente suave, corriente fuerte, sustrato duro, sustrato suave, vegetación acuática emergida, tanto dentro del río, como sus orillas, contenido de lodo y/o arena[3].

Los sedimentos fueron colocados en fundas con cierre hermético con sus respectivas etiquetas, con alcohol al 80% y con gotas de glicerina[3,4]. Se colectaron un total de cuarenta y cinco muestras de sedimento. Quince en cada una de los tres meses de muestreo.

La identificación de los taxas fue hasta familia, con respecto a los índices biológicos el índice IMEERA, es calcula-

Grupo de investigación de la Carrera de Ingeniería Ambiental: "Grupo de Protección Ambiental" (GPA), Universidad UTE, Ecuador.

Corresponding author: maria.endara@ute.edu.ec

Phylum	Clase	Orden	Familia	1500-3500
Anellidae	Hirudinea	Arhynchobdellid	Cylicobdellidae (*Cystobranchus sp.*)	9
Annellida	Hirudinea	Rhynchobdellida	Glossiphoniidae (*Helobdella festae; H. stagna*	3
Annellida	Oligochaeta	Haplotaxida	Todas las familias excepto Tubificidae: *Tubife*	2
Annellida	Oligochaeta	Haplotaxida	Tubificidae (*Tubifex*)	1
Arthopoda	Arachnoidea (Acari	Trombidiformes	Lymnessiidae (Hydracarina)	10
Arthopoda	Arachnoidea (Acari	Hydracarina	Arrenuridae (*Arrenurus*)	6
Arthopoda	Arachnoidea (Acari	Hydracarina	Hydrachnidae (*Hidrachna*)	5
Arthopoda	Arachnoidea (Acari	Hydracarina	Limnocharidae (*Limnochares americana*)	6
Arthopoda	Crustacea	Amphipoda	Hyalellidae (*Hyalella meinerti; H. cajasi*)	6
Arthopoda	Crustacea	Decapoda	Pseudothelphusidae	8
Arthropoda	Insecta	Coleoptera	Curculionioidea: Brachyceridae (*Neochetina;*	5
Arthropoda	Insecta	Coleoptera	Dryopidae	6
Arthropoda	Insecta	Coleoptera	Dytiscidae	4
Arthropoda	Insecta	Coleoptera	Elmidae	7
Arthropoda	Insecta	Coleoptera	Gyrinidae	9
Arthropoda	Insecta	Coleoptera	Haliplidae (*Haliplus*)	4
Arthropoda	Insecta	Coleoptera	Heteroceridae (*Heterocerus; Tropicus*)	4
Arthropoda	Insecta	Coleoptera	Hydraenidae	9
Arthropoda	Insecta	Coleoptera	Hydrophilidae	4
Arthropoda	Insecta	Coleoptera	Lampyridae	9
Arthropoda	Insecta	Coleoptera	Limnichidae	6
Arthropoda	Insecta	Coleoptera	Lutrochidae	6
Arthropoda	Insecta	Coleoptera	Noteridae	4
Arthropoda	Insecta	Coleoptera	Psephenidae	8
Arthropoda	Insecta	Coleoptera	Ptilodactylidae	7
Arthropoda	Insecta	Coleoptera	Scirtidae	9
Arthropoda	Insecta	Coleoptera	Sphaeridae	5
Arthropoda	Insecta	Coleoptera	Staphylinidae	5
Arthropoda	Insecta	Diptera	Athericidae	8
Arthropoda	Insecta	Diptera	Blepharoceridae	10
Arthropoda	Insecta	Diptera	Ceratopogonidae	4
Arthropoda	Insecta	Diptera	Chironomiidae (Todos los demás)	3
Arthropoda	Insecta	Diptera	Chironomiidae (*Chironomus* ROJO)	2
Arthropoda	Insecta	Diptera	Culicidae	3
Arthropoda	Insecta	Diptera	Dixidae	7
Arthropoda	Insecta	Diptera	Dolichopodidae	4
Arthropoda	Insecta	Diptera	Empididae	5
Arthropoda	Insecta	Diptera	Ephydridae	2
Arthropoda	Insecta	Diptera	Limoniidae	4
Arthropoda	Insecta	Diptera	Muscidae	3
Arthropoda	Insecta	Diptera	Psychodidae (*Maruina*)	6
Arthropoda	Insecta	Diptera	Psychodidae (*Psychoda* y *Clognia*)	2
Arthropoda	Insecta	Diptera	Sciomyzidae	3
Arthropoda	Insecta	Diptera	Simuliidae	7
Arthropoda	Insecta	Diptera	Stratiomyidae	4
Arthropoda	Insecta	Diptera	Syrphidae	1
Arthropoda	Insecta	Diptera	Tabanidae	4
Arthropoda	Insecta	Diptera	Tipulidae	4
Arthropoda	Insecta	Ephemeroptera	Baetidae	7
Arthropoda	Insecta	Ephemeroptera	Euthyplociidae	9
Arthropoda	Insecta	Ephemeroptera	Leptohyphidae	7
Arthropoda	Insecta	Ephemeroptera	Leptophlebiidae	9
Arthropoda	Insecta	Ephemeroptera	Oligoneuriidae	10
Arthropoda	Insecta	Hemiptera	Corixidae	5
Arthropoda	Insecta	Hemiptera	Gelastocoridae	6
Arthropoda	Insecta	Hemiptera	Gerridae	7
Arthropoda	Insecta	Hemiptera	Naucoridae	6
Arthropoda	Insecta	Hemiptera	Notonectidae	6
Arthropoda	Insecta	Hemiptera	Veliidae	7

Tabla 1A (Parte 1). Listado de las especies del índice BMWP/Ecu.

Arthropoda	Insecta	Lepidoptera	Crambidae	8
Arthropoda	Insecta	Lepidoptera	Pyralidae	8
Arthropoda	Insecta	Megaloptera	Corydalidae	6
Arthropoda	Insecta	Odonata	Aeshnidae	7
Arthropoda	Insecta	Odonata	Calopterygidae	7
Arthropoda	Insecta	Odonata	Coenagrionidae	7
Arthropoda	Insecta	Odonata	Gomphidae	8
Arthropoda	Insecta	Odonata	Libellulidae	7
Arthropoda	Insecta	Odonata	Polythoridae	8
Arthropoda	Insecta	Plecoptera	Gripopterygiidae	10
Arthropoda	Insecta	Plecoptera	Perlidae	9
Arthropoda	Insecta	Trichoptera	Anomalopsychidae	10
Arthropoda	Insecta	Trichoptera	Atriplectididae	10
Arthropoda	Insecta	Trichoptera	Calamoceratidae	10
Arthropoda	Insecta	Trichoptera	Glossossomatidae	8
Arthropoda	Insecta	Trichoptera	Helicopsychidae	7
Arthropoda	Insecta	Trichoptera	Hydrobiosidae	8
Arthropoda	Insecta	Trichoptera	Hidropsychidae (*Leptonema y Smicridea*)	7
Arthropoda	Insecta	Trichoptera	Hydroptilidae	7
Arthropoda	Insecta	Trichoptera	Leptoceridae	8
Arthropoda	Insecta	Trichoptera	Limnephilidae	9
Arthropoda	Insecta	Trichoptera	Odontoceridae	10
Arthropoda	Insecta	Trichoptera	Philopotamidae	8
Arthropoda	Insecta	Trichoptera	Polycentropodidae	7
Arthropoda	Insecta	Trichoptera	Xiphocentronidae	8
Coelenterata	Hydrozoa	Hidroida	Hydridae	10
Mollusca	Bivalvia	Veneroidea	Sphaeridae	4
Mollusca	Gastropoda	Basommatophora	Lymnaeidae	4
Mollusca	Gastropoda	Basommatophora	Physidae	3
Mollusca	Gastropoda	Basommatophora	Planorbidae	3
Nematomorpha		Gordioidea	Gordiidae	9
Platyhelmintes	Turbellaria	Tricladida	Dugesiidae	5
Platyhelmintes	Turbellaria	Tricladida	Planariidae	7

Tabla 1A (Parte 2). Listado de las especies del índice BMWP/Ecu.

CLASE	CALIDAD	RANGOS 376	
		MINIMO	MAXIMO
I	Muy Buena	>116	
II	Buena	96	115
II	Aceptable	76	95
IV	Dudosa	41	75
V	Crítica	11	40
VI	Muy Crítica	<10	

Tabla 1B. Valoración del índice BMWP/Ecu.

do con el Software CABIRA[5], mientras que los índices ABI y BMWP/Ecu se calculan a través de un listado de taxones identificados hasta familia con lo que se le denota un determinado puntaje de calidad, donde la sumatoria total de los puntajes obtenidos de la abundancia del mes de muestreo, es el resultado establecido con criterios de calidad de cuerpos hídricos (Tabla 1A y B). El índice EPT se calcula con la abundancia de las familias Ephemeroptera, Plecoptera y Trichoptera sobre la abundancia total por cien para obtener el porcentaje de EPT[6]. Para el análisis Biplot basado en la descomposición del ACP y ACC, se determinó con la ayuda del software PAST[7].

Los parámetros físico químicos fueron medidos in situ (pH, conductividad, turbidez y oxígeno disuelto) y en laboratorio (DBO_5, DQO, nitratos, amonio total, solidos totales, solidos suspendidos totales) siguiendo lo establecido por Standard Methods[8] en el monitoreo de parámetros físico químicos, los cuales fueron utilizados para el análisis estadístico, y para finalizar se los comparo con la normativa ambiental ecuatoriana[9].

Resultados

En la tabla 2 se pueden observar los datos físico químicos obtenidos en el presente estudio. Se recolectaron 1903 individuos de 15 diferentes familias, donde el 80,08% pertenecen a la familia Chironomidae 1524 individuos, el 11,98% es de la familia Hyalellidae (228 individuos), siendo estas las más abundantes dentro de los tres meses de muestreo. Las familias menos abundantes fueron Simulidae, Gerridae y Leptoceridae compartiendo un 0,05% de la abundancia total con 1 individuo encontrado en los meses de muestreo.

El resultado del porcentaje obtenido de la relación de EPT presentes en el río es de 1,05%, de acuerdo al cuadro de valoración, se obtiene que el resultado se encuentra en el rango de 0% a 24%, lo que indica que la calidad del agua dentro del río se califica como "MALA". En la Tabla 3 se indica el resultado total de la abundancia como también el resultado del índice EPT.

El índice ABI fue de 73 determinando que la calidad del agua se encuentra en un nivel "BUENO", por la presencia de Amphipodos, Odonatos y Trichopteros. En la Tabla 3, se mues-

tra el resultado de los índices ABI, IMEERA y BMW/ECU. Con IMEERA el agua se encuentra en un estado considerado como "BUENO" con un valor de 73. Con el índice BMWP / ECU, la calidad del agua fue "ACEPTABLE"[10].

El 94,43% de macroinvertebrados recolectados fueron colectores, 4,73% depredadores, 2,78% fijadores, 11,98% trituradores, 0,21% raspadores, 3,05% trepadores y 0,63% filtradores.

Se determinaron siete niveles tróficos, siendo el nivel de "colector" el de mayor porcentaje (94,43%) debido a la presencia de más de mil quinientos Chironomidos, como se presenta en la Figura 1.

En el análisis estadístico se realizó un ACC, donde el primer eje explicó el 82.3% de la variación y el segundo eje explico el 17.7%. En el Triplot del ACC se observa que el primer eje canónico mostró en su área positiva una gran relación entre el amonio total, DBO5, sólidos suspendidos totales, sólidos totales, turbidez y nitratos con los taxa Chironomidae, Tubificidae, Gerridae Leptoceridae Elmidae Simuliidae Philopotamidae Hydrophilidae. Por su parte el área negativa tuvo una mayor relación entre el DQO, conductividad, pH y oxígeno disuelto, los cuales estuvieron relacionados con los taxa Limnephilidae Hydraenidae Dolichopodidae Baetidae Ceratopogonidae Hyalellidae y Coenagrionidae. La relación entre los parámetros físico químicos, meses de muestreo y abundancia de individuos se observa en la Figura 2.

En el análisis Biplot basado en la descomposición de un ACP se obtuvo la relación entre los meses de muestreo con los macroinvertebrados. Siendo los meses de enero y febrero los más representativos, estos meses son más aptos para el desarrollo de la diversidad de macro bentos. Como se muestra en el componente 1 se encuentran los taxa Chironomidae, Tubificidae, Gerridae, Leptoceridae, Elmidae, Simuliidae, Philopotamidae, Hydrophilidae, Limnephilidae, Dolichopodidae, Ceratopogonidae, Hyalellidae y Coenagrionidae, siendo estos los más abundantes en los meses de enero y febrero. Mientras que en el componente 2 se encuentran los taxa Elmidae y Baetidae, siendo estos los más abundantes del mes de marzo. Figura 3.

Discusión

Los ríos con fondo arenoso carecen de gran diversidad de macroinvertebrados[11], al contrario, los fondos pedregosos y los que poseen algún tipo de vegetación tienden a tener una gran variedad de individuos, debido a que esta característica de sustrato les da a los macroinvertebrados las condiciones perfectas para su desarrollo en todo su ciclo de vida. En el estudio presentado dentro de cada una de las estaciones de muestreo se determinó dos tipos de bentos dentro del río Alambrado (arenoso y canto rodado), por lo que se observó que en determinados puntos del río la abundancia de familias no fue muy elevada, pero que en zonas pedregosas existía una gran variedad de familias y además macroinvertebrados que son considerados como indicadores de buena calidad de un cuerpo hídrico[11].

La variabilidad de los parámetros físico – químicos tienden a estar relacionados de manera directa con las diferentes condiciones meteorológicas. Los resultados presentados en este estudio nos dan a conocer que las características ambientales variaron según el mes en que se analizaron[5].

PARÁMETROS	UNIDADES	E1	E2	E3	PROMEDIO TRIMESTRAL
pH	--------	7.34	7.13	7.18	7.22
Oxígeno Disuelto	mg/L	6.48	6.00	6.40	6.29
Turbidez	NTU	19.84	18.61	18.51	18.98
Conductividad	µS/cm	247.39	200.93	129.05	192.46
Solidos Totales	g	0.07	0.23	0.04	0.11
Solidos Suspendidos Totales	g	0.16	0.07	0.06	0.09
Nitratos	NO_3	10.33	12.00	12.33	11.56
Amonio Total	NH_3	0.34	0.32	0.31	0.32
Demanda Química de Oxígeno	mg/L	36.33	36.67	34.00	35.67
Demanda Bioquímica de Oxígeno	mg/L	15.67	16.00	16.67	16.11

Tabla 2. Parámetros físico – químicos.

FAMILIA	ABUNDANCIA TRIMESTRAL	EPT	ABI	BMWP / ECU
Chironomidae	1524	0	2	3
Coenagrionidae	48	0	6	7
Turbificidae	26	0	1	1
Gerridae	1	0	5	7
Leptoceridae	1	1	8	8
Hyalellidae	228	0	6	6
Elmidae	13	0	5	7
Simuliidae	1	0	5	7
Philopotamidae	11	11	8	8
Hydrophilidae	2	0	3	4
Limnephilidae	4	4	7	9
Hydraenidae	28	0	5	9
Ceratopogonidae	8	0	4	4
Dolichopodidae	3	0	4	4
Baetidae	5	5	4	7
TOTAL	**1903**	**20**	**73**	**91**

Tabla 3. Resultado de abundancia total y índices EPT, ABI y BMWP / ECU.

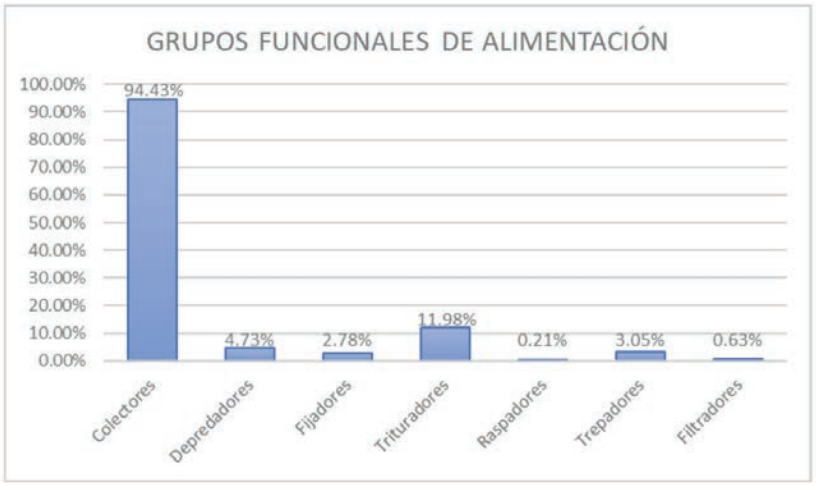

Figura 1. Grupos funcionales de alimentación y niveles tróficos.

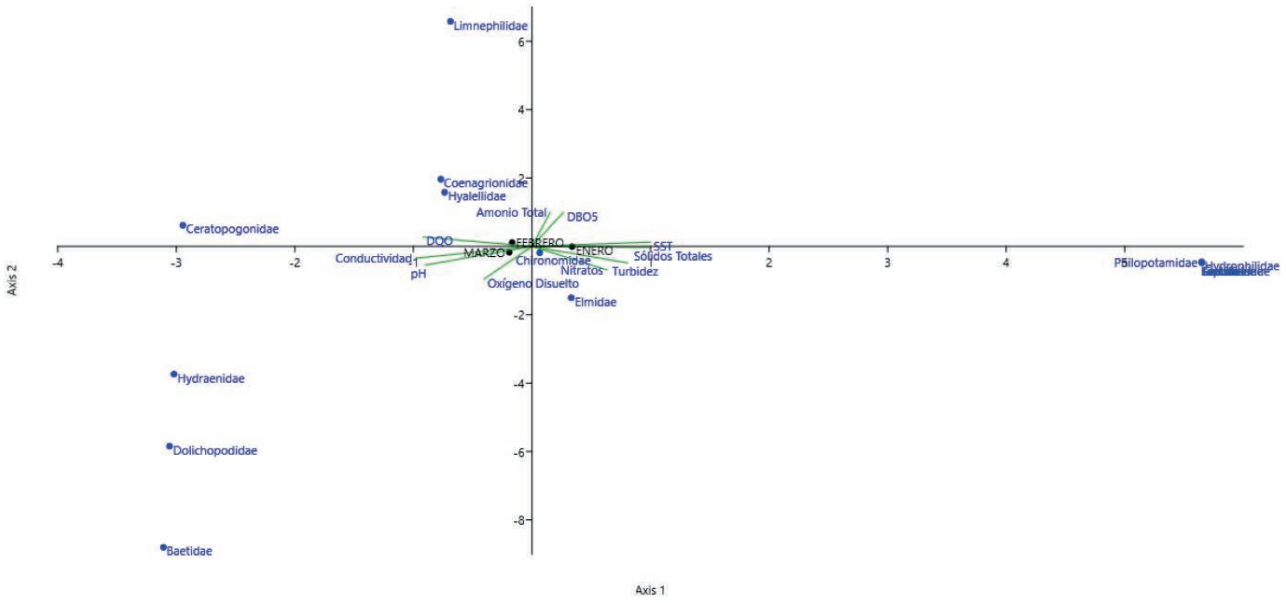

Figura 2A. Análisis de correspondencia canónica resultado trimestral.

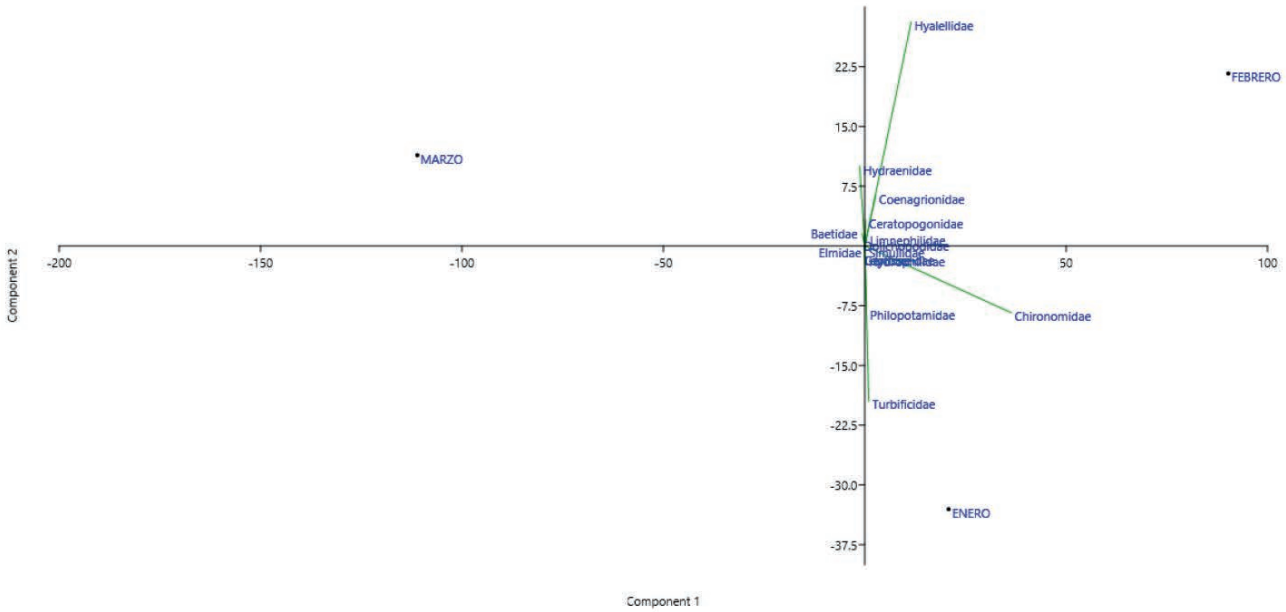

Figura 2B. Análisis de correspondencia canónica resultado trimestral.

Los parámetros físico – químicos medidos en estos tres meses se encuentran dentro de la norma planteada por la Autoridad Ambiental Ecuatoriana (Ministerio del Ambiente) con su Acuerdo Ministerial 097 – A en el Anexo 1 correspondiente a la calidad ambiental y descargas de efluentes al recurso agua. Cabe recalcar que el estudio utilizó la tabla 2 de la norma que son los criterios de calidad del agua para la preservación de la vida acuática y silvestre en aguas dulces, en aguas marinas y estuarios[9].

La carencia de familias de Ephemeropteros, Plecopteros y Trichopteros (EPT) en ríos alto andinos complica la utilización de este índice debido a que los resultados obtenidos son extremadamente bajos y estos no siempre están ligados a un impacto ambiental causado por las personas o por el medio ambiente en sí. En este estudio se observó la carencia de estos individuos pertenecientes a los órdenes de Ephemeropteros, Plecopteros y Trichopteros, por lo que da un resultado negativo de calidad del agua en el río[12].

En el análisis de los índices biológicos los resultados nos indican que el cuerpo de agua se considera con una calidad moderada; por lo tanto existe una varianza entre los resultados, por ende la principal causa que se le atribuye a éste comportamiento es a la altura, que por ser mayor de los 3.000 m.s.n.m este tipo de familias (EPT) no se desarrollan en ambientes fríos y por ende los resultados no son del todo ciertos, por lo que es recomendado utilizar otro tipo de índice que se encuentre adecuado para ecosistemas de páramo como el Índice Biótico Andino ABI o el Índice Multimétrico de Estado Ecológico de Ríos Altoandinos (IMEERA).

Como determina (6), en su estudio de calidad del agua en el río Tungurahua, dentro del Parque Nacional Cotopaxi, al ser un ecosistema de páramo similar al del estudio presentado los resultados del Índice Biótico Andino (ABI), son parecidos calificando a la calidad del agua como "MEDIA", debido a la presencia de familias que varían entre buenos y malos indicadores de calidad.

Según (13), en su proyecto de titulación "Influencia del cambio de uso del suelo sobre la fisicoquímica del agua y la composición de la comunidad de macroinvertebrados acuáticos de dos microcuencas en la zona del el Ángel, (Carchi-Ecuador)". Los resultados del Índice Multimétrico de Estado Ecológico de Ríos Altoandinos se encuentran relacionados con los resultados de esta investigación, ya que los lugares de estudio poseen características similares, debido a que ambos son ecosistemas de páramo andino y por ende las diferentes comunidades de macroinvertebrados encontradas tienden a tener las mismas características y ser parecidas casi en su totalidad, siendo diferentes únicamente por la influencia antropogénica.

En el estudio que realizó (14), dentro del río Alambrado en la Reserva Ecológica Antisana (REA), se determinaron diferentes métricas de estudio entre ellas los índices EPT, ABI y BMWP, dando como resultados que la calidad del agua del río Alambrado se encuentra calificada como "MALA", es por éste motivo que la REA se vio en la necesidad de volver a analizar estas métricas, por lo que en el estudio presentado se incorporaron diferentes índices, lo que dio a conocer que la calidad del agua dentro del río Alambrado cuatro años después se encuentra calificada como "MODERADA", pues se colectaron mayor cantidad de familias dentro del cuerpo de agua, como también macroinvertebrados calificados como buenos indicadores ambientales.

El nuevo índice para Ecuador indicó en este pilotaje que los resultados son similares en métricas de calificación de calidad de cuerpos hídricos, no obstante, existe una sensibilidad más amplia con el nuevo índice que con los otros índices biológicos, debido a que los parámetros físico-químicos en clima de páramo son variantes. Los resultados obtenidos en el mes de enero muestran una mayor sensibilidad con respecto al ABI e IMEERA, por lo que se nos presenta este nuevo índice más restrictivo con respecto a los pisos climáticos, ya que los grupos taxonómicos que se encuentran en este tipo de clima son resilientes a la contaminación y por ende van a tener mayores ponderaciones de calidad que en otros pisos climáticos.

Se determinó 1524 individuos pertenecientes al orden Díptera de la familia Chrinomidae, estos representan el 80,08% de toda la abundancia recolectada en los tres meses. La abundancia de estos tipos de macroinvertebrados según (4),es propia de los ecosistemas de páramos, debido a que estos tienden a desarrollarse de mejor manera en cuerpos hídricos andinos.

En la investigación realizada por (15) determino un biplot basado en la descomposición de ACP observando la relación existente entre los individuos recolectados y los lugares de muestreo, otorgando una mayor relación a los lugares donde obtuvieron mayor cantidad de individuos encontrados, lo que concuerda con los resultados obtenidos en esta investigación, ya que se observa una mayor relación directa con los meses que presentaron mayor abundancia. Con respecto al ACC se determinó una relación mayor en el primer eje de parámetros físico químicos con la abundancia total de taxas, de igual manera como fue planteado por Villalba se determina las variables ambientales que fueron relacionadas con las agrupaciones de individuos detectando cuales variables ambientales ayudan a un óptimo desarrollo de macrobentos y cuáles deben ser controladas para que exista una mejor calidad de agua basados en monitoreos de bioindicadores.

Conclusiones

La evaluación de la calidad del agua a través de macroinvertebrados en el río Alambrado, con los índices EPT, ABI, IMEERA y BMWP/ECU presentaron valores similares de calidad, donde se calificó al cuerpo hídrico con una calidad variante entre "MALA" y "MODERADA".

El 80,08% de los individuos recolectados pertenecieron a la familia Chironomidae, siendo esta familia la más abundante en todo el río Alambrado, este taxón se desarrolla en ecosistemas de páramo, por lo que es común encontrarlo a una altura de más de 3100 m.s.n.m. Las familias menos abundantes fueron Tubificidae, Gerridae y Elmidae 0,05%; esto se debe a que estos taxones se desarrollan en los periodos de sequía, por lo que en los periodos de transición y de lluvias fue baja la abundancia de estas familias.

La aplicación del biplot basado en la descomposición del ACP, determinó que los meses de enero y febrero fueron donde existió mayor abundancia de macroinvertebrados debido a las condiciones climáticas favorables para su desarrollo. El ACC determinó en el primer eje canónico, en su área positiva una gran relación entre el amonio total, DBO_5, sólidos suspendidos totales, sólidos totales, turbidez y nitratos con los taxa Chironomidae, Turbificidae, Gerridae Leptoceridae Elmidae Simuliidae Philopotamidae Hydrophilidae. Por su parte el área negativa tuvo una mayor relación entre el DQO, conductividad, pH y oxígeno disuelto, los cuales estuvieron relacionados con los taxa Limnephilidae Hydraenidae Dolichopodidae Baetidae Ceratopogonidae Hyalellidae y Coenagrionidae.

Referencias bibliográficas

1. Corroto F, Yalta J, Vásquez H, Gamarra O. Evaluación de la calidad ecológica del agua en la cuenca alta del río Imaza (Perú). INDES. 2014;3(2):20–9.
2. Machado V, Granda R, Endara A. Análisis de macroinvertebrados bentónicos e índices biológicos para evaluar la calidad del agua del río Sardinas, Chocó Andino ecuatoriano. Enfoque UTE. 2018;9(4):154–67.
3. Iza A. Diversidad de macroinvertebrados acuáticos y estado de conservación de la microcuenca del Río Pindo Mirador, Sector Estación Biológica "Pindo Mirador" [Internet]. Universidad UTE; 2015. Available from: http://repositorio.ute.edu.ec/bitstream/123456789/13893/1/63465_1.pdf
4. Santos M. Variabilidad de los factores físico - químicos del agua y su influencia sobre la comunidad de macroinvertebrados acuáticos en dos microcuencas del río El Ángel [Internet]. Universidad de las Américas; 2017. Available from: http://dspace.udla.edu.ec/bitstream/33000/7514/1/UDLA-EC-TIAM-2017-04.pdf
5. Villamarín C, Rieradevall M, Paul MJ, Barbour MT, Prat N. A tool to assess the ecological condition of tropical high Andean streams in Ecuador and Peru: The IMEERA index. Ecol Indic. 2013;29:79–92.
6. Ayala L. Variables hidromorfológicas y químicas en la determinación de macroinvertebrados en el río Tungurahua ubicado en el Parque Nacional Cotopaxi [Internet]. Universidad UTE; 2017. Available from: http://repositorio.ute.edu.ec/bitstream/123456789/14006/1/69894_1.Tesis_Ayala.pdf
7. Sánchez G, Gómez B, Delgado L, Rodrígez E, Chame E. Diversidad de escarabajos copronecrófagos (Coleoptera: Scarabaeidae: Scarabaeinae) en la Reserva de la Biosfera Selva El Ocote, Chiapas, México. Caldasia [Internet]. 2018;40(1):144–60. Available from: https://www.jstor.org/stable/90022795?seq=1#page_scan_tab_contents
8. Forero-Cespedes A, Reinoso-Flores G. Evaluación de la calidad del agua del río Opia (Tolima-Colombia) mediante macroinvertebrados acuáticos y parámetros fisicoquímicos. Caldasia [Internet]. 2013;35(2):371–87. Available from: www.jstor.org/stable/90008350
9. MAE. Acuerdo Ministerial 097 - A. Quito - Ecuador: Ministerio del Ambiente; 2015.
10. García CA. Evaluación de la calidad del agua en el río Alambrado, utilizando macroinvertebrados bentónicos como bioindicadores ambientales, dentro de la zona de influencia del Embalse de la Laguna de la Mica. Universidad UTE; 2019.
11. Roldán G. Bioindicación de la calidad del agua en Colombia: propuesta para el uso del método BMWP Col. 1st ed. Medellin - Colombia: Universdiad de Antioquia; 2003.
12. Hotaling S, Finn DS, Giersch J, Weisrock DW, Jacobsen D. Climate change and alpine stream biology: progress, challenges, and opportunities for the future. Biol Rev. 2017;92(4):2024–45.
13. Montalvo P. Influencia del cambio de uso del suelo sobre la fisicoquímica del agua y la composición de la comunidad de macroinvertebrados acuáticos de dos microcuencas en la zona del el Ángel, (Carchi-Ecuador). [Internet]. Universidad de las Américas; 2017. Available from: http://dspace.udla.edu.ec/bitstream/33000/7514/1/UDLA-EC-TIAM-2017-04.pdf
14. Cordero P. Calidad del agua para los ríos alto andinos, mediante indicadores biológicos [Internet]. Pontificia Universidad Católica del Ecuador; 2015. Available from: http://repositorio.puce.edu.ec/bitstream/handle/22000/8746/Calidad del agua para los ríos alto andinos%2C mediante indicadores biológicos. Pablo Cordero.pdf?sequence=1&isAllowed=y
15. Cerón-Vivas A, Gamarra Y, Villamizar M, Restrepo R, Arena R. Calidad de agua de la quebrada Mamarramos. Santuario de Flora y Fauna Iguaque, Colombia. Tecnol y ciencias del agua [Internet]. 2019;10(6):90–116. Available from: http://www.revistatyca.org.mx/ojs/index.php/tyca/article/view/1443/1652

Received: 4 mayo 2020
Accepted: 20 Agosto 2020

RESEARCH / INVESTIGACIÓN

Phytochemical screening and *in vitro* anti-inflammatory activity of ethanolic extract of *Epidendrum coryophorum* leaves

Irina Francesca González Mera[1], Orestes Darío López Hernández[2] and Vivian Morera Córdova[1*]
DOI. 10.21931/RB/2020.05.04.18

Abstract: *Epidendrum coryophorum* belongs to the Orchidaceae family. Traditional uses of some species for this genus include infusions of the leaves used for kidney problems, treat influenza, conjunctivitis, liver pain, relieve kidney symptoms, and hypoglycemic effect. This work's objective was to determine the phytochemical profile of the ethanolic extract of *Epidendrum coryophorum* leaves and to evaluate the potential anti-inflammatory activity *in vitro* of the extract employing the erythrocyte membrane stabilization method. The phytochemical screening carried out in this work suggested phenols, coumarins, flavonoids, tannins, steroids, and sterols in the ethanolic extract of *Epidendrum coryophorum* leaves. Cardiotonic glycosides and carbohydrates were also found. The ethanolic extract's UV-Vis spectrum showed absorption maxima at 268 nm and 332 nm, which could correspond to flavonoids of the flavonoid classes, 3-OH substituted flavonols, or isoflavones. The quantitative determination of total phenols of the ethanolic extract was carried out using the Folin-Ciocalteu method. The total phenolic content expressed as mg Gallic acid equivalent (G.A.E.) per gram of extract was found to be 19,96 mgGAE/g of *Epidendrum coryophorum*. The ethanolic extract of *Epidendrum coryophorum* leaves showed hemolysis inhibition values of 18,19% at 1,0 mg/mL, 38,98% at 1,5 mg/mL and 40,94% at 2,5 mg/mL compared with aspirin (positive control) giving values of 65,33% at 1,0 mg/mL, 72,26% at 1,5 mg/mL and 73,75% at 2,5 mg/mL. The values obtained for inhibition of hemolysis with ethanolic extract, compared with the values obtained with a pure anti-inflammatory, are significant and demonstrate anti-inflammatory activity in *Epidendrum coryophorum*.

Key words: *Epidendrum coryophorum*, total phenolic content, microencapsulation, anti-inflammatory activity.

Introduction

Inflammation is a body's normal physiological response when it tries to protect itself from cellular damage caused by pathogens, irritants, or physical damage. The inflammation function is to remove damaged and necrotic tissues generated by the causative agent and initiate tissue repair. A not adequately cured inflammation is the basis of hypersensitivity reactions and chronic diseases[1]. Current treatments to alleviate the symptoms of acute and chronic inflammation cause adverse effects, and in many cases, the treatments have low effectiveness[2]. An alternative may be to develop drugs based on plants that have been used in traditional medicine for many years. The analysis of natural products through biochemical, phytochemical, and pharmacological studies has allowed the identification and characterization of various active compounds capable of counteracting the effects of inflammation, including phenolic compounds[3-5].

The orchids, besides being used as ornamentals and food, are also used for medicinal purposes. The orchid's extracts are prepared from different parts of the plant. It could be tubers, leaves, rhizomes, stems, pseudobulbs, roots, flowers, sheaths, bulbs, and in some cases, the whole plant. They are prepared as an infusion, decoction, dried and ground, paste, Yin tonic, tincture, and juice[6,7]. These extracts are used as diuretics, antirheumatics, anticancer, hypoglycemic, anti-aging, antimicrobial, anticonvulsants, antivirals, and anti-inflammatories[8-13]. The genus Epidendrum (Orchidaceae) is found in the Andes, represented by 360 species, of which 178 are native species to the Andean forest[14,15]. Traditional uses of some species for this genus include infusions of the leaves for kidney problems, treat influenza, conjunctivitis, and hepatic pain; other authors report the use of orchids of this genus with hypoglycemic effect and to alleviate renal symptoms[16,17]. Despite the broad representation of genus Epidendrum in the Ecuadorian Andes and the wide use of orchids for medicinal purposes in many regions of the world, there are only a few scientific publications concerning the chemical composition and pharmacological properties of this genus. Regarding *Epidendrum coryophorum*, there are no scientific reports at all on this species.

There are different and varied methods to evaluate anti-inflammatory activity. These methods are classified as in vivo (if using animal models) or *in vitro* (when performed in a controlled environment outside of a living organism). Each of these methods is associated with some peculiarities, advantages, and disadvantages[18]. Although the *in vivo* models correlate well with the clinical picture and help understand the mechanisms of inflammation better, they are more complex and expensive. Among the *in vitro* methods, the method based on the stabilization of the erythrocyte membrane has gained wide popularity among researchers since it is based on the similarity of the erythrocyte membrane with the lysosomal membrane and its stabilization by the secondary metabolites of the plant extract is considered a good experimental indicator of the anti-inflammatory activity of secondary metabolites; additionally, it is a relatively simple method and is inexpensive.

This work's objective was to determine the phytochemical profile of the ethanolic extract of *Epidendrum coryophorum* leaves and to evaluate the potential anti-inflammatory activity *in vitro* of the extract employing the erythrocyte membrane stabilization method.

[1] Yachay Experimental Technology Research University, School of Chemical Sciences and Engineering, San Miguel de Urcuquí, Imbabura, Ecuador.
[2] Technical University of Ambato, Faculty of Food Science and Engineering, Biochemical Engineering Career, Ambato, Ecuador.

Corresponding author: vmorera@yachaytech.edu.ec

Materials and methods

Leaves preparation

The *Epidendrum coryophorum* specimens were acquired at Ecuadorian company Ecuagenera, Guayaquil (http://www.ecuagenera.com). The plants were kept in pots until the leaves were separated for processing. Using a scalpel, leaves were cut from the base of the plant. Then, leaves were washed separately with common water followed with distilled water to remove dust and particles. Subsequently, the leave was drained and dried in the shade at 25°C. The dried tissues were pulverized using an electric grinder and stored at -20°C until they were used[19].

Organic extraction

For the extraction of Epidendrum coryophorum leaves' phytochemicals, the solid-liquid extraction process was used with 70% ethanol as solvent[20]. The ratio of dry tissue powder and the organic solvent was 1:10 (w:v). Extraction was allowed to proceed for 48 hours with occasional manual stirring. Finally, the amber bottle with ground tissue, and the solvent was ultrasound for 1 hour at 25 °C. The solvent was filtered through filter paper with the vacuum's help, and the extract was stored in a new clean amber bottle, protected from light at 4 °C until use.

Phytochemical screening

Once the ethanolic extract from dried leaves was obtained, the preliminary phytochemical analysis applied simple, rapid, and selective phytochemical screening assays targeting the qualitative detection of secondary metabolites[21,22].

UV-Vis analysis

The ethanolic extract was diluted to 1:20 (v:v) with the same solvent. The spectrum was registered from 200 nm to 800 nm using a UV-VIS NIR Lambda 1050 spectrophotometer.

Total phenolic content

To determine the total phenolic content (TPC) in ethanolic extract of *Epidendrum coryophorum* leaves, a dilution of 1:10 (v:v) in distilled water was made. TPC was determined by Folin-Ciocalteu spectrophotometric method[23]. Gallic acid was used as reference material in concentrations of 0,02 mg/mL, 0,04 mg/mL, 0,06 mg/mL, 0,08 mg/mL, 0,10 mg/mL, 0,12 mg/mL, 0,14 mg/mL, 0,20 mg/mL and 0,30 mg/mL. The solutions were kept protected from light. For standard solutions and ethanolic extract, to 300 µL of the solution was added 150 µL of 10% Folin-Ciocalteau reagent, then the mixture was let to react for 3 minutes at room temperature. Next to each tube, 120 µL of 7,5% sodium carbonate was added and let them rest for 30 minutes in a dark place. At the end of the reaction, the absorbance was measured at 765 nm using a UV-VIS NIR Lambda 1050 spectrophotometer. The absorbance's values were extrapolated in the standard calibration curve. The results were expressed as mg in equivalents of Gallic acid (G.A.E.) per grams of dry material. The determination was performed in triplicate, and the results were expressed as mean ± S.D.

Microencapsulation

The extract was concentrated in a rotary evaporator at 30 °C, which allowed the ethanol's distillation from the mixture. Then, the concentrated extract was weighed, labeled, and stored in an Eppendorf tube at 4 °C, avoiding the metabolites' degradation. Then, the extract was first dissolved in Sacha inchi oil until most of the extract homogenize in the oil. So, for the microencapsulated extract matrix, it was used maltodextrin, Arabic gum, and water in a proportion of 30:30:30 (v:v:v). The mixture was homogenized using an Ultra turrax Pt25 I.K.A. at 25,000 rpm for 1 minute. For the microencapsulation, the Mini Spray Dryer Buchi B290 was used, which was fed with the respective combination, once the equipment conditions were verified to be adequate (-50 mbar, 150 °C inlet and 90 °C outlet)[24]. Microencapsulated extract was dissolved in PBS to reach concentrations of 1,0 mg/mL, 1,5 mg/mL, and 2,5 mg/mL.

Anti-inflammatory activity

Preparation of blood samples

The human red blood cell membrane stabilization method was used to study *in vitro* anti-inflammatory activity[25]. The human blood was obtained from two healthy volunteers who did not have used anti-inflammatory medications for at least a week and counted with a medical certificate to corroborate the health status. 3 mL of human blood was transferred to a conical tube and centrifuged for 10 min at 3000 rpm. The supernatant was taken out, and an equivalent volume of PBS was placed on the test tube to realize three consecutive washes to the erythrocyte suspension. After each extraction of plasma and the addition of PBS, the sample was centrifuged. 800 µL of the erythrocyte suspension was mixed with 1200 µL of PBS to form a suspension of 40% v/v in PBS.

Inhibition of heat-induced hemolysis

In 25 mL conical tubes were added 3 mL of the evaluated samples and 30 µL of 40% erythrocyte's suspension. The negative control was prepared using the same quantity of PBS instead of the sample. The microencapsulated extract and the commercial aspirin (positive control, from Sigma-Aldrich, USA) were evaluated at concentrations of 1,0 mg/mL, 1,5 mg/mL, and 2,5 mg/mL. All reaction mixtures were prepared in triplicates except the negative control. One conical tube of each reaction mixture was incubated for 20 min at 54 °C, and the other was left at room temperature. The negative control was incubated too. After 20 min of incubation, all test tubes were centrifuged at 3000 rpm for 10 min. The absorbance of supernatants was measured at λ = 560 nm[25]. The percentage of hemolysis inhibition was calculated according to the following expression:

$$\%\ hemolysis\ inhibition = \left[1 - \frac{A_I - A_{WI}}{A_{NC} - A_{WI}}\right] \times 100$$

Where: $A_{I.}$ represents the absorbance of the sample with incubation, $A_{W.I.}$ represents absorbance of the sample without incubation, and $A_{N.C.}$ represents the absorbance of the negative control.

Statistical analysis

Statistical analysis was performed by calculating the mean and standard deviation of the percentages of hemolysis inhibition for the extract's three concentrations. The used program was STATGRAPHICS Centurion XV, Version 15.2.05. The data were processed through a one-way analysis of variance (ANOVA), and subsequently, Duncan's test was performed, considering significant differences of at least $p < 0.05$.

Results and Discussion

The phytochemicals produced by plants have useful pharmacological activities for treating various diseases, including those that occur with inflammation. There are numerous studies and reviews on plants containing phytochemicals, specifically flavonoids, triterpenes, tannins, phenolic compounds, coumarins, and steroids; anti-inflammatory activity has been attributed[26-33]. However, very little has been investigated about these phytochemicals and their possible anti-inflammatory activity, especially in Epidendrum (Orchidaceae). In the ethanolic extract of *Epidendrum coryophroun* leaves, we found that phenols, coumarins, flavonoids, tannins, and anti-inflammatory activity were demonstrated. This work constitutes the first report on the phytochemical screening and anti-inflammatory activity of *Epidendrum coryophorum*.

Phytochemical screening

Phytochemical screening is one of the initial stages of phytochemical research, which allows the to determining qualitatively the main chemical groups present in the plant and guide the extraction and/or fractionation of the extracts, isolation and characterization of specific metabolites[34]. The phytochemical screening carried out in this work suggested phenols, coumarins, flavonoids, tannins, steroids and sterols in the ethanolic extract of *Epidendrum coryophorum* leaves. There were also found cardiotonic glycosides and carbohydrates. Anthocyanins, anthraquinones, flobatanins, saponins, proteins and free amino acids were not detected (Table 1). The presence of secondary metabolites in a given extract depends on the used solvent. For a solute (secondary metabolite) to be dissolved in a solvent, it is necessary that the solvent disaggregate the molecules and thus facilitate their solvation; this process depends on both the dielectric constant of the solvent and the solute's (secondary metabolites) and solvent's polarity. Generally, in ethanolic extracts, tannins, phenols, flavanols, terpenoids, sterols and alkaloids have been detected[35], which coincides with the type of metabolites detected in the ethanolic extract of *Epidendrum coryophorum* leaves (Table 1).

The phytochemical screening of ethanolic extract of *Epidenddrum coryophorum* leaves constitutes the first report on the presence of specific secondary metabolites in this species. However, phytochemical screening of other species belonging to the genus Epidendrum has been performed before. Cerna *et al.* evaluated the phytochemical content of ethanolic extracts of the species *Epidendrum blepharoclinium*, *Epidendrum blepharoclinium*, *Epidendrum cochlidium sp1*, *Epidendrum cochlidium sp2*, *Epidendrum jamiesonis*, *Epidendrum medusae*, *Epidendrum nocturnum*, *Epidendrum paniculatum*, *Epidendrum porphyreum*, *Epidendrum secundum*, *Epidendrum secundum*. Even though these authors' extraction conditions are not identical to those used in our work, they also found flavonoids in 5 species, saponins in 11 species, and tannins in 7 of the 11 studied[36].

UV-Vis analysis

UV-Vis spectroscopy is a technique that allows the detection of compounds in which can occur electronic transitions of the type π → π * and n → π * as a result of interaction with light in the ultraviolet and visible regions of the electromagnetic spectrum. The absorption maxima can be correlated with compounds containing π bonds and lone pairs of electrons[37]. In the UV-Vis spectrum of ethanolic extract of *Epidendrum coryophorum* leaves, the absorption maxima were recorded at 268 nm, 332 nm, 410 nm, 468 nm, 504 nm, 536 nm, 606 nm, and 664 nm. Of these maxima, the most intensive peaks (Peak 1-268 nm and Peak 2-332 nm, Figure 1A) could correspond to flavonoids of flavone, flavonols 3-OH substituted, or isoflavones classes. Flavonoids are natural pigments, especially abundant in plants' leaves, and their primary function is

	Secondary metabolites	Reaction	Results
Phenols	Phenols	Ferric chloride test	+
	Anthocyanin	a)	-
	Coumarins	b)	+
	Flavonoids	Ammonium test	+
	Tannins	Modified Braemer´s test	+
	Anthraquinones	Bornstrager´s test	-
	Flobatanins	Hydrochloric acid test	-
Terpenes	Terpenoids	Salkowski test	-
	Saponins	Froth test	-
	Steroids and sterols	Modified Lieberman – Burchardt test	+
Others	Cardiotonic glycosides	Modified Kellar – Kiliani test	+
	Proteins and amino acids	Ninhydrin test	-
	Carbohydrates	Benedict´s test	+
	Reducing sugars	Fehling´s test	-

a) 1,0 mL of ethanolic extract was mixed with 3,0 mL of water. Subsequently, 1,0 mL of 2 mol/L HCl and 1,0 mL of 0,5 mol/L ammonia were added. The appearance of red-pink color that turns blue-violet could indicate the presence of anthocyanins.
b) 1,0 mL of ethanolic extract was mixed with 1,0 mL of 10.0% NaOH. The formation of a yellow coloration could indicate the presence of coumarins in the extract.
(+) indicates the presence of the evaluated secondary metabolite
(-) indicates its absence.

Table 1. Secondary metabolites tested and detected by chemical reactions in the ethanolic extract of *Epidendrum coryophorum* leaves.

A

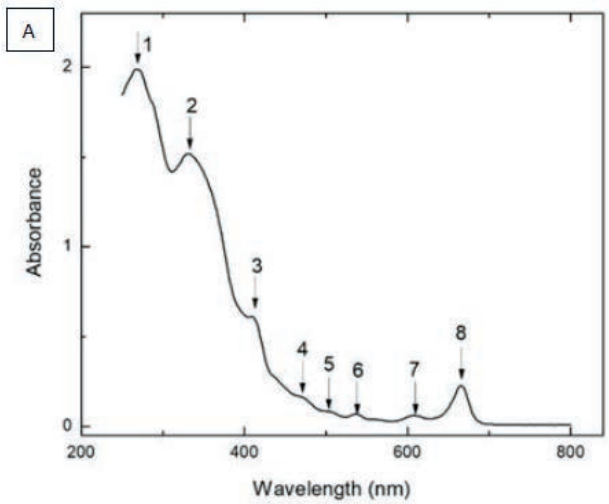

B

Peak number (λ max)	Flavonoid class	Typical range	
		Band II (λ max)	Band I (λ max)
1 (268 nm)	Flavone	250-280 (nm)	310-350 (nm)
2 (332 nm)	Flavonol 3-OH substituted	250-280 (nm)	330-360 (nm)
	Isoflavone	245-275 (nm)	310-330 (nm)

Figure 1. UV-Vis analysis of an ethanolic extract of *Epidendrum coryophorum* leaves. A: in the spectrum, the observed absorption maxima are indicated with arrows and numbers. B: correlation between the wavelengths of observed absorption maxima in the spectrum and typical ranges of absorption maxima wavelengths for some flavonoid classes.

to protect them from ultraviolet rays. The flavonoids have in their structure a standard diphenylpyran skeleton (C6-C3-C6), composed of two phenyl rings (A and B) linked through a pyran C ring (heterocyclic). This basic structure allows for a multitude of substitution patterns and variations in the C ring[38]. UV-Vis spectroscopy is a useful technique in the differentiation of flavonoids since the bands' position in the UV-Vis spectrum depends on the extent of conjugation and, therefore, on the nature of the C ring and the position of the phenyl group called ring B (C-2, C-3 or C-4 substituent). For these compounds, the UV-Vis spectrum presents two absorption maxima in the ranges from 310 to 360 nm and from 245 to 280 nm corresponding to bands I and II of rings B and A, respectively, according to the class of flavonoids (Figure 1B)[39].

Total phenolic content

Considering that several secondary metabolites were detected in the extract of Epidendrum coryophorum leaves classified as phenolic compounds[40], the TPC was determined using the Folin-Ciocalteu method as previously described. The value was calculated using a calibration curve with Gallic acid, whose equation resulted in $y = 8.8282x + 0.0328$ with $R^2 = 0.9987$. The TPC in the ethanolic extract was 19.96 mgGAE/g of *Epidendrum coryophorum* (Table 2). Values of TPC of *Epidendrum coryophorum* have not been reported before in the literature or other genus Epidendrum species.

Anti-inflammatory activity

The erythrocyte membrane stabilization test in the presence of microencapsulated ethanolic extract in an isotonic medium was positive and showed concentration-dependent anti-inflammatory activity. An increase in the percentage of hemolysis inhibition was observed as the amount of microencapsulated extract increased. The microcapsules of ethanolic extract of *Epidendrum coryophorum* leaves gave values of hemolysis inhibition of 18,19% at 1,0 mg/mL, 38,98% at 1,5 mg/mL, and 40,94% at 2,5 mg/mL in comparison with aspirin (positive control) giving values of 65,33% at 1,0 mg/mL, 72,26% at 1,5 mg/mL, and 73,75% at 2,5 mg/mL (Table 3). The results were statistically evaluated using the statistical method of ANOVA and presented statistical significance; that is, the treatments used were significantly different ($p < 0.05$). Therefore, the data were analyzed using Duncan's Test, with which we were able to corroborate the obtained results. The concentration of 1,00 mg/mL of the extract showed a significant difference concerning the concentrations of 1,5 mg/mL and 2,5 mg/mL of the extract itself and a lower percentage of hemolysis inhibition. However, the concentrations of 1,5 and 2,5 mg/mL of extract did not present significant differences between them and presented similar values of percentage of hemolysis inhibition. Similar behavior occurred in the case of aspirin (Figure 2). The erythrocyte membrane stabilization test is considered as an *in vitro* measure of the anti-inflammatory activity of drugs or extracts of plants[41]. The erythrocyte membrane is very similar to the membrane lysosomal so the effect of drugs on the stabilization of the erythrocyte membrane could be extrapolated to the stabilization of the lysosomal membrane; its stability is crucial since it can limit the inflammatory response, inhibiting the release of inflammation mediators as proteases and bactericidal enzymes[42].

Additionally, this test is a convenient, rapid, and inexpensive method to be applied for preliminary investigations on the anti-inflammatory activity of crude extracts of plants. Numerous investigations associate the presence of phenolic compounds in plants with the anti-inflammatory activity evaluated by this method[43]. Thus, we could assume that the observed anti-inflammatory activity can result from certain phenols' individual action in the extrac or of synergy between them[44]. Considering the coarse texture of the ethanolic extract after drying and to ensure the bioavailability of its active principles

Absorbance 1	mgGAE/gEc	Absorbance 2	mgGAE/gEc	Absorbance 3	mgGAE/gEc	Average	SD
0,620	22,17	0,525	18,58	0,539	19,11	19,96	1,94

The extract was analyzed by triplicate
GAE: Gallic acid equivalent
Ec: *Epidendrum coryophorum*
SD: standard deviation

Table 2. Total phenolic content of ethanolic extract from *Epidendrum coryophorum* leaves.

Concentrations of microencapsulated ethanolic extract	% of hemolysis inhibition	% of hemolysis inhibition	% of hemolysis inhibition	Average	SD
1,0 mg/mL	20,92	17,86	15,79	18,19	2,58
1,5 mg/mL	40,45	37,78	38,70	38,98	1,36
2,5 mg/mL	35,17	44,09	43,56	40,94	5,00
Concentrations of commercial aspirin					
1,0 mg/mL	65,70	66,50	63,78	65,33	1,40
1,5 mg/mL	73,76	73,40	69,61	72,26	2,30
2,5 mg/mL	75,13	73,42	72,71	73,75	1,24

SD: standard deviation

Table 3. Percentage of inhibition of hemolysis of the erythrocyte membrane for the three tested extract and control drug concentrations.

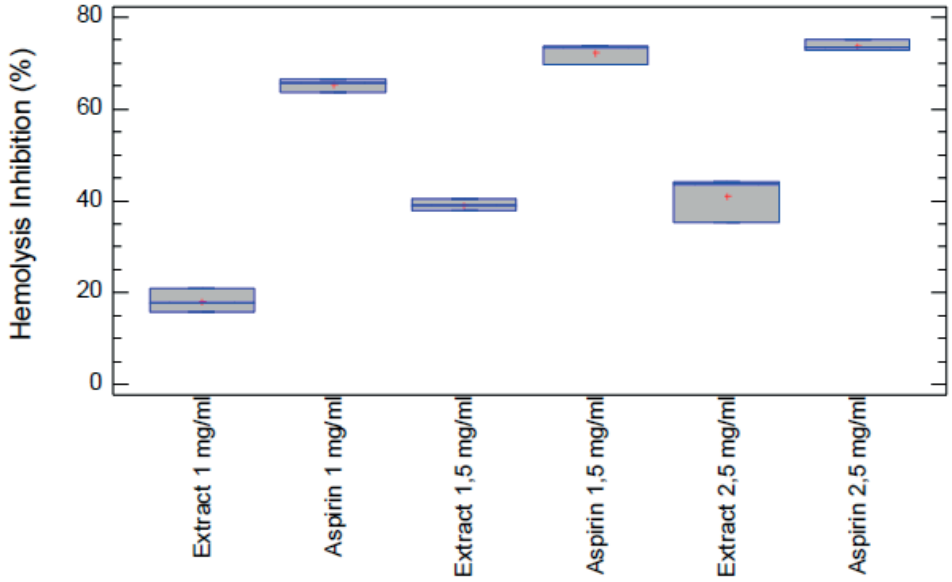

Figure 2. Percentages of hemolysis inhibition of the ethanolic extract of *Epidendrum coryophorum* leaves. Commercial aspirin was used as a positive control.
$p < 0.05$ was considered statistically significant in all analyses.

during the hemolysis inhibition test, it was microencapsulated using natural water-soluble polymers. During the microencapsulation procedure of the ethanolic extract of *Epidendrum coryophorum* leaves, the homogenization step is essential for forming the emulsion. This guarantees the formation of microcapsules with a polynuclear internal structure, which allows the dispersion of the microcapsules in water, forming a nanoemulsion on contact with the environment in which the cells are found and better dispersion of the active principles in the medium[45].

Conclusions

The phytochemical screening carried out in this investigation suggested the presence of phenols, coumarins, flavonoids, and tannins in the ethanolic extract of *Epidendrum coryophorum* leaves. The ethanolic extract's UV-Vis spectrum showed absorption maxima at 268 nm and 332 nm, which could correspond to flavonoids of the flavonoid classes, 3-OH substituted flavonols, or isoflavones. The ethanolic extract of *Epidendrum coryophorum* leaves contains phenolic compounds. The total phenolic content was found to be 19.96 mgGAE/g of *Epidendrum coryophorum*. The extract showed an erythrocyte membrane stabilization effect. The values obtained of hemolysis inhibition with ethanolic extract (crude extract) in comparison with those values obtained with a pure anti-inflammatory drug are significant and demonstrate anti-inflammatory activity in *Epydendrum coryophorum*. However, it should be mentioned that this study constitutes a preliminary study on the anti-inflammatory effect of this extract; therefore, it is suggested to expand the study of the anti-inflammatory effect using other methods and to consider the use of experimental animal models.

Acknowledgments

This research did not receive any specific grant from funding agencies in the public, commercial, or not-for-profit sectors.

Competing interest

The authors have no competing interests.

Bibliographic references

1. Cronkite D.A. and Strutt T.M. (2018) The Regulation of Inflammation by Innate and Adaptive Lymphocytes. Journal of Immunology Research, vol. 2018, Article ID 1467538, 14 pages, 2018. https://doi.org/10.1155/2018/1467538.
2. Recio M.C., Andujar I. and Rios, J.L. (2012) Antiinflammatory Agents from Plants: Progress and Potential. Current Medicinal Chemistry 19: 2088–2103. https://doi.org/10.2174/092986712800229069.
3. Maione F., Russo R., Khan H. and Mascolo, N. (2016). Medicinal plants with anti-inflammatory activities. Natural Product Research 30: 1343–1352. https://doi.org/10.1080/14786419.2015.1062761.
4. Duangjai Tungmunnithum, Areeya Thongboonyou, Apinan Pholboon and Aujana Yangsabai (2018) Flavonoids and Other Phenolic Compounds from Medicinal Plants for Pharmaceutical and Medical Aspects: An Overview. Medicines 5: 93-108. doi: 10.3390/medicines5030093.
5. Middleton E. and Kandaswami C. (1992) Effects of flavonoids on immune and inflammatory cell functions. Biochem. Pharmacol. 43: 1167–1179. doi: 10.1016/0006-2952(92)90489-6.
6. Gutiérrez R.M.P. (2010) Orchids: A review of uses in traditional medicine, its phytochemistry and pharmacology. Journal of Medicinal Plants Research 4: 592-638. DOI: 10.5897/JMPR10.012.
7. Vibha S., Hebbar Sushmitha S, Mahalakshmi, S.N. and Prashith Kekuda, T.R. (2019) A comprehensive review on ethnobotanical applications and pharmacological activities of Acampe praemorsa (Roxb.) Blatt. & McCann (Orchidaceae). Journal of Drug Delivery & Therapeutics 9: 331-336. DOI: http://dx.doi.org/10.22270/jddt.v9i1.2224.
8. Mamta Arora, Anupama Mahajan and Jaspreet K. Sembi (2017) A REVIEW ON PHYTOCHEMICAL AND PHARMACOLOGICAL POTENTIAL OF FAMILY ORCHIDACEAE. International Research Journal of Pharmacy 8: 9 – 24. DOI: 10.7897/2230-8407.0810176.
9. Arora M., Mahaian A. and Sembi, J.K. (2017) A review on phytochemical and pharmacological potential of family Orchidaceae. International Research Journal of Pharmacy 8: 9-24. DOI: 10.7897/2230-8407.0810176.
10. Attri L.K. (2016) Therapeutic potential of orchids. World Journal of Pharmaceutical Sciences 5: 438-446. DOI: https://doi.org/10.22270/jddt.v9i1.2224.
11. Chinsamy M., Finnie J.F. and Van Staden J. (2014) Anti-inflammatory, antioxidant, anti-cholinesterase activity and mutagenicity of South African medicinal orchids. South African Journal of Botany 91: 88–98. DOI: 10.1016/j.sajb.2013.12.004.
12. Mohammad M.H. (2011) Therapeutic orchids: traditional uses and recent advances — An overview. Fitoterapia 82: 102–140. DOI: 10.1016/j.fitote.2010.09.007.
13. Hossain M.M. (2011) Therapeutic orchids: traditional uses and recent advances - An overview. Fitoterapia 82:102-140. DOI: 10.1016/j.fitote.2010.09.007.
14. Jørgensen P.M. and León-Yánez S. (1999) Catalogue of the vascular plants of Ecuador. Monographs in Systematic Botany from the Missouri Botanical Garden 75: i-viii, 1-1182.
15. Endara L., Williams N. and León-Yánez S. (2009) Patrones de endemismo de orquídeas endémicas ecuatorianas: perspectivas y prioridades para la conservación. In: Pridgeon A M, Suarez JP (eds) Proceedings of the Second Scientific Conference on Andean Orchids. Universidad Técnica Particular de Loja, Loja, Ecuador, pp 63-70. https://doi.org/10.1117/12.2028244.
16. Tene V., Malagon O., Finzi P.V., Vidari G., Armijos Ch. and Zaragoza T. (2007) An ethnobotanical survey of medicinal plants used in Loja and Zamora-Chinchipe, Ecuador. Journal of Ethnopharmacology 111: 63–81. doi: 10.1016/j.jep.2006.10.032.
17. Novaes A.P., Rossi C., Poffo C., Junior E.P., Oliveira A.P., Schlemper V., Niero R., Cechinel-Filho V. and Burger C. (2001) Preliminary evaluation of the hypoglycemic effect of some Brazilian medicinal plants. Therapie. 56: 427β 430.
18. Ifeanyi F.E., Philip F.U., Ikechukwu P., Bonaventure C.O. and Osadebe P.O. (2019) In vitro and In vivo Models for Anti-inflammation: An Evaluative Review. INNOSC Theranostics and Pharmacological Sciences 2: 3-15. DOI: 10.36922/itps.v2i2.775.
19. Jhansi K., Venkatesh R. and Khasim, S.M. (2019) A Study on Phytochemical and Anticancer Activitiesvof Epiphytic Orchid Aerides odorata Lour. European Journal of Medicinal Plants 28: 1-21. https://doi.org/10.9734/ejmp/2019/v28i330135.
20. Belwal T., Dhyani P., Bhatt I.D., Rawal R.S. and Pande V. (2016) Optimization extraction conditions for improving phenolic content and antioxidant activity in Berberis asiatica fruits using response surface methodology (R.S. M). Food Chem. 207: 115–124. DOI: 10.1016/j.foodchem.2016.03.081.
21. Trease G. E. and Evans W. C. (1989) Trease and Evan's Textbook of Pharmacognosy. 13th Edition. Cambridge University Press, London. 546.
22. Behrooz Alizadeh Behbahani, Fakhri Shahidi, Farideh Tabatabaei Yazdi, Seyed Ali Mortazavi and Mohebbat Mohebbi. (2017) Antioxidant activity and antimicrobial effect of tarragon (Artemisia dracunculus) extract and chemical composition of its essential oil. Food Measure 11: 847–863. https://doi.org/10.1007/s11694-016-9456-3.
23. Shanaida M., Golembiovska O., Hudz N. and Wieczorek PP (2018) Phenolic compounds of herbal infusions obtained from some species of the Lamiaceae family. Current Issues in Pharmacy and Medical Sciences 31: 194–199. https://doi.org/10.1515/cipms-2018-0036.
24. Jyothi N.V.N., Prasanna P.M., Sakarkar S.N., Prabha K.S., Ramaiah P.S. and Srawan G.Y. (2010) Microencapsulation Techniques. Factors Influencing Encapsulation Efficiency. J. Microencapsul. 27: 187–197. https://doi.org/10.3109/02652040903131301.
25. Anosike C.A., Obidoa O. and Ezeanyika L.U. (2012) Membrane Stabilization as a Mechanism of the Anti-inflammatory Activity of Methanol Extract of Garden Egg (Solanum Aethiopicum). DARU, J. Pharm. Sci. 20: 1–7. https://doi.org/10.1186/2008-2231-20-76.
26. Adebayo S.A., Dzoyem J.P., Shai L.J. and Eloff J.N. (2015) The anti-inflammatory and antioxidant activity of 25 plant species used traditionally to treat pain in southern African. B.M.C. Complement Altern Med. 15: 159. doi: 10.1186/s12906-015-0669-5.
27. Adebayo S.A., Dzoyem J.P., Shai L.J. and Jacobus N.E. (2015) The anti-inflammatory and antioxidant activity of 25 plant species used traditionally to treat pain in southern African. B.M.C. Complement Altern Med 15: 159. https://doi.org/10.1186/s12906-015-0669-5.
28. Sowjanya R., Shankar M., Sireesha B., Naik A.E., Yudharaj P. and Priyadarshini R.R. (2017) An overview on inflammation and plant havinganti inflammatory activity. International journal of phytopharmacy research 7: 25-32. http://dx.doi.org/10.22270/jddt.v9i3.2906.
29. Lock O., Perez E., Villar M., Flores D. and Rojas R. (2016) Bioactive Compounds from Plants Used in Peruvian Traditional Medicine. Nat Prod Commun. 11: 315–37.
30. Sobeh M., El-Raey M., Rezq S., Abdelfattah M.A.O., Petruk G., Osman S., El-Shazly A.M., El-Beshbishy H.A., Mahmoud M.F. and Wink M. (2019) Chemical profiling of secondary metabolites of Eugenia uniflora and their antioxidant, anti-inflammatory, pain killing and anti-diabetic activities: A comprehensive approach. J Ethnopharmacol. 240: 111939. doi: 10.1016/j.jep.2019.111939.
31. Falcão T.R., de Araújo A.A., Soares L.A.L., de Moraes Ramos R.T., Bezerra I.C.F., Ferreira M.R.A., de Souza Neto M.A., Melo M.C.N., de Araújo R.F. and de Aguiar Guerra, A.C.V. (2018) Crude extract and fractions from Eugenia uniflora Linn leaves showed anti-inflammatory, antioxidant, and antibacterial activities. BMC Complement Altern. Med. 18: 84–90. DOI: 10.1186/s12906-018-2144-6.
32. Abima Shazhni J.R., Renu A. and Vijayaraghavan P. (2018) Insights of antidiabetic, anti-inflammatory and hepatoprotective properties of antimicrobial secondary metabolites of corm extract from Caladium x hortulanum. Saudi Journal of Biological Sciences 25: 1755–1761. https://doi.org/10.1016/j.sjbs.2018.03.013.
33. Napagoda M., Gerstmeier J., Butschek H., Lorenz S., Kanatiwela D., De Soyza S.D., Qader M., Nagahawatte A., Wijayaratne G.B., Svatoš A., Jayasinghe L., Koeberle A. and Werz O. (2018) Lipophilic extract of Leucas zeylanica, a multi-purpose medicinal plant in the tropics, inhibits key enzymes involved in inflammation and gout. J. Ethnopharmacol. 224: 474–481. DOI: 10.1016/j.jep.2018.04.042.

34. Łukasz Cies and Ruin Moaddela (2016) Comparison of analytical techniques for the identification of bioactive compounds from natural products Nat Prod Rep. 33: 1131–1145. doi:10.1039/c6np00016a.
35. S. Sasidharan, Y. Chen, D. Saravanan, K.M. Sundram and L. Yoga Latha (2011)Afr J Tradit Complement Altern Med. 8: 1-10.
36. Cerna M., Mencias F., Salazar T. and Gutiérrez S. Estudio Fitoquímico, Actividad Antioxidante de Especies de Orquídeas de Los Generos Epidendrum, Onicidium y Caucaea. BIONATURA 2018, 1 (1). https://doi.org/10.21931/RB/CS/2018.01.01.8.
37. Dhivya S.M. and Kalaichelvi K. (2017) UV-Visible Spectroscopic and FTIR Analysis of Sarcostemma brevistigma, Wight. and Arn. Int. J. Curr. Pharm. Res. 9: 46-49. https://doi.org/10.22159/ijcpr.2017.v9i3.18890.
38. Duangjai Tungmunnithum, Areeya Thongboonyou, Apinan Pholboon and Aujana Yangsabai. (2018) Flavonoids and Other Phenolic Compounds from Medicinal Plants for Pharmaceutical and Medical Aspects: An Overview. Medicines 5: 93-108 doi:10.3390.
39. Markham K.R. (1982) Techniques of flavonoids identification. Biological Techniques Series: Series editors: J.E. Treheme and P.H. Rubery. Academic Press, London p. 144.
40. Lattanzio V., Kroon P.A., Quideau S. and Treutter D. (2008) Plant phenolics – Secondary metabolites with diverse functions. In: Daayf F, Lattanzio V (eds) Recent advances in polyphenol research, vol 1. Wiley-Blackwell, Oxford, pp 1–35.
41. Debnath P.C., Das A., Islam A., Islam M.A., Hassan M.M., Gias Uddin S.M. (2013) Membrane stabilization – A possible mechanism of action for the anti-inflammatory activity of a Bangladeshi medicinal plant: Erioglossum rubiginosum (Bara Harina). Pharmacogn J. 5:104–107. DOI 10.1016/j.phcgj.2013.04.001.
42. Gadamsetty G., Maru S., Tyagi A. and Chakravarthula S.N. (2013) Anti-Inflammatory, Cytotoxic and Antioxidant Effects of Methanolic Extracts of Drypetes sepiaria (Euphorbiaceae). Afr J Tradit Complement Altern Med. 10: 274–82. DOI: 10.4314/ajtcam.v10i5.9.
43. Fabian I.E., Philip F.U., Ikechukwu P., Bonaventure C.O. and Patience O.O. (2019) In vitro and In vivo Models for Anti-inflammation: An Evaluative Review. INNOSC Theranostics and Pharmacological Sciences 2: 3-15. DOI: 10.36922/itps.v2i2.775.
44. Lijuan Z., Virgousb C. and Sia H. (2019) Synergistic anti-inflammatory effects and mechanisms of combined phytochemicals. 69: 19-30. https://doi.org/10.1016/j.jnutbio.2019.03.009.
45. López O.D., Nuñez Y., Menéndez R.A., Nogueira A., Reyes M.I., Toledo C., Pérez E. y Agüero S. (2010) Influencia del Proceso de Microencapsulación sobre el Efecto Farmacológico de los Lípidos Presentes en las Semillas de Cucurbita pepo L. Latin American Journal of Pharmacy 29 (4): 612-616.

Received: 22 September 2020
Accepted: 12 October 2020

CASE REPORTS / REPORTE DE CASO

Reporte de un caso con reacción a la polisulfona durante hemodiálisis. Clínica Reynadial, Guayaquil, 2020

Report of a case with a reaction to polysulfone during hemodialysis. Reynadial Clinic, Guayaquil, 2020

Mario Hernández[1], Elsa Bernal[2], Fresia Massuht[3], Emilio Fors[1], Yinet Ramírez[4], Ingrid Figueredo[4], Raúl Caballero[4], Martha Fors[5]

DOI. 10.21931/RB/2020.05.04.19

Resumen: El tratamiento de hemodiálisis (HD) presupone un cierto riesgo de reacciones adversas de hipersensibilidad, se han descrito casos de hipersensibilidad con membranas biocompatibles, como la polisulfona. En este artículo describimos el caso de un paciente que se realiza tratamiento de HD usando dializador de polisulfona, aproximadamente a los 10 minutos de iniciar presenta manifestaciones digestivas, caracterizada por diarreas liquidas, no relacionadas con evento alimenticio, sin flemas, ni contenido hemático, sin pujos ni tenesmo, presenta dolor abdominal difuso, vómitos e hipotensión arterial. Estas reacciones fueron consideradas como hipersensibilidad relacionada con el proceso de hemodiálisis, el cuadro clínico no reapareció en observaciones sucesivas cuando las sesiones se llevaron a cabo utilizando una membrana de celulosa.

Palabras clave: Hemodiálisis, membrana de polisulfona, reacción de hipersensibilidad.

Abstract: Hemodialysis (HD) treatment assumes a certain risk of adverse hypersensitivity reactions; cases of hypersensitivity with biocompatible membranes, such as polysulfone, have been described. In this article we describe the case of a patient who undergoes HD treatment using polysulfone dialyzer, approximately 10 minutes after starting, he presents digestive manifestations, characterized by liquid diarrhea, not related to eating events, without phlegm, or blood content, without straining or tenesmus, presents diffuse abdominal pain, vomiting and arterial hypotension. These reactions were considered as hypersensitivity related to the hemodialysis process, the clinical picture did not reappear in successive observations when the sessions were carried out using a cellulose membrane.

Key words: Hemodialysis, polysulfone membrane, hypersensitivity reaction.

Introducción

El realizar una sesión de hemodiálisis (HD) puede conllevar a riesgo de aparición de reacciones adversas de hipersensibilidad para el paciente, al estar su sangre en contacto con diferentes materiales de origen sintético[1]. Se ha descrito por varios autores reacciones de hipersensibilidad al óxido de etileno y a membranas de baja biocompatibilidad como el cuproamonio. También se han reportado casos de hipersensibilidad con membranas biocompatibles como la polisulfona, e incluso con polisulfona asociada a polivinilpirrolidona (PVP)[1,2].

En la literatura hay ejemplos de reacciones anafilácticas y anafilactoides o intolerancia a distintos tipos de membranas sintéticas en el mismo paciente[3,4,5], lo cual se atribuye a las diferencias en manufactura y a la cantidad de PVP utilizada para hidrofilizar la membrana.

Se ha evidenciado ausencia de reacción anafilactoide con el uso de un dializador de polisulfona en placas que no utilizan PVP como amalgamante, lo cual induce a pensar en un papel significativo de este producto en el desarrollo de la reacción. En ninguno de estos casos el cambio de dializador supuso la desaparición de las crisis y el desarrollo de urticaria crónica con eosinofilia. Otras causas que valorar serían la retrofiltración de endotoxinas en membranas de alta permeabilidad (ausente en membranas de baja permeabilidad), la hipersensibilidad a hierro intravenoso o el uso de inhibidores de la enzima convertidora de angiotensina (IECA).

Estas reacciones han inducido a realizar una evaluación no solo de las ramas y del dializador sino también de los procesos de esterilización que incluyen como principal factor el óxido de etileno y a los diferentes y numerosos medicamentos utilizados en el tratamiento de la Enfermedad Renal Crónica (ERC) como son la heparina, soluciones de hierro, vitaminas y las eritropoyetinas.

Intuir una reacción de hipersensibilidad en este tipo de pacientes es extremadamente difícil por lo que hay que analizar la situación de los pacientes afectados por la enfermedad de base, los estigmas de ERC y las comorbilidades que frecuentemente los afectan.

Las membranas son el elemento fundamental del tratamiento de HD, puesto que a través de ellas se realizan la filtración, la difusión y otros procesos físicos responsables de la detoxificación de la sangre y la eliminación de los metabolitos de desecho orgánico, estas membranas semipermeables tienen su origen en materiales naturales como la celulosa, el papel almidonado y otros derivados del algodón que se usaron en la etapa experimental e inicial de la nefrología en el mundo contemporáneo, precisamente este tipo de membranas eran poco toleradas, lo que obligo a la búsqueda de nuevos materiales que ofrecieran mejores índices de eficiencia y eficacia en la depuración de toxinas y filtración de agua, comenzaron a utilizarse materiales con cualidades físico-químicas donde la

[1] Clínica Reynadial, Guayaquil, Ecuador. Hospital General IESS Babahoyo, Los Ríos, Ecuador.
[2] Universidad Técnica de Babahoyo, Ecuador.
[3] Clínica Reynadial. Hospital General IESS Sur Valdivia, Guayaquil, Ecuador.
[4] Clínica Reynadial, Guayaquil, Ecuador.
[5] Universidad de las Américas, Quito, Ecuador.

Corresponding author: martha.fors@udlanet.ec

porosidad, el espesor, la hidrofilia, la conductividad alcanzaron una diversidad, en la misma medida que se lograba mejorar ostensiblemente la biocompatibilidad.

Las polisulfonas ocupan un lugar importante en el desarrollo de las membranas dializadoras y han generado una indudable mejoría en los resultados del tratamiento hemodialítico, pero también hay evidencias científicas de reportes de hipersensibilidad a este tipo de membranas sintéticas.

La Clínica Reynadial es un centro de atención dedicado a brindar Servicio de Hemodiálisis a pacientes portadores de Enfermedad Renal Crónica grado V. Brinda servicios desde el año 2016 y ha sido fiel seguidora de los Protocolos de tratamiento elaborados por las Autoridades del Ministerio de Salud Pública (MSP) y el Instituto Ecuatoriano de Seguridad Social (IESS), así como una continua actualización de técnicas y procederes tomando como modelo las normas Europeas y Americanas y la medicina basada en evidencia, lo que permite brindar una atención de excelencia en el tratamiento de 140 pacientes.

En términos generales la Hemodiálisis se practica 3 veces por semana durante 4 horas; En REYNADIAL como protocolo se maneja la diálisis Hipotérmica (Temperatura del líquido de dializado en 35°C), con NA ajustado al perfil de los pacientes y sumando monitoreo de la tensión arterial y frecuencia cardiaca, el peso se estima por clínica y ajustes orientados a través de la realización de la medición ultrasónica del diámetro de la vena cava inferior y la Bioimpedancia, de manera tal que los parámetros fundamentales se manejan con estándares que permiten la calidad en hemodiálisis.

En este estudio reportamos un primer caso de hipersensibilidad a membranas sintéticas de polisulfona, en el que se realizó una revisión exhaustiva de todas las potenciales causas de aparición de esta condición como las anafilactoides, hemodinámicas y cardiovasculares. que pudieran explicar la sintomatología presentada que finalmente fueron corregidas al sustituir las membranas de polisulfona por membranas semisintéticas de triacetato, la cual logra un Kt y un volumen convectivo adecuados, con buen perfil de biocompatibilidad e inflamatorio, lo que la convierte en una posibilidad más de tratamiento en pacientes alérgicos a membranas sintéticas.

Reporte de caso

Paciente NCLQ de 75 años de edad, con antecedentes de Diabetes Mellitus, Tuberculosis pulmonar e Hipertensión Arterial de más de 15 años de evolución, así como Enfermedad Renal Crónica (ERC), que fue referido a Hemodiálisis(HD) el 24 de junio del 2019, con catéter yugular derecho, anemia (hemoglobina 7,7 g/l), hipoalbuminemia discreta, y presentando al examen físico: edemas de miembros inferiores, palidez cutáneo mucosa, con peso de 60.9 kg y tensión arterial (TA) de 160/60.

En el transcurso de los 2 meses iniciales en HD este paciente solo presentó elevación de la tensión arterial durante las sesiones de hemodiálisis, así como una positiva evolución de su síndrome de ERC con desaparición de los edemas en miembros inferiores, ascenso de los valores de Hemoglobina y serinemia, destacando la permanencia de valores absolutos elevados de eosinofilia.

En el mes de octubre (15/10/2019) se realiza exitosamente una fistula arteriovenosa (FAV); desde el punto de vista de la analítica mantenía la eosinofilia, habiendo ya corregido la anemia con hemoglobina en valores de 11g/ l.

En el mes de noviembre del 2019 el paciente comienza con manifestaciones de diarreas liquidas, sin flemas, ni contenido hemático, ni alimenticio, acompañadas de dolor abdominal difuso, sin pujos ni tenesmo al comienzo de la sesión (10 minutos) así como astenia, mejorando pasada una hora en tratamiento (si se mantenía conectado), a veces con necesidad de desconexión y reconexión. En el mes de diciembre, a lo anterior se agregan náuseas, epigastralgia e hipotensión arterial, después de 15 a 20 minutos de conectado a la hemodiálisis, por lo que se investigan otras causas probables especialmente hemodinámicas, ya que se asociaba su morbilidad intradialítica a la previa realización de la FAV ; es de señalar la repetición de estos episodios en cada sesión de hemodiálisis, hasta entonces realizadas con filtros de polisulfona de al menos 3 compañías manufactureras distintas.

Los cambios de filtro a otra polisulfona, definitivamente no se mostraron eficaces en la reducción de los síntomas de este paciente. (Tabla 1)

Tipo de membrana	FECHA
FX 8	24/6/2019
REVACLEAR 300	**28/6/2019**
FX 8	19/8/2019
P18	**2/9/2019**
FX 8	18/9/2019
FX 60	**1/11/2019**
REVACLEAR 300	24/12/2019
P 18	**26/12/2019**
SUREFLUX	28/12/2019

Tabla 1. Cambios de membranas al paciente.

Tampoco el uso de hidrocortisona, antihistamínicos y oxígeno con máscara produjeron mejorías ostensibles. Se realiza un ecocardiograma pensando en la posibilidad de un bajo gasto, obteniéndose un resultado normal con F/E 65%; el electrocardiograma también fue normal; la exploración con ECO de los diámetros de vena cava inferior e índice caval expresaron adecuada volemia. Se observan los resultados de los exámenes de laboratorio en la Tabla 2. La eosinofilia se mantuvo todo el periodo incluso después del cambio de membrana.

Analizando otras posibilidades y teniendo en cuenta informaciones sobre casos de reacción de hipersensibilidad a las membranas sintéticas, se decide pasar a membranas celulósicas eligiendo Sureflux N10 de NIPRO (triacetato de celulosa). Una vez utilizada esta membrana desaparecen inmediatamente todos los síntomas, y manteniéndose asintomático a partir de entonces hasta la fecha de este reporte.

Discusión

La composición de las membranas dializadoras desde el uso de celulosa a membranas sintéticas, los métodos de esterilización para la eliminación de óxido de etileno y la utilización de otros materiales en el dializador y los tubos como son diferentes pegamentos, aglutinantes, plásticos, látex y siliconas han evolucionado para mejorar la biocompatibilidad. A pesar de esta biocompatibilidad mejorada, no se ha observado una disminución en las reacciones de hipersensibilidad que aparecen en los pacientes que reciben hemodiálisis[5,6].

Un aumento en el número de informes sobre reacciones

	JUNIO	JULIO	AGOSTO	SEPTIEMBRE	OCTUBRE	NOVIEMBRE	DICIEMBRE	ENERO	FEBRERO
LEUCOCITOS	8.56	8.26	10.9	12.4	8.53	8.03	8.59	13.00	8.000
EOSINOFILOS %	12.5	15.3	23	19.4	22	29	24	20.4	40.2
CONTEO ABSOLUTO	1.070	1.270	2.520	2.410	1.900	0.700	0.900	2.654	1.415
PLAQUETAS	286.000	364.000	325.000	233.000	232.000	166.000	178.000	305.000	230.000

Tabla 2. Resultados de exámenes de laboratorio.

de hipersensibilidad ha creado alarma y ha provocado una advertencia por parte de las autoridades sanitarias españolas sobre los riesgos de las membranas de polisulfona[1,7,8].

Existen reportes de que 1 de cada 20 a 50 pacientes tiene probabilidades de experimentar una reacción anafilactoide con un nuevo dializador, lo que indica que la magnitud del problema es grande[9]. Desde ya hace varios años, se reportó que la incidencia de reacciones era de 0.17 por 1000 sesiones con membranas de celulosa y 4.2 por 1000 sesiones con membranas sintéticas[10].

La morbilidad intradialítica extrema de este cas nos insinuaba la necesidad de profundizar en la pesquisa de situaciones parecidas pero quizás de menor intensidad que pudieran estar presentes en nuestros pacientes polisintomáticos y relacionadas con membranas sintéticas con la misma probable fisiopatogenia, por lo que decidimos indagar en manifestaciones clínicas de hipersensibilidad (prurito, urticaria, broncoespasmo, opresión precordial, hipotensión arterial, dolor abdominal, vómitos, diarreas, molestias) generadas durante el proceso dialítico proceder ante la duda a cambiar el dializador por celulósico, evaluando resultados clínicos demostrables.

Las manifestaciones en este paciente fueron recidivantes y generadas en el proceso de la hemodiálisis o relacionadas con el uso de una membrana de polisulfona. Al realizar el cambio de ésta, las manifestaciones clínicas desaparecieron.

Puede haber reacciones tanto con celulosa como con membranas sintéticas, aunque las membranas sintéticas, en la actualidad, causan más reacciones alérgicas. Es posible que el uso de otros materiales como la PVP pueda aumentar la probabilidad de sufrir una reacción de hipersensibilidad en estos pacientes.

Se deben descartar otras causas de reacciones alérgicas como látex, hierro intravenoso, heparina y formaldehído en pacientes que sufren reacciones de hipersensibilidad en diálisis.

Conclusiones

Las reacciones de hipersensibilidad pueden ocurrir con cualquier tipo de membranas, pero el reciente aumento en los casos publicados relacionados con las membranas sintéticas de polisulfona nos advierte de esta posibilidad, por lo que el personal que atiende a pacientes en hemodiálisis debe estar atento a cualquier manifestación de este tipo. El triacetato de celulosa parece ser una buena alternativa para estos pacientes.

Referencias bibliográficas

1. Sánchez-Villanueva Rafael J., González Elena, Quirce Santiago, Díaz Raquel, Álvarez Laura, Menéndez David et al. Reacciones de hipersensibilidad a membranas sintéticas de hemodiálisis. Nefrología (Madr.) [Internet]. 2014 [citado 2020 Jul 01]; 34(4): 520-525. Disponible en: http://scielo.isciii.es/scielo.php?script=sci_arttext&pid=S0211-69952014000400012&lng=es. http://dx.doi.org/10.3265/Nefrologia.pre2014.May.12552.
2. Arenas MD, Gil, MT, Carretón MA, Moledous A, Albiach B. Efectos adversos a polisulfona durante la sesión de hemodiálisis. Nefrología, 27(5):638-642
3. Caruana RJ, Hamilton RW, Pearson FC. Dialyzer hypersensitivity syndrome: possible role of allergy to ethylene oxide. Report of 4 cases and review of the literature. Am J Nephrol 1985;5:271-4.
4. Kuragano T, Kuno T, Takahashi Y, Yamamoto C, Nagura Y, Takahashi S, et al. Comparison of the effects of cellulose triacetate and polysulfone membrane on GPIIb/IIIa and platelet activation. Blood Purif 2003;21:176-82
5. Ebo DG, Bosman JL, Couttenye MM, Stevens WJ. Haemodialysis-associated anaphylactic and anaphylactoid reactions. Allergy 2006;61:211-20.
6. Butani L, Calogiuri G: Hypersensitivity reactions in patients receiving hemodialysis. Ann Allergy Asthma Immunol 2017; 118: 680–684.
7. González Sanchidrián S, Labrador Gómez PJ, Marín Álvarez JP, Jiménez Herrero MC, Castellano Cerviño I, Gallego Domínguez S, Sánchez-Montalbán JM, Deira Lorenzo J, Davin Carrero E, Planco Candelario S, Gómez-Martino Arroyo JR: Reacción a membranas sintéticas en hemodiálisis. Nefrología 2016; 36: 707–709.
8. Martín-Navarro JA, Gutiérrez-Sánchez MJ, Petkov-Stoyanov V: Hypersensitivity to synthetic hemodialysis membranes. Nefrologia 2014; 34: 807–808.
9. Nicholls AJ. Hypersensitivity to hemodialysis: the United Kingdom experience. Artif Organs. 1987;11(2):87-89. doi:10.1111/j.1525-1594.1987.tb02634.x
10. Simon P, Potier J, Thebaud HE. Facteurs de risque des réactions aiguës d'hypersensibilité en hémodialyse: enquête prospective multicentrique sur six mois dans l'Ouest de la France [Risk factors for acute hypersensitivity reactions in hemodialysis]. Nephrologie. 1996;17(3):163-170

Received: 24 septiembre 2020
Accepted: 10 octubre 2020

CASE REPORTS / REPORTE DE CASO

Síndrome de Sweet asociado a Neoplasias. Reporte de un caso

Sweet Syndrome is associated with neoplasms. Report of a case

Adrian Isacc Nieto Jiménez

DOI. 10.21931/RB/2020.05.04.20

Resumen: El Síndrome de Sweet es una entidad que se manifiesta clínicamente por la presencia de placas eritematosas, pústulas y/o ampollas. En la histología se evidencia un denso infiltrado de neutrófilos. Al igual que otras dermatosis neutrofílicas, se caracteriza por una buena respuesta al tratamiento con esteroides y dapsona. En el 20% de los casos se asocia a enfermedades malignas, representando las hematológicas el 85% y los tumores sólidos el 15% restante. Se presenta una paciente de 46 años de edad con antecedentes de Leucemia Linfoblàstica, que consultó por la aparición de placas eritematosas, violáceas en el dorso de las manos con un estudio histopatológico que evidenció un Síndrome de Sweet.

Palabras clave: Neutrofilia, vasculitis, Síndrome de Sweet.

Abstract: The Sweet Syndrome is an entity that is manifested clinically by badges erythematous, pocks, and limited bladders. In the histology, a dense one is evidenced by infiltrated neutrophils. Like another Neutrophilic dermatosis, it is characterized by an excellent answer to steroids and dapsone treatment. Twenty percent of cases are associated with malignancies; 85% of them involve hematologic malignancies and the remaining 15%, solid tumors. A 46-year-old patient with a history of Lymphoblastic Leukemia is presented that consulted for the appearance of badges erythematous, violaceous in the back of the hands with a histopathological examination showed the Sweet Syndrome.

Key words: Neutrophilia, vasculitis, Sweet Syndrome.

Introducción

En el año 1964, el Dr. Robert Douglas Sweet describió una dermatosis a la cual denominó enfermedad de "Goom-Button", en homenaje a las dos primeras pacientes en las que se observó esta entidad. Posteriormente, recibe el nombre de dermatosis neutrofílica febril y aguda, por sus características clínicas y humorales. Actualmente, se prefiere el nombre de Síndrome de Sweet[1].

Este se caracteriza por cinco rasgos principales: 1) aparición brusca de placas eritemato-dolorosas a nivel de la cabeza, cuello y extremidades superiores; 2) fiebre; 3) leucocitosis neutrofílica; 4) denso infiltrado dérmico a predominio polimorfonuclear; 5) rápida respuesta a la terapéutica esteroidea[2,3]. Esta entidad se ha clasificado en cinco grupos: idiopático o clásico, para inflamatorio, para neoplásico, secundario a drogas y asociado a embarazo[3]. La mayoría de los pacientes pertenecen al primer grupo. En el 20% de los casos se encontró asociación con enfermedades malignas, representando las hematológicas el 85% de las mismas y los tumores sólidos el 15% restante. Con respecto a las neoplasias hematológicas, la leucemia mieloide aguda es la que se observa más frecuentemente; y en cuanto a los tumores sólidos, aproximadamente 2/3 de los casos corresponden a carcinomas del tracto genitourinario[2].

El diagnóstico de dicho síndrome es, a menudo, el signo de presentación de una neoplasia nueva o recurrente. A su vez, la presencia de anemia, un recuento anormal de plaquetas, la ausencia de neutrofilia, la localización y formas de presentación atípicas de las lesiones, deben alertar a la búsqueda de neoplasias, ya que estos hallazgos no son comunes de observar en la forma idiopática de dicho síndrome[2,4].

Si bien la resolución espontánea del cuadro clínico puede ocurrir en semanas a meses, el tratamiento de elección son los esteroides, los cuales producen la remisión del mismo a pesar de la neoplasia subyacente[5].

En Cuba el comportamiento de esta entidad poco frecuente se registra asociado en primer lugar a la Leucemia, en edades de 42 a 51 años de edad, seguido de otros tumores sólidos del tracto genitourinario. Se reportan cerca de 6 casos en ciudad de La Habana del Síndrome de Sweet relacionados con Linfoma no Hodgking, en Villa Clara no se encontraron reportes[6].

Caso Clínico

Se trata de un paciente del sexo femenino, de 46 años de edad, con antecedentes de Leucemia Linfoblàstica de 2 años de evolución, que fue hospitalizada por un episodio de fiebre de 4 días, con toma del estado general. Además, presentó lesiones en placa eritematovioláceas e infiltradas, bien definidas, de diversos tamaños, redondeadas en el dorso de la mano derecha. (Figura 1)

La infiltración es más marcada en la lesión en placa al dorso del segundo dedo de dicha mano, con aspecto pseudovesiculoso. (Figura 2) Las lesiones se acompañaban de discreto ardor y sensación de quemazón, sobre todo en las lesiones más extensas. Se indicó tratamiento por el servicio de Hematología con Imipenem y Ciprofloxacino, porque se encontró también un foco séptico a nivel de la cavidad oral, persistiendo la fiebre.

Complementarios realizados

Biometría hemática: Arroja anemia ligeraHb-10 G/L con neutropenia.

VIH, Antígeno de superficie para Hepatitis B y C: normales.

LDH, Perfil hepático y renal. Rx de tórax y Ultrasonido abdominal y ginecológico (sin alteraciones)

Cultivos y hemocultivos: Negativos.

[1] Especialista en primer grado en Medicina General Integral y Dermatología, Profesor Asistente, Diplomado en Hematodermias, Investigador Agregado, Hospital Pediátrico Provincial: José Luis Miranda, Santa Clara, Cuba.

Corresponding author: adrianisacnj@gmail.com

Se realizó Biopsia cutánea donde se observó la presencia de acantosis y espongiosis en la epidermis, y de importante edema e infiltración

polimorfonuclear a nivel dérmico. En base a la clínica y al estudio histopatológico, se arribó al diagnóstico del síndrome de Sweet.

Se le indicó tratamiento con Prednisona a razón de 1 mg/kg de peso diario más Dapsone con rápida resolución del cuadro cutáneo en 17 días.

Figura 1. En esta figura se observan lesiones en placas múltiples con bordes definidos eritematosa papulosas en el dorso de la mano derecha.

Comentario

El Síndrome de Sweet o dermatosis neutrofílica febril y aguda, es una entidad de etiología desconocida, que se caracteriza por la presencia de fiebre; leucocitosis neutrofílica; la aparición abrupta de placas y nódulos eritemato-dolorosos a predominio de la cabeza, cuello y extremidades superiores; un denso infiltrado dérmico polimorfonuclear sin vasculitis y la rápida respuesta al tratamiento con corticoides, coincidiendo con nuestro caso[2].

La mayoría de los pacientes presentan la forma clásica o idiopática, representando la forma paraneoplásica el 20% de los casos. La mayor parte corresponde a neoplasias hematológicas, como pudimos constatar en el caso presentado. La enfermedad maligna más común corresponde a la leucemia mieloide aguda. Sin embargo, también se han observado asociaciones con trastornos mieloproliferativos, linfoproliferativos, síndrome mielodisplásico y carcinomas[7].

Habitualmente, el Síndrome de Sweet se presenta en forma coincidente o precediendo a la neoplasia, pero también se ha informado la aparición de la misma hasta un año posterior a dicho síndrome[3,7].

El compromiso extra cutáneo se observa en una alta proporción (cercano al 50%) de los pacientes con síndrome de Sweet asociado a neoplasias, especialmente a nivel musculoesquelético y renal. Con menor frecuencia, también puede existir afección ocular, pulmonar, hepática, digestiva, pancreática, esplénica, ganglionar, cardiaca y del sistema nervioso central[8].

La incidencia de este Síndrome es baja en América Latina[9]. En varias literaturas se describe el predominio en el sexo femenino, aunque otros autores no discriminan en cuanto el sexo y edad de presentación[10].El diagnóstico positivo se realiza con las manifestaciones clínicas y el estudio histológico, aunque en ocasiones resulta complejo por la similitud con otras dermatosis neutrofilicas[8].

Figura 2. Aquí se observa la lesión más extensa, infiltrada hacia los bordes en el dorso el segundo dedo.

La terapéutica esteroidea junto al Dapsone produjo la remisión de las lesiones cutáneas, al igual que lo observado en la literatura[9]. La terapéutica de primera elección, tanto para el síndrome de Sweet idiopático como el asociado a neoplasias, corresponde a los corticoides sistémicos con los cuales se obtiene una rápida respuesta del cuadro clínico. Se utiliza prednisona a dosis entre 30-60 mg/día por vía oral durante cuatro a seis semanas, con descenso progresivo de la dosis. Existen otras alternativas terapéuticas como el yoduro de potasio, la colchicina, indometacina, clofazimina y ciclosporina[9,10].

Recientemente, se ha publicado un caso de síndrome de Sweet recalcitrante asociado con síndrome mielodisplásico, que respondió con éxito al tratamiento con talidomida[11].

El pronóstico es variable y depende si está o no asociado a una neoplasia subyacente. Puede involucionar de forma espontánea[8,11].

Conclusiones

El Síndrome de Sweet se asocia frecuentemente a neoplasias, sobre todo Hematológicas. Ante un paciente con lesiones sospechosas de esta entidad, con síntomas acompañantes, se debe descartar un tumor asociado. Es importante la valoración de los pacientes con Síndrome de Sweet por la especialidad de Hematología.

Referencias bibliográficas

1. Byun, J.W.; Hong, W.K.; Song, H.J.; Han, S.H.; Lee, H.S.; Choi, G.S.; Shin, J.H.: A case of neutrophilic dermatosis of the dorsal hands with concomitant involvement of the lips and Sweet Syndrome. Ann Dermatol. 2013; 22: 106-109.
2. Cohen PR, Kurzrock R. Sweet's syndrome and malignancy. Am J Med. 2014; 82:1220-6. 3.
3. Cohen PR, Kurzrock R. Sweet's síndrome revisited: a review of disease concepts. Int J Dermatol. 2015; 42:761-78.
4. Cohen PR, Talpaz M, Kurzrock R. Malignancy-associated Sweet's syndrome: review of the world literature. J Clin Oncol. 2016; 6:1887-97.
5. Hussein K, Nanda A, Al-Sabah H, Alsaleh QA. Sweet's syndrome (acute febrile neutrophilic dermatosis) associated with adenocarcinoma of prostate and transitional cell carcinoma of urinary bladder. J Eur Acad Dermatol Venereol. 2016; 19:597-9.
6. Registro Estadístico de Salud Nacional. Síndrome de Sweet y Neoplasias Oncoproliferativas. La Habana. Cuba. 2017.
7. Gómez Vázquez M, Sánchez-Aguilar D, Peteiro C, Toribio J. Sweet's syndrome and polycythaemia vera. J Eur Acad Dermatol Venereol. 2017; 19:382-3.
8. Culp L, Crowder S, Hatch S. A rare association of Sweet's syndrome with cervical cancer. Gynecol Oncol. 2017; 95:396-9.
9. Nobeyama Y, Kamide R. Sweet's syndrome with neurologic manifestation: case report and literature review. Int J Dermatol. 2018; 42:438-43.
10. Gibson L, Dicken C, Flach D. Neutrophilic dermatoses and myeloproliferative disease: report of two cases. Mayo Clin Proc. 2018; 60:735-40.
11. Del Pozo J, Martínez W, Pazos JM, Yebra-Pimentel MT, García Silva J, Fonseca E. Concurrent Sweet's syndrome and leukemia cutis in patients with myeloid disorders. Int J Dermatol. 2019; 44:677-80.

Received: 24 septiembre 2020
Accepted: 11 octubre 2020

CASE REPORTS / REPORTE DE CASO

Coexistencia de hemorragia subaracnoidea aneurismática accidentada y tromboembolia pulmonar en paciente con COVID-19. Reporte de un caso

Coexistence of accident aneurismatic subarachnoid hemorrhage and pulmonary thromboembolic in a patient with COVID-19. Report of a case

Jorge Luis Vélez Páez[1], Santiago Xavier Aguayo Moscoso[1], Christian Leonardo Mora Coello[2], Wilson Daniel Alava Muñoz[3], María José Proaño Constante[2], Erika Lizeth Sananay Auquilla[2]

DOI. 10.21931/RB/2020.05.04.21

Resumen: El COVID-19 es causado por el SARS-CoV2, un coronavirus beta, que actualmente es responsable de una pandemia con alta tasa de contagiosidad y mortalidad a nivel mundial. Este virus, a más de su impacto a nivel pulmonar, puede desencadenar una tormenta de citocinas proinflamatorias que dañan el endotelio vascular generando endotelitis, disfunción endotelial y alta prevalencia de eventos trombóticos. Clínica y analíticamente la expresión de este fenómeno se evidencia con niveles elevados de dímero D, trombosis venosa y/o arterial, embolia pulmonar, enfermedades cerebrovasculares y cardiovasculares y trombosis microvascular difusa. Dado que el endotelio es un órgano vital en la regulación del tono vascular y la homeostasis, su afectación conduce a vasoconstricción, isquemia, infarto e inflamación y esto posiblemente cause debilitamiento de su estructura.
En él siguiente reporte de caso, narramos la historia de un paciente con neumonía por SARS-CoV2, que presentó concomitancia de alteraciones endoteliales hemorrágicas y trombóticas, expresadas por una hemorragia subaracnoidea aneurismática accidentada y una tromboembolia pulmonar submasiva.

Palabras clave: SARS-CoV2, COVID-19, hemorragia subaracnoidea, aneurisma cerebral, tromboembolia pulmonar.

Abstract: COVID-19 is caused by SARS-CoV2, a beta coronavirus currently responsible for a pandemic with a high rate of contagiousness and mortality worldwide. In addition to its impact at the lung level, this virus can trigger a storm of proinflammatory cytokines that damage the vascular endothelium, generate endothelium, endothelial dysfunction, and a high prevalence of thrombotic events. Clinically, this phenomenon's expression is evidenced by high D-dimer levels, venous and arterial thrombosis, pulmonary embolism, cerebrovascular and cardiovascular diseases, and diffuse microvascular thrombosis. Since the endothelium is a vital organ in regulating vascular tone and homeostasis, its involvement leads to vasoconstriction, ischemia, infarction, and inflammation, which possibly causes a weakening of its structure.
In the following case report, we narrate the history of a patient with SARS-CoV2 pneumonia, who presented concomitance of hemorrhagic and thrombotic endothelial alterations, expressed by an accidental aneurysmal subarachnoid hemorrhage and submassive pulmonary thromboembolism.

Key words: SARS-CoV2, COVID-19, subarachnoid hemorrhage, cerebral aneurysm, pulmonary thromboembolism.

Introducción

El COVID-19 es causado por el SARS-CoV2, un coronavirus beta, que actualmente es responsable de una pandemia con alta tasa de contagiosidad y mortalidad a nivel mundial[1]. El impacto pulmonar de ésta enfermedad está dado por hipoxemia secundaria a daño alveolar directo y aumento de los productos de degradación de la fibrina[2], especialmente el dímero D[3,4]; por lo que los síntomas de enfermedad embólica pulmonar y neumonía viral suelen coexistir y solaparse en algunos casos[5-7].

Este virus, a más de su impacto a nivel pulmonar, puede desencadenar una tormenta de citocinas proinflamatorias que dañan el endotelio vascular generando endotelitis, disfunción endotelial y alta prevalencia de eventos trombóticos[8]. Clínica y analíticamente la expresión de este fenómeno se evidencia con niveles elevados de dímero D, trombosis venosa y/o arterial, embolia pulmonar, enfermedades cerebrovasculares, cardiovasculares y trombosis microvascular difusa. Dado que el endotelio es un órgano endocrino, paracrino y autocrino dinámico con un papel vital en la regulación del tono vascular y la homeostasis, su afectación conduce a vasoconstricción, isquemia, infarto e inflamación y esto posiblemente cause debilitamiento de su estructura[9,10].

En el siguiente reporte de caso, narramos la historia de un paciente con neumonía por SARS-CoV2, que presentó concomitantemente alteraciones endoteliales hemorrágicas y trombóticas, expresadas por una hemorragia subaracnoidea aneurismática accidentada y una tromboembolia pulmonar submasiva.

Caso Clínico

Varón de 63 años, con antecedentes de tabaquismo desde hace 40 años (Índice de paquete año 40). Acudió por tos seca y alza térmica de 6 días de evolución que se agrava y progresa a taquipnea, desaturación de oxígeno (O2) hasta 83% y disnea. No antecedente de eventos traumáticos ni compromiso neurológico.

Ingresó por emergencia, donde pese a administración de O2 a alto flujo no mejoró su oxigenación y persistió con taquip-

[1] Hospital Pablo Arturo Suárez, Ecuador.
[2] Hospital Pablo Arturo Suárez, Pontificia Universidad Católica del Ecuador.
[3] Hospital Pablo Arturo Suárez, Universidad Central del Ecuador.

Corresponding author: jlvelez@uce.edu.ec

nea, por lo que en 12 horas ingresó a ventilación mecánica invasiva, requirió alta concentración de O2 (FiO2 75%) y elevada presión positiva al final de la expiración (PEEP) 14cmH2O, por ello fue transportado a la Unidad de Terapia Intensiva (UTI) a las 72 horas de ingreso hospitalario.

En UTI, fue admitido bajo sedación y analgesia profunda más relajación muscular, RASS-3, pupilas de 2mm, con reflejo fotomotor, oculocefálico y corneal presente bilateralmente. Signos vitales de ingreso: TA 140/78mmHg, TAM 102mmHg, FC 62, FR 24, SO2 98%, sin requerimiento de vasopresores y bajo ventilación mecánica invasiva, en secuencia mandatoria continua, controlada por presión, con PaO2/FiO2 menor a 100 mmHg pese a FiO2 de 100% y PEEP de 15, por lo que se procedió a ventilación en posición prona. Recibió cobertura antimicrobiana empírica con aminopenicilina más macrólido, además corticoides y anticoagulación por valores elevados de dímero D y ferritina respectivamente. (Tabla 1)

Después de 48 horas de ventilación en prono, se evidencia bradicardia sinusal de 24 horas de evolución (Figura 1), con frecuencia cardíaca de 33 lpm sin compromiso en la hemodinamia; mejoró su oxigenación, con PaO2/FiO2 de 194 mmHg y con PEEP < 10mmHg por lo que se indicó despronación y retorno al decúbito supino. Posterior a la despronación presentó parada cardiorrespiratoria de 1 minuto con retorno de la circulación espontánea luego de aplicar protocolo de reanimación cardiovascular avanzada.

Posterior al evento de parada cardiaca; se encontró midriasis pupilar bilateral de 5 milímetros y ausencia de reflejos del tallo encefálico, por lo que, se solicitó estudios de imagen cerebral y pulmonar.

La tomografía simple de cráneo mostró una hemorragia subaracnoidea temporo-parietal derecha y frontal izquierda (Figura 2).

Posteriormente se realizó una angiotomografía cerebral que reveló una imagen hiperdensa de 6.1x5x5.4 centímetros, volumen aproximado 316 mililitros con relación a sangrado que se extiende hacia sistema ventricular, que desplaza la línea media hacia la izquierda 8.8 milímetros (Figura 3A); una dilatación aneurismática de base ancha 3.5 milímetros, saco aneurismático 4.6x3.8 a nivel de arteria cerebral media derecha en la bifurcación hacia segmento M2. (Figura 3B). Y la angiotomografía de tórax mostró defectos de llenado a nivel de la rama terminal de la arteria pulmonar derecha en relación con tromboembolia pulmonar aguda. (Figura 3C).

Posterior a los hallazgos, la evolución del paciente fue mala, presentó choque refractario y falleció a las 72 horas de su ingreso a la UTI.

Discusión

Éste reporte de caso de infección por SARS-CoV2; es elocuente de la clínica variada del virus, presenta afección hemorrágica que coexiste con trombótica a nivel de dos órganos diferentes como el cerebro y el pulmón respectivamente; además de hipoxemia propia de la presentación clásica del virus y bradiarritmia por efecto cardíaco directo.

De manera particular en el ámbito neurológico existe mayor predisposición a enfermedades cerebrovasculares: de tipo isquémico agudo, trombosis del seno venoso, hemorragia cerebral, encefalopatía hemorrágica necrotizante aguda y hemorragia subaracnoidea que fue lo que finalmente dió un desenlace fatal a nuestro enfermo[11-15].

La arritmia en el COVID-19, es relativamente frecuente con una incidencia de 16,7% de forma general y de 44% en pacientes críticamente enfermos de forma particular[16]; la respuesta inflamatoria excesiva desencadena injuria miocárdica y miocarditis, además de otras posibles noxas cardíacas como

ANALÍTICA DE INGRESO					
LEUCOCITOS	9.40 K/µL	TIEMPO DE PROTROMBINA	11,4 seg	FERRITINA	>1650 ng/ml
NEUTRÓFILOS%	91,6%	TIEMPO DE TROMBOPLASTINA	24,3 seg	DIMERO D	5492,2 ng/ml
LINFOCITOS %	4,4%	INR	1,08	DESHIDROGENASA LÁCTICA	1216 U/L
PLAQUETAS	277.000 K/µL	TROPONINA I	0,024 ng/ml	SODIO / POTASIO	146 / 4,4 meq/L
HEMOGLOBINA	14,2 g/dL	NITRÓGENO UREICO	19 mg/dL	CLORO	108 meq/L
HEMATOCRITO	41,8%	CREATININA	0,64 mg/dL	INTERLEUQUINA 6	22 pg/ml

Tabla 1. Analítica de ingreso a la unidad de terapia intensiva.

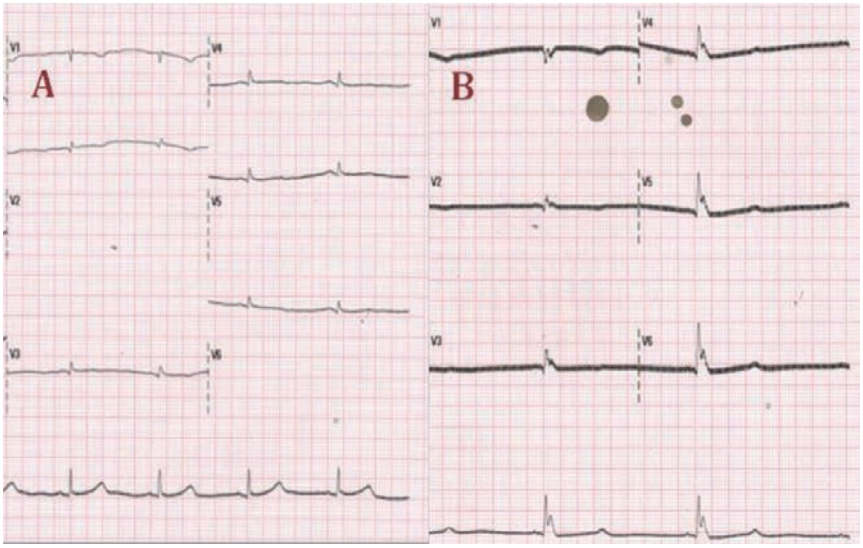

Figura 1. Elecardiografía al ingreso (A) y al momento de la bradicardia (B), que muestra frecuencias cardíacas de 53 y 33 latidos por minuto respectivamente.

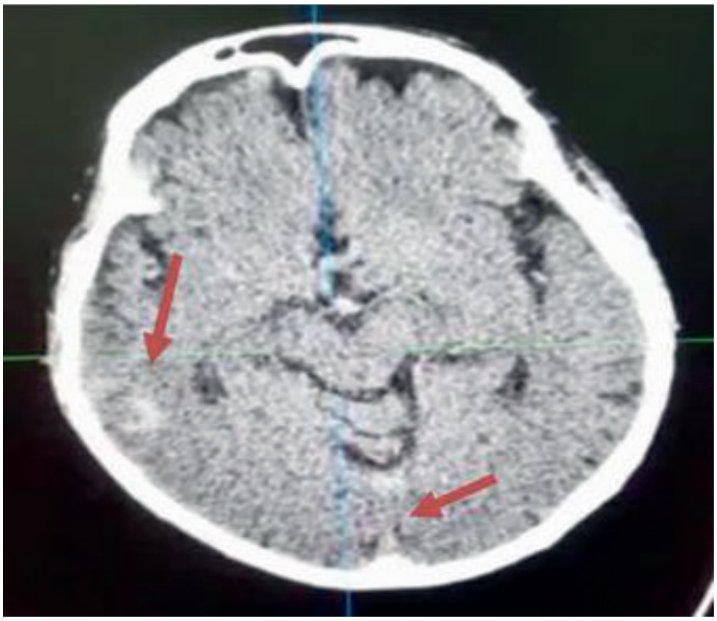

Figura 2. Tomografía simple de cráneo que muestra hemorragia subaracnoidea temporo-parietal derecha y frontal izquierda (flechas rojas).

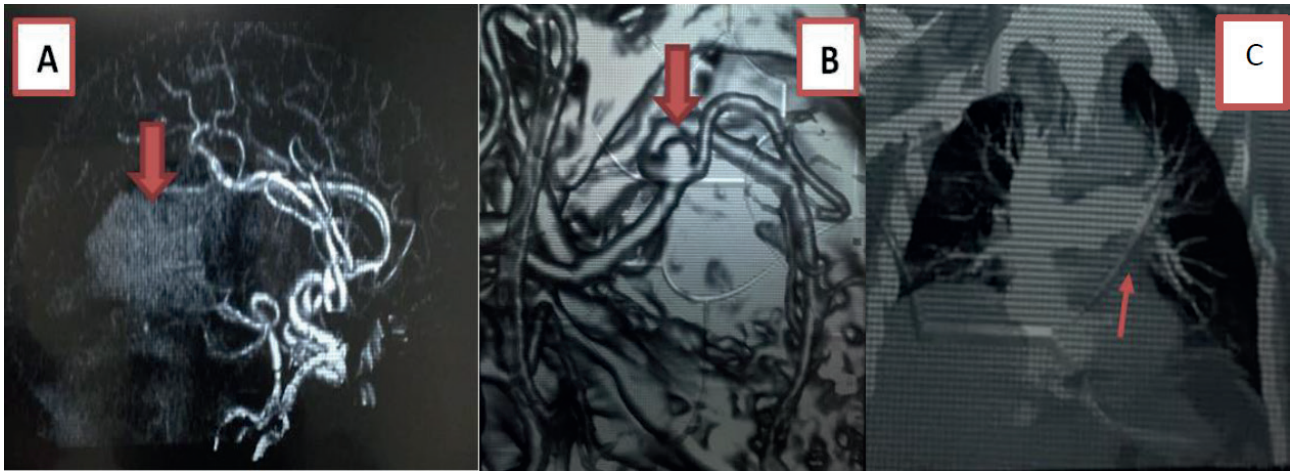

Figura 3. La figura 3 muestra en A la hemorragia subaracnoidea de gran volumen (flecha roja), en B la dilatación aneurismática en arteria cerebral media derecha (flecha roja) y en C muestra el trombo a nivel de la rama terminal de la arteria pulmonar derecha.

la ruptura de placas ateromatosas y trombosis coronaria[17]. En nuestro paciente la bradiarritmia se pudo haber explicado desde causas farmacológicas como el uso de opioides hasta miocárdicas y neurológicas directas inducidas por el virus, que parecen ser las responsables finales de la misma.

El SARS-CoV2 es neurotrópico mediante 2 mecanismos, la diseminación retrógrada hematógena y neuronal[12].

En la vía hematógena, el virus se une a los receptores de la Enzima Convertidora de Angiotensina 2 (ECA2), expresados en el endotelio capilar de la barrera hematoencefàlica (BHE), así infecta leucocitos y los disemina en el sistema nervioso central (SNC). La vía neuronal, es la otra ruta de entrada, el virus infecta las neuronas periféricas y las utilizan para generar transporte axonal y así ingresar al SNC a través del nervio olfatorio, ya que muchos receptores ECA2 se expresan ampliamente en las células epiteliales de la mucosa oral y nasal[15,18].

El SRAS-Cov2, induce tormentas de citoquinas, provocando inflamación sistémica con altos niveles de IL-6, IL-1β y TNFα.[19]; esto puede desencadenar lesión endotelial, por descomposición del colágeno y aumento de la permeabilidad de la BHE inducida por la metaloproteinasa-9 (MMP-9); que rompe el colágeno de la membrana basal de la pared vascular y una reacción inflamatoria disregulada por respuesta exagerada de los linfocitos T helper 1 (TH1) y macrófagos[20-22]. Esto podría explicar la inestabilidad aneurismática con rotura posterior y hemorragia subaracnoidea catastrófica en nuestro paciente.

La coexistencia de tromboembolismo pulmonar, es explicable por los fenómenos trombóticos que son cada vez más descritos y estudiados en COVID-19, se producen por disfunción endotelial y endotelitis que llevan a la formación de trombos. Se ha determinado la presencia de estructuras de inclusión viral en las células endoteliales que ingresan a través del receptor ECA2, reclutan células inmunes e inducen apoptosis. Además en los vasos pulmonares existe un síndrome trombo-inflamatorio obstructivo (MicroCLOTS), que se caracteriza por el desarrollo de trombosis pulmonar microvascular. Finalmente el endotelio está cubierto por una estructura que es el glicocálix, degradada directamente por el virus que desencadenaría todos los eventos descritos[9,23].

Conclusiones

El presente caso clínico es relevante al informar sobre la habilidad del virus para dañar el endotelio vascular de formas diversas, que van desde la propensión a la trombosis hasta la hemorragia y el debilatimiento vascular con rotura. Esperamos que la experiencia aquí presentada aporte nuevas herramientas para conocer la amplia gama clínica del SARS Cov2 y permita a la comunidad mèdica tener más instrumentos clínicos para diagnosticar éste mal.

Contribuciones de los autores

JV, SA, CM, WA, MP, ES participaron en la concepción, realización, redacción y revisión de la versión final.

Fuentes de financiamiento

Este artículo ha sido financiado por los autores.

Conflicto de interés

Los autores declaran no tener ningún conflicto de interés.

Referencias bibliográficas

1. Organización Mundial de la Salud. Nuevo coronavirus 2019 (COVID-19) [Internet]. Oms. 2020 [cited 2020 Jul 8]. Available from: https://www.who.int/es/emergencies/diseases/novel-coronavirus-2019
2. Pons S, Fodil S, Azoulay E, Zafrani L. The vascular endothelium: the cornerstone of organ dysfunction in severe SARS-CoV-2 infection. Crit Care [Internet]. 2020 Dec 16;24(1):353. Available from: https://ccforum.biomedcentral.com/articles/10.1186/s13054-020-03062-7
3. Klok FA, Kruip MJHA, van der Meer NJM, Arbous MS, Gommers DAMPJ, Kant KM, et al. Incidence of thrombotic complications in critically ill ICU patients with COVID-19. Thromb Res [Internet]. 2020 Jul;191(January):145–7. Available from: https://linkinghub.elsevier.com/retrieve/pii/S0049384820301201
4. Thachil J, Srivastava A. SARS-2 Coronavirus–Associated Hemostatic Lung Abnormality in COVID-19: Is It Pulmonary Thrombosis or Pulmonary Embolism? Semin Thromb Hemost [Internet]. 2020 May 12;1(212). Available from: http://www.thieme-connect.de/DOI/DOI?10.1055/s-0040-1712155
5. Franco-López Á, Poveda JE, Gilabert NV. Tromboembolismo Pulmonar en los pacientes con COVID-19. Angiografía con tomografía computarizada: resultados preliminares. J Negat No Posit Results. 2019;5(6):616–30.
6. Xie Y, Wang X, Yang P, Zhang S. COVID-19 Complicated by Acute Pulmonary Embolism. Radiol Cardiothorac Imaging [Internet]. 2020 Apr 1;2(2):e200067. Available from: http://pubs.rsna.org/doi/10.1148/ryct.2020200067
7. Ioan A-M, Durante-López A, Martínez-Milla J, Pérez-Calvo C, Santos A. Pulmonary embolism in COVID-19. When nothing is what it seems. Rev Española Cardiol (English Ed [Internet]. 2020 Apr;(x):3–5. Available from: https://linkinghub.elsevier.com/retrieve/pii/S1885585720301705
8. Pons S, Fodil S, Azoulay E, Zafrani L. The vascular endothelium: The cornerstone of organ dysfunction in severe SARS-CoV-2 infection. Crit Care. 2020;24(1):4–11.
9. Ciceri, F.; Beretta, L.; Scandroglio, A.M.; Colombo, S.; Landoni, G.; Ruggeri, A.; Peccatori, J.; D'Angelo, A.; De Cobelli, F.; Rovere-Querini, P.; et al. microvascular COVID-19 lung vessels obstructive thromboinflammatory syndrome (MicroCLOTS): An atypical acute respiratory distress syndrome working hypothesis. Crit. Care Resusc. 2020. Available online: https://pubmed.ncbi.nlm.nih.gov/32294809/(accessed on 30 May 2020).
10. Bonetti, P.O.; Lerman, L.O.; Lerman, A. Endothelial dysfunction: A marker of atherosclerotic risk. Arterioscler. Thromb. Vasc. Biol. 2003, 23, 168–175. [CrossRef] [PubMed]
11. Spence JD. Cryptogenic Stroke. N Engl J Med [Internet]. 2016 Sep 15;375(11):e26. Available from: http://www.nejm.org/doi/10.1056/NEJMc1609156
12. Moriguchi T, Harii N, Goto J, Harada D, Sugawara H, Takamino J, et al. A first case of meningitis/encephalitis associated with SARS-Coronavirus-2. Int J Infect Dis [Internet]. 2020 May;94(-January):55–8. Available from: https://linkinghub.elsevier.com/retrieve/pii/S1201971220301958
13. Aguayo, Santiago; Mora, Christian; Proaño, María; Revelo, Edwin; Vélez J. Accidente cerebrovascular trombótico en paciente con COVID-19, reporte de un caso. Rev científica INSPILIP [Internet]. 2020;(May):0–12. Available from: http://www.inspilip.gob.ec/
14. Bohmwald K, Gálvez NMS, Ríos M, Kalergis AM. Neurologic Alterations Due to Respiratory Virus Infections. Front Cell Neurosci [Internet]. 2018 Oct 26;12(October):1–15. Available from: https://www.frontiersin.org/article/10.3389/fncel.2018.00386/full
15. Guo Y, Korteweg C, McNutt MA, Gu J. Pathogenetic mechanisms of severe acute respiratory syndrome. Virus Res [Internet]. 2008 Apr;133(1):4–12. Available from: https://linkinghub.elsevier.com/retrieve/pii/S0168170207002663
16. Backer JA, Klinkenberg D, Wallinga J. Incubation period of 2019 novel coronavirus (2019-nCoV) infections among travellers from Wuhan, China, 20–28 January 2020. Eurosurveillance [Internet]. 2020 Feb 6;25(5):1–6. Available from: https://www.eurosurveillance.org/content/10.2807/1560-7917.ES.2020.25.5.2000062
17. Bansal M. Cardiovascular disease and COVID-19. Diabetes Metab Syndr Clin Res Rev [Internet]. 2020 May;14(3):247–50. Available from: https://linkinghub.elsevier.com/retrieve/pii/S1871402120300539
18. Xu H, Zhong L, Deng J, Peng J, Dan H, Zeng X, et al. High expression of ACE2 receptor of 2019-nCoV on the epithelial cells of oral mucosa. Int J Oral Sci [Internet]. 2020 Dec 24;12(1):8. Available from: http://dx.doi.org/10.1038/s41368-020-0074-x
19. Muhammad S, Haasbach E, Kotchourko M, Strigli A, Krenz A, Ridder DA, et al. Influenza virus infection aggravates stroke outcome. Stroke. 2011;42(3):783–91.
20. Hackenberg KAM, Rajabzadeh-Oghaz H, Dreier R, Buchholz BA, Navid A, Rocke DM, et al. Collagen Turnover in Relation to Risk Factors and Hemodynamics in Human Intracranial Aneurysms. Stroke. 2020;1624–8.
21. Zhang HF, Zhao MG, Liang GB, Yu CY, He W, Li ZQ, et al. Dysregulation of CD4+ T Cell Subsets in Intracranial Aneurysm. DNA Cell Biol. 2016;35(2):96–103.
22. Hasan D, Hashimoto T, Kung D, Loch MacDonald R, Richard Winn H, Heistad D. Upregulation of cyclooxygenase-2 (COX-2) and microsomal prostaglandin E2 synthase-1 (mPGES-1) in wall of ruptured human cerebral aneurysms: Preliminary results. Stroke. 2012;43(7):1964–7.
23. Varga, Z., Flammer, A. J., Steiger, P., Haberecker, M., Andermatt, R., Zinkernagel, A. S., Mehra, M. R., Schuepbach, R. A., Ruschitzka, F., & Moch, H. (2020). Endothelial cell infection and endotheliitis in COVID-19. The Lancet, 395(10234). https://doi.org/10.1016/S0140-6736(20)30937-5

Received: 24 Septiembre 2020
Accepted: 20 Octubre 2020

REVIEW / ARTÍCULO DE REVISIÓN

Therapeutic Approach For COVID-19 – Clinical Challenges And Implementation

Faizan Ahmad[1*], Abhichandan Das[2], Shariq Suleman[3], Upasana Pathak[2] and Sabiha Naaz[3]
DOI. 10.21931/RB/2020.05.04.22

Abstract: SAR-CoV-2 originated from China with first case reporting from Wuhan, has been declared as pandemic by WHO on March 11 2020, which has affected millions of people around the globe with 213 countries and territories infected worldwide. It has caused the death of around 0.6 million individuals with no specific or promising vaccines or treatment available until now to prevent COVID 19, which has been approved; this has led the world to a global crisis not only on the health front but also affected the economic sectors. Researchers across the globe are working around the clock with their level best to discover promising therapeutic approaches for COVID 19, but till now for the treatment, only 3 therapeutics have been approved, including dexamethasone in U.K. and Japan, Avigan in Russia, Italy, and China and remdesivir in Japan and Australia; also convalescent plasma therapy is seen to be effective in critical cases of COVID-19, however, there are limitations with the use of this plasma therapy like the time point of treatment, optimal dose as the dose may vary with number of patients the particular therapeutic effects of convalescent plasma therapy will be further explored in randomized clinical trials. Several complete multinational studies are investigating alternative therapies. More than 100 countries entered a cooperation to evaluate applicants for high-profile COVID-19 diagnosis with this most massive WHO's cooperation. According to WHO's information, there are 28 vaccine candidates under clinical evaluation, with 6 of them entering phase 3. This review emphasizes the allopathic approaches along with the Chinese herbal medicine for the prevention of COVID-19. This paper also includes a brief discussion on the vaccine and nutritional supplements.

KeyWords: SAR-CoV-2, COVID-19, therapeutics, drugs, vaccines.

Introduction

The novel coronavirus (Severe Acute Respiratory Syndrome Coronavirus 2) is the epigenetic modification of COVID-19, which was first identified at the end of 2019 in Wuhan, China[1,2]. The SARS-CoV and SARS-CoV-2 spike proteins are 77.5% identical to the primary A.A. (amino acid) sequence and bind to ACE2 protein (human angiotensin-converting-enzyme -2) as RBD (Receptor Binding Domain) bind firmly to ACE2 receptors present in human and bat[3]. Researchers found that SARS-CoV-2 RBD has a higher binding affinity than SARS-CoV RBD to receptor ACE2[3].

Due to the rapid increase in this CoV disease, on January, 31 World Health Organization (WHO) declared COVID-19 a public health emergency of international concern[2]. The virus has infected >3 million people around the globe and killed > 2 lakh people worldwide[2]. On March 11 2020, COVID-19 was declared as a pandemic disease by WHO[4]. SARS CoV2 is mainly transmitted in humans to humans through coughing and sneezing, leading to severe complications like septic shock, coagulation dysfunction, ARDS with multiple organ failure[4]. Looking into the rapid increase in patient numbers daily, required for promising therapeutic intervention[1].

In this review, almost all therapeutic approach is available for the COVID-19 treatment ranging from drugs to Chinese herbal medicine, vaccines and convalescent plasma therapy has been discussed[1,5].

Drugs and treatments available

COVID-19 has been considered one of the biggest challenges in the modern era faced by medicine. Scientists and researchers are continually seeking remedies and medications to save infectious people's lives and maybe even avoid infection. Though F.D.A has yet not approved any drug completely, but It provided authorization for emergency usage to others, with some of them being widely used, others giving promising evidence, and few of them being used as a tentative alternative.

Some of the drugs have been discussed below.

ANTIMALARIAL

Choloroquine and Hydroxychloroquine

Mechanism of action - Inhibition of RNA and DNA polymerase enzymes and inhibition of ACE2 cellular receptor. It was initially used to treat malaria and later approved for other diseases such as lupus, and rheumatoid arthritis, a less toxic version of chloroquine is known as hydroxychloroquine. This drug proved as one of the most controversial drugs during the initial phase Scientists have found that both medications will inhibit the coronavirus from replicating in cells during the small studies but later in March, WHO launched a randomized clinical trial to check the effectiveness of the drug against COVID-19[6,7].

RNA DEPENDENT

Remdesiver (GS-5734)

Mechanism of action - Drug evades proofreading by viral exoribonuclease enzyme[8].

It was the first drug to get the FDA's emergency authorization; this was initially tested against Ebola and Hepatitis C. Initial findings from the trials which began this season indicated that the medication might shorten the recovery period for people hospitalized with Covid-19 from 15 to 11 days[8,9].

[1] Department of Medical Elementology and Toxicology, Jamia Hamdard, Delhi, India.
[2] Centre for Biotechnology and Bioinformatics, Dibrugarh University, Assam, India.
[3] Department of Biotechnology, Jamia Hamdard, Delhi, India.

Corresponding author: 1996faizanahmad@gmail.com

Favipiravir

Mechanism of action - Inhibits viral RNA synthesis[9].

Initially used for influenza, shows mixed evidence in its use against COVID-19 during trials. Limited research carried out in March suggested the medication could be effective in expunging the coronavirus from the airway, although the findings of broader, well-designed clinical trials are still awaited[8,9].

Ribavirin

Mechanism of action – It is a nucleoside inhibitor that stops viral mRNA capping and viral RNA synthesis[7,8,9].

The antiviral properties of Ribavirin on the immune system was 1st observed with the treatment of hepatitis. It was also used for the treatment during SARS and MERS outbreak, which significantly showed the viral load reduction when given individually or in other antiviral drugs. A phase 2 randomized trial was conducted for COVID-19 when a combination of drug, including ribavirin (oral nucleoside analog), interferon beta-1b (injectable), and lopinavir-ritonavir (oral protease inhibitor) was found to be effective in suppressing COVID-19 although this study had several limitations[9,10,11].

SUPPORTIVE THERAPY

Tocilizumab

Mechanism of action – Inhibited IL-6-mediated signaling[10].

Tocilizumab belongs to the IgG1 class, a recombinant humanized monoclonal antibody, Aimed at both the soluble and the Interleukin's membranous forms receptor 6 (IL-6). It was initially used to treat severe rheumatoid arthritis, systemic juvenile idiopathic arthritis, giant cell arteritis, and life-threatening cytokine release syndrome induced by chimeric antigen receptor T cell therapy. In a study, the patients were treated with Either intravenous or subcutaneous tocilizumab, and the quality of care relative to routine practice. The correlation with tocilizumab usage became greater during reviews of the total mortality risk separately, although the study had many limitations as the comparison was not randomized[11,12].

Sarilimuab

Mechanism of action – Binds to membrane-bound receptors & soluble IL-6 receptors (sIL-6 R & mIL-6 R)[3].

Sarilimuab precisely binds to the IL-6 receptor and demonstrates to block IL-6-mediated signaling. IL-6 is an immune system protein developed in high quantities in rheumatoid arthritis patients and correlated with disease development, joint damage, and other systemic problems. It is being tested for it's potential to suppress COVID-19-associated overactive inflammatory immune response based on reports of significantly elevated rates of IL-6 in seriously ill coronavirus patients. But during the phase 3 trial of sarilimuab (kevzara) in the U.S., it was announced that the use of this drug requires mechanical ventilation and did not fulfill its primary and secondary endpoints when compared with placebo; depending on this result, the trial has been stopped[11].

Siltuximab

Mechanism of action – Binds to both membrane-bound receptors & soluble IL-6 receptors (sIL-6R & mIL-6R)[12].

Siltuximab is an IL-6 focused mAb approved by the United States Food and Drug Administration (FDA) and the European Medicines Agency (EMA), among other regulatory bodies, for the treatment of patients with multicentered Castleman disease (MCD) who are found to be negative in human immunodeficiency virus (HIV) and human herpesvirus-8 (HHV-8). As it is an inhibitor of IL-6, Prevents the escalation of IL-6 in the cytokine storm responsible for getting the elevated CRP concentrations during COVID-19. However, the drug has been approved for several clinical trials but has not been approved by the FDA for complications related to COVID-19[13].

Leronliamb

Mechanism of action - Leronliamb mitigate cytokine storm and enhance immune response[8].

Leronlimab is a humanized IgG4 mAb research that blocks CCR5, a cellular receptor significant in HIV infection, tumor metastases, and other diseases like NASH. Recently, a small clinical study found that leronlimab would minimize viral load from plasma and help rebuild the COVID-19 patient immune system. Within seven days of diagnosis, seriously ill patients reported rapid immune regeneration and extubation, according to IncellDx;. However, this was a small-scale study, although extensive randomized placebo-based studies are also going on to evaluate drug efficacy, where it has shown positive results[8].

Anakinra

Mechanism of action - Inhibit binding of IL-1 beta & IL-1 alpha to the IL-1 type-1- receptor (IL-1R1)[12].

Anakinra is a non-glycosylated recombinant 17 kD Human receptor antagonist IL-1, with a limited half-life about 3–4 hours, with a strong health profile. It has been used for the treatment of rheumatoid arthritis. In a study, it was observed that this drug had been proved effective in the hyperinflammatory phase of COVID-19 where the level of CRP decreases with anakinra treated patient, and the respiratory functions have also seen improving; although, it also had several limitations like all other drugs and immunomodulators being considered[13].

SOME DIFFERENT DRUGS USED FOR TREATMENT OF COVID-19

Corticosteroids

Both advantageous and injurious clinical effects have been documented in patients with other pulmonary infections, using corticosteroids (mostly prednisone or methylprednisolone), but Corticosteroids were examined with contradictory findings in critically ill patients with an acute respiratory distress syndrome (ARDS). Seven randomized, controlled trials, which included 851 patients, assessed corticosteroid use in ARDS patients. A meta-analysis of these test results showed that corticosteroid therapy lowered all-cause mortality risk compared to placebo. The COVID-19 Treatment Guidelines Panel (the Panel) suggested using dexamethasone based on a preliminary report from the RECOVERY trial, for the patients who are mechanically ventilated or either require supplement oxygen. However, the patients that do not require supplemental oxygen should not be given dexamethasone. In case it is not available other alternative glucocorticoids such as prednisone, methylprednisolone, or hydrocortisone are recommended. However, there is a risk of adverse side effects with these drug-drug interactions that should be closely monitored[14].

Metronidazole

Metronidazole is an antibiotic category of nitro-imidazole that has the potential to cure infectious diseases which have also been used to cure COVID-19; the treatment with this drug

to COVID-19 patients led to an appropriate cytokine reduction stated by Gharebaghi et al., the main concern here is the effect of this drug on the significant cytokine reduction. In a study, IL-12 has been proved as a marker that can further help researchers identify patients infected with COVID-19 during early infection, MTZ inhibits IL-12 from binding to the IL-12 receptors by altering the surface and volume of IL-12. Few other drugs such as metronidazole phosphate, metronidazole benzoate, acyclovir, tetrahydrobiopterin, and 1- [1- (2- hydroxyethyl) -5-nitroimidazole-2-yl] - N-methylmethanimine oxide have also been approved by the U.S. Food and Drug Administration (FDA) during their virtual screening as they work in the same manner like MTZ. Other reasons can be modifications in the position of methyl and hydroxyl functional groups in MTZ have triggered IL-12 active sites' inhibition. Therefore, this drug can be hope in COVID-19 treatment[15].

Bronchodilators

Bronchodilators are the medicine that relaxes the lungs' muscle and widens the bronchi, making patient breathing easier. Mainly there are three types of bronchodilators which are Beta 2 agonists, Anticholinergics, and Theophylline[16].

It is useful in treating patients of COVID-19 who has a history of chronic obstructive pulmonary disease (COPD) or underlying asthma[3].

Anticoagulant

Anticoagulants are medicines that prevent blood clots. The most common anticoagulant is warfarin, and some different anticoagulants are rivaroxaban, dabigatran, apixaban, and edoxaban. The Anti-coagulation is not recommended for the COVID -19 patient who has confirmed Venous thromboembolism (VTE)[3].

Convalescent plasma therapy

Convalescent plasma is adoptive immunotherapy that was practiced in the 1918 influenza epidemic to save from viruses and protect the lungs from severe damage[18]. In the 1918 crisis of influenza, A (H1N1) virus, early implementation of convalescent blood products decreased the absolute risk of pneumonia-related mortality up to 21%[19]. Neutralizing antibodies adhere to the spike-protein virus, which contributes to confirmation of the spike and could cause the peculiar result of better access into human cells through the IgFc- receptor[20]. Convalescent Plasma therapy is the antibody-dependent enhancement of entry (ADE). A convalescent plasma therapy blood sample is collected from the person who recovers from COVID-19 infection, and then serum is isolated from the sample[5]. The separated serum containing antibodies generated against the target antigen is given in the infected person to combat the virus's infection. As antibodies bind to the antigen, the immune response is neutralized or activated[29]. Hence, identifying the monoclonal-antibody of humans that neutralizes SARS-COV-2 5. Until now, there is no effective treatment for SARS-COV-2 because of the absence of evidence[22]. Convalescent plasma therapy is effective as antibodies from convalescent plasma suppress viremia[22]. Immunoglobulin's or convalescent plasma is seen to be effective in critically ill patients. The convalescent treated patient has to stay in the hospital for a shorter period with a lower mortality rate in patients who are not treated with convalescent plasma[24]. The primary immune response is usually response development in patients during 10 to 14 days, followed by virus clearance[22]. According to the Public Republic of China National Health Commission, convalescent therapy diagnosis will fellow principle[1]. First, the disease course should not extend 3 weeks, as well as the patient should have positive viremia or viral nucleic acid certified by clinical experts. Second, their plasma infusion dose is determined for critically ill patients according to the patient's weight 200-500ml (45 ml/kg) and depends upon the clinical situation[24]. According to the study, 5 patients with a reported COVID-19 & ARDS (Acute Respiratory Disease Syndrome) case obtained convalescent plasma with 2 consecutive transfusions of 200 ml - 250 ml of convalescent plasma with a cumulative dose of 400 ml[25]. After convalescent plasma infusion within a 3 day body temperature normalized in 4 to 5 patients, and the score of sequential organ failure access (SOFA) decreased[25]. Patients were negative with SARS COV2 neutralizing antibodies within 12 days of

Serial no	Interventions	Funding Agency	Phase of trial	Beginning of trial	Estimated end
1.	Chloroquine	University of Oxford	N/A	MAY 2020	MAY 2022
2.	Remdesivir	Capital Medical University	3	05-02-2020	27-04-2020
3.	Hydroxychloroquine	Shanghai Public Health Clinical Center	3	6-02-2020	31-12-2020
4.	Human immunoglobulin	Peking Union Medical College Hospital	2&3	10-02-2020	30-06-2020
5.	Arbidol (umifenovir)	Jieming QU, Ruijin Hospital	4	7-02-2020	30-12-2020
6.	Recombinant human interferon alpha2 beta	Tongji Hospital	1	1-03-2020	30-06-2020
7.	Darunavi cobicistat Combination	Shanghai Public Health Clinical Center	3	30-01-2020	31-12-2020
8.	Thalidomide	First Affiliated Hospital of Wenzhou Medical University	2	18-02-2020	30-05-2020
9.	Methylprednisolone	Peking Union Medical College Hospital	2	26-01-2020	25-12-2020
10.	Combinations foseltamivir, favipiravir, and chloroquine	Rajavithi Hospital	3	15-03-2020	30-11-2020
11.	Xiyanping Combined with lopinavir-ritonavir	Jiangxi Qingfeng Pharmaceutic al	N/A	14-03-2020	14-04-2021
12.	Xiyanping combined with lopinavir-ritonavir	Jiangxi Qingfeng Pharmaceutic al	N/A	19-02-2020	14-12-2020
13.	TCM combination with lopinavir-ritonavir, a-interferon via aerosol	Beijing302 Hospital	N/A	22-01-2020	22-01-2021
14.	Bromhexine hydrochloride	Second Affiliated Hospital of Wenzhou Medical University	N/A	16-02- 2020	30-04- 2020
15.	Fingolimod	1°Affiliated Hospital of Wenzhou Medical University	2	22-02-2020	1-06-2020
16.	Bevacizumab	Qilu Hospital of Shandong University	2 and 3	FEBRUARY Y 2020	MAY 2020
17.	Ivermectin	Monash University in Melbourne, Australia	In-vitro laboratory study	further clinical trials need to be completed	further clinical trials need to be completed

Table 1. Clinical trials of drugs for COVID-19[17].

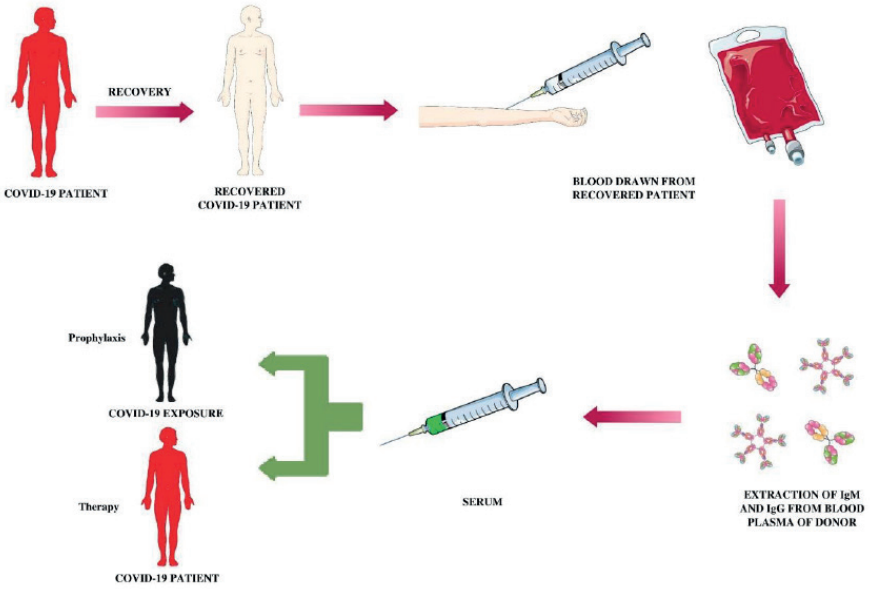

Figure 1. Convalescent plasma therapy path.

transfusion, and 14 patients recovered from ARDS after 12 days of transfusion, and within the 2 weeks of treatment, 3 patients were weaved from ventilation[3]. After convalescent plasma transfusion, there is a reduction in pulmonary lesions during chest C.T. examination of the patient. There are no severe adverse effects reported so convalescent plasma therapy could be successful in patients infected with SARS-COV-2[25].

Vaccine

Vaccines play a crucial role in not only protecting an individual but the entire community, as it trains the body's immune system to identify and attack against the virus while encountering it. At present more than 100 projects are being worked on around the world for the COVID-19 vaccine. Many collaborations have formed around the globe, such as COVAX, with 150 countries involved. COVAX is co-led by Gavi, the Coalition for Epidemic Preparedness Innovations (CEPI), and the WHO. Its goal is to promote the production and manufacture of COVID-19 vaccines and ensure equal and reasonable access for all countries globally. The ACT Accelerator is a ground-breaking global partnership to speed up the growth, output, and equal access to COVID-19 studies, treatments, and vaccinations[18,19,28,29].

Several vaccines are under clinical and pre-clinical trials, and researchers are putting their best to discover a vaccine against this novel coronavirus. According to the document drafted by the world health organization, vaccines include 26 candidate vaccines under clinical trial with candidates including viral vectors, RNA, DNA, protein subunits; apart from these, 139 candidates are under pre-clinical evaluation. Some of the vaccines under clinical trial are discussed below.

RNA vaccine

There are 5 RNA vaccines under clinical trial currently with the first one being 1273 mRNA vaccine developed by Modern Tx Inc and NIAID (Cambridge, MA, USA) convert SAR COV2 viral protein sequence into mRNA when induced into the body[34,35]. This vaccine is encapsulated within a lipid-nanoparticle and developed by the SARS- COV-2 virus against spike glycoprotein(s) where the administration route is intramuscular. The mRNA-1273 is under phase 3 clinical trial (NCT no.- NCT04470427). Another one is BioNTech/Fosun Pharma/Pfizer with vaccine candidate 3 LNP mRNAs being in phase 3 with the route of administration intramuscular; the rest are in phase 1 and 2 with trails still going on[18,19,28,29].

DNA vaccine

There is 4 DNA vaccine with all of them being in phase 1/2 where vaccine candidates are DNA plasmid either with adjuvant or with electroporation with intradermal/ intramuscular route of administration[18,19,28,29].

Virus-Like Particle Vaccine

There is only one VLP vaccine under clinical evaluation sponsored by Medicago Inc., where the candidate is plant-derived VLP adjuvanted with GSK or Dynavax adds administered through intramuscular route under phase 1 clinical trial[18,19,28,29].

Protein Subunit Vaccine

There are 7 vaccine candidates out of which the one in phase 2 clinical trial is manufactured by Anhui Zhifei Longcom Biologic Pharmacy Co., Ltd. Where vaccine candidate is Adjuvanted recombinant protein (RBD-Dimer) administered through the intramuscular route. The other 6 are either in phase 1/2 or in phase 1,[18,19,28,29].

Non-Replicating Viral Vector Vaccine

There are 4 vaccines under clinical evaluation from which the one manufactured by the University of Oxford/AstraZeneca with vaccine candidate ChAdOx1-S is administered through intramuscular route in under phase 3 of the clinical trial while the rest is in phase ½,[18,19,28,29].

Traditional Chinese Herbal (TCM) medicine

The government of China uses TCM (Traditional Chinese Medicine) with conventional medicine in approximately 26 provinces to treat COVID-19. On February 17, the NHC (National Health Commission) of the Public Republic of China treatment 85.20% of the total confirmed cases with TCM. Till March 1 2020, almost 50 trials (16.5%) out of 303 ongoing clinical trials include using TCM 14 cases (4.6%), including combined treatment with western medicine & TCM[29,30]. Below, the list of Traditional Chinese Medicine has been discussed.

S.NO	COMPANY	TYPE OF VACCINE	PHASE
1.	University of Oxford/AstraZeneca	ChAdOx1-S	PHASE 3
2.	CanSino Biological Inc./Beijing Institute of Biotechnology	Adenovirus Type 5 Vector	PHASE 3
3.	Gamaleya Research Institute	Adeno-based (rAd26-S+rAd5-S)	PHASE3
4.	Sinovac	Inactivated	PHASE 3
5.	Beijing Institute of Biological Products/Sinopharm	Inactivated	PHASE 3
6.	Moderna/NIAID	LNP-encapsulated mRNA	PHASE 3
7.	BioNTech/Fosun Pharma/Pfizer	3 LNP-mRNAs	PHASE 3
8.	Anhui Zhifei Longcom Biopharmaceutical/Institute of Microbiology, Chinese Academy of Sciences	The adjuvanted recombinant protein (RBD-Dimer)	PHASE 2
9.	Novavax	Full-length recombinant SARS CoV-2 glycoprotein nanoparticle vaccine adjuvanted with Matrix M	PHASE 2
10.	Curevac	mRNA	PHASE 2
11.	Institute of Medical Biology, Chinese Academy of Medical Sciences	Inactivated	PHASE 1/2
12.	Research Institute for Biological Safety Problems, Rep of Kazakhstan	Inactivated	PHASE 1/2
13.	Inovio Pharmaceuticals/ International Vaccine Institute	DNA plasmid vaccine with electroporation	PHASE 1/2
14.	Osaka University/ AnGes/ Takara Bio	DNA plasmid vaccine + Adjuvant	PHASE 1/2
15.	Cadila Healthcare Limited	DNA plasmid vaccine	PHASE 1/2
16.	Genexine Consortium	DNA Vaccine (GX-19)	PHASE 1/2
17.	Bharat Biotech	Whole-Virion Inactivated	PHASE 1/2
18.	Janssen Pharmaceutical Companies	Ad26COVS1	PHASE 1/2
19.	Kentucky Bioprocessing, Inc	RBD-based	PHASE 1/2
20.	Sanofi Pasteur/GSK	S protein (baculovirus production)	PHASE 1/2
21.	Arcturus/Duke-NUS	mRNA	PHASE 1/2
23.	Clover Biopharmaceuticals Inc./GSK/Dynavax	Native like Trimeric subunit Spike Protein vaccine	PHASE 1
24.	Vaxine Pty Ltd/Medytox	Recombinant spike protein with Advax™ adjuvant	PHASE 1
25.	University of Queensland/CSL/Seqirus	Molecular clamp stabilized Spike protein with MF59 adjuvant	PHASE 1
26.	Medigen Vaccine Biologics Corporation/NIAID/Dynavax	S-2P protein + CpG 1018	PHASE 1
27.	Instituto Finlay de Vacunas, Cuba	RBD + Adjuvant	PHASE 1
28.	FBRI SRC VB VECTOR, Rospotrebnadzor, Koltsovo	Peptide	PHASE 1
29.	West China Hospital, Sichuan University	RBD (baculovirus production expressed in Sf9 cells)	PHASE 1
30.	Institute Pasteur/Themis/Univ. of Pittsburg CVR/Merck Sharp & Dohme	Measles-vector based	PHASE 1
31.	Imperial College London	LNP-nCoVsaRNA	PHASE 1
32.	People's Liberation Army (PLA) Academy of Military Sciences/Walvax Biotech.	mRNA	PHASE 1
33.	Medicago Inc.	Plant-derived VLP adjuvanted with GSK or Dynavax adjs.	PHASE 1

Table 2. Different types of vaccine for trial[28].

S.NO	TCM NAME	PHASE
1.	*Tan Re Qing Capsules*	0
2.	*Tan ReQing Injection*	4
3.	*Xue Bi Jing Injection*	0
4.	*Lian Hua Qing Wen Capsule /Granule*	4
5.	*Jing Yin Granule*	4
6.	*Gu Biao Jie Du Ling*	0
7.	*Re Du Ning Injection*	0
8.	*Xi Yan Ping Injection*	4
9.	*Shuang Huang Lian Oral Liquid*	4
10	*Shen Qi Fu Zheng Injection*	4
11.	*Shen Fu Injection*	4
12.	*Kang BingDu Granules*	4
13.	*Jin Yin Hua Tang*	0
14.	*Ke Su Ting Syrup /Ke Qing Capsule*	4

Table 3. Different types of Chinese herbal medicine[29,30].

Micronutrients

Various micronutrients like iron, zinc, vitamin A, C, D, and selenium play a vital role in our immunocompetence[31,32]. We will discuss some micronutrients that are essential for decreasing the risk of COVID-19[31,32].

Vitamin D

Vitamin D has the property to regenerate epithelial lining and can alleviate acquired immunity[27]. Based on a meta-analysis, vitamin D plays a vital role in minimizing the alveolar damage during Acute Respiratory Tract Infection. Evidence showed that vitamin D has an almost 12% protective effect against viral and bacterial respiratory tract infection so, supplementation intake needs to be started before infection. The mechanism behind the use of Vitamin D lies in the stimulation of cathelicidins and defensins that we can increase the concentration of Anti-inflammatory cytokines and reduce the level of pro-inflammatory cytokines can induce inflammation and pneumonia. Vitamin D also decreases the replication of viruses, so, based on this data, vitamin D can play an influential role in decreasing the role of COVID-19[31,32].

Vitamin A

Vitamin A deficiency people are more prone to viral infection and various other influenza, measles, virus, etc. Vitamin A enhances the level and function of N.K. (Natural-Killer Cells), B-cells, T-cells, neutrophils, and macrophages or monocytes[31,32].

Vitamin C (L-ascorbic acid)

In early days literature, high doses of intravenous Vitamin C during sepsis during ARDS have a protective effect[31,32]. HDIVC reduces DNA plasma cells, which play a significant role in sepsis-induced multiple organ failure inflammations. Thus, vitamin C can be useful micronutrients that can decrease the risk of COVID -19[31,32].

Conclusions

Global vaccination study and engineering initiative to tackle the pandemic COVID-19 had no history on pace and scale. The R & D area's frequency suggests that vaccines under

emergency usage or related protocols should be accessible by early 2021. It will mark a significant shift from the conventional vaccine delivery process, which requires more than 10 years on average compared to the rapid 5-year production cycle for the first Ebola vaccine. This novel vaccine production includes phases of concurrent and competitive growth, creative regulatory processes, and production capability scaling. Along with the vaccines, scientists and researchers worldwide are working day and night on drugs and immunotherapy that would be proven effective and efficient in fighting a pandemic number of drugs and immunomodulators under randomized clinical trials. However, none of them has got the approval from FDA, but these vaccines and drug can be the only effective way in which this world can combat this COVID-19 pandemic, which has affected not only the health sector but lead to a significant loss in the economic sector in countries around the globe.

Conflict of interest

The authors declare no conflict of interest.

Funding

No source of funding.

Bibliographic references

1. Divya R, Santosh D. Therapeutic Application of Chloroquine and Hydroxychloroquine in Clinical Trials for COVID-19: A systematic review. medRxiv preprint doi:https://doi.org/10.1101/2020.03.22.20040964
2. Arun G, Margherita B, Dana S et al. Drug Development and Medicinal Chemistry Efforts Toward SARS-Coronavirus and Covid-19 Therapeutics Chem Med Chem doi : https://doi.org/10.1002
3. Tim Smith, PharmD, BCPS; Jennifer Bushek, PharmD; Aimée LeClaire, PharmD, COVID-19 Drug Therapy BCPS; Tony Prosser, PharmD Clinical Drug Information | Clinical Solutions
4. Shudong Z, Xialing G, Kyla G et al. Emerging Therapeutic Strategies for COVID-19 Patients Discoveries 2020, Jan-Mar, 8(1): e105 DOI: 10.15190/d.2020.2
5. Govindarajan K, Venkadapathi J, Saminathan R et al. A short review on antibody therapy for COVID-19New Microbes and New Infections S2052-2975(20)30034-2 https://doi.org/10.1016/j.nmni.2020.100682
6. Emanuele N, Nicola P , Tomasso et.al. National Institute for the Infectious Diseases "L. Spallanzani", IRCCS. Recommendations for COVID-19 clinical management Infectious Disease Reports 2020; 12:8543 doi:10.4081/idr.2020.8543
7. Binqing F, Xialing Xu, Haiming Wei Fu. J Transl Med (2020) 18:164 https://doi.org/10.1186/s12967-020-02339-3
8. Jahan S. Khalili , Hai Zhu , Nga Sze Amanda Mak et.al, Novel coronavirus treatment with ribavirin: Groundwork for an evaluation concerning COVIDβ 19J Med Virol. 2020;92:740–746.
9. Dimitar P Treatment of Covid-19 Infection. A Rationale for Current and Future Pharmacological Approach E.C. Pulmonology and Respiratory Medicine 9.4 (2020):38-58
10. Ritesh G ,Anoop M et.al, Contentious issues and evolving concepts in the clinical presentation and management of patients with COVID-19 infection with reference to use of therapeutic and other drugs used in Co-morbid diseases (Hypertension, diabetes etc) Diabetes & Metabolic Syndrome: Clinical Research and & Reviews 14(2020) 1871-4021
11. Giovanni Guaraldi*, Marianna Meschiari*, Alessandro Cozzi-Lepri et al., tocilizumab in patients with severe COVID-19: a retrospective cohort study Lancet Rheumatol 2020; 2: e474–84 Published Online June 24, 2020 https://doi.org/10.1016/ S2665-9913(20)30173-9
12. Reza G, Fatemeh H, Mohammad M et al. Metronidazole; a Potential Novel Addition to the COVID19 Treatment Regimen Archives of Academic Emergency Medicine. 2020;8(1): e40
13. Naidi Y, Han S Targeting the Endocytic Pathway and Autophagy Process as a Novel Therapeutic Strategy in COVID-19 International Journal of Biological Sciences 2020; 16(10): 1724-1731. doi: 10.7150/ijbs.45498
14. Corticosteroids Coronavirus Disease COVID 19 https://www.covid19treatmentguidelines.nih.gov/immune-based-therapy/immunomodulators/corticosteroids
15. Zamora-Ledezma, C.; C., D.F.C.; Medina, E.; Sinche, F.; Vispo, N.S.; Dahoumane, S.A.; Alexis, F. Biomedical Science to Tackle the COVID-19 Pandemic: Current Status and Future Perspectives. Molecules 2020, 25, 4620. https://www.nhs.uk/conditions/bronchodilators/9/4/2020Bronchodilators - NHS
16. Judith Stewart COVID-19: Prevention & Investigational Treatments
17. Miguel M. Compounds with Therapeutic Potential against Novel Respiratory 2019 Coronavirus Antimicrobial Agents and Chemotherapy 64:e00399-20.https://doi.org/10 1128/AAC.00399-20.
18. Anne C , Hui G , David K . Treatment of COVID-19: old tricks for new challenges . Critical care (2020) 24:91 https://doi.org/10.1186/s13054-020-2818-6 COVID-19: Clinical information and treatment guidelines FIP Health Advisory 1-13
19. Cynthia L, Qiongqiong Z, Yingzhu Let al. Research and Development on Therapeutic Agents and Vaccines for COVID-19 and Related Human Coronavirus Disease ACS Central Science .2020,6,315-331
20. Yuxin Y, Woo S, Yoong P The First 75 Days of Novel Coronavirus (SARS-CoV-2) Outbreak: Recent Advances, Prevention, and Treatment Int. J. Environ. Res. Public Health 2020, 17, 2323; doi:10.3390/ijerph17072323
21. Wen C, Ulrich S, Peter H et al. Current Tropical Medicine Reports https://doi.org/10.1007/s40475-020-00201-6
22. Yang Y, Md I , Jin W et al. Int. J. Biol. Sci. 2020; 16(10): 1708-1717. doi: 10.7150/ijbs.45538
23. Deng Z , Kun W, Xue Z et al. Journal of Integrative Medicine In silico screening of Chinese herbal medicines with the potential to directly inhibit 2019 novel coronavirus
24. Amin G, Sadaf N, Torsak T et al. Individual risk management strategy and potential therapeutic options for the COVID-19 pandemic Clinical Immunology https://doi.org/10.1016/j.clim.2020.108409
25. Erin M, Jason P Coronavirus Disease 2019 Treatment: A Review of Early and Emerging Options DOI: 10.1093/ofid/ofaa105
26. Zamora-Ledezma, C.; C., D.F.C.; Medina, E.; Sinche, F.; Santiago Vispo, N.; Dahoumane, S.A.; Alexis, F. Biomedical Science to Tackle the COVID-19 Pandemic: Current Status and Future Perspectives. Molecules 2020, 25, 4620
27. Jun R, Al Z, Xi W Traditional Chinese medicine for COVID-19 treatment Pharmacological Research 155 (2020) 104743
28. Chang L Traditional Chinese medicine is a resource for drug discovery against 2019 novel coronavirus (SARS-CoV-2) Journal of Integrative Medicine https://doi.org/10.1016/j.joim.2020.02.004 2095-4964
29. Emanuela F. Vademecum for the treatment of people with COVID-19. Edition 2.0, 13 b. March 2020 Le Infezioni in Medicina, n. 2, 143-152, 2020
30. Pierre T, Xavier, Pascal M Collecting and evaluating convalescent plasma for COVID-19 treatment: why and how doi: 10.1111/vox.12926

Received: August 21 2020
Accepted: October 21 2020

REVIEW / ARTÍCULO DE REVISIÓN

Development of research on COVID-19 by the World Scientific Community in the first half of 2020

Daniel Tinôco[1*] and Suzana Borschiver[2]

DOI. 10.21931/RB/2020.05.04.23

Abstract: The World Scientific Community has carried out several studies on the novel coronavirus, responsible for the current COVID-19 pandemic. This study aimed to verify the development level and research evolution on COVID-19, summarizing experts' main trends in the first half of 2020. The most cited articles focused on understanding the disease, addressing aspects of its transmission, viral activity period, symptoms, health complications, risk factors, and the estimate of new cases. These papers also focused on the treatment/prevention and management of COVID-19. Several drugs and alternative treatments have been investigated, such as the convalescent plasma transfusion and stem cell transplantation, while an efficient vaccine is developed. Prevention and control measures, such as social isolation and immediate case identification, were also investigated. Therefore, the main COVID-19 trends were identified and classified in disease, treatment/prevention, and pandemic management, contributing to scientific understanding and future studies.

KeyWords: Novel coronavirus; SARS-CoV-2; COVID-19 scientific development; COVID-19 evolution; COVID-19 trends.

Introduction

At the end of December 2019, in Wuhan's city in China, a novel coronavirus appeared, responsible for a severe acute respiratory syndrome, similar to the one in 2003, called SARS-CoV-2. A month later, the World Health Organization (WHO) declared that the coronavirus disease 2019 (COVID-19) outbreak consisted of a Public Health Emergency of International Importance, after H1N1 (2009), Poliomyelitis (polio) (2014), Ebola in West Africa (2014), Zika (2016), and Ebola in the Democratic Republic of Congo (2019). In March 2020, WHO declared the COVID-19 pandemic[1].

In the first half of 2020 alone, the COVID-19 pandemic was marked by more than 11.6 million infected people, more than 500,000 deaths, and 216 affected countries worldwide, according to WHO. Until this moment, the USA and Brazil were the countries with most disease cases[2].

With the emergence and advancement of COVID-19, the world scientific community began a series of investigations and research to understand the behavior of the novel coronavirus in the human body, the consequences of the disease caused by it, and the most effective treatment for the combating of the COVID-19 pandemic. Furthermore, several studies have presented disease management guidelines or held discussions about implementing public health policies by the affected countries' governments[3,4]. Social isolation measures, rapid identification of suspected cases, and the tracking and follow-up of potential contacts between infected and non-infected were the main strategies suggested as efficient in preventing and controlling the COVID-19[4].

In this study, a prospection of scientific articles about COVID-19 was carried out, aiming to establish the scientific trajectory of the disease and identifying the development level of worldwide research on the novel coronavirus in recent months, specifically from February to June 2020. The selected papers were classified according to their approach, highlighting the transmission aspects, symptoms, risk factors, proposed treatments, clinical tests, and measures to prevent and control the disease.

Scientific Studies

China, the USA, and the U.K. were the countries with the most papers on COVID-19 cited by the scientific community. About 28% of the scientific investigations were performed by Chinese research institutions and universities, followed by 16% from the USA and 11% from the U.K. Several studies were conducted in hospitals by health professionals linked or not to the academy (Figure 1). Medical associations from different countries and national and international scientific research centers, such as the Centers for Disease Control and Prevention (USA) 5 have also developed research on the subject.

About 60% of the papers presented disease aspects, whose main nomenclatures were: COVID-19, SARS-CoV-2 (acute respiratory syndrome coronavirus 2), Novel coronavirus pneumonia, and Wuhan pneumonia. The novel coronavirus origin was attributed to two animals, the bat and the pangolin. For the bats, two types of viruses have been reported: bat-SL-CoVZC45 and bat-SL- CoVZXC21[6]. For the pangolins, the Pangolin-CoV was identified[7]. About 23% of the papers corresponded to the disease's treatment and prevention investigations, and 17% discussed COVID- 19 management (Figure 2). Many studies on the disease were due to the novelty of this virus, in which, despite the experience with Sars-CoV in 2003, little was known about the treatment and control forms. Therefore, in the first months, specialists investigated the disease mostly to understand it and control it.

Scientific Trajectory

The scientific trajectory revealed essential aspects for the understanding of the COVID-19. Approximately 70% of the papers discussed the disease in March 2020, 50% approached the treatment and prevention in February 2020, and 30% suggested management measures of disease in May 2020 (Figure 3). The search for treatment before a complete understanding of the disease can be explained by the novelty and the rapid advance of COVID-19, which in February 2020 required immediate action to control the infection. With the disease development and the scientific research advancement, about 67% of the investigations in June 2020 focused on understanding the disease.

[1] Department of Biochemical Engineering, School of Chemistry, Federal University of Rio de Janeiro, Brazil.
[2] Department of Organic Processes, School of Chemistry, Federal University of Rio de Janeiro, Brazil.

Corresponding author: dneto@peq.coppe.ufrj.br

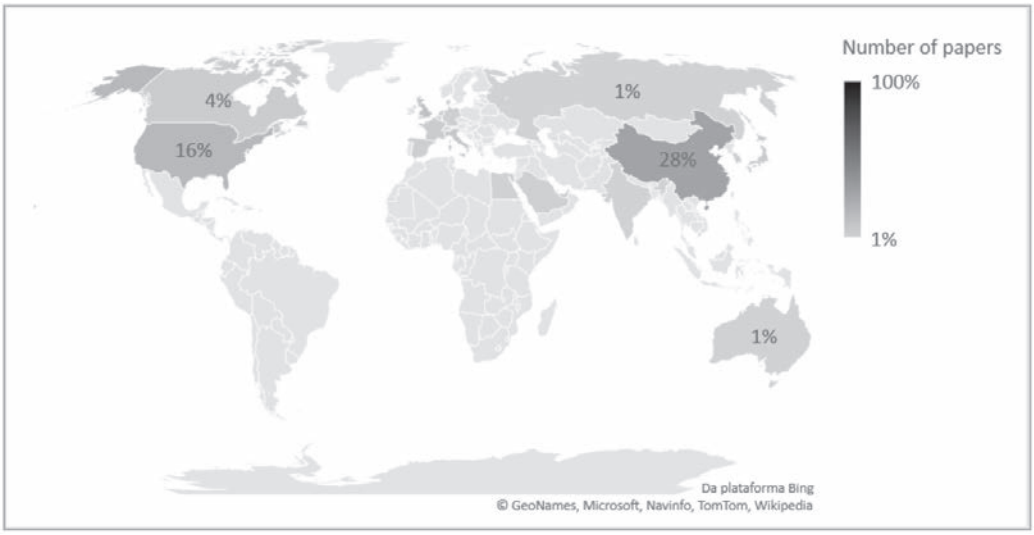

Figure 1. The most cited papers on COVID-19 by country.

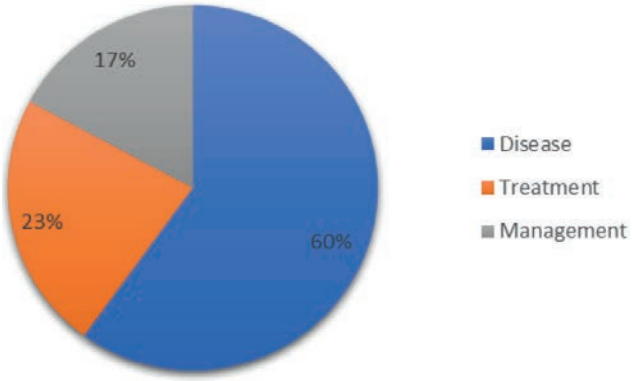

Figure 2. Main approaches on COVID-19 of the most cited papers.

Disease

COVID-19 was characterized as flu, capable of generating complications in the human respiratory system, such as pneumonia. People with comorbidities or old age were more prone to the most severe disease stage, transmitted through direct contact with infected people and the air. The symptomatic period was more extended than that of ordinary flu, and the transmissibility and infectivity were considered more significant than SARS-CoV, with the prediction of many more contaminated and deaths. The research focus reporting the disease has varied over the months. In February 2020, the concern was to predict the disease's behavior, while in June 2020, it was to identify the health complications caused by COVID-19. The other disease aspects, such as transmission, time, symptoms, and risk factors, were addressed according to their identification and occurrence in the infected people (Figure 4).

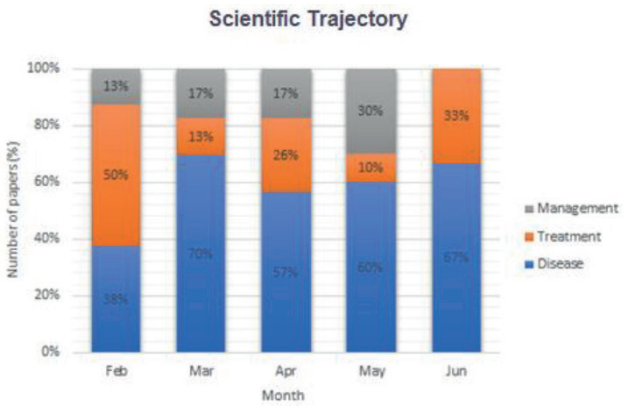

Figure 3. Scientific trajectory on COVID-19 investigations in terms of disease, 107 treatment/prevention and management approaches.

Transmission

Two types of transmission have been identified in scientific research: secondary and tertiary transmissions. In both cases, the transmission occurred through direct contact by droplets exchanged between infected and healthy people, as verified by previous studies[6]. The secondary transmission was also attributed to hospital transmission and contact between asymptomatic and healthy patients. However, the COVID-19 expansion in the world has been attributed to international travel, especially by people from China[6]. One of China's first transmission cases occurred with a 54-year-old Korean man who lived in Wuhan, China. Upon returning to Korea, the man transmitted the disease to a friend (secondary route), who, in turn, transmitted it to his wife, son, and another friend (tertiary route)[8]. At the beginning of the pandemic, both transmission types were also reported in scientific articles; however, in March 2020, the only secondary transmission was reported. In the following months until June 2020, the novel coronavirus's transmission type was not reported by the most cited papers (Figure 5A). The closure of borders and international airports possibly contributed to the reduction of tertiary transmissions in the world.

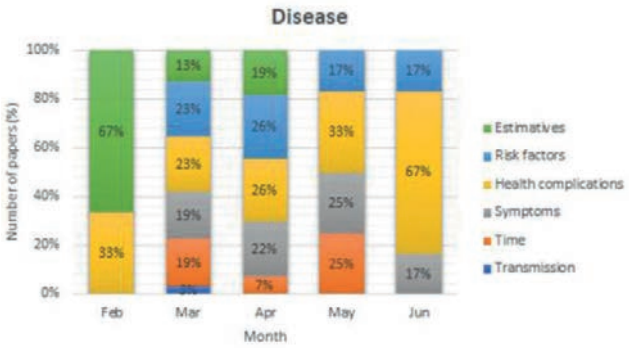

Figure 4. Main disease aspects identified in research on COVID-19.

Time

The novel coronavirus' behavior and the disease manifestation were correlated with the incubation, communicable, and symptomatic periods, and viral shedding (Figure. 5B). The average incubation period was 5 days[4], similar to the SARS time, within the expected range for MERS (between 5 and 7 days), and less than the non-SARS (3 days)[9]. However, other studies have reported an average time between 5 and 7 days, such as 5.8 days[10], 6.4 days[6,11], and 6.7 days[12]. The incubation period determination contributes to the monitoring, surveillance, control, and estimation of COVID-19[9]. The incubation period was investigated between March and May 2020, in at least 67% of the papers, possibly because it represents an important control factor for disease transmission.

The communicable period corresponds to the interval between the positive clinical diagnosis and the negative tests for COVID-19. The average communicable period was 9.5 days, reaching up to 21 days for asymptomatic cases[13]. The average COVID-19 symptoms period was 11.5 days in 97.5% of patients, with an interval of 1.2 days between the onset of symptoms and hospitalization. Disease development was also expected after 14 days of active monitoring or quarantine in about 101 cases for every 10,000[9]. The viral shedding median was 20 days, reaching up 37 days in cured patients. The viral shedding has also been identified in killed patients. For the treated patients with antivirals, in the severe and in the critical stages, the viral shedding median was 22, 19, and 24 days, respectively[14]. These four-time parameters were mostly researched between March and May 2020, at least 17% of published studies.

Symptoms

The main COVID-19 symptoms were fever, cough, sputum, chills, fatigue, shortness of breath, headache, and olfactory and gustatory disorders. Several asymptomatic cases have also been identified worldwide (Figure 5C). Fever was the most common symptom among patients, and the first identified early in the pandemic[15], followed by dry cough[6], fatigue or myalgia, and headache[12,16]. The onset of fever and cough occurred, respectively, in 5 and 7 days[8], being the fever classified as mild (37.3-38.9 °C) or moderate (38.1-39 °C)[16]. The onset of fatigue occurred in 8 days[17].

Other symptoms also verified in COVID-19 patients were sputum[18], chills, shortness of breath or dyspnea[12,17], diarrhea, and olfactory and gustatory disorders[19]. In almost 86% of patients, olfactory dysfunctions were identified while gustatory dysfunctions in 88% of those evaluated in a European clinical study on these symptoms. Both dysfunctions were not associated with nasal obstruction, and the women were more affected than men[19].

Asymptomatic cases were also identified. In a study, 24 asymptomatic cases were evaluated. Approximately 21% developed symptoms, such as fever, cough, and fatigue during hospitalization, and at least 21% had complications in the lungs[13]. In another study, the COVID- 19 proportion of asymptomatic cases reached 32%, higher than measles (8%), and lower than polio (90-95%)[11]. The information on asymptomatic cases can help COVID-19 infection control and prevent a second outbreak.

Health complications

COVID-19 is an acute respiratory syndrome that can progress to pneumonia. Clinical evidence of this complication was performed by chest computed tomography (C.T.), which identified bilateral abnormalities, peripheral (showing air bronchograms), ill-defined, and ground-glass opacification[20,21]. These abnormalities predominantly involved the lower lobes of the right lung[16,22]. The multifocal peripheral ground-glass image pattern and mixed opacity prevalent in the lower lung can be seen in the first week of the disease, although many infected people do not have these complications previously[18]. Furthermore, patients may have multiple lobe involvement, interlobular septal thickening[23], unilobar inverted halo[24], traction bronchiectasis, and architectural distortion[25]. The diagnosed lesions included irregular lesions, large confluent, and small nodular lesions[24], being the diffuse or irregular shape, with ground-glass opacity consolidation, observed between 1 and 3 weeks from disease onset[18,22]. Irregular lesions were identified mainly in the lower lobes and along the pleura, while nodular lesions were distributed in the white-vascular bundle forms[24]. These anomalies have also been identified in asymptomatic patients, thus being additional evidence to the laboratory results for an early COVID-19 diagnosis[22]. Chest CT showed a low rate of COVID-19 misdiagnosis, being, therefore, an option for rapid diagnosis of the disease, although it is limited in the identification of the virus type responsible for pulmonary complications[26]. Only in May 2020, at least 80% of papers reported studies about other pulmonary complications caused by COVID-19 (Figure 5D).

The COVID-19 patients have also shown a decrease in blood oxygen saturation (hypoxemia), a reduced white blood cell count (leukopenia), with a specific reduction in lymphocytes (lymphopenia), and changes in C-reactive protein[18]. Many patients had higher levels of Pt, APTT (activated partial thromboplastin time), d-dimer, lactate dehydrogenase, PCT (procalcitonin), ALB (albumin), and aspartate aminotransferase[14,25]. Patients with previous lung tumors showed edema, exudate, focal reactive pneumocyte hyperplasia with irregular inflammatory cell infiltration, and multinucleated giant cells in the initial phase of COVID-19, even though hyaline membranes were not prominent[28].

Psychosomatic issues, such as anxiety, stress, and depression during the COVID-19 pandemic, were observed, especially in March and April 2020, in at least 10% of the most cited papers. An online survey with more than 1,200 people was conducted in 194 Chinese cities. More than half of the interviewees reported moderate to severe psychological impact, 16.5% depressive symptoms, approximately 29% anxiety, and just over 8% some stress. The survey also found that just over 75% of respondents had concerns about family members' contamination. The most severe levels of mental health complications have been identified among women, especially students[29].

Risk factors

The main risk factors for COVID-19 involved age, gender, and comorbidities such as hypertension, diabetes, heart disease, and cancer (Figure 5E). Age was considered the leading risk factor by the scientific community since the advanced age increased hospital deaths by a ratio of 1:10[14]. The average age was 63-64 years, for the most severe cases[15,30]. China and the USA have seen more severe cases in people over the age of 65[5]. The children with an average age of 8 years presented mild to moderate symptoms or were diagnosed as asymptomatic in most cases[31]. When associated with the male gender, underlying comorbidities, and progressive radiographic deterioration[13,22], the death probability was even more remarkable. Hypertension, diabetes,

and coronary heart disease were identified as comorbidities critical to COVID-19[14,30]. Obesity was also verified[32]. Patients with acute kidney injury (AKI) had a higher risk of hospital death[33]. Cancer was also assessed as an essential risk factor, whose clinical management requires structure, preparation, and agility on the oncology community[34], primarily due to the immunocompromise of patients undergoing invasive cancer treatment[35].

Estimative

Some scientific studies estimated the number of cases, mortality rate, and contact tracing (especially the zero case) since the beginning of the COVID-19 pandemic (Figure 5F). The increase of cases worldwide was related to international travel and late social isolation established by countries, leading to an immediate outbreak of COVID-19, as previously seen in Italy and Spain, and after in the USA and Brazil. The mortality rates in China and Italy became identical and equal to 2.3%, with older adults' predominance. The failure to identify the Italian zero case may have influenced that rate[36]. Travel ban measures in Wuhan (China) contributed to the reduction of about 80% of predicted imported cases in mid-February 2020, despite a predicted disease progression delay of only 3 to 5 days. Travel restrictions would only effectively alter the COVID- 19 progress if combined with a reduction of at least 50% in the community transmissions[37]. Travel restrictions were also beneficial in reducing the average number of daily reproductions in Wuhan, which dropped from 2.35 to 1.05 a week after adopting these measures[38]. All estimates were made using the exponential growth rate from Chinese exported cases for COVID-19, where the necessary number of reproduction (secondary transmission) and the mortality rate could be determined. The COVID-19 pandemic was predicted from two scenarios: from a single case and using the growth rate adjusted with other parameters. Mortality rates ranged from 5.3% to 8.4%, while the number of secondary cases ranged from 2.1 to 3.2 for the scenarios, respectively[39]. In May and June 2020, research on the COVID-19 cases' estimation was not among the most cited papers in the period, possibly due to disease stabilization in many countries and the interest in other more critical disease aspects.

Treatment and Prevention

COVID-19 treatments have included strategies to control the disease's leading symptoms and health complications due to the limitations in the rapid development of a vaccine against the

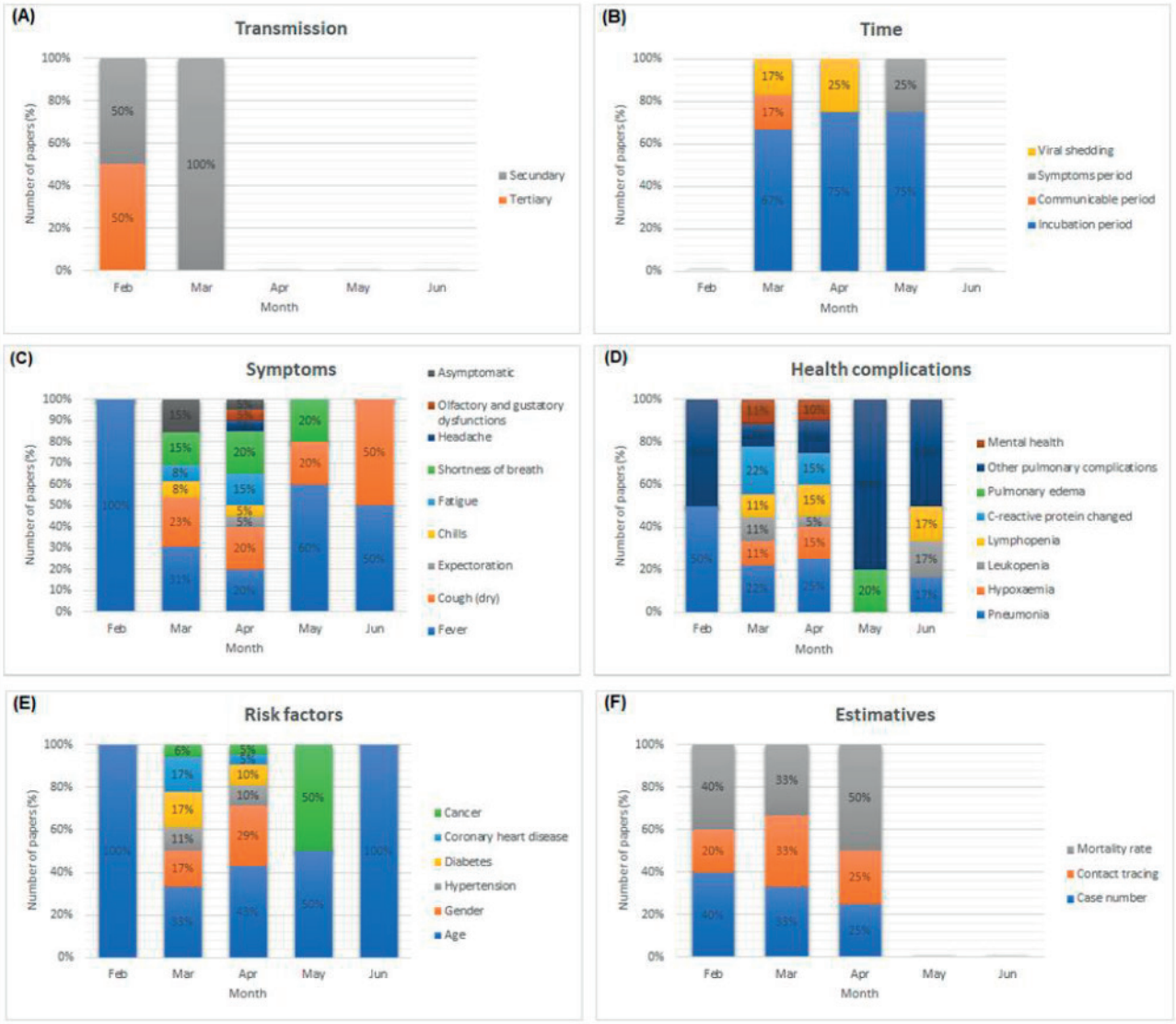

Figure 5. Scientific trajectory on COVID-19 disease in terms of (A) Transmission. (B) Time. (C) Symptoms. (D) Health complications. (E) Risk factors. (F) Estimative.

SARS-CoV-2. Therefore, different drugs have been investigated since February 2020 as treatment measures, considered palliative and not preventive ones. Medicaments used to fight other viruses have been widely carried out. Alternatively, antibody transfusion and stem cell transplantation have been evaluated in some studies (Figure 6).

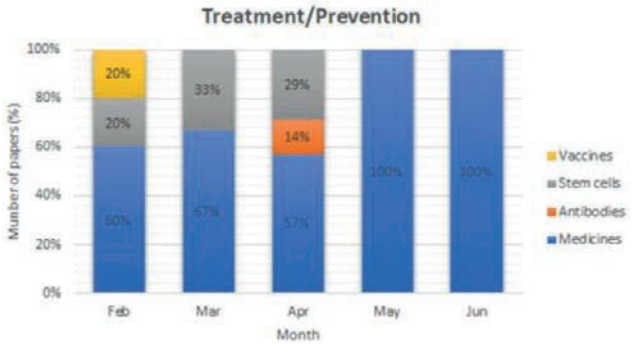

Figure 6. Main treatment and prevention approaches identified in research on COVID-19.

Medicines

Several antiviral drugs have been investigated (Figure 7). Lopinavir-ritonavir was used to treat HIV (human immunodeficiency virus) and was used to treat COVID-19 since it had previous results *in vitro* and clinical studies against SARS-CoV. It was prescribed twice a day for 14 days to infected adult patients, and the results were compared to the standard COVID-19 treatment. There was no improvement in patients who used lopinavir-ritonavir[40]. However, the first case of COVID-19 in Korea was treated with lopinavir-ritonavir, which significantly reduced the viral β- coronavirus loads[8].

Nucleotide inhibitors such as Anti-HCV used to fight hepatitis C by inhibiting RNA polymerase[41], and inhibitors of the Renin-Angiotensin-Aldosterone System (RAAS), considered vasoactive peptides[42] were also investigated. Examples of anti-polymerase drugs with positive results for the COVID-19 treatment were sofosbuvir, IDX-184, ribavirin, and Remdesivir[41,43]. The RAAS inhibitors have been indicated in severe clinical cases, especially in patients with comorbidities related to heart disease. However, the real activity of these inhibitors in combating COVID-19 has been researched. The angiotensin-converting enzyme 2 (ACE2) is considered responsible for coronavirus infection since it functions as a receptor. Studies suggested that RAAS inhibition favors ACE2 overexpression, causing viral activity to increase[42]. Therefore, further studies involving RAAS inhibitors must be carried out to verify their real benefits against COVID- 19.

Other essential drugs investigated were chloroquine and hydroxychloroquine, which have generated much discussion in the scientific community, although about 20 clinical studies have been carried out in several Chinese hospitals with different coronaviruses SARS-CoV and SAR- CoV-2. These drugs have been used effectively to combat malaria, Q fever, and Whipple's disease, and in a recent study, the chloroquine helped reduce pneumonia, duration of symptoms, and viral shedding of COVID-19, without causing severe side effects[44]. Investigations of drugs such as methylprednisolone, moxifloxacin, interferon alfa-2b physicochemical inhalation, meropenem[17,45], Kaletra, corticoids[16], Arbidol and IFN-α[46], and the COVID-19 therapies[16] have also been reported.

Vaccines

According to WHO, it will take at least 18 months for a vaccine against the novel coronavirus to be completed,

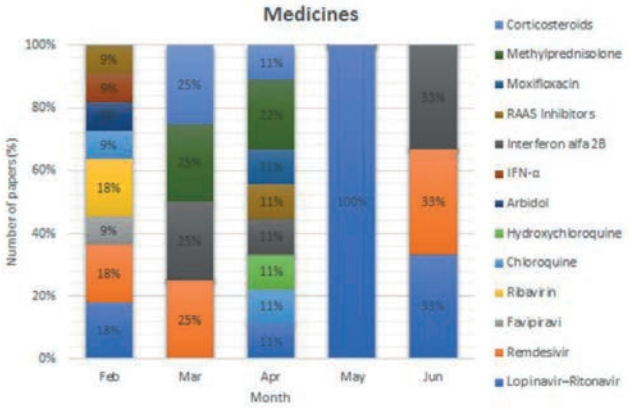

Figure 7. Scientific trajectory on COVID-19 treatment in terms of medicines.

although different research groups and experts are in a real scientific race for its fast development[47]. Currently, treatments only combat symptoms, acting as anti-inflammatory and antiviral drugs. Experience with immunological studies of SARS-CoV and its similarity to SARS-CoV-2 allowed the tracking and identification of B and T cell epitopes in SARS-CoV immunogenic structural proteins, also identified in SARS-CoV-2. As no epitope mutations were observed in more than 120 SARS-CoV-2 sequences, they were considered useful in researching a new vaccine, with complete and global coverage[48]. Other vaccines have also been investigated, but not reported in the most cited articles in the first half of 2020, possibly because they are confidential research or in little advanced development stages.

Antibodies and Stem Cells

Alternative COVID-19 treatments have included the convalescent plasma (C.P.) transfusion from recently cured donors containing neutralizing antibodies[23], and the mesenchymal stem cells (CTMs) transplantation[49]. C.P. therapy was considered efficient in severe COVID-19 cases, contributing to the viremia disappearance in 7 days after the transfusion. An increase in the lymphocyte number and a reduction in C-reactive protein was seen within days, and the lung injuries were absorbed within 7 days[23]. C.P. therapy also helped stabilize body temperature and remove mechanical ventilators, which happened 3 weeks after the transfusion[50]. In turn, the transplantation of MSCs had an immunomodulatory function, which was responsible for an improvement in the pulmonary functions of the patients 2 days after the transplant, a hospital discharge after 10 days, and a general clinical improvement after 14 days. The MSCs transplantation contributed to increased lymphocytes, decreased C-reactive protein, and the disappearance of immune cells secreting overactive cytokines[50]. Although a limited number of people have undergone both treatments, they are promising in combating the novel coronavirus and potential interest in future investigations.

Management of COVID-19

The management of COVID-19 involved control strategies that range from outstanding medical care and personal hygiene to the social isolation measures. Furthermore, the clinical case determination and the disease importation control, either between countries or between regions of the same country, have been necessary measures for the effective control of COVID-19 (Figure 8). Although these strategies have been prioritized differently from February to June 2020,

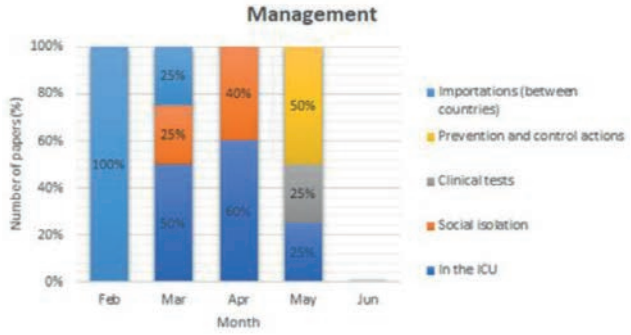

Figure 8. Main management approaches identified in research on COVID-19.

they have all been equally important in reducing the number of cases or stabilizing the COVID-19 and overcoming it in the coming months.

In the Intensive Care Unit (ICU)

The care for patients admitted to the ICU has involved adopting special medical measures and protocols, which could ensure health professionals' safety and patients' well-being. The main procedures included the infection control (risks of SARS-CoV-2 transmission), laboratory tests, supportive care (continuous renal replacement - CRRT, invasive mechanical ventilation[32], extracorporeal membrane oxygenation - ECMO[47], hemodynamic support[3]), and COVID-19 therapy[3]. Some procedures were considered specific and necessary in patients with COVID-19, such as emergency tracheal intubation, predicted or unexpected difficult tracheal intubation, cardiac arrest, anesthetic care, and tracheal extubating[51] (Figure 9A). Although ventilatory support was mostly reported in April 2020 in 56% of the most cited papers, all measures related to care in the ICU were used equally in May 2020, possibly due to the disease's peak in many countries in this period.

Social Isolation

Social isolation was a measure used to contain viruses such as SARS and COVID-19, by reducing the disease peak and flattening the curve over time, to ensure sufficient time for the government to implement public health care measures[52]. The main social isolation measures included the closure of schools and workplaces non-essential (non-food and non-health) and people's reduced movement on the streets[52]. Countries that took a long time to implement quarantine measures suffered the consequences of the accelerated increase in cases of COVID-19[53]. Although COVID- 19 and SARS differ in terms of transmissibility, infectious period, and disease spread, measures taken to control SARS have helped to control COVID-19, such as syndromic surveillance, immediate isolation of infected patients, and strict application of vertical quarantine (lockdown)[4]. Mathematical models considering social isolation and contact tracing could predict the positive impacts on the new COVID-19 cases, thus contributing to the outbreak control[10]. The early relaxation of social isolation compromised COVID-19 control. Therefore, it is necessary to have a strict contact control between people and a policy willing to implement social distance measures until the disease stabilizes and decreases[52].

Prevention and Control Procedures

Other COVID-19 prevention and control measures included personal hygiene care such as handwashing after direct contact with infected people or with the environment, the distancing of wild and farm animals[6], the use of alcohol 70%, and masks in public places. Cancer and dental medicine patients must be treated using particular protocols to reduce the contamination risk[54]. Access to information is crucial for the correct and conscious procedure implementations to combat the novel coronavirus.

Clinical tests

The COVID-19 diagnoses were carried out by direct and indirect assays, from the determining nucleic acids, immunohistochemical stains, and image tests involving 18F-FDG PET/CT (Figure. 9B). The clinical test based on viral nucleic acid was the primary technique reported[13,28,55]. Immunohistochemical stains are still under development[28], and the 18F-FDG PET/CT test was able to identify the presence of COVID-19 in tested positive patients. The 18F-FDG PET/CT teste consists of a hybrid technique between positron emission tomography (PET) and conventional computed tomography (C.T.), using the 18F-Fluordeoxiglicose (FDG), a glucose analog, as a tracer. This technique allows for obtaining metabolic and anatomical information. Tomography images helped identify ground-glass peripheral opacities, pulmonary consolidations in lung lobes, and lung lesions with lymph node involvement in patients with COVID-19[56].

Importation

A critical study on vulnerability to COVID-19 in developing countries, especially in Africa, was carried out. The COVID-19 importation was related to the recipient country's ability to respond to the outbreak. Countries such as Egypt, Algeria, and South Africa presented a higher importation risk of the novel coronavirus, but a high capacity to control the disease. Countries such as Ethiopia, Nigeria, Sudan, Angola, Ghana, Tanzania, and Kenya with moderate risk showed high vulnerability to control the outbreak. The same was verified for the provinces of Guangdong, Fujian, and Beijing city[57]. This study can be used to reference countries with limited preparedness to deal with COVID-19, suggesting the adoption of intensified surveillance and resource allocation. Non-African countries can also use these measures.

Conclusions

It was possible to establish the development level of scientific research on SARS-CoV-2, summarizing the major studies carried out in the first half of 2020, and highlighting the scientific community's main discussions on the disease, treatment/prevention, and management of COVID-19. This compilation study can help future research by identifying knowledge gaps in coronavirus and its disease. Furthermore, the information contained herein may be used in studies on new drugs capable of combating this viral infection, developing vaccines in a shorter period, and on measures to control new COVID-19 cases. This study also helps to understand the disease behavior and proposing solutions for the resumption of economic and social activities by affected countries based on scientific knowledge. All the experience gained with COVID-19 should be used to anticipate future scenarios and establish more effective control procedures to reduce new pandemics' probability in the coming years.

Acknowledgments

The authors greatly acknowledge the Coordination for the Improvement of Higher Education Personnel (CAPES), the

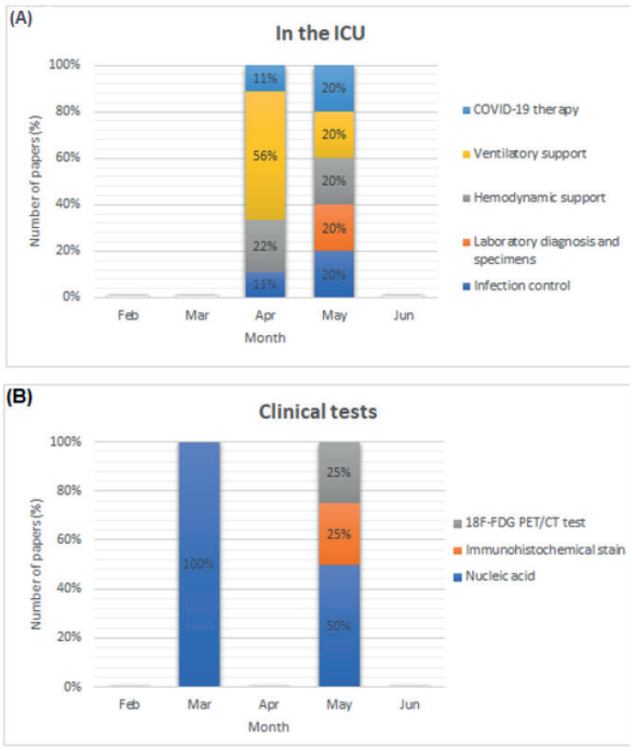

Figure 9. Scientific trajectory on COVID-19 management in terms of (A) Procedures in the ICU. (B) Clinical tests.

National Council for Scientific and Technological Development (CNPq), and the Research Support Foundation of the State of Rio de Janeiro (FAPERJ) for giving financial support for scientific investigation of this paper.

Author contributions

D.T. and S.B conceived the scientific prospecting project. D.T. searched for the most cited papers on the Web of Science. D.T. and S.B. contributed to the data analysis. D.T. wrote the manuscript, and S.B. revised the text.

Competing interests

The authors declare that there are no competing interests.

Data and materials availability

All data are available in the main text or the supplementary materials.

Ethics statement

The authors confirm that the ethical policies of the journal, as noted on the journal's author guidelines page, have been adhered to. No ethical approval was required as this is a review article with no original research data.

Bibliographic references

1. Pan American Health Organization. Coronavirus Disease (COVID-19) pandemic [Internet]. [cited 2020 Jul 2]. Available from: https://www.paho.org/en
2. Wordl Health Organization. Coronavirus disease (COVID-19) pandemic [Internet]. [cited 2020 Jul 2]. Available from: https://www.who.int/emergencies/diseases/novel-coronavirus-2019
3. Alhazzani W, Møller MH, Arabi YM, Loeb M, Gong MN, Fan E, et al. Surviving Sepsis Campaign: guidelines on the management of critically ill adults with Coronavirus Disease 2019 (COVID-19) [Internet]. Vol. 46, Intensive Care Medicine. Springer Berlin Heidelberg; 2020. 854–887 p. Available from: https://doi.org/10.1007/s00134-020-06022-5
4. Wilder-Smith A, Chiew CJ, Lee VJ. Can we contain the COVID-19 outbreak with the same measures as for SARS? Lancet Infect Dis [Internet]. 2020;20(5):e102–7. Available from: http://dx.doi.org/10.1016/S1473-3099(20)30129-8
5. Bialek S, Boundy E, Bowen V, Chow N, Cohn A, Dowling N, et al. Severe outcomes among patients with coronavirus disease 2019 (COVID-19) - United States, February 12-march 16, 2020. Morb Mortal Wkly Rep. 2020;69(12):343–6.
6. Lai CC, Shih TP, Ko WC, Tang HJ, Hsueh PR. Severe acute respiratory syndrome coronavirus 2 (SARS-CoV-2) and coronavirus disease-2019 (COVID-19): The epidemic and the challenges. Int J Antimicrob Agents [Internet]. 2020;55(3):105924. Available from: https://doi.org/10.1016/j.ijantimicag.2020.105924
7. Zhang T, Wu Q, Zhang Z. Probable Pangolin Origin of SARS-CoV-2 Associated with the COVID-19 Outbreak. Curr Biol [Internet]. 2020;30(7):1346-1351.e2. Available from: https://doi.org/10.1016/j.cub.2020.03.022
8. Lim J, Jeon S, Shin HY, Kim MJ, Seong YM, Lee WJ, et al. The Author's response: Case of the index patient who caused tertiary transmission of coronavirus disease 2019 in Korea: The Application of lopinavir/ritonavir for the treatment of COVID-19 pneumonia monitored by quantitative RT-PCR. J Korean Med Sci. 2020;35(7):1–6.
9. Lauer SA, Grantz KH, Bi Q, Jones FK, Zheng Q, Meredith HR, et al. The incubation period of coronavirus disease 2019 (CoVID-19) from publicly reported confirmed cases: Estimation and application. Ann Intern Med. 2020;172(9):577–82.
10. Hellewell J, Abbott S, Gimma A, Bosse NI, Jarvis CI, Russell TW, et al. Feasibility of controlling COVID-19 outbreaks by isolation of cases and contacts. Lancet Glob Heal. 2020;8(4):e488–96.
11. Mizumoto K, Kagaya K, Zarebski A, Chowell G. Estimating the asymptomatic proportion of coronavirus disease 2019 (COVID-19) cases on board the Diamond Princess cruise ship, Yokohama, Japan, 2020. Eurosurveillance. 2020;25(10):1–5.
12. Tian S, Hu N, Lou J, Chen K, Kang X, Xiang Z, et al. Characteristics of COVID-19 infection in Beijing. J Infect [Internet]. 2020;80(4):401–6. Available from: https://doi.org/10.1016/j.jinf.2020.02.018
13. Hu Z, Song C, Xu C, Jin G, Chen Y, Xu X, et al. Clinical characteristics of 24 asymptomatic infections with COVID-19 screened among close contacts in Nanjing, China. Sci China Life Sci. 2020;63(5):706–11.
14. Zhou F, Yu T, Du R, Fan G, Liu Y, Liu Z, et al. Clinical course and risk factors for mortality of adult inpatients with COVID-19 in Wuhan, China: a retrospective cohort study. Lancet [Internet]. 2020;395(10229):1054–62. Available from: http://dx.doi.org/10.1016/S0140-6736(20)30566-3
15. Bhatraju PK, Ghassemieh BJ, Nichols M, Kim R, Jerome KR, Nalla AK, et al. COVID-19 in critically ill patients in the Seattle region — Case series. N Engl J Med. 2020;382(21):2012–22.
16. Wan S, Xiang Y, Fang W, Zheng Y, Li B, Hu Y, et al. Clinical features and treatment of COVID-19 patients in northeast Chongqing. J Med Virol. 2020;(March):1–10.
17. Xu Z, Shi L, Wang Y, Zhang J, Huang L, Zhang C, et al. Pathological findings of COVID-19 associated with acute respiratory distress syndrome. Lancet Respir Med [Internet]. 2020;8(4):420–2. Available from: http://dx.doi.org/10.1016/S2213-2600(20)30076-X
18. Yang W, Cao Q, Qin L, Wang X, Cheng Z, Pan A, et al. Clinical characteristics and imaging manifestations of the 2019 novel coronavirus disease (COVID-19):A multi-center study in Wenzhou city, Zhejiang, China. J Infect [Internet]. 2020;80(4):388–93. Available from: https://doi.org/10.1016/j.jinf.2020.02.016

19. Lechien JR, Chiesa-Estomba CM, De Siati DR, Horoi M, Le Bon SD, Rodriguez A, et al. Olfactory and gustatory dysfunctions as a clinical presentation of mild-to-moderate forms of the coronavirus disease (COVID-19): a multicenter European study. Eur Arch Oto-Rhino-Laryngology [Internet]. 2020;2(0123456789). Available from: https://doi.org/10.1007/s00405-020-05965-1
20. Bernheim A, Mei X, Huang M, Yang Y, Fayad ZA, Zhang N, et al. Chest CT findings in coronavirus disease 2019 (COVID-19): Relationship to duration of infection. Radiology. 2020;295(3):685–91.
21. Pan F, Ye T, Sun P, Gui S, Liang B, Li L, et al. Time course of lung changes at chest C.T. during recovery from Coronavirus disease 2019 (COVID-19). Radiology. 2020;295(3):715–21.
22. Shi H, Han X, Jiang N, Cao Y, Alwalid O, Gu J, et al. Radiological findings from 81 patients with COVID-19 pneumonia in Wuhan, China: a descriptive study. Lancet Infect Dis [Internet]. 2020;20(4):425–34. Available from: http://dx.doi.org/10.1016/S1473-3099(20)30086-4
23. Duan K, Liu B, Li C, Zhang H, Yu T, Qu J, et al. Effectiveness of convalescent plasma therapy in severe COVID-19 patients. Proc Natl Acad Sci U S A. 2020;117(17):9490–6.
24. Yoon SH, Lee KH, Kim JY, Lee YK, Ko H, Kim KH, et al. chest radiographic and ct findings of the 2019 novel coronavirus disease (Covid-19): Analysis of nine patients treated in korea. Korean J Radiol. 2020;21(4):498–504.
25. Zhao W, Zhong Z, Xie X, Yu Q, Liu J. Relation between chest C.T. findings and clinical conditions of coronavirus disease (covid-19) pneumonia: A multicenter study. Am J Roentgenol. 2020;214(5):1072–7.
26. Li Y, Xia L. Coronavirus disease 2019 (COVID-19): Role of chest C.T. in diagnosis and management. Am J Roentgenol. 2020;214(6):1280–6.
27. Thachil J, Tang N, Gando S, Falanga A, Cattaneo M, Levi M, et al. ISTH interim guidance on recognition and management of coagulopathy in COVID-19. J Thromb Haemost. 2020;(March):1023–6.
28. Tian S, Hu W, Niu L, Liu H, Xu H, Xiao SY. Pulmonary Pathology of Early-Phase 2019 Novel Coronavirus (COVID-19) Pneumonia in Two Patients With Lung Cancer. J Thorac Oncol [Internet]. 2020;15(5):700–4. Available from: https://doi.org/10.1016/j.jtho.2020.02.010
29. Wang C, Pan R, Wan X, Tan Y, Xu L, Ho C.S., et al. Immediate psychological responses and associated factors during the initial stage of the 2019 coronavirus disease (COVID-19) epidemic among the general population in China. Int J Environ Res Public Health. 2020;17(5).
30. Wu J, Li W, Shi X, Chen Z, Jiang B, Liu J, et al. Early antiviral treatment contributes to alleviate the severity and improve the prognosis of patients with novel coronavirus disease (COVID-19). J Intern Med. 2020;2:1–11.
31. Qiu H, Wu J, Hong L, Luo Y, Song Q, Chen D. Clinical and epidemiological features of 36 children with coronavirus disease 2019 (COVID-19) in Zhejiang, China: an observational cohort study. Lancet Infect Dis [Internet]. 2020;20(6):689–96. Available from: http://dx.doi.org/10.1016/S1473-3099(20)30198-5
32. Richardson S, Hirsch JS, Narasimhan M, Crawford JM, McGinn T, Davidson KW, et al. Presenting Characteristics, Comorbidities, and Outcomes among 5700 Patients Hospitalized with COVID-19 in the New York City Area. JAMA - J Am Med Assoc. 2020;323(20):2052–9.
33. Cheng Y, Luo R, Wang K, Zhang M, Wang Z, Dong L, et al. Kidney disease is associated with in-hospital death of patients with COVID-19. Kidney Int [Internet]. 2020;97(5):829–38. Available from: https://doi.org/10.1016/j.kint.2020.03.005
34. Ueda M, Martins R, Hendrie PC, McDonnell T, Crews JR, Wong TL, et al. Managing Cancer Care During the COVID-19 Pandemic: Agility and Collaboration Toward a Common Goal. J Natl Compr Canc Netw. 2020;18(4):1–4.
35. Alβ Shamsi HO, Alhazzani W, Alhuraiji A, Coomes EA, Chemaly RF, Almuhanna M, et al. A Practical Approach to the Management of Cancer Patients During the Novel Coronavirus Disease 2019 (COVID β 19) Pandemic: An International Collaborative Group . Oncologist. 2020;2019:1–10.
36. Porcheddu R, Serra C, Kelvin D, Kelvin N, Rubino S. Similarity in Case Fatality Rates (CFR) of COVID-19/SARS-COV-2 in Italy and China. J Infect Dev Ctries. 2020;14(2):125–8.
37. Chinazzi M, Davis JT, Ajelli M, Gioannini C, Litvinova M, Merler S, et al. The effect of travel restrictions on the spread of the 2019 novel coronavirus (COVID-19) outbreak. Science (80-). 2020;368(6489):395–400.
38. Kucharski AJ, Russell TW, Diamond C, Liu Y, Edmunds J, Funk S, et al. Early dynamics of transmission and control of COVID-19: a mathematical modelling study. Lancet Infect Dis. 2020;20(5):553–8.
39. Jung S, Akhmetzhanov AR, Hayashi K, Linton NM, Yang Y, Yuan B, et al. Real-Time Estimation of the Risk of Death from Novel Coronavirus (COVID-19) Infection: Inference Using Exported Cases. J Clin Med. 2020;9(2):523.
40. Cao B, Wang Y, Wen D, Liu W, Wang J, Fan G, et al. A trial of lopinavir-ritonavir in adults hospitalized with severe covid-19. N Engl J Med. 2020;382(19):1787–99.
41. Elfiky AA. Anti-HCV, nucleotide inhibitors, repurposing against COVID-19. Life Sci. 2020;248(January).
42. Vaduganathan M, Vardeny O, Michel T, McMurray JJV, Pfeffer MA, Solomon SD. Renin–Angiotensin–Aldosterone System Inhibitors in Patients with Covid-19. N Engl J Med [Internet]. 2020 Apr 23;382(17):1653–9. Available from: http://www.nejm.org/doi/10.1056/NEJMsr2005760
43. Grein J, Ohmagari N, Shin D, Diaz G, Asperges E, Castagna A, et al. Compassionate use of remdesivir for patients with severe Covid-19. N Engl J Med. 2020;382(24):2327–36.
44. Colson P, Rolain JM, Lagier JC, Brouqui P, Raoult D. Chloroquine and hydroxychloroquine as available weapons to Fight COVID-19. Int J Antimicrob Agents [Internet]. 2020;55(4):105932. Available from: https://doi.org/10.1016/j.ijantimicag.2020.105932
45. Zhu L, Xu X, Ma K, Yang J, Guan H, Chen S, et al. Successful recovery of COVID-19 pneumonia in a renal transplant recipient with long-term immunosuppression. Am J Transplant. 2020;(March):1–5.
46. Dong L, Hu S, Gao J. Discovering drugs to treat coronavirus disease 2019 (COVID-19). Drug Discov Ther. 2020;14(1):58–60.
47. Jiang F, Deng L, Zhang L, Cai Y, Cheung CW, Xia Z. Review of the Clinical Characteristics of Coronavirus Disease 2019 (COVID-19). J Gen Intern Med. 2020;35(5):1545–9.
48. Ahmed SF, Quadeer AA, McKay MR. Preliminary identification of potential vaccine targets for the COVID-19 Coronavirus (SARS-CoV-2) Based on SARS-CoV Immunological Studies. Viruses. 2020;12(3).
49. Leng Z, Zhu R, Hou W, Feng Y, Yang Y, Han Q, et al. Transplantation of ACE2- Mesenchymal stem cells improves the outcome of patients with covid-19 pneumonia. Aging Dis. 2020;11(2):216–28.
50. Shen C, Wang Z, Zhao F, Yang Y, Li J, Yuan J, et al. Treatment of 5 Critically Ill Patients with COVID-19 with Convalescent Plasma. JAMA - J Am Med Assoc. 2020;323(16):1582–9.
51. Cook TM, El-Boghdadly K, McGuire B, McNarry AF, Patel A, Higgs A. Consensus guidelines for managing the airway in patients with COVID-19: Guidelines from the Difficult Airway Society, the Association of Anaesthetists the Intensive Care Society, the Faculty of Intensive Care Medicine and the Royal College of Anaesthetist. Anaesthesia. 2020;785–99.
52. Prem K, Liu Y, Russell TW, Kucharski AJ, Eggo RM, Davies N, et al. The effect of control strategies to reduce social mixing on outcomes of the COVID-19 epidemic in Wuhan, China: a modelling study. Lancet Public Heal. 2020;5(5):e261–70.
53. Remuzzi A, Remuzzi G. COVID-19 and Italy: what next? Lancet [Internet]. 2020;395(10231):1225–8. Available from: http://dx.doi.org/10.1016/S0140-6736(20)30627-9
54. Meng L, Hua F, Bian Z. Coronavirus Disease 2019 (COVID-19): Emerging and Future Challenges for Dental and Oral Medicine. J Dent Res. 2020;99(5):481–7.
55. Xia W, Shao J, Guo Y, Peng X, Li Z, Hu D. Clinical and C.T. features in pediatric patients with COVID-19 infection: Different points from adults. Pediatr Pulmonol. 2020;55(5):1169–74.
56. Qin C, Liu F, Yen TC, Lan X. 18F-FDG PET/CT findings of COVID-19: a series of four highly suspected cases. Eur J Nucl Med Mol Imaging. 2020;47(5):1281–6.
57. Gilbert M, Pullano G, Pinotti F, Valdano E, Poletto C, Boëlle PY, et al. Preparedness and vulnerability of African countries against importations of COVID-19: a modeling study. Lancet. 2020;395(10227):871–7.

Received: Oct 1 2020
Accepted: Oct 25 2020

NEWS AND VIEWS

La Fragata Portuguesa o Aguamala (*Physalia physalis*): Importancia en la salud pública

The Portuguese man-of-war or bluebottle (*Physalia physalis*): Public health importance

Joxmer Scott-Frías[1], Esmeralda Mujica de Jorquera[2]

DOI. 10.21931/RB/2020.05.04.24

Resumen: La Fragata Portuguesa (*Physalia physalis*) es un llamativo sifonóforo colonial de aguas abiertas que vive entre la interface aire y mar. Sus tentáculos se caracterizan por producir dolorosas lesiones que en raros casos ha causado la muerte de la persona. En el Atlántico, los arribazones de *Physalia* están siendo más comunes en los últimos años, lo que causa el incremento de las afecciones a los humanos. En inicios de marzo 2020, se registró un arribazón de *Physalia* en el Litoral Central venezolano (mar Caribe). Por este motivo se procedió a documentar el evento y suministrar información adecuada que permita conocer más sobre estos animales, así como su importancia en la salud pública. Se revisan las medidas que deben ser consideradas al detectar su presencia, primeros auxilios e indicaciones recomendadas para el tratamiento por parte del personal médico.

Palabras clave: Fragata Portuguesa, *Physalia physalis*, salud pública, primeros auxilios, tratamientos.

Abstract: -The Portuguese man-of-war (*Physalia physalis*) is a distinctive colony of open water siphonophores that lives at the sea-air interface. This animal is known to produce painful injuries that have caused people's death in rare cases. In the Atlantic, the arrivals of *Physalia* are becoming more common in recent years, causing an increase in humans' accidents. In early March 2020, *Physalia's* arrival was recorded on the Venezuelan Central Coastline (Caribbean Sea). For this reason, we proceeded to document the event and provide adequate information to learn more about these animals and their importance in public health. The measures that should be considered when detecting their presence, first aid, and recommended indications for medical personnel treatment are reviewed.

Key words: Portuguese man-of-war, *Physalia physalis*, public health, first aid, treatments.

Características de la Fragata Portuguesa

La Fragata Portuguesa es un animal relacionado con las medusas (aguamalas), anémonas y corales, todos estos organismos forman parte de los Cnidarios, un grupo primitivo de seres vivos que se asocian principalmente a los fondos marinos[1]. El nombre científico de la Fragata Portuguesa es *Physalia physalis* (Linnaeus, 1758), que se lee (= Fisalia fisalis), así todos podemos reconocerla en cualquier idioma del mundo; pues los nombres comunes pueden variar entre región y país. Por esto también es conocida como Carabela Portuguesa, Barquito Portugués, Hombre de Guerra Portugués, Botella Azul, Aguamala o Falsa Medusa debido a su forma de "barco a velas", coloración o relación con las medusas. Sin embargo, el término Medusa Azul genera confusión y es inadecuado, porque *Physalia* no pertenece al grupo de las medusas verdaderas (clase Scyphozoa)[2,3]. La diferencia se encuentra en que *Physalia* forma parte de un grupo de organismos llamados Sifonóforos (pertenecientes a la clase Hydrozoa), en el que varios individuos conforman una colonia donde cada uno desempeña funciones diferentes como flotar, alimentarse, defenderse o reproducirse. En cambio el cuerpo de las medusas verdaderas corresponde a un único individuo con todas las funciones presentes en dicho ejemplar. Podemos comparar los sifonóforos con una colonia de hormigas en donde encontramos juntas cooperando a la reina, soldados y obreras, cada una con funciones únicas que mantienen la actividad de la colonia entera. Sin embargo, en *Physalia* todos estos individuos están unidos, conformando al ejemplar que consiste principalmente de un flotador; que es una vejiga membranosa llena de gas y con forma de vela. Esta estructura también es la encargada del desplazamiento del animal que es impulsado por el viento, mientras que desde el cuerpo central se extienden numerosos tentáculos de color azul intenso (Fig. 1).

Importancia en el ambiente

Al igual como ocurre en las medusas, los sifonóforos como *Physalia* se comportan como depredadores, cumpliendo con el importante papel de contribuir en la ecología y equilibrio de los mares. Entre estas funciones se encuentra el reciclaje de nutriente, indispensable para el sustento del ecosistema marino[4]. Las medusas y los sifonóforos controlan las poblaciones de los pequeños animales que forman parte del plancton (o zooplancton), así como a los pequeños peces y sus larvas que capturan con los tentáculos. Es por esto que también se han evaluado sus efectos no deseados sobre las pesquerías comerciales[5]. Por otro lado, *Physalia* además es presa de otras especies con importancia ecológica, como peces, tortugas y babosas marinas como el Dragón Azul (*Glaucus atlanticus* Forster, 1777).

Distribución geográfica

Physalia está presente en todos los mares tropicales, desde el Atlántico, Indico hasta el Pacífico. Es una especie principalmente oceánica, pero llega a las costas por acción del viento que las arrastra hasta la orilla. Es por esto que podemos encontrarla en las playas del mar Caribe en ciertas épocas del año. En el caso particular de las costas de Venezuela, su presencia se registra con mayor frecuencia entre los meses de

[1] Laboratorio de Ecología de Sistemas Acuáticos, Instituto de Ecología y Zoología Tropical (IZET – UCV), Caracas, Venezuela.
[2] Investigador independiente, Venezuela.

Corresponding author: joxmer@gmail.com

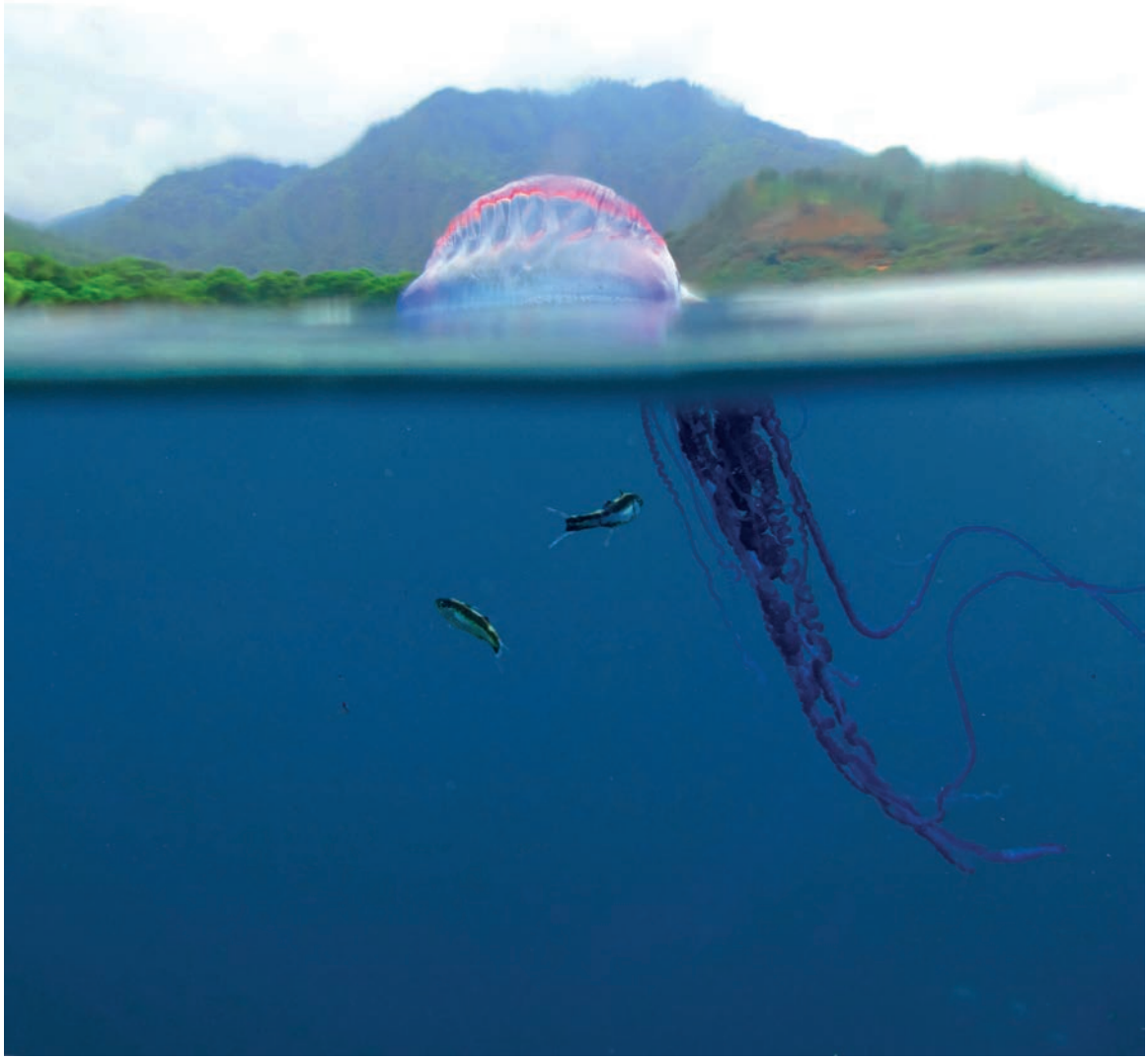

Figura 1. Fragata Portuguesa (*Physalia physalis*) junto a dos Peces Pastorcillos (*Nomeus gronovii* (Gmelin, 1789)), comensal/depredador de *Physalia*. Fotografía tomada en abril 30, 2016, Chichiriviche de la Costa (estado La Guaira, Caribe venezolano: 10º33'08'' N, 67º14'19'' W). Fotógrafo © Joxmer Scott-Frías.

enero y mayo, momento en el que su alimento es más abundante y los vientos alisios del noreste soplan con mayor intensidad hacia la costa. Aunque los avistamientos de la especie pueden ser esporádicos y erráticos. Es por esto último que no se puede predecir cuándo o dónde ocurrirán los arribazones de Physalia, ni la escala o magnitud del número de ejemplares que llegarán a la costa. En países con costa atlántica como Brasil, Cuba, Francia y México, los arribazones de *Physalia* se han vuelto más comunes en los últimos años[4,6,7]. Adicionalmente estos eventos coinciden con los periodos vacacionales, aumentando así los accidentes con la especie.

Un evento reciente en Venezuela

Durante los días 7 y 8 de marzo de 2020, se observó la presencia de varios ejemplares de *Physalia*. Esto ocurrió en aguas frente a la ensenada de Patanemo y Yapazcua (estado Carabobo, mar Caribe venezolano: 10º27'19'' N, 67º55'26'' W y 10º28'19'' N, 67º53'57'' W respectivamente). Miembros de la organización ambiental Cachiri, llevaron algunos ejemplares hasta la costa y alertaron a través de las redes sociales la presencia de estos animales, así como los riesgos potenciales que representan. Por otro lado, ejemplares flotando frente a Patanemo, fueron avistados y confirmados por la Instructora de Buceo Iris Santana, Directora del centro de buceo La Tienda de Buceo. En los días posteriores (12 de marzo) se reportó la evacuación temporal de Playa Grande en Choroní[8](estado Aragua, Venezuela: 10º30'28'' N, 67º35'51'' W), ubicada a más de 30 Km al este de los primeros avistamientos y que se encuentra entre las playas más visitada del Litoral Central venezolano (Fig. 2). Aunque fue llamativa la cantidad de ejemplares observados, no se reportaron personas afectadas durante todo el evento. Dada la poca frecuencia de este tipo de fenómenos, así como la conducción de la información ofrecida por parte de los medios y redes sociales, hemos tenido la intención de brindar información adecuada que permita conocer más sobre estos animales, su importancia en la salud pública, así como las medidas que se deben considerar al detectar su presencia.

Eventos como el descrito anteriormente, aunque ocurren de forma esporádica, han sido documentados previamente en Venezuela. Por ejemplo, durante el periodo comprendido entre diciembre de 2006 y 2007, se trataron 59 pacientes con lesiones producidas por *Physalia* en la costa de Adicora (estado Falcón, mar Caribe)[9]. Sin embargo, únicamente los casos más representativos alcanzan la luz pública, lo que dificulta una evaluación efectiva de la frecuencia y magnitud de estos eventos.

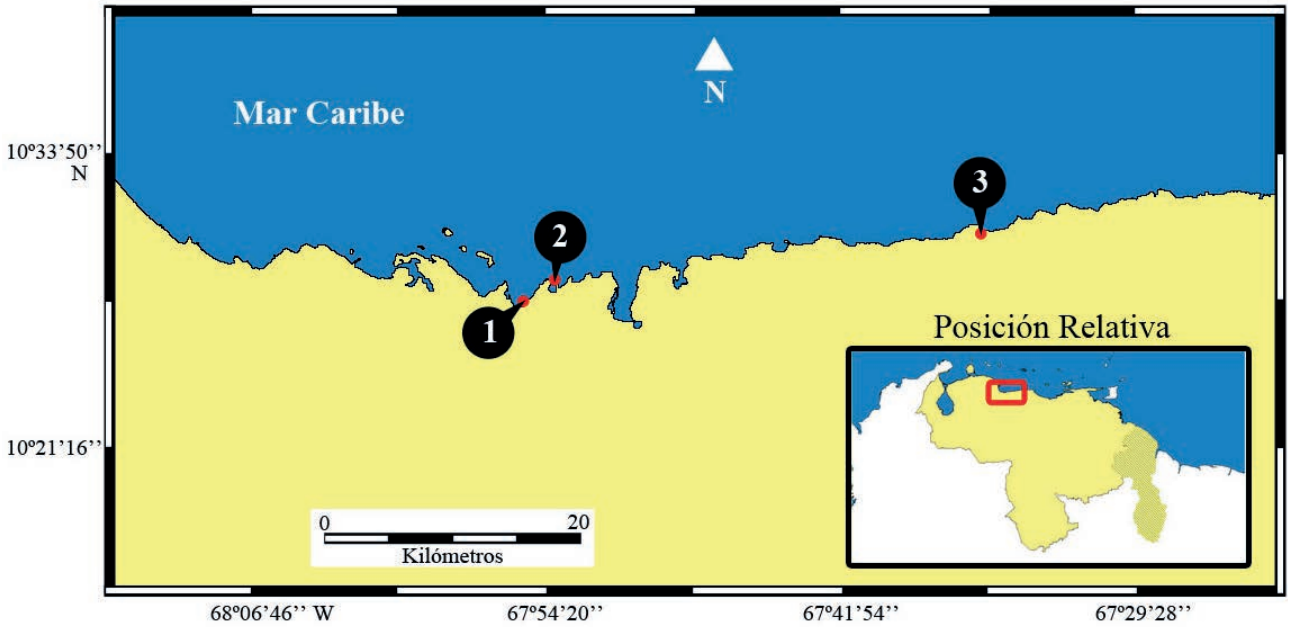

Figura 2. Ubicación espacial de las localidades en donde se reportaron avistamientos de *Physalia* entre los días 7 y 12 de marzo de 2020. Litoral Central, mar Caribe venezolano: (1) Ensenada de Patanemo y (2) Yapazcua (estado Carabobo). (3) Playa Grande en Choroní (estado Aragua).

Lesiones o "picaduras" de los Cnidarios

Como todos los Cnidarios, tanto corales, anémonas, medusas y *Physalia* capturan su alimento usando los tentáculos. Estos cuentan con células urticantes diminutas en forma de cápsulas llamadas cnidocidos. Estás células al entrar en contacto con su presa o una persona desprevenida, pueden inyectar un veneno por medio de los nematocistos, que son proyecciones similares a agujas microscópicas[7]. Las dosis y componentes del veneno varían entre las especies de Cnidarios y a su vez sus efectos en las personas dependerán de la edad, contextura física, grado de la lesión, área afectada y el desarrollo de alergias. En por esto que las lesiones y su magnitud no necesariamente serán similares entre diferentes personas. Mientras que otras especies de medusas y sifonóforos presentes en la región del Caribe, se sabe que la intensidad y gravedad de estas lesiones son menores, *Physalia* representa la principal especie de Cnidario con riesgos a la salud pública en la región. Esto se debe a que su picadura es dolorosa y los efectos del veneno pueden ocasionar complicaciones en la salud del afectado. En algunos casos documentados, estos accidentes han ocasionado la muerte de la persona[6]. Es por esto que la Organización Mundial de la Salud (OMS) incluyó a *Physalia* en el listado de "especies peligrosas" para la salud humana dentro de las Guías para Ambientes Seguros en Aguas Recreacionales[10].

Por otro lado, un aspecto interesante referente a las toxinas de los Cnidarios, es su aplicación en el área de la salud. En donde se han desarrollado diferentes tratamientos a partir de la purificación de estas sustancias en laboratorios, con el propósito de salvar vidas. Estos procedimientos médicos han sido empleados como alternativas para el tratamiento de enfermedades virales como el SIDA, trastornos cardiacos y terapias contra el cáncer[11,12]. Motivo adicional para reconocer y apreciar el valor específico de estos animales.

Protocolo ante el avistamiento de ejemplares en las playas

Se recomienda conservar una distancia prudencial del animal y notificar de inmediato a las autoridades del lugar. El flotador, también llamado neumatóforo es inerte, por lo que no cuenta con las células urticantes. Un funcionario o personal capacitado, puede retirarla del agua de forma segura, tomándola por el flotador con cuidado y extendiendo el brazo lo más lejano del cuerpo. Este procedimiento no debe ser realizado por los bañistas debido a los riesgos y medidas que deben ser consideradas. Se debe tener especial cuidado con los tentáculos de *Physalia*, que en algunos ejemplares pueden alcanzar 10 metros de largo, no son visibles debajo del agua y pueden estar fragmentados en el mar. Por esto, a pesar de ser retirado el animal pueden quedar restos de tentáculos en el agua. Así mismo se debe evitar el uso de redes o mallas para su captura, que puedan causar la fragmentación de los tentáculos.

Hay que estar atentos porque si se observa un ejemplar, existe la posibilidad que otros también hayan sido arrastrados hasta la playa por los vientos. Una recomendación que se debe adoptar en los balnearios públicos, es si la cantidad de animales supera los 5 ejemplares por cada 100 metros de playa, lo más prudente para resguardar la salud de las personas es comunicarse con las autoridades de la localidad para que se encarguen de cerrar temporalmente el balneario hasta que finalice el arribazón. Esta medida debe ser acatada con responsabilidad por el bien de la salud pública. Además, las observaciones realizadas en otras especies de Cnidarios pelágicos indican que en la mayoría de los casos la duración de estos eventos es breve y ocurren de forma puntual, afectado sólo una extensión específica de la región o provincia[13,14].

Procedimientos en caso de picadura (Primeros auxilios)

La primera recomendación es mantener la calma y ante todo NO tocar, rascar o restregar la lesión. Luego usando pinzas de cejas o con los dedos protegidos por guantes o bolsa plástica, se debe retirar los tentáculos y el resto del material azul que se encuentre sobre la piel y el traje de baño. Es muy importante hacer esto antes de lavar la lesión.

Para lavar la lesión se recomienda hacerlo con abundante agua de mar. El agua de mar se debe tomar en un recipiente alejado de la zona en donde ocurrió el accidente con *Physalia*, para garantizar que no contenga restos fragmentados de los tentáculos.

Si se cuenta con vinagre de cocina sin diluir (concentración: 3-5%), también se puede usar para limpiar la lesión. Aunque esta medida es recomendada, no es obligatoria. Lo más importante es que luego de aplicar estos primeros auxilios, la persona sea trasladada inmediatamente al centro de atención sanitaria más cercano. Es necesario realizar esto porque aunque la lesión parezca leve en un principio, con el paso del tiempo pueden presentarse complicaciones en la salud.

Medidas que no se deben implementar

Todas las medidas mencionadas a continuación están contraindicadas porque podrían causar que empeore la lesión: (1) No se debe limpiar la lesión con agua dulce, orina, licor ni algún otro líquido. Las variaciones en las condiciones que rodean las células urticantes (cnidocitos), como cambios en la presión osmótica, pueden ocasionar la activación de un mayor número de células e incrementar la lesión. (2) No aplicar hielo, arena o cremas corporales. (3) Nunca se debe secar ni frotar el área afectada con prendas de tela como toallas. (4) Evitar la exposición al sol de la lesión.

Indicaciones para el personal médico

Estas indicaciones están dirigidas al personal de la medicina. Reiteramos que en caso de sufrir algún accidente con *Physalia* u otra lesión de seriedad causada por fauna marina, la persona debe ser trasladada al centro de atención sanitaria más cercano en donde será atendido por un profesional en el área. Bajo ninguna circunstancia deberá automedicarse o restar importancia por presentar sintomatología leve, porque es posible desarrollar complicaciones post-lesión.

Haddad *et al.*[15] estudiaron la etiología de las lesiones cutáneas producidas por Cnidarios en la costa de Brasil. En este trabajo muestran el aspecto característico de las lesiones por *Physalia*, que son visibles como largas marcas lineales entrecruzadas, lo que permite reconocerlas y diferenciarlas de las lesiones que causan otras especies[15]. A partir de la extensión del área afectada es posible también evaluar la severidad de la lesión.

Para el pretratamiento por el personal médico, se deben revisar las soluciones sugeridas en Wilcox *et al.*[16], específicamente aquellas que producen porcentajes de descargas de cnidocitos menores a 0,6% (ver Tabla 2, en Wilcox *et al.*[16]). Entre estas soluciones de uso tópico se encuentran el agua de mar, vinagre blanco (3-5%), gluconato de cobre (30 mM en 110 mM de solución salina), la lidocaína (4%) y el spray comercial Sting No More ®.

Otro tratamiento aplicado para aliviar el dolor, con buenos resultados aparentes, consiste en la inmersión del área afectada en agua caliente a 45 ºC durante 20 minutos[17]. Primero es necesario asegurarse haber realizado los primeros auxilios antes descritos. Además, se debe verificar previamente que el nivel de calor es tolerable, esto lo tiene que realizar el personal médico ya que la víctima puede tener alterada la sensibilidad al dolor.

El tratamiento dependerá del criterio médico basado en el manejo sintomático. Se recomienda que los centros asistenciales cercanos a las zonas costeras cuenten con antihistamínicos, corticoesteroides, antipiréticos y AINES. Cazorla-Perfetti *et al.*[9] indican que todos los pacientes presentaron dolores intensos, urticaria y trastornos sistémicos (disnea, fiebre, malestar general, taquicardia). El tratamiento de los síntomas descritos por estos autores, según la evaluación del paciente, incluyó loratadina (administrado por vía oral, 3-10 mg/día por 10 días), hidrocortizona (vía intravenosa, un vial de 500 mg; 5 mg/kg en niños), y acetaminofén para el dolor y la inflamación (tabletas de 500 mg y suspensión para niños de 15 mg/kg; cada 6 horas por 3 días). Insistimos en advertir que estos tratamientos, deben ser aplicados únicamente bajo la supervisión de un profesional de la medicina.

Conclusiones

La Fragata Portuguesa (*Physalia physalis*) constituye un organismo de interés tanto por su importancia ecológica, los aportes potenciales en la investigación médica y sus efectos en la salud pública. Esto último debido a los riesgos que representan para los humanos por el incremento en la frecuencia de los arribazones observados en el Atlántico. El arrastre por los vientos de esta especie oceánica a las playas, la coincidencia de estos eventos durante los periodos vacacionales, las considerables lesiones que pueden causar, así como el hecho que los accidentes con esta especie pueden ser motivo de consulta médica, hace necesario que *Physalia* sea conocida por los profesionales de la medicina y autoridades. Tantos aquellos que trabajan en centros asistenciales, guardaparques, salvavidas, policías y bomberos que ejercen acciones sanitarias y de resguardo en toda la zona costera. Los futuros estudios desarrollados en el Caribe, que permitan evaluar los patrones y factores que rigen la biología de la especie, serán de utilidad para estimar la frecuencia y magnitud de los arribazones de *Physalia*, así como reducir sus efectos perjudiciales.

Recomendaciones

Entre las labores necesarias para la capacitación de las personas, se encuentra el desarrollo de programas educativos que permita a los niños reconocer a *Physalia*, así como los riegos que representa a la salud, porque estos pueden confundir el animal con algo inofensivo e intenten manipularlo. Por otro lado, se debe invertir en la información y capacitación del personal de atención primaria sobre la manipulación de la especie, así como la aplicación de los primeros auxilios. Las lesiones de *Physalia* pueden presentar complicaciones sistémicas potencialmente mortales, por esto se debe desarrollar programas de vigilancia epidemiológica, especialmente en visitantes y viajeros de las zonas costeras.

Agradecimientos

Queremos agradecer a la médica Ana C. Pereira D. y el biólogo Julio C. Morón por sus valiosos aportes que permitieron mejorar este manuscrito.

Referencias bibliográficas

1. Losada FJ, Marques Pauls S. Cnidarios. En: Aguilera M, Azocar A, González Jiménez E, eds. Biodiversidad en Venezuela, Volumen 1. Caracas, Venezuela: Fundación Polar y Ministerio de Ciencias y Tecnología. Fondo Nacional de Ciencia, Tecnología e Innovación (Fonacit); 2003:228-241.
2. Zoppi E. Distribución vertical del zooplancton en el golfo y extremo este de la fosa de Cariaco. Bol Inst Ocean Univ Oriente. 1961;1(1):219-247.
3. Gasca R, Loman-Ramos L. Biodiversidad de Medusozoa (Cubozoa, Scyphozoa e Hydrozoa) en México. Rev Mex Biodivers. 2014;85:154-163. doi:10.7550/rmb.32513
4. Ponce DP, López E. Medusas, las bailarinas del mar. CONABIO Biodiversitas. 2013;109:1-6.
5. Purcell JE, Arai MN. Interactions of pelagic cnidarians and ctenophores with fish: A review. Hydrobiologia. 2001;451:27-44. doi:10.1023/A:1011883905394

6. Labadie M, Aldabe B, Ong N, et al. Portuguese man-of-war (Physalia physalis) envenomation on the Aquitaine Coast of France: An emerging health risk. Clin Toxicol. 2012;50(7):567-570. doi:10.3109/15563650.2012.707657
7. Haddad V, Virga R, Bechara A, da Silveira FL, Morandini AC. An outbreak of Portuguese man-of-war (Physalia physalis - Linnaeus, 1758) envenoming in Southeastern Brazil. Rev Soc Bras Med Trop. 2013;46(5):641-644. doi:10.1590/0037-8682-1518-2013
8. Castillo M de los Á. Ejecutan evacuación temporal en Choroní por presencia de medusas. El Aragüeño.com.ve. https://elaragueno.com.ve/2020/03/12/ejecutan-evacuacion-temporal-en-choroni-por-presencia-de-medusas/. Publicado en marzo 12, 2020.
9. Cazorla-Perfetti DJ, Loyo J, Lugo L, et al. Epidemiology of the cnidarian Physalia physalis stings attended at a health care center in beaches of Adicora, Venezuela. Travel Med Infect Dis. 2012;10(5-6):263-266. doi:10.1016/j.tmaid.2012.09.007
10. OMS. Guidelines for safe recreational water environments, Volumen 1: Coastal and fresh waters. Ginebra, Suiza; 2002.
11. Balamurugan E, Venkata Reddy B, Padmanaban Menon V. Antitumor and antioxidant role of Chrysaora quinquecirrha (Sea Nettle) nematocyst venom peptide against ehrlich ascites carcinoma in Swiss Albino mice. Mol Cell Biochem. 2010;338:69-76. doi:10.1007/s11010-009-0339-3
12. Becerra-Amezcua MP, González-Márquez H, Guzmán-Garcia X, Guerrero-Legarreta I. Medusas como fuente de productos naturales y sustancias bioactivas. Rev Mex Ciencias Farm. 2016;47(2):7-21.
13. Baumann S, Schernewski G. Occurrence and public perception of jellyfish along the German Baltic coastline. J Coast Conserv. 2012;16(4):555-566. doi:10.1007/s11852-012-0199-y
14. Rodríguez G, Clarindo G, McKnight L. Jellyfish outbreaks in coastal city beaches from a management perspective. Coast Cities their Sustain Futur. 2015;1:277-288. doi:10.2495/cc150231
15. Haddad V, da Silveira FL, Migotto ÁE. Skin lesions in envenoming by cnidarians (Portuguese man-of-war and jellyfish): Etiology and severity of accidents on the Brazilian coast. Rev Inst Med Trop Sao Paulo. 2010;52(1):47-50. doi:10.1590/S0036-46652010000100009
16. Wilcox CL, Headlam JL, Doyle TK, Yanagihara AA. Assessing the efficacy of first-aid measures in Physalia sp. envenomation, using solution and blood agarose-based models. Toxins (Basel). 2017;9(5):149. doi:10.3390/toxins9050149
17. Loten C, Stokes B, Worsley D, Seymour JE, Jiang S, Isbister GK. A randomised controlled trial of hot water (45° C) immersion versus ice packs for pain relief in bluebottle stings. Med J Aust. 2006;184(7):329-333. doi:10.5694/j.1326-5377.2006.tb00265.x

Received: 10 julio 2020
Accepted: 15 septiembre 2020

NEWS AND VIEWS

Mechanisms of Nuclear Transport in the cell: RNA exosome in *Saccharomyces cerevisiae*

Bruna Rech[1] and Fernando A. Gonzales-Zubiate[2]

DOI. 10.21931/RB/2020.05.04.25

Abstract: Ribonucleases (RNases) functions in the cell include precise maturation of non- coding RNAs and degradation of specific RNA transcripts that are no longer necessary. RNAses are present in the cell as single units or assembled as multimeric complexes; one of these complexes is the RNA exosome, a highly conserved complex essential for RNA processing and degradation. In the yeast *Saccharomyces cerevisiae*, the RNA exosome comprises eleven subunits, two with catalytic activity: Rrp6 and Rrp44, where the Rrp6 subunit is exclusively nuclear. Despite the RNA exosome has been intensively investigated since its discovery in 1997, only a few studies were accomplished concerning its nuclear transport. This review describes recent research about cellular localization and transport of this essential complex.

Key words: Ribonucleases, exosome, nuclear transport, Rrp6, Rrp44, RNA processing, RNA degradation.

Introduction

RNA exosome is a multiprotein RNase involved in the modification of all RNAs in the cell; its primary function includes exonucleolytic and endonucleolytic cleavage of pre-ribosomal RNA (pre-rRNA), messenger RNA (mRNA), small nuclear RNA (snRNA), and small nucleolar RNA (snoRNA)[1]. Other RNA exosome substrates were described and included a significant group of long noncoding RNAs (lncRNAs): cryptic unstable transcripts (CUT) in yeast and upstream promoter transcripts (PROMPT) in humans, prematurely terminated RNA (ptRNA), enhancer RNA (eRNA) and long intergenic RNA (lincRNA)[2] (Figure 1). Highly conserved throughout evolution, exosome complex can be found in several species such as *Archaea*, *Saccharomyces cerevisiae*, *Drosophila melanogaster*, *Arabidopsis thaliana*, *Mus musculus*, and humans, to mention some. In *Saccharomyces cerevisiae*, the exosome is present in both nucleus and cytoplasm, fulfilling different functions depending on its substrates. Two structures compose the exosome core: a barrel-like with six different subunits, each containing an inactive RNase PH domain (Rrp41, Rrp42, Rrp43, Rrp45, Rrp46, Mtr3); and a cap, capping this barrel with three RNA binding subunits (Rrp4, Rrp40, Csl4). The catalytic subunits bind to opposite sides of the core: Rrp44 with endo- and exonucleolytic activities is present in both nuclear and cytoplasmic exosome[3-5]; Rrp6 with a 3'-5' exonucleolytic activity present only in the nuclear exosome[6] (Figure 2).

The nuclear exosome[7,8] processes degradation of incorrectly processed RNAs and maturation of ribosomal RNAs, small nuclear RNAs and small nucleolar RNAs. Furthermore, cytoplasmic exosome plays a vital role in regulating mRNA biogenesis's gene expression by mRNA degradation[9,10].

Nuclear transport of exosome

Nuclear transport is primarily mediated by specific interactions between a karyopherin, a protein transporter, and signal sequences (NLS; Nuclear Localization Signal) present in the cargo proteins[11,12] (Figure 3). In *Saccharomyces cerevisiae*, there is one karyopherin: Srp1. Besides, there are 14 karyopherins β: ten of which are involved in transport to the nucleus (importins - Kap95, Kap104, Sxm1/Kap108, Mtr10, Kap114, Nmd5, Kap120/Lph2, Pse1/Kap121, Kap122, Kap123), three are involved in transport to the cytoplasm (exportins - Cse1, Crm1/Xpo1, Los1), and one karyopherin is involved in transport in both directions, Msn5[13]. Interaction of karyopherins Srp1 and Kap95 with Rrp6 were observed initially in protein purification experiments[14-17] and co-immunoprecipitation experiments using Rrp6 as bait showing a surprising number of karyopherins: Kap95, Srp1, Kap114, Kap123, Sxm1, and Cse1[18].

Presence of NLSs in exosome subunits

In-silico and experimental analysis showed three subunits containing NLSs in their sequence: Rrp6, Rrp43, and Rrp44. Subunit Rrp43 contains a potential NLS between the residues 203 and 213: $_{203}$LKMKRKWSYVL$_{213}$ identified using the software NLS Mapper and NLStradamus[19,20]. No experiments are available to test if this motif could serve as a nuclear localization signal.

Subunit Rrp6 showed the presence of a three different NLSs in its sequence

NLS1 sequence $_{104}$NSKSRGSDLQYLGEFSGKNFSPTKRVEKP$_{132}$ identified by NLS Mapper and NLStradamus[19,20]. NLS2: $_{153}$KEKPNALKPLSESLRLVDDDENNPSHYPHPY$_{183}$, contains a multipartite proline–tyrosine nuclear localization signal called PY-NLS with a C- terminal R/H/K-X2–5-P-Y motif within a positively charged region of approximately 30 amino acids[18,21]. They could be recognized by importins Kap104, Sxm1/Kap108, Kap121, Kap114, Nmd5/Kap119, and Kap95[22-24].

NLS3: $_{697}$RQQKKRRFDPSSSDSNGPRAAKKRRPA$_{723}$, a classical NLS at the C-terminal region of Rrp6 that could be recognized by importin α Srp1[25]. It was observed that lack of any of the mentioned NLSs in the Rrp6 sequence lead to a partial mislocalization in the cell[18].

Subunit Rrp44 showed to possess three NLSs

NLS1: $_{172}$RAIRKTCQWYSEHLKPY$_{188}$, similar to Rrp6-NLS2 with a nuclear localization signal PY-NLS, NLS1 is located PinC domain of Rrp44[26].

NLS2 is located in the cold shock domain 2 CSD2[26] be-

[1] Fertility Medical Group, Sao Paulo, Brazil.
[2] School of Biological Sciences and Engineering, Yachay Tech University, Ecuador.

Corresponding author: fgonzales@yachaytech.edu.ec

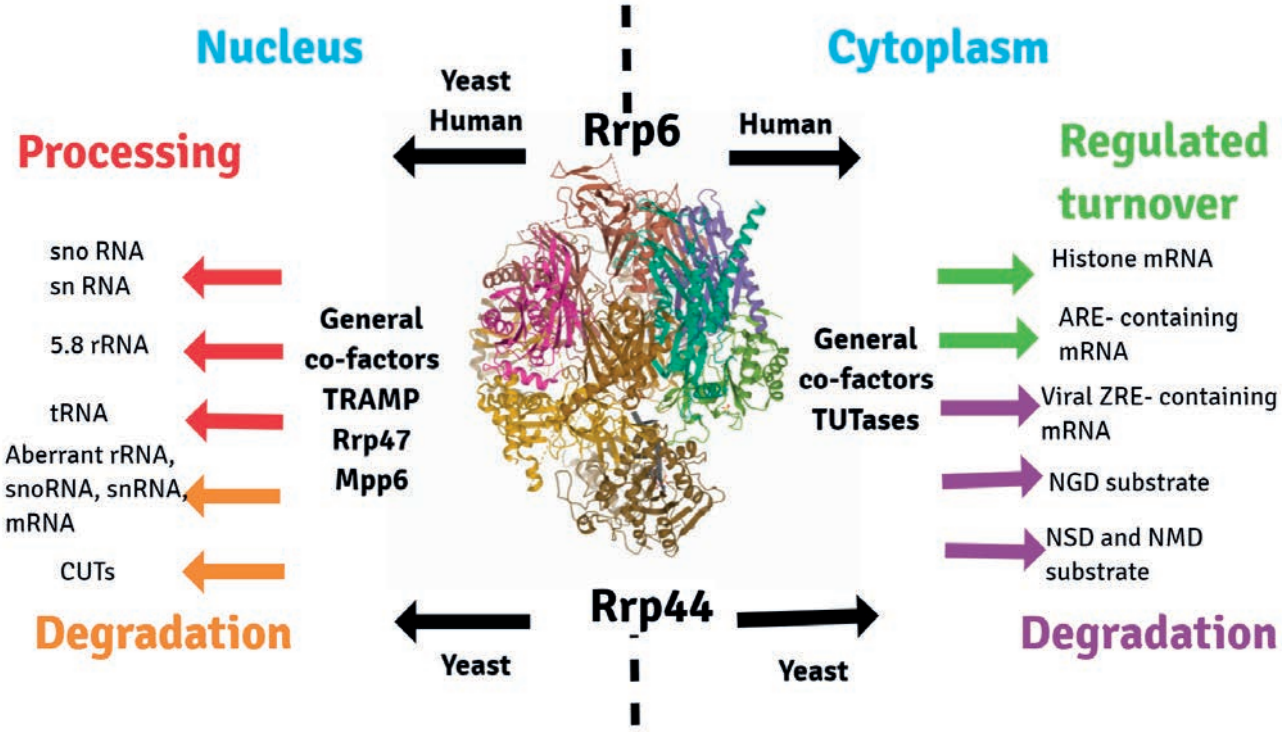

Figure 1. RNA quality control by the exosome for aberrant mRNA, tRNA, rRNA, and other noncoding RNA (ncRNA) species in every cell compartment. Arrows indicate the localization of active nucleases Rrp6 and Rrp44. TRAMP (complex consists of helicase Mtr4, polyA polymerase Trf4 or Trf5, and RNA-binding proteins Air1 or Air2), TUTases (terminal RNA uridylyltransferases). CUTs (Cryptic unstable transcripts), upstream promoter transcripts (PROMPTs), and upstream noncoding transcripts (UNTs). ARE (AU-rich instability element). Aberrant mRNAs with translation defects: NMD (Nonsense-mediated decay), NSD (non-stop decay), and NGD (no-go decay).

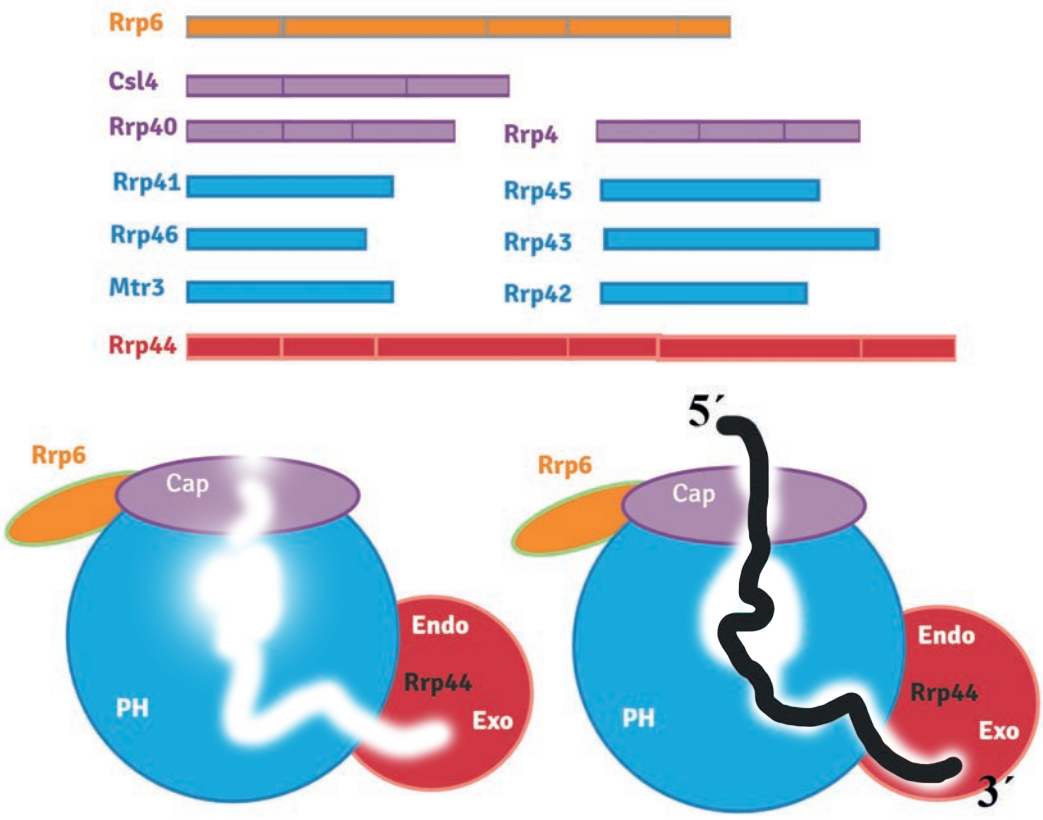

Figure 2. Exosome structure in yeast. A. Cap and barrel-like structures of exosome in purple and blue, respectively. Associated nucleases are in red (Rrp44) and orange (Rrp6). B. RNA-free form of the exosome. C. RNA going through the exosome channel to be processed.revistabionatura.com/2020.05.04.25.html

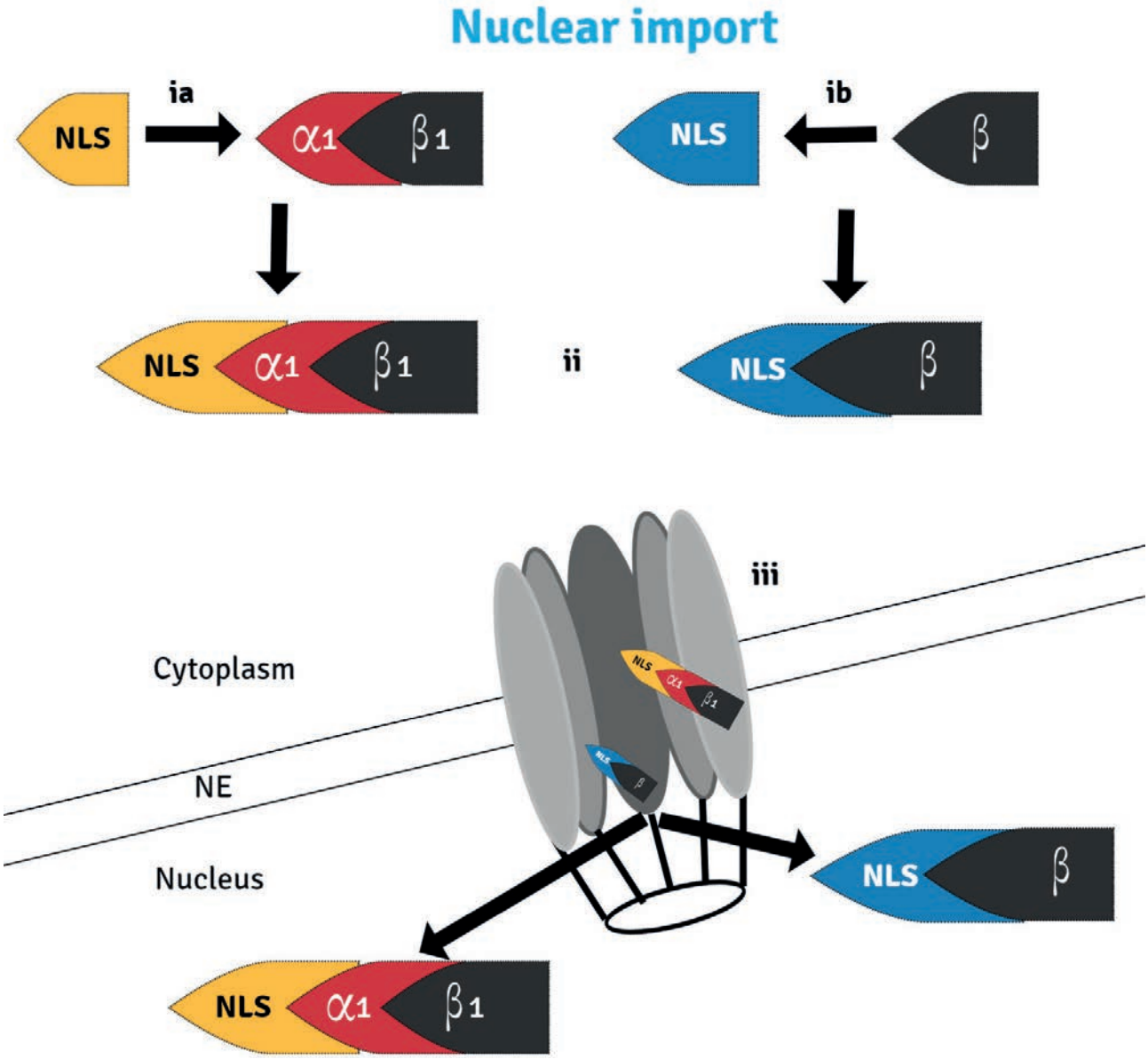

Figure 3. Nuclear transport through the Nuclear Pore Complex requires the recognition and binding of NLS-containing cargo proteins by either the importins α/β1 heterodimer (ia) or importin β alone (ib) on the cytoplasm. Once bound (ii), the transport complex moves through the NPC (iii) via a series of transient interactions between importin β and nucleoporins in the NPC.

tween the residues 370 and 401 of Rrp44 $_{370}$RRLLAKDAMIAQRSKKIQPTAKVVYIQRRSWR$_{401}$ and contains the consensus NLS R/K-X2-L-XnV/Y-X2-V/I-X-K/R-X3-K/R that can be recognized by the importins Kap114, Kap95, Kap123, Pse1, and Kap104[27].

NLS3 is located at the C-terminus of Rrp44: $_{988}$DPITSKRKAELLLK$_{1001}$. This NLS is similar to the NLS in Drosophila Rrp44 (dDis3), which is recognized by importin-3[28,29]. From the three NLSs presents in Rrp44 sequence, NLS1 is the most critical signal for Rrp44 nuclear import. NLS1, together with either NLS2 or NLS3 is sufficient for Rrp44 nuclear localization[18].

The presence of three nuclear localization signals in both Rrp6 and Rrp44 and more of one karyopherin involved in their nuclear transport confirm overlapping and redundancy in the import pathways.

Depletion of karyopherins affect the localization of exosome subunits

Depletion of essential karyopherin Srp1 in the cell after 14 hours showed Rrp6 visualized in the cytoplasm, although Rrp6 remained concentrated in the nucleus; levels of Rrp6 decreased upon inhibition of Srp1 expression, it could suggest when not efficiently transported to the nucleus, Rrp6 may be destabilized[18]. Inhibition of karyopherin Kap95 expression for 14 hours strongly affected Rrp6 localization; Rrp6 was observed in the cytoplasm and concentrated in the nucleus. Surprisingly, the deletion of the karyopherin Sxm1/Kap108 gene affected the localization of Rrp6 partially Sxm1 is not essential for growth but Rrp6 was detected in the cytoplasm, and its mislocalization was more robust at 37°C. These results showed that Rrp6 could associate with different importins for its transport to the nucleus[18].

Localization of Rrp44 in wild-type cells is mainly in the nucleus with a weak signal in the cytoplasm. The depletion of Srp1 or Kap95 levels in the cell leads to Rrp44 partial mislocalization, evidenced by a strong signal in the cytoplasm. Unlike Rrp6, the depletion of Sxm1 did not show any effect on Rrp44 localization[30].

Conclusions

The RNA exosome is localized in the cytoplasm and the nucleus (specifically in the nucleolus). Although its predominantly nuclear localization, only three exosome subunits contain NLSs in their sequence, and from these three, two have shown to be transported by karyopherins: Rrp6 and Rrp44. It is already known that Srp1 and Kap95 are the karyopherins involved in the nuclear transport of Rrp44 and Rrp6, with the extra help of karyopherin Sxm1 for Rrp6 transport. However, it is uncertain how the rest of the subunits are transported to the nucleus or transported independently or as a complex. Only further studies will help to elucidate these questions and better understand the transport mechanisms of this complex.

Bibliographic references

1. Allmang C, Kufel J, Chanfreau G, Mitchell P, Petfalski E, Tollervey D. Functions of the exosome in rRNA, snoRNA and snRNA synthesis. EMBO J [Internet]. 1999 Oct 1;18(19):5399–410. Available from: http://www.pubmedcentral.nih.gov/articlerender.fcgi?artid=1171609&tool=pmcentrez&rendertype=abstract
2. Ogami K, Chen Y, Manley JL. RNA surveillance by the nuclear RNA exosome: Mechanisms and significance. Noncoding RNA. 2018;4(1).
3. Liu Q, Greimann JC, Lima CD. Reconstitution, activities, and structure of the eukaryotic RNA exosome. Cell [Internet]. 2006 Dec 15 [cited 2012 Apr 8];127(6):1223–37. Available from:http://www.ncbi.nlm.nih.gov/pubmed/17174896
4. Makino DL, Baumgärtner M, Conti E. Crystal structure of an RNA- bound 11-subunit eukaryotic exosome complex. Nature [Internet]. 2013 Mar 7 [cited 2013 Nov 5];495(7439):70–5. Available from: http://www.ncbi.nlm.nih.gov/pubmed/23376952
5. Dziembowski A, Lorentzen E, Conti E, Séraphin B. A single subunit, Dis3, is essentially responsible for yeast exosome core activity. Nat Struct Mol Biol. 2007;14(1):15–22.
6. Burkard KTD, Butler JS. A Nuclear 3 β -5 β Exonuclease Involved in mRNA Degradation Interacts with Poly (A) Polymerase and the hnRNA Protein Npl3p A Nuclear 3β -5β Exonuclease Involved in mRNA Degradation Interacts with Poly (A) Polymerase and the hnRNA Protein Npl3p. 2000;20(2).
7. Houseley J, LaCava J, Tollervey D. RNA-quality control by the exosome. Nat Rev Mol Cell Biol [Internet]. 2006;7(7):529–39. Available from: http://www.ncbi.nlm.nih.gov/pubmed/16829983
8. Allmang C, Kufel J, Chanfreau G, Mitchell P, Petfalski E, Tollervey D. Functions of the exosome in rRNA, snoRNA and snRNA synthesis. EMBO J [Internet]. 1999 Oct 1;18(19):5399–410. Available from: http://www.pubmedcentral.nih.gov/articlerender.fcgi?artid=1171609&tool=pmcentrez&rendertype=abstract
9. Anderson JSJ, Parker R. The 3′ to 5′ degradation of yeast mRNAs is a general mechanism for mRNA turnover that requires the SKI2 DEVH box protein and 3′ to 5′ exonucleases of the exosome complex. 1998;17(5):1497–506.
10. Oliveira CC, Gonzales FA, Zanchin NIT. Temperature-sensitive mutants of the exosome subunit Rrp43p show a deficiency in mRNA degradation and no longer interact with the exosome. Nucleic Acids Res [Internet]. 2002 Oct 1;30(19):4186–98. Available from: http://www.pubmedcentral.nih.gov/articlerender.fcgi?artid=140545&tool=pmcentrez&rendertype=abstract
11. Xu D, Farmer A, Chook YM. Recognition of nuclear targeting signals byKaryopherin-β proteins. Curr Opin Struct Biol. 2010;20(6):782–90.
12. Lange A, Mills RE, Lange CJ, Stewart M, Devine SE, Corbett AH. Classical nuclear localization signals: Definition, function, and interaction with importin β . J Biol Chem. 2007;282(8):5101–5.
13. Mosammaparast N, Pemberton LF. Karyopherins: from nuclear-transport mediators to nuclear-function regulators. Trends Cell Biol [Internet]. 2004 Oct [cited 2013 Nov 5];14(10):547–56. Available from: http://www.ncbi.nlm.nih.gov/pubmed/15450977
14. Ho Y, Gruhler A, Heilbut A, Bader GD, Moore L, Adams S, et al. Systematic identification of protein complexes in Saccharomyces cerevisiae by mass spectrometry. 2002;415(January):2–5.
15. Gavin A-C, Bösche M, Krause R, Grandi P, Marzioch M, Bauer A, et al.Functional organization of the yeast proteome by systematic analysis of protein complexes. Nature [Internet]. 2002 Jan 10;415(6868):141–7. Available from: http://www.ncbi.nlm.nih.gov/pubmed/11805826
16. Gavin A-C, Aloy P, Grandi P, Krause R, Boesche M, Marzioch M, et al. Proteome survey reveals modularity of the yeast cell machinery. Nature [Internet]. 2006 Mar 30 [cited 2014 Jan 29];440(7084):631–6. Available from: http://www.ncbi.nlm.nih.gov/pubmed/16429126
17. Synowsky S a, van Wijk M, Raijmakers R, Heck AJR. Comparative multiplexed mass spectrometric analyses of endogenously expressed yeast nuclear and cytoplasmic exosomes. J Mol Biol [Internet]. 2009 Jan 30 [cited 2013 Nov 5];385(4):1300–13. Available from:http://www.ncbi.nlm.nih.gov/pubmed/19046973
18. Gonzales-Zubiate FA, Okuda EK, Da Cunha JPC, Oliveira CC. Identification of karyopherins involved in the nuclear import of RNA exosome subunit Rrp6 in Saccharomyces cerevisiae. J Biol Chem. 2017;292(29):12267–84.
19. Kosugi S, Hasebe M, Tomita M, Yanagawa H. Systematic identification of cell cycle-dependent yeast nucleocytoplasmic shuttling proteins by prediction of composite motifs. Proc Natl Acad Sci U S A. 2009;106(14):10171–6.
20. Nguyen Ba AN, Pogoutse A, Provart N, Moses AM. NLStradamus: a simple Hidden Markov Model for nuclear localization signal prediction. BMC Bioinformatics. 2009;10:202.
21. Lee BJ, Cansizoglu AE, Suel KE, Louis TH, Zhang Z, Chook YM. Rules for Nuclear Localization Sequence Recognition by Karyopherin b2. Cell. 2006;126(3):543–58.
22. Suel KE, Gu H, Chook YM. Modular Organization and Combinatorial Energetics of Proline – Tyrosine Nuclear Localization Signals. PLoS Biol. 2008;6(6).
23. Lee C, Hodgins DC, Calvert JG, Welch SKW, Jolie R, Yoo D. The nuclear localization signal of the PRRS virus nucleocapsid protein modulates viral replication in vitro and antibody response in vivo. Adv Exp Med Biol. 2006;581:145–8.
24. Süel KE, Chook YM. Kap104p imports the PY-NLS-containing transcription factor Tfg2p into the nucleus. J Biol Chem. 2009;284(23):15416–24.
25. Phillips S, Butler JS. Contribution of domain structure to the RNA 3 end processing and degradation functions of the nuclear exosome subunit Rrp6p. 2003;1098–107.
26. Lebreton A, Tomecki R, Dziembowski A, Séraphin B. Endonucleolytic RNA cleavage by a eukaryotic exosome. Nature [Internet]. 2008 Dec 18 [cited 2012 Mar 11];456(7224):993–6. Available from: http://www.ncbi.nlm.nih.gov/pubmed/19060886
27. Fries T, Betz C, Sohn K, Caesar S, Schlenstedt G, Bailer SM. A novel conserved nuclear localization signal is recognized by a group of yeast importins. J Biol Chem. 2007;282:19292–301.
28. Graham AC, Davis SM, Andrulis ED. Interdependent nucleocytoplasmic trafficking and interactions of Dis3 with Rrp6, the core exosome, and importin- β 3. 2009;10(5):368–85.
29. Mamolen M, Smith A, Andrulis ED. Drosophila melanogaster Dis3 N- terminal domains are required for ribonuclease activities, nuclear localization and exosome interactions. Nucleic Acids Res. 2010;38(16):5507–17.
30. Okuda EK, Gonzales-Zubiate FA, Gadal O, Carla C. Oliveira. Nucleolar localization of the yeast RNA exosome subunit Rrp44 hints at early pre-rRNA processing as its main function. J Biol Chem. 2020;(1):1–9.

Received: 10 August 2020
Accepted: 16 October 2020

NEWS AND VIEWS

Modeling the strategies to eradicate rats introduced in the Galapagos Islands

Camila Velastegui[1], Mary Pulgar-Sánchez[1], Kevin Chamorro[2]

DOI. 10.21931/RB/2020.05.04.26

Abstract: The Galapagos Islands are well known for their incredible biodiversity and the inspiration for Charles Darwin's natural evolution theory. It is an ecosystem that has evolved without predators, so their native species are unfit for competition. As a result, this biodiversity has been threatened by invasive species like rats (Black and Norwegian). Nowadays, the primary strategy to control rats is by having drones that disperse a unique poisoned bait. Our study aims to mathematically model the strategies to eradicate rats in islands, based on previously reported processes. As a result, we are obtaining the approximated time to reduce its population as much as being eradicated, without threatening the coexisting species. We also propose a suitable alternative to be applied in the Galapagos Islands to recover their biodiversity richness. We find that rats' introduction has caused a decrease in the native species due to having specific traits that make them fitter in different situations. The best method to control species in such a sensitive environment is by the use of anticoagulant rodenticides. The current method used for eradicating rats seems to be the most profitable even though there is not enough information to see the collateral consequences of the poison technique. Furthermore, we propose this theoretical study complemented with in situ samplings to corroborate our hypothesis and improve our prediction model.

Key words: Invasive species, rodenticides, eradication, prediction model, strategies, Galapagos Islands.

Introduction

Islands developed as isolated ecosystems resulted in species evolution with restricted native competence and the inability to compete with predators. Then the presence of foreign species directly treats island biodiversity worldwide. The introduction of mammals, specifically the presence of invasive rodents, is among the most problematic species in islands[1] by being responsible for changes in the ecosystem and many extinctions to date[2]. There are records of invasive rodents on 80% of the significant islands globally, and how it is still unceasingly introduced[3] that worries conservationists. Rodents represent more than a problem for the conservation of biodiversity; they are a threat to humans' health with whom overlap its habitat by being an imminent disease vector[4]. The rats' ease of adaptation, lifespan, and rapid spread, complemented by the warm, favorable climate of the islands, have made rats a tricky pest to deal with[5].

The need to recover species and restore island conservation has driven the development of eradication techniques as one of the most cost-effective tools[6], even though in large islands, this is often impossible[7]. Eradication of invasive species is based on (i) all target animals (rodents) are put at risk by the eradication technique(s), (ii) target animals must be removed at a rate exceeding their rate of increase at all densities, (iii) immigration must be zero[8]. However, native species are also at risk. So, this requires special attention. Meanwhile, the process must be done as fast as possible to avoid eliminating a new generation of invaders. Eradication is performed by delivering a lethal dose of rodenticide to each rodent; this bait containing rodenticide can be distributed either by hand-broadcast or in bait stations on small islands, but for larger islands, eradication by an aerial broadcast of bait is required to ensure suitable bait availability[5,9,10]. However, there is a failure rate of 16.1% of eradication from the overall eradication processes reported[5,11]. Mathematical models and, in particular, models applied to biology can be an essential tool to understand the dynamics of a phenomenon[12], which allows the prediction of the impact of a determined process with variables pre-established that saves monetary, ecological investment, labor, and time.

Galapagos Islands are an exact representation of biodiversity; however, it has been affected by introducing the rodents *Rattus rattus*, *R. norvegicus*, *R. exulans*, and *Mus musculus*[13] that arrive at the archipelago on whaling boats and pirate ships since the late 1600s[14]. Human colonies spread together with rats' dispersing along the island at unknown dates of arrival[15]. These introduced species caused a decrease in the population of endemic species principally in two ways: the first one is eating the eggs and the second by eating the other species' food. The Galapagos Islands have always been a key example of Charles Darwin's theory of evolution. Though, the species he detected at the time has been gradually lost. Darwin recorded in 1835, the first species of the black rat on the island Santiago and progressively new researchers recorded more rodent species[16]. Black rats drove the extinction of four endemic rodents and a terminal decline of fauna, to mention sea- and land-bird populations and even the endangered status of one race of giant tortoise[16–18]. At present, there are two endemic genera of rats, *Oryzomys* and *Nesoryzomys*[16].

In Galapagos Islands, there have been attempts to eradicate rodents; one of them occurred in 1988 at Pinzon Island with rodenticide bait dumps and hand broadcast of baits containing brodifacoum and coumatetralyl that were unsuccessful[19,20]. North Seymour Island was hand baited in 2007 with wax blocks containing brodifacoum and successfully eradicating black rats[21]. The first aerial broadcast of brodifacoum baits occurred in 2011 at Rabida and Pinzon Islands and managed to eliminate invasive black rats. For this procedure, it captured and held the Pinzon tortoises (*Chelonoidis ephippium*), Pinzon lava lizards (*Microlophus duncanensis*), and Galapagos hawks (*Buteo galapagoensis*) species to mitigate the direct impact of the rodenticide[15,22]. The rodenticide bait has led to non-target animals'

[1] School of Biological Sciences and Engineering, Yachay Tech University, Hacienda San José s/n, San Miguel de Urcuquí, Ecuador.
[2] School of Mathematical and Computational Sciences, Yachay Tech University, Hacienda San José s/n, San Miguel de Urcuquí, Ecuador.

Corresponding author: mary.pulgar@yachaytech.edu.ec

poisoning, especially raptors whose diet is not restricted only to rodents[23]. For instance, in 2011, after the eradication plan in Pinzon, all captive Galapagos hawks were released, and from days to months later, it was found that 22 of them died by anticoagulant toxicosis by brodifacoum in the liver due to rodenticide exposition of lava lizards, part of hawks diet[13,24].

This paper aims to evaluate an alternative use of rodenticide with reduced secondary effects and obtain a theoretical approximation by designing a mathematical equation that may predict the process before being applied in situ. Simultaneously, suggesting the control and management of strategies to eradicate rats in the Galapagos Islands. All based on the successful plans carried out in other case studies to promote the conservation of endemic species in the archipelago and avoid the rapid extinction of more species. Our study begins with an analysis of the three main strategies for eradicating rats, where the assumptions for our study are introduced. The base equation for our mathematical model is then shown and is followed by the model equations along with each parameter and estimated value to use. Then, in results and discussion, the best alternatives and the eradication time of rats in the Galapagos Islands are analyzed and compared. Finally, this work ends with the conclusions of our study and future work.

Methods

Eradication strategies and model assumptions

We had considered three main strategies for the eradication of rats. The first strategy is poisoning, the second is killing by trapping, and the third one is inducing infertility.

The poisoning strategy is based on the use of rodenticides that had been broadly applied in rat eradication programs, some with success and others with some failures[6]. Anticoagulant rodenticides are the most widely used poisoned technique. They inhibit the synthesis of clotting factors dependent on vitamin-K in the liver, which results in internal hemorrhaging, leading to death typically within 3–10 days[25]. The rodenticides are designed specially to kill rats, although non-target species could also be affected. There are some reports about the affection of non-target species due to rodenticides, especially in vertebrates[6]. The rate of success of rodenticide use depends on rats' ability to differentiate the toxins, which produce offspring capable of avoiding bait stations. For our model, we assume that the poisoning strategy is by using bait stations and that eventually, the rats will learn how to distinguish poison.

The second method analyzed is the use of traps, which are more acceptable within urban populations[27]. Trapping is recommended for sensitive environments where rat populations are prominent, as it has the most significant capture rate. The use of traps needs continuous monitoring, which requires more costs, but at the same time, it avoids affecting the capture of non-target species and also can be used as a way of monitoring the rat population within an island. This is an essential parameter before assisting the application of any eradication methods[28]. The use of traps also induces the development of trap shyness such that they learn to avoid traps. For that reason, a period of pre-baiting to familiarize the rats with the traps is recommended[29]. Due to this, the strategy could have a small-time lag from their initiation of the trap strategy and population decrease. Therefore, the use of traps is more recommended in places with high human density. In the Galapagos Islands, it is recommended in the populated islands, which are Baltra (Seymour), Floreana, Santa Cruz, San Cristóbal, and Isabela, and with a large population of rats. In our model, we assume that live traps are widely distributed in the islands and that rats will learn to avoid traps.

The third strategy consists of inducing sterility. The use of chemosterilants could have changed the behavior and structure of the population. Induced sterilty may be temporary or permanent and can affect males or females[30]. Depending on how the sterility is induced by chemosterilants or modified females' introduction, different outcomes could arise. In the Galapagos Islands, where it is not recommended to introduce any new animal, it is suggestable to induce infertility by chemosterilants like androgens. The sterilization strategy has higher specificity than traps. One of the main disadvantages of sterilization is the time lag between sterilization and decreased population size. In the present study, we applied the sterile induced in females because female rats mate several times (higher than 90 per hour with different males)[30]. The sterilization method that we are considering is the spread of androgens that induce infertility in females. We are assuming that rats do not learn how to identify the androgen bait. Just one intervention with androgen is needed, and we induce sterility for the remaining of the rat's lifetime.

In addition to the eradication methods described above, we also consider joining two strategies to get a better output of rats' eradication in the islands. For this purpose, we consider the case of applying poisoning and sterilization strategy. The assumptions will be the same as the eradication methods. The other assumptions for this method are applied at the same time. So, the same rate of rats dying from poison could be infertile or fertile.

Application of the Logistic equation

Rat populations grow in an essentially logistic pattern until the limit of the habitat's carrying capacity is approached[30]. It means that rat populations tend to increase exponentially, but they lower their increasing rate when the carrying capacity is reached. We had constructed our equations modeling the different eradication methods based on the logistic equation [1], where r is the rate of population increase. *N* is the number of individuals in the population. *K* is the carrying capacity[31]. We are assuming no time lags, no migration among islands or with the continent, and no influence of genetic variation.

$$\frac{dN}{dt} = rN\left(1 - \frac{N}{K}\right) \qquad [1]$$

To evaluate the best method to control rats, we varied the parameter "*r*" that regulates the increased population rate. For each method, we are calculating "*r*" that will result from the strategy applied. We consider that each eradication method has a different *r*. The calculation of *r* depends on the rate of births and deaths to the population. All the calculations and rates presented were defined by months.

Four factors will influence the rate of births. The first factor is the proportion of adults in the population (γ). In the model presented, we consider as an adult the population capable of producing offspring. The second factor is the average offspring that a rat produces per month (α). The third parameter is the female proportion within the population because they are the ones that produce offspring, so they are the ones that produce an increase in the population (β). For this parameter, the value of 0.5 is assumed, which means equal proportions. This is due to various reports showing there was an equal distribution of gender within the rats. The last factor is the fertility rate of females (δ), which is directly correlated with the proportion of pregnant female rats.

The rate of deaths is the sum of the rate of rats that die naturally (ω) and rats that die due to the eradication method. In our case, just the first method of eradication, the use of poison, we consider the rate of natural deaths and rats' rate died by poison. This last rate is calculated, considering that rats learn how to distinguish the poison. The equation developed by Gentry in 1971 describes this rate [2], where ϕ is the rate of rats dying by poison A_1, is the fraction of rats that will be poisoned if the rats will not realize that they are being poisoned, Q is the fraction of rats that do not learn to distinguish poison, and A_2 describes how fast the rats learn how to distinguish poison[32].

$$\phi = A_1(Q + (1 - Q)e^{-A_2}) \quad [2]$$

The second method of eradication is very similar to the first method because here, we also had rats that learn to avoid traps. Therefore, the rate of rats dying by traps will be influenced by B_1 (the fraction of rats that will be trapped if the rats will not realize that they are being trapped). P is the fraction of rats that do not learn to distinguish traps and B_2 describes how fast the rats learn how to distinguish traps[32].

For the third eradication method, the deaths will be just influenced by the fraction of rats that die due to natural causes. The change in this equation is the fertility rate that will decrease due to the induced sterility (i). . In the mixed strategies, we are using the same parameters as their respective eradication methods.

Model Equations and parameters of the Strategies analyzed

Summarizing all the descriptions above, we developed the following equations for the eradication methods. Equations [3], [4], [5], [6] describes the poisoning strategy, trapping strategy, sterilization strategy, and the combination of poisoning and infertility strategies, respectively:

$$\frac{dN}{dt} = (\gamma\alpha\beta\delta - [\omega + A_1(Q + (1 - Q)e^{-A_2})])N\left(1 - \frac{N}{K}\right) \quad [3]$$

$$\frac{dN}{dt} = (\gamma\alpha\beta\delta - [\omega + B_1(P + (1 - Q)e^{-B_2})])N\left(1 - \frac{N}{K}\right) \quad [4]$$

$$\frac{dN}{dt} = (\gamma\alpha\beta(\delta - i) - \omega)N\left(1 - \frac{N}{K}\right) \quad [5]$$

$$\frac{dN}{dt} = (\gamma\alpha\beta(\delta - i) - [\omega + A_1(Q + (1 - Q)e^{-A_2})])N\left(1 - \frac{N}{K}\right) \quad [6]$$

The values of the parameters described before were estimated from previous reports about the behavior of rats. In some cases, the parameters calculated were an average of various reports. The values and parameters are summarized in Table 1.

After finding all the parameters, we calculate the respective "r" values and then replace them in the logistic equation solution [7]. For the estimation of the carrying capacity, we calculated based on the total area of the islands that had rats in Galapagos, which is 6937 km^2,[22], and the home range of rats being 150 square feet[38]. To estimate the rats' initial population on the island, we consider the density of 4.6 rats per ha reported on one island of Galapagos[39].

$$N(t) = \frac{KN_0}{N_0 + (K - N_O)e^{-rt}} \quad [7]$$

Results and Discussion

To find the best strategy to eradicate rats, we must first solve each of the differential equations presented in [3],[4], and [5]. The results obtained considering the previous variables and restrictions presented by the model are presented in Fig. 1. We discover that the strategy that produces a more significant reduction is by poison with -0.20, the second is induced infertility with -0.12, and the trapping method with -0.11. It can be seen that the strategy of spreading poison is the one that makes our logistic equation tend to 0 more quickly.

The primary data found for the poison methodology to be most significant is the value of the intrinsic growth rate, which will influence rats' data that learn about the detection of the poison or the trap it is pretending to use. Besides, this data is highly influenced if we contrast it with the logistic equation's solution [4] since they are strictly within an exponential. So it will be what predominates for the behavior at zero that is expected for eradication. On the other hand, the infertility strategy has a supervised factor since the population of infertile rats must be better controlled with the rat eradication process. If we contrast it with equation [3], we observe that the variable induced infertility ratio is the independent variable with more weight to give a better growth rate. The poison propagation strategy is one of the most common to be used according to the reviewed literature, which suggests that it is the most effective strategy in the different places that have been applied.

As we can see in Fig. 1, even though poisoning is the best strategy, it does not result in the ideal time to reduce rats' population because if there is a long enough time lag, there could be a resurgence of rats. There have been reports that approximately after 2 years, there is a relapse of rat infestations and the percentage of rat incidence increase along the time[40]. However, when we used two techniques, it had a better result in eradicating rats, as shown in Fig. 3. The mixed strategy of poisoning and sterility the ones with highest values we got an r of -0.52 and got an eradication before two years, which ultimately is the aim.

With the results obtained, it is possible to consider the predicted times for the eradication of rats in each of the islands belonging to the Galapagos Archipelago that have the presence of rats as in Fig. 2, representing a population of rats N = 1 for each one of them and time in months. Therefore, in the solution of the logistic regression equation [6], we will be able to obtain the different times (t) according to the area in square kilometers (km^2) in which rats are exterminated applying the poison strategy. The results are presented in Table 2.

As we can see, the larger the island area, the longer it will take to eradicate rats, having a direct relationship between the area of the island and time. Still, the time of poisoning with rodenticide, despite being found as the most effective, takes a prolonged time, but this time is reduced notably if complemented with the other strategies. This fact is essential when avoiding new births since the generation time of rats is short.

Conclusions

The best strategy to recover biodiversity after the ecosystem has been affected by alien species' introduction is its eradication. The most viable and effective way found is the use of rodenticides and their dispersion through bait stations. The most widely used rodenticide is an anticoagulant of second-generation brodifacoum. The eradication time is dependent on the area of the island and its rodent population density. By

Parameter	Description	Estimate	Citation
γ	Adults proportion	0.43	33
α	Average offspring	3.70	34
β	Females proportion	0.50	34
δ	Fertile rats proportion	50.50	34
ω	Mortality rate due to natural causes	0.17	35
A_1	Poisoned rats	0.72	32
Q	Rats do not distinguish poison	0.26	32
A_2	Learning rats	0.75	32
B_1	Death by trapping	0.55	27,29,36
B_2	Rats learned to avoid traps	0.71	37
P	Rats did not distinguish traps	0.28	32,37
i	Infertility induced proportion	0.45	32

Table 1. Values of the parameters used in the calculations.

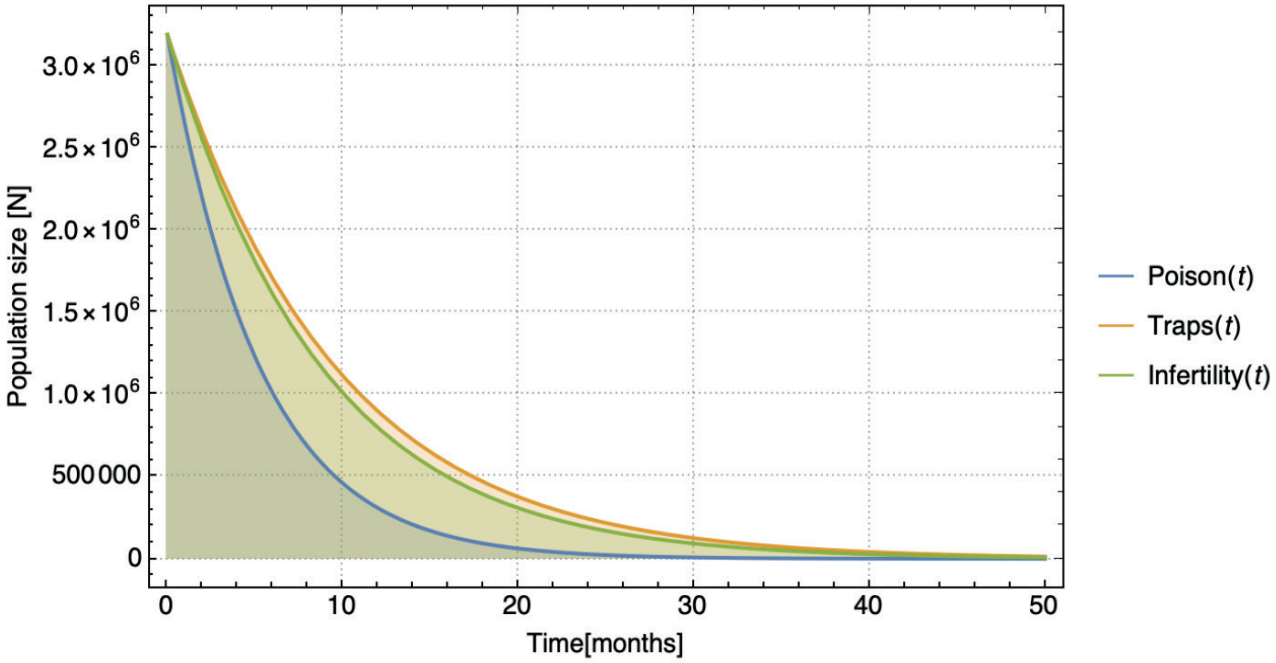

Figure 1. Population growth of the application of the three strategies.

combining the poisoning and sterility induced strategies, time is significantly reduced compared to the individual application. In the case of the Galapagos archipelago, Isabela Island needs the most time with 28.02 months, while the island we can eliminate rodents the fastest is Bartolomé, the smallest, in about a year. It has to be taken into account that the target animals inhabit the island, but if it is human-populated and if there are animals that coexist in the same habitat.

The application of a mathematical model to this situation allows us to simulate the eradication of rats without the need to experiment in situ, which is the best in the least amount of time. This allows us to save financial expenses and time to carry out this work. It is crucial to have actual data from the islands to improve the model and get closer to real-time to offer better suggestions regarding invasive species' eradication processes.

Future work

We look forward to finding a budget for the studio and monitoring the ecology of rodents in the Galapagos Islands and how it has affected biodiversity. There is insufficient quantitative information on the critical archipelago and introduced

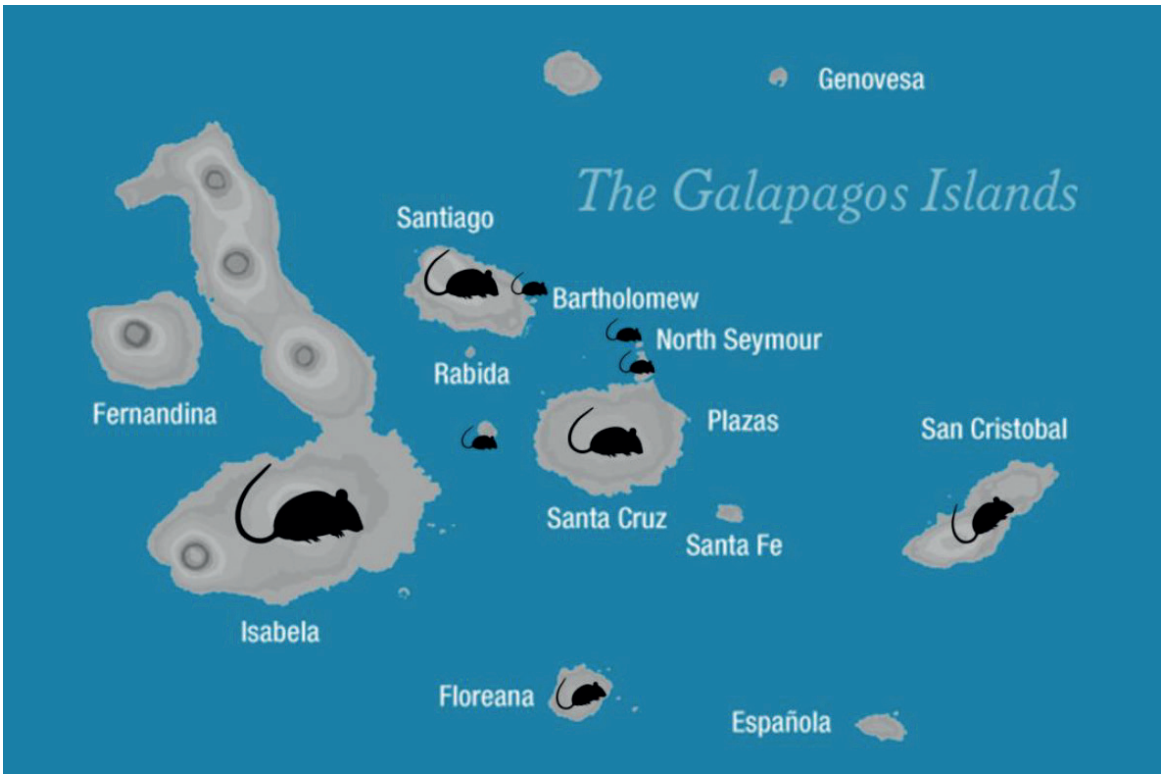

Figure 2. Map of the Islands that have registered the presence of rats.

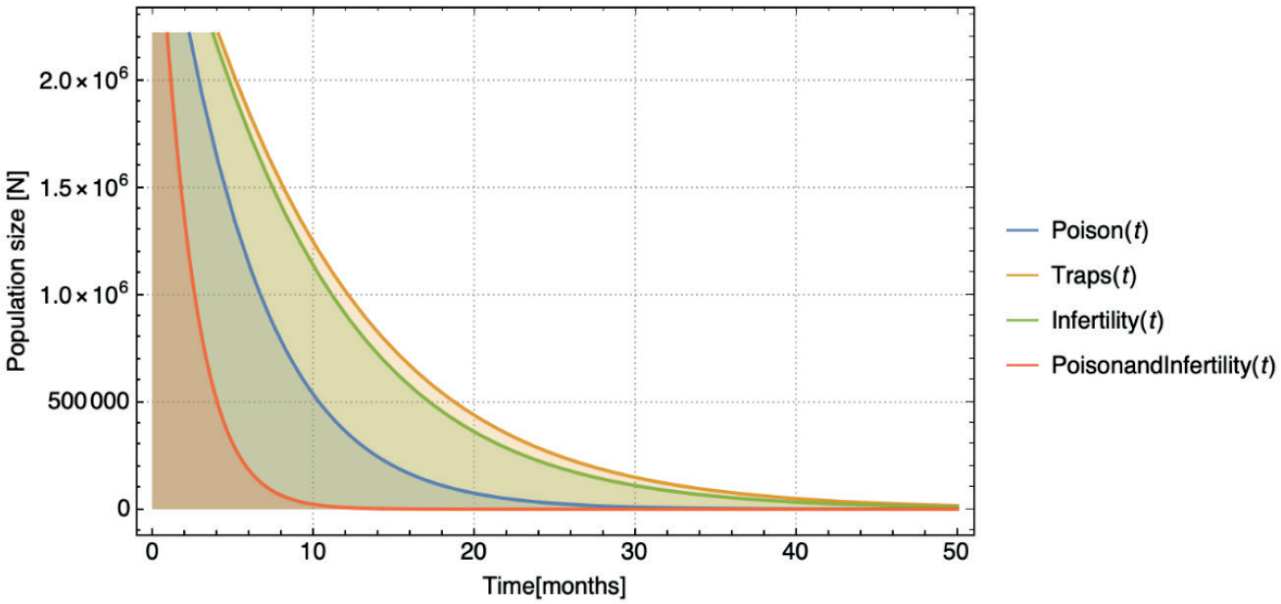

Figure 3. Population growth of the 3 strategies and the combination of poison and infertility.

species of rodents. With this, we will continue to improve our mathematical model and subsequently form part of a rescue plan for the site's critical biodiversity.

Bibliographic references

1. Hilton GM, Cuthbert RJ. The catastrophic impact of invasive mammalian predators on birds of the UK Overseas Territories: A review and synthesis. Ibis (Lond 1859) 2010; 152: 443–458.
2. Towns DR, Atkinson IAE, Daugherty CH. Have the harmful effects of introduced rats on islands been exaggerated? Biol Invasions 2006; 8: 863–891.
3. Atkinson I, Western D, Pearl MC. Introduced animals and extinctions. In: Conservation for the twenty-first century. Oxford University Press: New York, 1989, pp 54–79.
4. Fundación Charles Darwin (FCD) y WWF-Ecuador. Atlas de Galápagos, Ecuador: Especies Nativas e Invasoras. 2018.
5. Russell JC, Holmes ND. Tropical island conservation: Rat eradication for species recovery. Biol Conserv 2015; 185: 1–7.
6. Howald G, Donlan CJ, Galván JP, Russell JC, Parkes J, Samaniego A et al. Invasive rodent eradication on islands. Conserv Biol 2007; 21: 1258–1268.
7. Duron Q, Shiels AB, Vidal E. Control of invasive rats on islands and priorities for future action. Conserv Biol 2017; 31: 761–771.

Island	Area (km^2)	Estimated population of rats on the island (individuals)	Time (months) at which N=1 by applying poisoning strategy	Time (months) at which N=1 by poisoning and induced infertility strategies
Isabela	4588	4381540	72.84	28.02
Santa Cruz	986	941630	65.16	25.06
Santiago	585	558675	62.55	24.06
San Cristóbal	558	532890	62.31	23.97
Floreana	172	164260	56.43	21.70
Bartolome	1.24	1184.2	31.76	12.22
Baltra	27	25785	47.17	18.14
North Seymour	1.9	1814.5	33.90	13.04
Pinzon	18.15	17333.25	45.18	17.38

Table 2. Area of each island with the presence of rats registered and the predicted time to reach population equals 1.

8. Cromarty P, Broome K, Cox A, Empson RA, Hutchinson WM, McFadden I. Eradication planning for invasive alien species on islands – the approach developed by the New Zealand department of conservation. Turn Tide Erad Invasive Species 2002; : 85–91.
9. Pott M, Wegmann AS, Griffiths R, Samaniego-Herrera A, Cuthbert RJ, Brooke M de L et al. Improving the odds: Assessing bait availability before rodent eradications to aid in selecting bait application rates. Biol Conserv 2015; 185: 27–35.
10. Pitt WC, Driscoll LC, Sugihara RT. Efficacy of rodenticide baits for the control of three invasive rodent species in Hawaii. Arch Environ Contam Toxicol 2011; 60: 533–542.
11. Brown D, Tershy B, Pitt WC, Cuthbert RJ, Wegmann A, Keitt B et al. Successes and failures of rat eradications on tropical islands : a comparative review of eight recent projects. 2019; : 120–130.
12. Delgadillo Alemán ES, Carrillo Kú AR, Vela Arévalo LV. Modelación matemática del control de plagas en un cultivo de brócoli. Rev del Dpto Matemáticas y Física la UAA 2006; : 3–20.
13. Rueda D, Carrion V, Castano P, Cunninghame F, Fisher P, Hagen E et al. Preventing extinctions: planning and undertaking invasive rodent eradication from Pinzon Island, Galapagos. invasives scaling up to meet challenge Occas Pap SSC 2019; : 51–56.
14. Patton JL, Yang SY, Myers P. Genetic and morphologic divergence among introduced rat populations (rattus rattus) of the galÁpagos archipelago, ecuador. Syst Biol 1975; 24: 296–310.
15. Patton JL, Hafner MS. Biosystematics of the Native Rodents of the Galapagos Archipielago, Ecuador. Patterns Evol Galapagos Org 1983; : 539–567.
16. Key G, Muñoz EH. Distribution and current status of rodents in the Galápagos. Not Galapagos 1994; 53: 21–25.
17. Cruz JB, Cruz F. Conservation of the Dark-rumped Petrel Pterodroma phaeopygia of the Galápagos Islands, 1982-1991. Bird Conserv Int 1996; 6: 23–32.
18. Steadman DW, Stafford TW, Donahue DJ, Jull AJT. Chronology of Holocene vertebrate extinction in the Galápagos Islands. Quat Res 1991; 36: 126–133.
19. Harper GA, Zabala J, Carrion V. Monitoring of a population of Galápagos land iguanas (Conolophus subcristatus) during a rat eradication using brodifacoum. Isl invasives Erad Manag 2011; : 309–312.
20. Cayot L, Rassmann K, Tillmich F. Are marine iguanas endangered on islands with introduced predators. Not ... 1994; : 3–5.
21. Harper G., Carrion V. Introduced rodent in the Galapagos: colonisation, removal and the future. Isl Invasives Erad Manag Proc Int Conf Isl Invasives 2011; : 63–66.
22. Campbell KJ, Carrión V, Sevilla C. Increasing the scale of successful invasive rodent eradications in the Galapagos Islands. Galapagos Rep 2011-2012 2013; : 194–198.
23. Nakayama SMM, Morita A, Ikenaka Y, Mizukawa H, Ishizuka M. A review: Poisoning by anticoagulant rodenticides in non-target animals globally. J Vet Med Sci 2019; 81: 298–313.
24. Rueda D, Campbell KJ, Fisher P, Cunninghame F, Ponder JB. Biologically significant residual persistence of brodifacoum in reptiles following invasive rodent eradication, Galapagos Islands, Ecuador. Conserv Evid 2016; 13: 38.
25. Hadler MR, Sahdbolt. RS. Novel 4-hydroxycoumarin anticoagulants active against resistant rats. Nature 1975; 253: 277–282.
26. Booth L, Eason C, Spurr E. Literature review of the acute toxicity and persistence of brodifacoum to invertebrates. Sci Conserv 2001; : 1–9.
27. Roomaney R, Ehrlich R, Rother H-A. The acceptability of rat trap use over pesticides for rodent control in two poor urban communities in South Africa. Environ Health 2012; 11: 32.
28. Ji W, Craig J. An evaluation of the efficiency of rodent trapping methods: The effect of trap arrangement, cover type, and bait. N Z J Ecol 1999; 23.
29. Thompson H V. Experimental live trapping of rats, with observations on their behaviour. Br J Anim Behav 1953; 1: 96–111.
30. Jackson WB. Biological and behavioural studies of rodents as a basis for control. Bull World Health Organ 1972; 47: 281–286.
31. Gotelli N. Gotelli_2008_A primer of Ecology (4ed).pdf. 2008.

32. Gentry JW. Evaluation of Rat Eradication Programs. Environ Sci Technol 1971; 5: 704–709.
33. Morlan HB, Bernice C. U, Dent JE. DOMESTIC rats, rat ectoparasites and typhus control. Public Health Monogr 1952; 14: 1–37.
34. Panti-May JA, Carvalho-Pereira TSA, Serrano S, Pedra GG, Taylor J, Pertile AC et al. A Two-Year Ecological Study of Norway Rats (Rattus norvegicus) in a Brazilian Urban Slum. PLoS One 2016; 11: e0152511–e0152511.
35. Davis DE. The Characteristics of Rat Populations. Q Rev Biol 1953; 28: 373–401.
36. Theuerkauf J, Rouys S, Jourdan H. Efficiency of a New Reverse-Bait Trigger Snap Trap for Invasive Rats and a New Standardised Abundance Index. Ann Zool Fennici 2011; 48: 308–318.
37. Taylor KD, Hammond LE, Quy RJ. The Reactions of Common Rats to Four Types of Live-Capture Trap. J Appl Ecol 1974; 11: 453–459.
38. Brown RZ. Biological Factors in Domestic Rodent Control: Training Guide. U.S. Consumer Protection and Environmental Health Service, Environmental Control Administration, 1969https://books.google.com.ec/books?id=h0o9Gu_CSFQC.
39. Harper GA, Bunbury N. Invasive rats on tropical islands: Their population biology and impacts on native species. Glob Ecol Conserv 2015; 3: 607–627.
40. Smith WW. Rat, Flea, and Murine Typhus Recurrence Following Eradication Measures. Public Health Rep 1958; 73: 469–474.

Received: 10 July 2020
Accepted: 10 November 2020

BIOETHICS /BIOÉTICA

Bioethical Guidelines of 'Extreme Triage' Under Covid: The Question of 'Possible Lives' in Latin America

Abril Saldaña-Tejeda
DOI. 10.21931/RB/2020.05.04.27

Abstract: The essay briefly looks into the bioethical guide of extreme triage and resource allocation based on known co-morbidities (i.e., obesity, hypertension, and diabetes). I invite to reflect upon how a focus on individual responsibility under COVID-19 occludes major structural problems while silencing the social factors behind the heath disaster that we are witnessing today. The essay argues that chronic diseases are not merely the result of genetic makeup or individual choices but are instead profoundly linked to poverty, systemic racism, structural violence, and lack of care. Debates on extreme triage guidelines and resource allocation illuminate a series of ethical shortcomings that preexisted COVID-19. Even if guidelines clearly state that criteria such as race, gender, or class will not be taken into account when deciding how to allocate limited medical resources, these categories are deeply linked to health disparities, and therefore, on people's possibilities of surviving the pandemic.

Key words: COVID-19, bioethics, extreme traige, comorbidites, health inequalities.

Assuming a shortage of medical resources to treat patients with Covid-19, many Latin American countries have discussed or established bioethical guides for limited resource allocation in the case of a public health emergency or what is known as 'extreme triage.' Under the principle of social justice, these guides propose to allocate resources to save as many lives as possible. Countries such as Chile, México, Argentina, Colombia, Brazil, and Uruguay have discussed the establishment of triage teams to administer scarce resources based on two main criteria: the possibility that a patient will improve and survive (that is, the presence vs. the absence of co-morbidities) and the time the patient will take to recover. In many countries, the additional recommended principle is to allocate resources to those who can have more years of life saved. That is, younger patients.

An emergency resource allocation strategy certainly involves abandoning the Hippocratic Oath, the idea of equality between people, and the sacredness of life. However, in a crisis like the one we are experiencing now, health professionals require direction to proceed in the event of facing limited resources in a scenario that seems inevitable. Bioethical procedures need to be discussed and agreed upon before impromptu and discretionary decisions are made by health professionals overwhelmed by the physical and emotional burden of the current crisis. Helen Ouyang[1], a New York emergency department doctor, vividly describes her experience in the midst of the pandemic as hospitals get flooded by patients, dead and alive. Her experience demonstrates the need for bioethical guidance on 'extreme triage' for those at the front of the pandemic risking their own physical and emotional lives to save the lives of others. However, there is also a need to question some of the assumptions behind these triage guidelines.

Bioethical triage guidelines have sparked a heated debate across the globe[2]. Bioethicists have been accused of playing God by deciding who deserves the chance to live and who doesn't. In many countries, public opinion has forced bioethicists to rewrite and retract many of the recommendations for limited medical resource allocation. Many complaints have been directed towards the utilitarian ethics that often inform 'extreme triage' guidelines that propose the allocation of scarce medical resources with the sole idea of saving as many lives as possible. The most prominent criticisms were focused on age discrimination.

For instance, in Mexico, some went as far as comparing the bioethical triage guidelines to Nazi's atrocities against those perceived as old or ill[3]. In Argentina, a group of bioethicists questioned age as a factor in decision making since a young individual can suffer from more severe pathologies than an older one, and therefore be less likely to survive the virus[4]. In contrast to the outcry over what many perceived as age discrimination, little has been said about co-morbidities as a factor that would make someone less likely to survive. This is especially problematic as there is growing evidence to suggest that many chronic diseases are not merely the result of genetic makeup or individual choices but are instead profoundly linked to poverty, systemic racism, structural violence, and lack of care[5]. Failing to look at the preexisting conditions of our health systems and the struggles of those suffering from chronic diseases before Covid-19 could easily imply that critical medical resources are denied to those for whom the state has already failed to protect. As Palmer[6] suggests, when highlighting how wellness is increasingly being presented as a lifestyle choice, 'even before the pandemic, they [the chronically ill] had been used to the medical system giving up on them before they were given a chance.' Moreover, many of those that are being identified as particularly 'at risk' of Covid-19 are being denied the care they regularly receive as surgeons or hospitals find themselves overwhelmed by the Covid-19 crisis[7]. Given the economic toll of the pandemic, it seems unlikely that health care systems around the world will be able to maintain [in many countries, already inefficient] pre- Covid-19 levels of care for patient groups.

As a society, we decide on the allocation of resources on a daily basis. Triage guidelines have merely illuminated a series of ethical shortcomings that preexist in the crisis. Even as guidelines state that criteria such as race, gender, or class will not be taken into account when deciding how to allocate limited medical resources, these categories are indeed involved in the configuration of health disparities, and therefore, on the likelihood of someone surviving the virus. Since 2015, Latin America has seen a severe increase in poverty rates and extreme poverty that directly affects health inequalities[8]. Covid-19 has

University of Guanajuato, Mexico.

Corresponding author: abrilsaldana@ugto.mx

exposed the extent of such inequalities across the Latin American region. For instance, there are disproportionate rates of infection and death among indigenous peoples. As of May 18th, there were up to 20,000 confirmed cases of Covid-19 among indigenous peoples from the Amazonia and in its 2,400 territories across eight countries[9]. Black Brazilians are said to be 62 percent more likely to die from the virus than whites, not only because of unequal access to health services but also because of the close correlation between race and chronic diseases such as diabetes and hypertension[10]. Women constitute up to 70 percent of health workers across the region; they are not only at the front of the pandemic but are also the target of attacks by those fearing contamination[11].

In some cases, domestic violence is taking more women's lives than Covid-19, and women are disproportionately taking the burden of domestic and care work during lockdown[12]. Finally, migrants, refugees, and displaced people are also being disproportionately affected by Covid-19, not only because of stigmatization in host countries but also because of the impact of border shutdowns that have left thousands of people trapped, without basic needs for survival[13]. In the case of Mexico, people treated at a private hospital were said to be 60 percent less likely to die by COVID-19 than those in public health units[14]. Up to 71 percent of COVID-19 fatalities were among people with the educational attainment of primary school or less (i.e., incomplete primary school, no studies), and up to 46 percent were retired, unemployed or part of the informal economy[15]. As these numbers suggest, race, class, and other social factors are directly behind the devastating effects of COVID-19. A bioethical approach to the allocation of medical resources under Covid-19 must consider that many of the bodies marked as 'more likely to survive the virus' were previously configured by colonial histories of racism, violence, and dispossession[16-18]. As Barnes *et al.*[19] suggest, 'care always has a past and how we respond to past injustices is one of the largest ethical questions we need to face.' Bioethics must engage with our regional past to address our present and future practices of care.

Covid-19 doesn't exist in isolation and requires that we consider social and structural conditions as preexisting and problematic[20]. Some of these conditions are embodied by individuals (i.e., age or co-morbidities), but others are found in institutional practices and policy approaches to address Covid-19. A preexisting condition could be found in the current denigration of our health systems or the so-called 'care deficit' as the effect of the international migration from Latin America. However, another preexisting condition could be the place of bioethics in the region and the low impact that research has had in policy-making[21]. We must confront the possible limits of bioethics to account for the political nature of the new place that science and medicine have in the world of politics to face unexpected challenges such as Covid-19[22].

Bulcock[23] describes the general features that distinguish Ibero-American from American bioethics. She identifies the communitarian character of the former versus the individualistic or autonomy-centered of the latter. The author looks at the central role of physicians and theologians in the development of an Ibero-American bioethics that identified itself as a social and political movement. In contrast, the establishment of American bioethics was institutionalized by academia and philosophy departments. Some Latin American theoretical approaches assert such distinction. For instance, complex, intervention, and protection bioethics are all theoretical models critical of individualistic and autonomy-centered approaches and all engage with a broader view of bioethics capable of encompassing human rights, public health, and social inequality[24-25]. However, confronting Covid-19 from a bioethical approach requires us to problematize the very notion of the community before and after the crisis. Following Esposito, we must rethink the basis of our political and social relations to unveil how, in the name of the 'common', we have reactivated the worst forms of structural violence[26]. Mestizaje, as the foundational myth found in many of the region's national histories, is one example of how in the name of a 'common' origin, indigenous, black, and Asian ancestries were to be violently and progressively erased from national identities. Mestizaje is still today the logic that works to deny the persistence of racist practices across many countries in Latin America through the idea that we have all a shared past, and we are all mixed[27].

In the post-pandemic world, bioethics must go beyond procedures and ethical committees to fully understand the challenges ahead. Following Esposito[28], Covid-19 presents a particular biopolitical dynamic that manifests in three particular features: the change of focus from individuals to population segments (i.e., identification and surveillance of 'at risk' and 'a risk' groups); a process where politics becomes medicalized, and medicine gets politicized, and finally, the increasing entanglement of political and biological life that allows for the transference of democratic action to states of emergency. If we aim to fully grasp the way forward, we must explore the political implications of these processes in our own contexts. For instance, in Mexico, Giovanni López, a 30-year-old bricklayer, was beaten to death by police officers for not wearing a face mask in public. As Giovanni's unlawful killing shows, police brutality must be seen as another preexisting condition that complicates the forced implementation of state measures to care for the broader population under Covid-19.

The current focus on the body (i.e., the presence of co-morbidities) seems to work as a mechanism to leave the state unaccountable for the political and social roots of health inequalities. This notion of the body as private or apolitical could also be behind the stigmatization and condescending practices that often occur when labeling whole groups of people as vulnerable[29]. For instance, a private amusement park in the city of Monterrey, northeast Mexico, announced that people [perceived by staff as] suffering from obesity were to be forbidden entrance for their protection from coronavirus[30]. The park didn't specify how its staff would be able to 'diagnose' someone as obese or if measures would be implemented to avoid discrimination. Companies are starting to refuse to hire people with chronic diseases, over 55 years of age, and other forms of 'risks' under COVID-19[31]. People are reported being denied entrance into casinos (gambling businesses) if they are perceived as obese for 'their own protection.' Other forms of COVID-19'S co-morbidities that are not seen as easy to diagnose through sights, such as diabetes or hypertension, are allowed to occupy these spaces freely. This leads us to ask, who or what are these businesses 'protecting'? What forms and meanings the notion of 'protection' or 'care' take in these cases? We must be attentive to the way these notions are used and how they are heavily charged with complex and, sometimes, contradictory meanings.

Conclusions

When it comes to the current state of emergency, it is also crucial to think about new and old forms of power in the region and their potential impact when managing the administration of life under Covid19. We must engage with a bioe-

thical approach to the allocation of care not only in times of emergencies but through the everyday care responsibilities grounded in democracy. As Tronto[32] suggests, 'democracy is not simply giving people a voice. It is giving people a voice in the allocation of caring responsibilities'. Following a theoretical tradition that attempts to go beyond an autonomy-centered approach to bioethics, we must engage with a democracy centered on care, one that could genuinely grasp the particular caring needs and obligations of states during and after Covid-19. As Garland-Thomson[33] suggests, disability bioethics reminds us of the need to transform medical subjects into political ones. Bioethical guides for extreme triage must acknowledge that decisions to allocate limited care during a health crisis are often shaped by past injustices and by the health inequalities that result from structural violence. It is only by accounting for those silenced and complex stories embodied by patients before arriving at the emergency room that we could truly engage with an ethical practice of care.

Funding

A Wellcome Small Grant supported this publication in Humanities and Social Science. Reference: 218699/Z/19/Z

The Medical Anthropology Blog Series published a previous version of this essay at the University of Central London: https://medanthucl.com/2020/09/15/bioethical-guidelines-of-extreme-triage-under-covid-the-question-of-possible-lives-in-latin-america/

Bibliographic references

1. Ouyang H. I'm an E.R. Doctor in New York. None of Us Will Ever Be the Same. The New York Times. April 14th 2020. Available from: https://www.nytimes.com/2020/04/14/magazine/coronavirus-er-doctor-diary-new-york-city.html. [Accessed October 28th 2020].
2. Del Missier G. Overwhelmed by the virus: the issue of extreme triage. Alphonsian Academy Blog. March 27th 2020. Available from: https://www.cssr.news/2020/03/overwhelmed-by-the-virus-the-issue-of-extreme-triage/ [Accessed 28th October 2020].
3. Miranda P. UNAM se deslinda de guía que relega a ancianos con Covid-19. El Universal. April 15th 2020. Available from: https://www.eluniversal.com.mx/nacion/expertos-critican-guia-que-prioriza-jovenes-sobre-ancianos-con-covid-19 [Accessed 28th October 2020].
4. Woites A M. Especialistas en bioética reflexionan sobre los desafíos que se afrontan ante el nuevo coronavirus Télam. 17 April 2020. Available from: https://www.telam.com.ar/notas/202004/453069-bioetica-salud-coronavirus-pandemia.html?fbclid=IwAR2aQodB5IGW20ecxcY0N18sbowDJ2ur-dWIWODX2bmgUKINfUSqza3v4BA [Accessed 28th October 2020].
5. Burnett C, Carney M A, Carruth L, Chard S, Dickinson, M, Howard M. Anthropologists Respond to The Lancet EAT Commission. Revista Bionatura. 2020. 5 (1): 1023-1024. Available from: doi: 0.21931/RB/2020.05.01.2.
6. Palmer A. Wellness is a seductive lie-and it is changing how we treat illness. The Guardian. June 22nd 2020. Available from: https://www.theguardian.com/books/2020/jun/22/wellness-is-a-seductive-lie-abi-palmer-sanatorium [Accessed 28th October 2020].
7. Manderson L, Wahlberg A. Chronic Living in a Communicable World. Medical Anthropology. 2020;39(5):428-439. Available from: doi: 10.1080/01459740.2020.1761352
8. Abramo L, Cecchini S, Ullmann H. Addressing health inequalities in Latin America: the role of social protection. Ciência & Saúde Coletiva. 2020, 25(5): 1587–1598. Available from: doi: 10.1590/1413-81232020255.32802019
9. Organización Panamericana de Salud. Directora de la OPS llama a proteger a los grupos vulnerables de los efectos de la pandemia de COVID-19. 19 May 2020. Available from: https://www.paho.org/es/noticias/19-5-2020-directora-ops-llama-proteger-grupos-vulnerables-efectos-pandemia-covid-19.[Accessed 28th October 2020].
10. Genot, L. In Brazil, Coronavirus Hits Blacks Harder Than Whites. Barron's. May 7th 2020. Available from: https://www.barrons.com/news/in-brazil-coronavirus-hits-blacks-harder-than-whites-01588886404 [Accessed 28th October 2020].
11. United Nations Population Fund. Covid-19 a Gender Lens: protecting sexual and reproductive health and rights and promoting gender equality. March 2020 Available from: https://www.unfpa.org/sites/default/files/resource-pdf/COVID-19_A_Gender_Lens_Guidance_Note.pdf [Accessed 28th October 2020].
12. Regnér A. Frente al coronavirus, las mujeres somos la primera línea de defensa. The Washington Post. 7 April 2020. Available from: https://www.washingtonpost.com/es/post-opinion/2020/04/07/frente-al-coronavirus-las-mujeres-somos-la-primera-linea-de-defensa/ [Accessed 28th October 2020].
13. Segnana J. La situación de los migrantes en América Latina en el contexto del COVID-19', PNUD América Latina y el Caribe. 19 May 2020. Available from: https://www.latinamerica.undp.org/content/rblac/es/home/blog/2020/la-situacion-de-los-migrantes-en-america-latina-en-el-contexto-d.html. [Accessed 28th October 2020].
14. Solís, P., Carreño H. 2020. 'COVID-19 Fatality and Co-morbidity Risk Factors among Confirmed Patients in Mexico'. MedRxiv. 2020: 1-8. Available from: https://doi.org/10.1101/2020.04.21.
15. Hernández Bringas H. Mortalidad por COVID-19 en México. Notas preliminares para un perfil sociodemográfico. Notas de Coyuntura del CRIM 2020 (36):1–7. Available from: http://doi.org/10.22201/crim.001r.2020.36
16. Yates-Doerr E. The Weight of Obesity: Hunger and Global Health in Postwar Guatemala. Oakland: University of California Press; 2015.
17. Gálvez A. Eating NAFTA: Trade, Food Policies, and the Destruction of Mexico. Oakland: University of California Press; 2018.
18. Mendenhall E. Rethinking Diabetes: Entanglements with Trauma, Poverty, and HIV. Ithaca and London: Cornell University Press; 2019.
19. Barnes M, Brannelly T, Ward L, Ward N. Introduction: the critical significance of care. In: Barnes M, Brannelly T, Ward L, Ward N (eds.) Ethics of Care: Critical Advances in International Perspective. Bristol: Policy Press; 2015. p. 3–19.
20. Mendenhall E. Why Social Policies Make Coronavirus Worse. Available from: https://www.thinkglobalhealth.org/article/why-social-policies-make-coronavirus-worse [Accessed 28th October 2020].
21. Garcia L F, Fernandes M S, Moreno J D, Goldim J R. Mapping Bioethics in Latin America: History, Theoretical Models, and Scientific Output. Journal of Bioethical Inquiry. 2019, 16(3):323–331. Available from: doi: 10.1007/s11673-019-09903-7.
22. Hernández Martínez C N. De Van R Potter a Michel Foucault o de la bioética a la biopolítica como estrategia de análisis en el debate en torno a las biotecnologías. In: Corona Fernández J. (coord.) Poder y subjetividad. Emplazamientos para una reflexión sobre el presente. México: Itaca/Universidad de Guanajuato; 2019. p. 95-119.
23. Bulcock J A. The Many Beginnings of Bioethics: A Comparison of American and Ibero-American Bioethics and the Possibility of a Global Bioethics. In: Pessini L, Paul de Barchifontaine C, and Lolas Stepke F (eds) Ibero-American Bioethics. History and Perspectives. London and New York: Springer; 2010. p. 379–386.
24. Garcia, L. F., Fernandes, M. S., Moreno, J. D., & Goldim, J. R. (2019). Mapping Bioethics in Latin America: History, Theoretical Models, and Scientific Output. Journal of Bioethical Inquiry, 16(3), 323-331.Goldim, JR. Revisiting the beginning of bioethics: the contribution of Fritz Jahr (1927). Perspect Biol Med. 2009, 52(3):377-380. Available from: doi: 10.1353/pbm.0.0094.

25. Port D, Garrafa V. Bioética de intervenção: Considerações sobre a economia de Mercado [Intervention bioethics: Considerations on market economy]. Revista Bioética. 2005, 13(1): 1122–1132.
26. Bird G, Short J. Community, immunity, and the proper an introduction to the political theory of Roberto Esposito. Angelaki. 2013,18(3): 1–12. Available from: doi: 10.1080/0969725X.2013.834661.
27. Moreno Figueroa M. Distributed intensities: Whiteness, mestizaje and the logics of Mexican racism. Ethnicities. 2010, 10(3): 387-401. Available from: doi: 10.1177/1468796810372305.
28. Esposito R. Biopolítica y coronavirus. Available from: https://www.filco.es/biopolitica-y-coronavirus/ [Accessed 28th October 2020].
29. Luna F. (2019). Revisiting Vulnerability: Its Development and Impact. In Controversies in Latin American Bioethics. In: Lopez E, Rivera M (eds) Controversies in Latin American Bioethics. London and New York:Springer, 2019. p. 67-81.
30. Zuñiga F. Personas con obesidad, niños y adultos mayores no podrán entrar al parque Fundidora. 4 July 2020. Milenio. Available from: https://www.milenio.com/ciencia-y-salud/sociedad/coronavirus-personas-obesidad-entrar-parque-fundidora
31. Casasola, Tania. 17 de septiembre, 2020 'El COVID nos trajo discriminación': Niegan empleo por tener diabetes, hipertensión y obesidad. Animal Político. Available from: https://www.animalpolitico.com/2020/09/covid-niegan-empleo-enfermos-diabetes-hipertension-obesidad-discriminacion/
32. Tronto J. Democratic caring and global care responsibilities. In: Barnes M, Brannelly T, Ward L, Ward N. (eds.) Ethics of Care: Critical advances in international perspective. Bristol: Policy Press; 2015.p. 21–30.
33. Garland-Thomson R. CRISPR and Human Identity: Governing Germline Gene Editing. 30 years of the Genome Integrating and Applying ELSI Research. Columbia University. June 15th 2020. Available from: https://www.mhe.cuimc.columbia.edu/our-divisions/division-ethics/elsi-virtual-forum/elsi-virtual-forum-video-recordings [Accessed 2 November 2020].

Received: 15 August 2020
Accepted: 3 November 2020

El Centro de Biotecnología de la ESPOL, CIBE

Genera, aplica, transfiere y difunde las soluciones biotecnológicas que demanda el sector agroindustrial de la costa ecuatoriana.

Sus fortalezas se enfocan en servicios de análisis o de investigación aplicada que puedan proveer soluciones a problemas particulares de la agricultura.

Tipos de ensayos

- Clínica de plantas.
- Servicios analíticos.
- Servicios de bioensayos.

Servicios más requeridos

- Diagnóstico de enfermedades en cultivos agrícolas.
- Estudio de sensibilidad de Sigatoka Negra a fungicidas.
- Cuantificación de fitohormonas, perfil de ácidos grasos por CG-EM.
- Cuantificación de polifenoles y flavonoides, actividad antioxidante.
- Extensión agrícola.

Productos que puede evaluar

- Cultivos agrícolas con presencia de enfermedades causadas por patógenos (bacterias, virus y hongos).
- Bioproductos o bioinsumos con impacto en el rendimiento de cultivos.
- Fungicidas o productos similares para el control de Sigatoka Negra.

Nuestra visión es ser el líder nacional en biotecnología en beneficio del desarrollo de la sociedad ecuatoriana.

V Congreso Internacional de Biotecnología y Biodiversidad

CIBB 2020

MODALIDAD VIRTUAL

XVII INTERNATIONAL BANANA CONVENTION 2020 VIRTUAL

ALIANZA ESTRATÉGICA PARA SEGUIR AVANZANDO EN TIEMPO DE PANDEMIA

Dra. Paloma Moncaleán
NEIKER BRTA - BIOALI CYTED

NEIKER MEMBER OF BASQUE RESEARCH & TECHNOLOGY ALLIANCE

Dra. Daynet Sosa
CIBE - ESPOL

espol Centro de Biotecnología

PROGRAMA IBEROAMERICANO

bioali CYTED

CIENCIA Y TECNOLOGIA PARA EL DESARROLLO

La salud del futuro: Nanomedicina

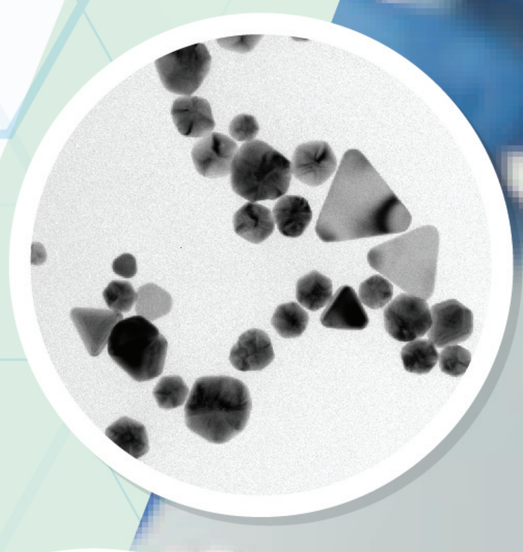

Aplicación de nanopartículas en Medicina, Veterinaria, Cultivo Vegetal, Agricultura y Acuicultura

INTERNATIONAL BIONANOTECHNOLOGY NETWORK

CONACYT Consejo Nacional de Ciencia y Tecnología

Universidad Nacional Autónoma de México

www.redinternacionaldebionanotecnologia.org /Red-Internacional-de-Bionanotecnología

http://bionn.org/ letyens@outlook.com 52-(646)-1366446


UNIVERSIDAD
YACHAY
TECH
SOMOS LA PRIMERA UNIVERSIDAD
DEL ECUADOR
CON MAYOR RELEVANCIA EN
PUBLICACIONES
CIENTÍFICAS
FUENTE: www.natureindex.com/country-outputs/Ecuador


UNIVERSIDAD
YACHAY
TECH
DE LA CURIOSIDAD ACADÉMICA
A LA INNOVACIÓN TECNOLÓGICA
ESCUELA DE
CIENCIAS MATEMÁTICAS
Y COMPUTACIONALES
ESCUELA DE
CIENCIAS FÍSICAS
Y NANOTECNOLOGÍA
ESCUELA DE
CIENCIAS QUÍMICAS
E INGENIERÍA
ESCUELA DE
CIENCIAS DE LA TIERRA,
ENERGÍA Y AMBIENTE
ESCUELA DE
CIENCIAS BIOLÓGICAS
E INGENIERÍA